

TECHNISCHE UNIVERSITÄT MÜNCHEN

Fakultät für Chemie

WACKER-Lehrstuhl für Makromolekulare Chemie

Precision Polymerization of *Michael*-type Monomers: Benefits and Limitations of Main Group Element Catalysts

Michael Weger

Vollständiger Abdruck der von der Fakultät für Chemie der Technischen Universität München zur Erlangung des akademischen Grades eines

Doktors der Naturwissenschaften

genehmigten Dissertation.

Vorsitzender:

Priv.-Doz. Dr. Gerd Gemmecker

Prüfer der Dissertation

1. Prof. Dr. Dr. h.c. Bernhard Rieger
2. apl. Prof. Dr. Wolfgang Eisenreich
3. Prof. Dr. Ingo Krossing (schriftliche Beurteilung)
Prof. Dr. Klaus Köhler (mündliche Prüfung)

Die Dissertation wurde am 22.10.2019 bei der Technischen Universität München eingereicht und durch die Fakultät für Chemie am 28.11.2019 angenommen.

„Den Wissenschaftlern geht es wie den Chaoten. Es ist alles da, man muss es nur suchen.“

- Franz Kern -

Die vorliegende Arbeit wurde in der Zeit von August 2016 bis Oktober 2019 am WACKER-Lehrstuhl für Makromolekulare Chemie, Technische Universität München, unter Betreuung von Herrn *Prof. Dr. Dr. h.c. Bernhard Rieger* angefertigt.

Acknowledgements

Mein besonderer Dank gilt Herrn Prof. Dr. Dr. h.c. Bernhard Rieger für die Aufnahme an seinem Lehrstuhl und die Möglichkeit, meine Doktorarbeit unter seiner Anleitung anfertigen zu dürfen. Die mir gewährten Freiräume und die hervorragenden Arbeitsbedingungen am Lehrstuhl habe ich sehr genossen. Mit vielen, manchmal auch hartnäckigen, aber immer sachlichen und sehr wertvollen Diskussionen haben wir einige Projekte erfolgreich beendet und neue in die Wege geleitet, was mir sehr viel Freude bereitet hat.

Zu großem Dank bin ich auch Dr. Alexander Pöthig und Prof. Dr. Wolfgang Eisenreich verpflichtet, die beide entscheidend am erfolgreichen Fortschritt meiner Arbeit beteiligt waren. Während ich zusammen mit Dr. Pöthig ein komplexes Kooperationsprojekt durchführen konnte, das nur mit seinem kristallographischen Fachwissen möglich war, steuerte Prof. Eisenreich mit größter Geduld unverzichtbares Fachwissen zur Inbetriebnahme und wissenschaftlichen Nutzung des neuen Lehrstuhl-NMR-Geräts bei.

Des Weiteren möchte ich mich ganz herzlich bei meinem Mentor Dr. Carsten Troll bedanken, der mir immer mit Rat und Tat zur Seite stand und für die sehr gute Organisation des Lehrstuhls verantwortlich ist. Danken möchte ich auch Dr. Sergei Vagin und Frau Bauer, die jederzeit als Anlaufstelle für diverse Probleme zur Verfügung standen.

Zudem bin ich Dr. Philipp Altmann („Altmann Analytics“) für seinen superschnellen SC-XRD Service und David Mayer, Dr. Julius Hornung und Dr. Markus Drees für die äußerst hilfreichen theoretischen Studien dankbar. Ohne euch wäre meine Arbeit in dieser Form nicht möglich gewesen, was ebenso für meine drei Masteranden Fabian Schmidt, Jonas Breitsameter und Waldemar Schmidt gilt. Ihr habt entscheidend zu meiner Thesis beigetragen und es war mir immer eine Freude, mit euch zusammenzuarbeiten. Genauso möchte ich meinen Vorgängern Dr. Maximilian Knaus und Raphael Grötsch danke sagen für die vielfältigen Themen, die ihr mir hinterlassen habt, und dafür, dass ihr mir auch nach eurer Zeit am Lehrstuhl für Fragen zur Verfügung gestanden seid. Natürlich gilt auch meinen zahlreichen Bacheloranden, Praktikanten und Auszubildenden mein Dank, die die letzten Jahre wichtige Arbeit für mich geleistet haben.

An die Zeit am WACKER-Lehrstuhl werde ich mich immer mit Freude zurückerinnern, was vor allem an der sehr kollegialen Atmosphäre und den hilfsbereiten Kollegen liegt. Sowohl mit der Generation, die vor mir angefangen hat, (Martin, Daniel, Tobi, Theresa, Philipp, Rike,...) als auch mit denen, die kurz nach mir mit ihrer Promotion begonnen haben, (Basti, Tom, Marc) konnte man fachliche Diskussionen führen wie auch lustige (Bier)Abende verbringen. Und ich bin mir sicher, dass die „junge“ Generation dem in nichts nachstehen wird.

Der Studienstiftung des deutschen Volkes, die meine Promotion großzügig über das Promotionsstipendium unterstützt hat, bin ich sehr verbunden.

Außerhalb des Lehrstuhls möchte ich im Speziellen der sogenannten „Damm“-Gruppe herzlich danken. Wir hatten während Studium und Promotion eine super Zeit mit seriösen Lerngruppen, unvergesslichen Urlauben und feucht-fröhlichen Abenden, die hoffentlich nach unseren erfolgreichen Promotionen weiterbestehen werden. Zudem will ich die Herrenmannschaft und die Vorstandskollegen der Tennisabteilung des TV Geisenhausen erwähnen, die mich nach anspruchsvollen Laborwochen in kürzester Zeit auf andere Gedanken gebracht haben.

Mein größter Dank gilt abschließend meiner Familie, insbesondere meinen Eltern Monika und Hans. Auch wenn ihr anfangs etwas verwundert über meinen Studienwunsch wart, habt ihr mich bedingungslos moralisch, finanziell und essenstechnisch unterstützt und mir das ermöglicht, wo ich jetzt stehe. Auch möchte ich meinem Onkel und „Zweitmentor“ Roland danken, der mich auf die Fährte der Chemie gebracht hat und für jegliche Fragen chemischer und nicht-chemischer Art zur Verfügung stand. Last but not least: Danke, liebste Kathi! Danke, dass du mir auch während der Promotion als helfende Hand zur Seite gestanden bist. Danke, dass du meine Launen jederzeit ertragen hast und mir immer den Rücken freigehalten hast. Danke für das gestern, für das heute und für das morgen.

List of Abbreviations

AN	acrylonitrile
<i>at</i>	atactic
BHT	2,6-di-tert-butyl-4-methylphenoxide
BLP	bridged <i>Lewis</i> pair
CF	carbon fiber
CGC	constrained geometry complex/catalyst
CLA	classic <i>Lewis</i> adduct
COSY	correlation spectroscopy
Cp	cyclopentadienyl
Cp*	pentamethylcyclopentadienyl
DAAA	<i>N,N</i> -dialkyl/aryl acrylamide
DAMA	<i>N,N</i> -dialkyl methacrylamide
DAVP	dialkyl vinylphosphonates
DEVP	diethyl vinylphosphonates
DFT	density functional theory
DMAA	<i>N,N</i> -dimethyl acrylamide
DMSO	dimethyl sulfoxide
DMVP	dimethyl vinylphosphonates
EBI	ethylene-bridged bis(indenyl)
en	ethylenediamine
Et	ethyl
ESI MS	electrospray ionization mass spectroscopy
FLP	frustrated <i>Lewis</i> pair
GTP	group transfer polymerization
HETCOR	two-dimensional heteronuclear (¹³ C- ¹ H) correlation
HMQC	heteronuclear multiple-bond correlation spectroscopy

List of Abbreviations

HSQC	heteronuclear single-quantum correlation spectroscopy
ILP	interacting <i>Lewis</i> pair
INEPTLR	long range insensitive nuclear enhanced by polarization transfer
IR	infrared
HPDE	high density poly(ethylene)
Ind	indenyl
IPOx	2- <i>isopropenyl</i> -2-oxazoline
<i>it</i>	isotactic
LCST	lower critical solution temperature
LA	<i>Lewis</i> acid
LB	<i>Lewis</i> base
LP	<i>Lewis</i> pair
LPP	<i>Lewis</i> pair polymerization
<i>m</i>	meso
Me	methyl
MMA	methyl methacrylate
γ MMBL	γ -methyl- α -methylene- γ -butyrolactone
<i>n</i> BA	<i>n</i> -butyl acrylate
NBO	natural bond orbitals
<i>n</i> Bu	<i>n</i> -butyl
NHC	<i>N</i> -heterocyclic carbene
NHO	<i>N</i> -heterocyclic olefin
NMR	nuclear magnetic resonance
<i>N,N</i> -DMF	<i>N,N</i> -dimethyl formamide
PDI	polydispersity index
PP	poly(propylene)
<i>r</i>	racemic

List of Abbreviations

REM	rare earth metal
SC-XRD	single crystal X-ray diffraction
SOHIO	standard oil of ohio
<i>st</i>	syndiotactic
<i>t</i> BuMA	<i>tert</i> -butyl methacrylate
T_g	glass transition temperature/point
THF	tetrahydrofuran
T_m	melting point
TMS	trimethylsilane
TOCSY	total correlation spectroscopy
TOF	turnover frequency
TON	turnover number
UV	ultraviolet
VF	vinyl fluoride
2VP	2-vinylpyridine
4VP	4-vinylpyridine
VPA	vinylphosphonic acid

Publication List

- M. Weger,[‡] M. M. Giuman,[‡] M. G. Knaus,[‡] M. Ackermann, M. Drees, J. Hornung, P. J. Altmann, R. A. Fischer, B. Rieger*. Single-Site, Organometallic Aluminum Catalysts for the Precise Group Transfer Polymerization of *Michael*-Type Monomers. *Chem. Eur. J.* **2018**, *24*, 14950 – 14957.
- M. Weger,[‡] R. K. Grötsch,[‡] M. G. Knaus, M. M. Giuman, D. C. Mayer, P. J. Altmann, E. Mossou, B. Dittrich, A. Pöthig,* B. Rieger*. Non-Innocent Methylene Linker in Bridged *Lewis* Pair Initiators. *Angew. Chem. Int. Ed.* **2019**, *58*, 9797 – 9801; Nicht-unschuldiger Methylen-Linker in verbrückten *Lewis*-Paar-Initiatoren. *Angew. Chem.* **2019**, *131*, 9902 – 9906.
- M. Weger,[‡] P. Pahl,[‡] F. Schmidt,[‡] B. S. Soller, P. J. Altmann, A. Pöthig, G. Gemmecker, W. Eisenreich,* B. Rieger*. Isospecific Group Transfer Polymerization of Diethyl Vinylphosphonate and Multidimensional NMR Analysis of the Polymer Microstructure. *Macromolecules* **2019**, *52*, 7073 – 7080.
- M. Weger, M. G. Knaus, M. M. Giuman, M. Drees, A. Pöthig, B. Rieger*. Taking Control over the Polymerization of Acrylonitrile with Highly Active Main Group Element Catalysts. *Submitted to Angew. Chem. Int. Ed.*

Publications beyond the scope of this thesis:

- A. Schaffer, M. Weger, B. Rieger*. From Lanthanide-mediated High Precision Group Transfer Polymerization of *Michael*-type Monomers to Intelligent, Functional Materials. *Eur. Polym. J.* **2020**, *122*, 109385.

[‡] These authors contributed equally; * Corresponding authors

Conference contributions:

- M. Weger, B. Rieger. Single-site, Organometallic Aluminum Catalysts for the Precise Group Transfer Polymerization of *Michael*-type Monomers, Biennial Meeting of the GDCh-Division of Macromolecular Chemistry **2018**, Karlsruhe, poster presentation.
- M. Weger, B. Rieger. All for Aluminum: A Single-Component, Main Group Element Mediated Group Transfer Polymerization, 258th American Chemical Society National Meeting & Exposition **2019**, San Diego, oral presentation.

Table of Contents

Acknowledgements	IV
List of Abbreviations	VI
Publication List	IX
Table of Contents	X
1. Introduction	1
2. Importance and Characteristics of Catalytic Precision Polymerizations	3
2.1 Monomer Scope	4
2.2 Metal-mediated Group Transfer Polymerization	6
2.2.1 Nonbridged Catalysts	7
2.2.2 Bridged Catalysts	9
2.2.3 C-H Bond Activation	11
2.3 Lewis Pair Polymerization	12
2.4 Analysis of the Tacticity	15
2.5 Stereocontrol Mechanisms	20
2.6 The Special Case Acrylonitrile	22
3. Aim of this Thesis	25
4. Single-site, Organometallic Aluminum Catalysts for the Precise Group Transfer Polymerization of <i>Michael</i> -type Monomers	30
5. Non-Innocent Methylene-Linker in Bridged Lewis Pair Initiators	41
6. Taking Control over the Polymerization of Acrylonitrile with Highly Active Main Group Element Catalysts	47
7. Isospecific Group-Transfer Polymerization of Diethyl Vinylphosphonate and Multidimensional NMR Analysis of the Polymer Microstructure	53
8. Excursus: Polymer-Analogous Reactions as Novel and Controlled Pathway to Polyacrylonitrile and its Well Adjustable Copolymers	62
9. Summary and Outlook	69
10. Zusammenfassung und Ausblick	75

Table of Contents

11. Bibliography	81
12. Appendix	88
12.1 Supporting Information for Chapter 4	88
12.2 Supporting Information for Chapter 5	91
12.3 Supporting Information for Chapter 6	92
12.4 Supporting Information for Chapter 7	114

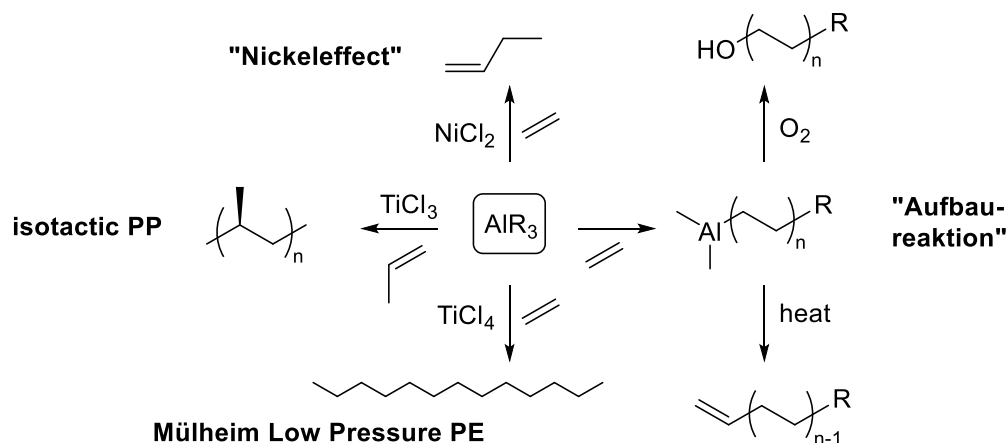
1. Introduction

Plastics have been key enablers for innovations in the past 150 years and due to their broad scope of applications and superior properties, they have replaced other classic materials such as metals, ceramics, wool, or wood. The engineering applications of polymers are widespread and our modern consumer-based society is impossible to imagine without synthetic materials. During the last years, several new families of functional polymers have been reported which provide an improved set of properties and therefore show enhanced potential in more challenging applications compared to the commodity polymers. To achieve the required precise control of the macromolecular architecture, it is inevitable to develop new, smart, and more efficient processes for the synthesis of functional polymers. In polymer chemistry, this challenge can be met with the development of suitable catalysts.^[1] Catalysts minimize energy costs, ensure the formation of the desired product, and even enable the rational design of unprecedented polymer architectures.

In a broad sense, the propagation of all polymerization reactions can be seen as catalytic as multiple monomers are consumed per reactive initiating molecule. For a better distinction of those initiating compounds, the terms “initiators” and “catalysts” are used, depending on whether one or several polymer chains are produced by one reagent. The definition of an initiator is precise for free radical, cationic, or anionic polymerization techniques. In contrast, in catalytic polymerizations, the catalyst can either relate to the initiating ligand or to the metal center being responsible for the activation and stabilization of the monomer and growing chain end. To overcome this terminological conflict, according to the literature, the term “catalyst” is used in this thesis when referring to the activation and addition of the monomer.^[2] Whereas complexes are often termed as catalysts, only one polymer chain is formed per metal center and the turnover number (TON) is strictly one for living polymerizations in contrast to the classic catalysis definition.

The historic starting point of polymerization catalysis were the discoveries of *Ziegler* and *Natta* during the 1950s. Their effective catalytic methods for carbon-carbon bond forming polymerization reactions are milestones in the organometallic and stereoselective polymerization chemistry.^[3] The so-called “*Ziegler'sche Aufbaureaktion*” constitutes the groundwork for the catalytic olefin polymerization. In this reaction, ethylene inserts in the Al-C bond of triethylaluminum (AlEt_3) to form higher aluminum alkyls. Today the “*Aufbaureaktion*” is still being applied for the manufacturing of 1-olefins as well as straight chain alcohols. Additionally, high purity alumina is obtained through oxidation of the aluminum

alkyls as commercially valuable side product. Shortly afterwards, nickel contamination of an autoclave was recognized to prevent ethylene propagation in the presence of aluminum alkyls and to favor chain termination. In the presence of nickel salts, aluminum alkyls gave exclusively the ethylene dimer 1-butene. The more detailed investigation of *Ziegler's "Nickeffect"* ultimately led to the discovery of *Ziegler's Mülheim low pressure process* for the catalytic ethylene polymerization. When zirconium and titanium compounds were added to aluminum alkyls, high molecular weight linear high density poly(ethylene) (HDPE) was formed at atmospheric pressure and room temperature. The group of *Giulio Natta* succeeded to polymerize propylene using *Ziegler's* catalyst system. *Natta* immediately recognized that the poly(propylene) (PP) obtained with crystalline α - TiCl_3 and AlEt_3 is composed of different diastereoisomers with very different physical properties. His new concept of polymer stereoregularity had extensive impact on the progress of polymer science and technology and led to the targeted design of transition metal catalysts with enantiomorphic active sites for stereospecific polymerizations.^[4]



Scheme 1. The initial catalytic processes of the olefin polymerization starting from aluminum alkyls (AlR_3).

As shown in Scheme 1, aluminum compounds played a decisive role for the discovery of the catalytic olefin polymerization. However, the use of alanes as (co)catalysts is not restricted to the polymerization of nonpolar olefins. Organoaluminum catalysts combined with *Lewis* bases are already known for the precision polymerization of polar monomers like acrylates and further *Michael*-type monomers.^[5,6] In general, main group compounds have experienced a renaissance in the last decades and have emerged as non-toxic, fairly abundant and efficient replacements of transition and rare earth metals. Thus, organoaluminum compounds are promising, but hardly explored candidates for promoting the precise conversion of *Michael*-type monomers and could substitute the well-known single-component and single-site non-main group element catalysts which are mostly based on expensive, dwindling resources.

2. Importance and Characteristics of Catalytic Precision Polymerizations

The need for new materials has driven the polymer research in recent years, even though the majority of the industrially produced plastics are based on only a few commodity polymers. Due to their specific chemical groups, functional polymers form the basis for new and smart materials with enhanced properties and are increasingly becoming a focus of research activities. The number of available functionalities tailored by the introduction of heteroatoms like O, N and P is vast. In combination with macromolecular organization and self-assembly principles, a wide range of new functional materials is accessible.^[1]

Synthesizing these types of polymers requires high precision and control with regard to composition, microstructure and molecular weight. The attainment of this goal was enabled by the prolific coupling of polymer science with organometallic chemistry. Remarkable successes were achieved in the production of revolutionary polyolefin materials by coordinative-anionic (co)polymerization of nonpolar 1-olefins using single-site catalysts such as metallocenes and related discrete nonmetallocene metal complexes.^[7]

The development process for catalysts being suitable for coordinative-anionic polymerizations has already been instigated several decades ago. Shortly after *Ziegler* and *Natta* received the Nobel Prize for their groundbreaking findings regarding the catalytic polymerization of nonpolar olefins in 1963, their catalysts were already employed for syndiospecific polymerization of methyl methacrylate (MMA) and for copolymerization of MMA with acrylonitrile (AN).^[8] However, active species, polymerization mechanism and degree of polymerization control were unknown and further attempts shared the issues of low activities and broadened dispersities.^[9] Two subsequent, independent communications reported in 1992 marked the beginning of the controlled/living polymerization of acrylic monomers using discrete metal complexes. These are seminal works of *Yasuda et al.* involving neutral, single-component lanthanocenes for living MMA polymerization and of *Collins* and *Ward* involving a two-component metallocene system for high-conversion polymerization of MMA, consisting of cationic zirconocenium complex as catalyst and neutral zirconocene as initiator.^[10,11]

The significant advances in the precision polymerization of polar vinyl monomers since 1992 are summarized in the following sections mostly by the examples of two important methods: On the one hand, the rare earth metal-mediated group transfer polymerization (REM-GTP) following a *Yasuda*-type mechanism, on the other hand, the more recently introduced and main group element-based *Lewis* pair polymerization (LPP).

2.1 Monomer Scope

By far, the most commonly used monomers for the coordinative-anionic polymerization are the (meth)acrylates, especially MMA. Acrylates polymerize two orders of magnitude faster than methacrylates, but the reactions show a living behavior only in rare cases. This issue is attributed to the lacking α -methyl group and the resulting deprotonation or migration of an initiating molecule to this position.^[12] Beside MMA, further methacrylates are of high interest due to promising possible applications. One of the most interesting examples in this context is furfuryl methacrylate. The reactive furfuryl substituent offers the possibility to cross-link the corresponding polymer *via* UV irradiation or to conduct post polymerization modification *via* [4+2] cycloaddition.^[13] Its beneficial properties such as a low shrinkage volume and the low reaction heat of polymerization make its corresponding polymer an ideal candidate for substituting materials like PMMA.^[14] The well-known *n*- and *t*-butyl methacrylates are already utilized for commercial materials and thereby in the focus of catalytic approaches.^[15] Nevertheless, there is a bunch of further monomers which exhibit a structural similarity to (meth)acrylates. The most important so-called *Michael*-type structures are depicted in Figure 1.

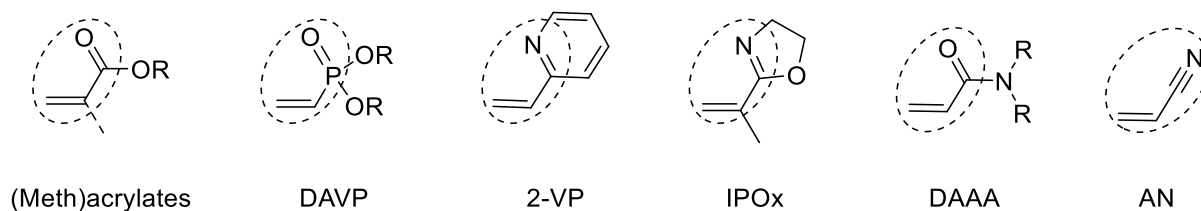


Figure 1. Structural motif of different *Michael*-type monomers.

Within this class, the poly(dialkyl vinylphosphonates) (PDVPP) have attracted much attention, especially due to their thermoresponsive behavior and access to poly(vinylphosphonic acid) (PVPA) through saponification. Due to the biocompatibility and low toxicity of these polymers, their use in biomedical fields is attractive, with applications as diverse as non-fouling coatings, tissue engineering, drug delivery systems, and cell proliferation surfaces.^[16] However, a well-controlled polymerization of DAVP is hard to establish, since radical and anionic synthesis routes often only lead to incomplete conversion of the monomers and provide materials with low molecular weights. Recently, it was shown that various REM-GTP catalysts constitute a superior alternative to the radical and anionic methods.^[17]

Block copolymers consisting of the mentioned DAVP with 2-vinylpyridine (2VP) help to tailor the lower critical solution temperature (LCST) and self-assemble to multi-responsive micelles.^[18] In addition to this, a variable design of the initiator molecule renders the synthesis of a biocompatible and water-soluble material which can be further functionalized for

biomedical application fields.^[19,20] Furthermore, the homopolymers of 2VP show a distinct pH sensitivity resulting in a wide range of applications and are well accessible with different polymerization methods.^[21] Noteworthy is also the regioisomer of 2VP, the non-classic *Michael*-monomer 4-vinylpyridine (4VP), which exhibits an extended unsaturated system. P(4VP) has not been accessible *via* GTP thus far, though the resulting polymer shows various promising application areas, for example as interface layer for organic solar cells.^[22]

A second monomer, whose polymerization also proceeds *via* a nitrogen-metal coordination, is 2-*isopropenyl*-2-oxazoline (IPOx). P(oxazolines) have already proven their beneficial properties in various applications in biomedicine.^[23,24] Whereas P2VP can be obtained at elevated temperatures *via* radical polymerization or at low temperatures using classic anionic polymerization methods, in case of IPOx, these methods lead to incomplete conversion or high polydispersities.^[17] Thus, this monomer offers potential for a specific catalyst design in coordinative-anionic procedures.

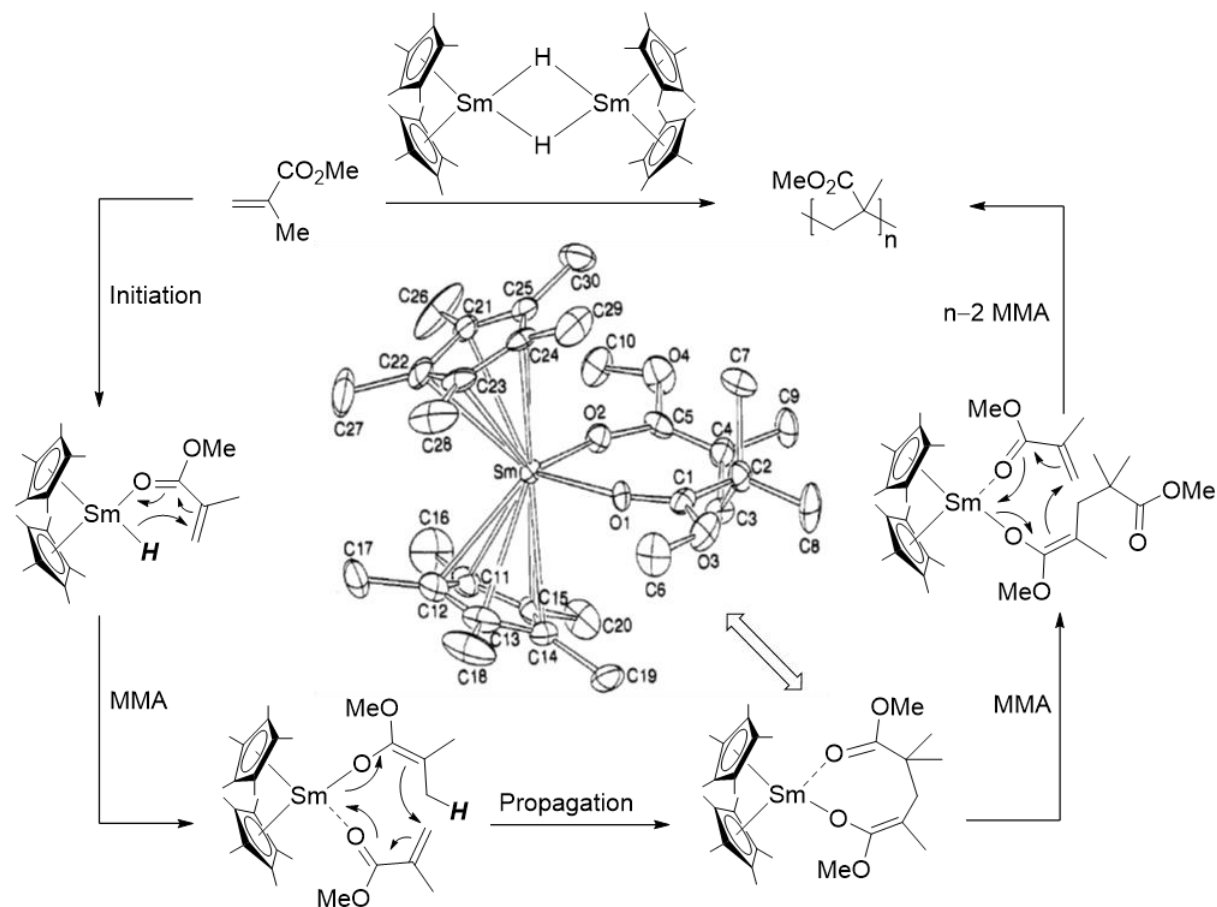
Further *Michael*-type monomers comprising a nitrogen atom are the *N,N*-dialkyl/aryl acrylamides (DAAA) that are well accessible with coordinative-anionic methods. The solubility and thermoresponsive behavior of DAAA vary depending on the hydrophobicity of the substituents at the amide groups. However, metalorganic catalysts are inactive toward polymerization of monosubstituted *N*-alkyl acrylamides. The origin of this problem can be found either in the presence of the slightly acidic amide hydrogen or in the formation of single addition products.^[25] Furthermore, the inability to polymerize *N,N*-dialkyl methacrylamides (DAMA) with coordinative-anionic approaches is noteworthy. The incompatibility is attributed to a twisted, nonconjugated monomer conformation between the vinyl and carbonyl double bonds, a result of steric repulsions between the α -methyl group or the vinyl proton and the *N*-alkyl group of DAMA. This twisted conformation results in a less effective π overlap between these two functional groups and thus leads to unstable amide enolate intermediates upon nucleophilic attack by the initiator. NMR studies show that chemical shifts and peak separations for the vinyl protons and carbonyl carbons of the nonpolymerizable DAMA more closely resemble those of nonconjugated vinyl monomers than those of polymerizable, conjugated monomers.^[26]

The last monomer within this class is AN which is of special importance. It is the only one containing a triple bond combined with a highly electron deficient structure and requires a specific treatment. Therefore, the properties of AN and its important polymer serving as precursor for carbon fibers are discussed in chapter 2.6 in greater detail.

2.2 Metal-mediated Group Transfer Polymerization

Almost ten years before the seminal works of *Yasuda et al.* and *Collins and Ward*, the term “group transfer polymerization” (GTP) was established by the group of *Webster*.^[27] They discovered a controlled polymerization of acrylic monomers by a silyl ketene acetal and a nucleophilic or *Lewis* acidic catalyst. The term “GTP” was initially based on the postulated associative propagation mechanism in which the silyl group remains bound to the same polymer chain and is transferred intramolecularly to the next monomer through hypervalent silicon anions. However, several lines of key experimental evidence now are more consistent with a dissociative mechanism, which involves an ester enolate as propagating species and a rapid, reversible complexation (termination) of small concentrations of enolate anions with a silyl ketene acetal or its polymer homologue.^[28]

Whereas the molar weights were limited to 20 – 30 kg/mol for these systems, the single-component metallocenes from *Yasuda et al.* were able to produce higher molecular weight PMMA with very narrow dispersities.^[11] The living and syndiospecific polymerizations were catalyzed by organolanthanide complexes like $[(Cp^*)_2SmH]_2$ (Scheme 2). To elucidate the



Scheme 2. Postulated mechanism and eight membered cyclic transition state, including the corresponding molecular structure, for the polymerization of MMA by *Yasuda et al.*^[11]

mechanism, 2:1 adduct of MMA and the catalyst was isolated and investigated with SC-XRD. Accordingly, initiation occurs *via* coordination of the carbonyl moiety of the first MMA molecule to the metal center and subsequent nucleophilic transfer of the hydride to the C-C double bond. A conjugated addition of the second monomer gives rise to the isolated transition state, bearing one MMA molecule in enolate- and the other in keto-form resulting in an eight membered cycle. Owing to the livingness of the lanthanocene-catalyzed polymerizations of both methacrylates and acrylates, Cp*₂SmMe(THF) was utilized for the successful synthesis of well-defined MMA-*n*-butyl acrylate (*n*BA) diblock copolymer as well as MMA(hard)-*n*BA (soft)-MMA(hard) triblock copolymers, which exhibited good elastic properties.^[29]

2.2.1 Nonbridged Catalysts

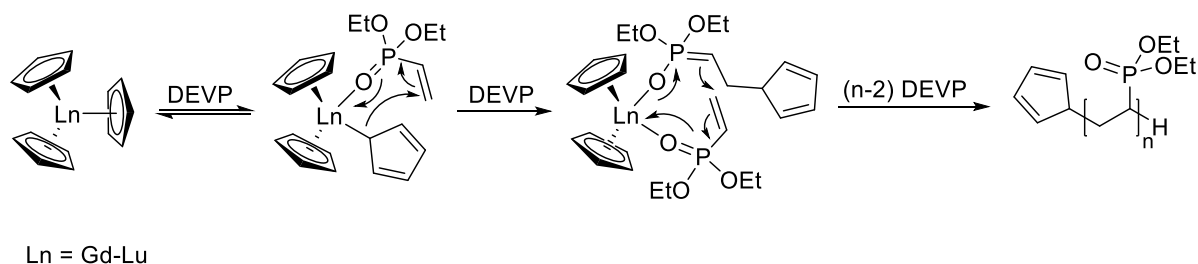
Methyl lanthanocenes, Cp*₂LnMe(THF), and AlMe₃ complexes of lanthanocenes, Cp*₂Ln(μ -Me)₂AlMe₂, behaved in a fashion similar to [Cp*₂SmH]₂ toward MMA and other methacrylates polymerization. The polymerization activity increases with an increase in ionic radii of the Ln metal (Sm > Y > Yb > Lu) within the series.^[30,31] Lanthanocenes incorporating amido ligands as initiators polymerized MMA to syndiotactic (*st*-)PMMA with varying molecular weight distributions, depending on metal and polymerization temperature. Polymerization activity and polymer tacticity remained comparable to those achieved by hydrido or hydrocarbyl initiating ligands. It is particularly noteworthy that even the divalent ytterbium homoleptic hydrocarbyl complex Yb[C(Me₃Si)₃]₂ is modestly active for MMA polymerization but produces highly isotactic (*it*-)PMMA with high molecular weight and a narrow dispersity at -78 °C.^[32] Further studies uncovered the relationship between the ligand structure and the microstructure of obtained PMMA when single component cationic zirconocenes were used. While MMA polymerization with [Me₂CCpIndZrMe(THF)][BPh₄] was highly isospecific at room temperature, using symmetric [Me₂CCp₂ZrMe(THF)][BPh₄] led to *st*-PMMA at low temperatures.^[33]

The MMA polymerization by lanthanocenes is typically carried out in toluene, but polar solvents including THF and Et₂O can also be used without noticeably influencing the polymerization results. This observation is notable because this is in sharp contrast to the classic anionic polymerization of MMA initiated by organometallic lithium reagents, where solvents are decisive for determining the tacticity of PMMA produced due to competition between counterion coordination to chain-end and monomer vs solvation.^[34]

Once more, *Yasuda et al.* established the catalysts with the highest activity and degree of control, when going beyond methacrylate polymerization. Trivalent lanthanocenes Cp*₂LnMe(THF) (Ln = Sm, Y) provided the solution for the challenge of a controlled

polymerization of α -acidic acrylates. These compounds remarkably catalyzed the extremely rapid and also living polymerization of alkyl acrylates to high molecular weights and narrow dispersities.^[29,35] The initiation and propagation mechanism for the acrylate polymerization was thought to proceed in the same fashion as described for the methacrylate polymerization. The acrylate polymerization catalyzed by lanthanocenes is considerably faster than the methacrylate polymerization by the same catalysts, achieving high monomer conversions and high initiator efficiencies in seconds. The apparent rate of acrylate polymerization increases with an increase in the steric bulk of the acrylate R group in the order $n\text{Bu} > \text{Et} > \text{Me}$, presumably due to the electronic effect of the alkyl group, in contrast to methacrylates.^[30,31]

The very similar complexes of the Cp_2LnX type were introduced for the polymerization of DAVP by *Rieger et al.*^[36] The initiation can proceed either *via* abstraction of the acidic α -CH of the vinylphosphonate (e.g., for $\text{X} = \text{Me}, \text{CH}_2\text{TMS}$), *via* nucleophilic transfer of X to a coordinated monomer (e.g., for $\text{X} = \text{Cp}, \text{SR}$) or *via* a monomer-induced ligand-exchange reaction forming Cp_3Ln in equilibrium (e.g., for $\text{X} = \text{Cl}, \text{OR}$), which serves as the active initiating species (Scheme 3).^[37]



Scheme 3. GTP of diethyl vinylphosphonate (DEVP) catalyzed by lanthanide complexes.

The REM-GTP of DAVP showed a living behavior in contrast to anionic and radical methods, resulting in narrow molecular weight distributions and easily adjustable molecular weights. Additionally, this enabled the synthesis of block copolymers in consideration of the relative coordination strength to the metal center, and thus smart materials with a tailored thermoresponsivity.^[24]

Besides the commonly employed metallocenes, *Mashima et al.* showed that en-diamido (en = ethylenediamine) yttrium catalysts are well suitable for the controlled polymerization of 2VP.^[38] The idea of non-metallocene compounds was taken up by the group of *Rieger* and ensured for further expansion of the monomer scope. The recently developed $(\text{ONOO})^{\text{R}}\text{Y}(\text{CH}_2\text{TMS})(\text{THF})$ catalysts were active for the precision polymerization of DAVP, 2VP, IPOx and *N,N*-dimethyl acrylamide (DMAA).^[39]

2.2.2 Bridged Catalysts

The controlled and, in addition, highly isospecific synthesis of PDMAA was already presented by *Chen* and *Mariott* in 2004.^[40] This living and rapid polymerization also provided access to P(*N,N*-diaryl acrylamides) and was catalyzed by the racemic zirconocenium ester enolate cation *rac*-(EBI)Zr⁺(THF)[OC(OiPr)=CMe₂][MeB(C₆F₅)₃]⁻ under ambient conditions (Figure 2). The isospecific nature of this catalyst toward the polymerization of both methacrylates and acrylamides enabled the synthesis of the well-defined isotactic PMMA-*b*-PDMAA stereodiblock copolymer.^[41] This was by far not the first use of an *ansa*-metallocene in the polymerization of *Michael*-type monomers. A multitude of bridged lanthanocenes were reported to be suitable for the conversion of MMA, mainly applied to control the stereoregularity of PMMA. Even though most of them showed a high stereospecificity, the activities were low and the polymerizations proceeded rather uncontrolled with respect to molecular weight distribution and initiator efficiency.^[42] To overcome this issue, it is worthwhile looking at *ansa*-zirconocenes and bridged, nonmetallocene REM complexes (Figure 2).

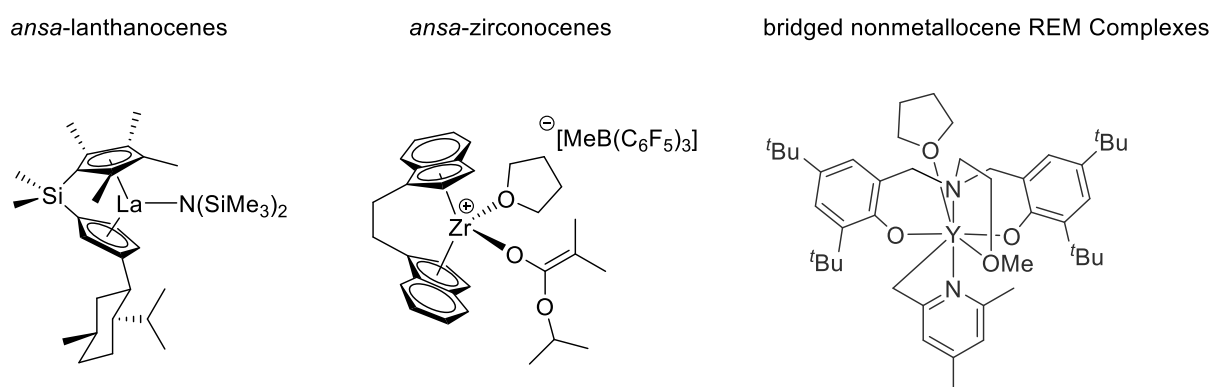


Figure 2. Illustrative catalysts for the isospecific polymerization of *Michael*-type monomers.

Bolig and *Chen* applied the beforementioned preformed cationic zirconocenium ester enolate, an *ansa*-C_{2v}-ligated catalyst, in the highly isospecific polymerization of MMA.^[43] This structure simulates the proposed active propagating species, thus in essence bypassing the slow chain-initiation step. Therefore, it not only significantly enhances the polymerization activity and initiator efficiency compared to the methyl-based catalyst, it also enables a living and well-controlled polymerization process. Furthermore, *ansa*-C₁-ligated zirconocenes exhibited a comparable isospecificity, whereas *ansa*-C_s-ligated zirconocenes were found to produce highly *st*-PMMA.^[44,45]

In the area of bridged, nonmetallocene REM complexes, it was discovered that highly *it*-PMMA can be produced by a bis(pyrrolylaldiminato)samarium hydrocarbyl complex at 0 °C.^[46] This complex displays molecular C₁ symmetry with the two pyrrolylaldiminato ligands adopting an

approximate C_2 arrangement. A racemic, *trans*-1,2-diaminocyclohexane-bridged bis(iminophosphonamido)yttrium complex also catalyzed isospecific MMA polymerization.^[46,47] The group of *Rieger* reported on a toolbox of nonmetallocene lanthanides, which can be utilized as highly active and isospecific catalysts for the precise REM-GTP of DMAA.^[48]

An additional well-known type of catalyst for stereospecific polymerizations are the so-called constrained geometry complexes (CGC). These half-sandwich metal complexes incorporating linked Cp amido ligands have been employed very successfully, even for commercial purposes, in the (co)polymerization of nonpolar olefins using group 4 metals. This concept was prolifically transferred to polar monomers, in particular to MMA. A cationic CGC zirconocenium ester enolate complex afforded highly isotactic PMMA at low temperatures (Figure 3).^[49] Unlike the isostructural, cationic (CGC)Zr alkyl complex, which is inactive for MMA polymerization at high or low temperatures, the cationic Ti alkyl complex effected living and syndiospecific (co)polymerization of MMA with acrylates and methacrylates at ambient temperature.^[50] The corresponding chiral cationic (CGC)Ti ester enolate complex, which simulates the structure of the active propagating species, behaved similarly to that of the (CGC)Ti alkyl complex. On the other hand, *Carpentier et al.* found that the Ti alkyl complex effectively catalyzed polymerization of *n*-butyl acrylate with higher TOFs, producing polymers with a broader dispersity and a similar syndiotacticity compared to PMMA.^[51] The moderately active Yttrium alkyl complexes of CGC type polymerize *tert*-butyl acrylate to median molecular weight, atactic polymers.^[52] Quantitative monomer conversion was achieved only at low monomer to catalyst ratios.

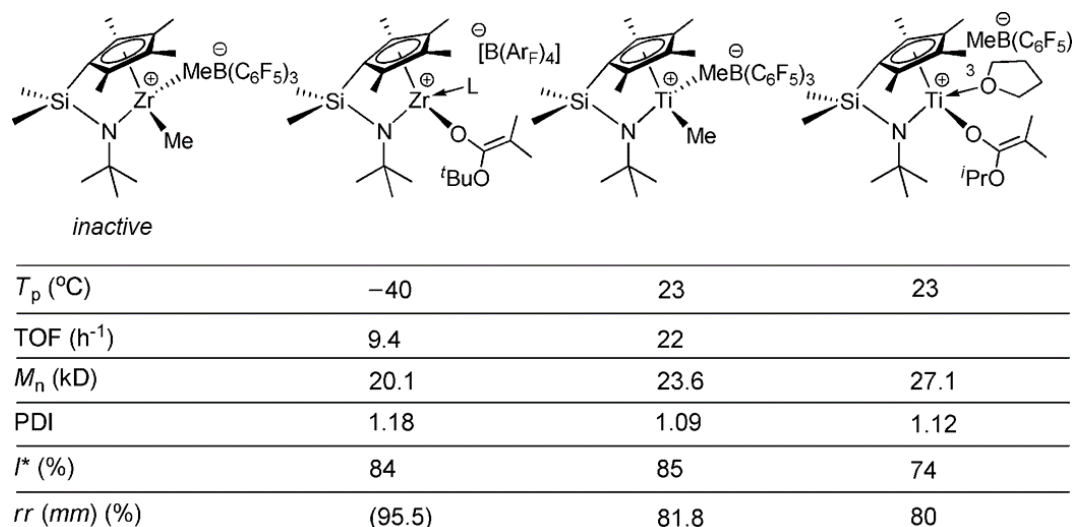
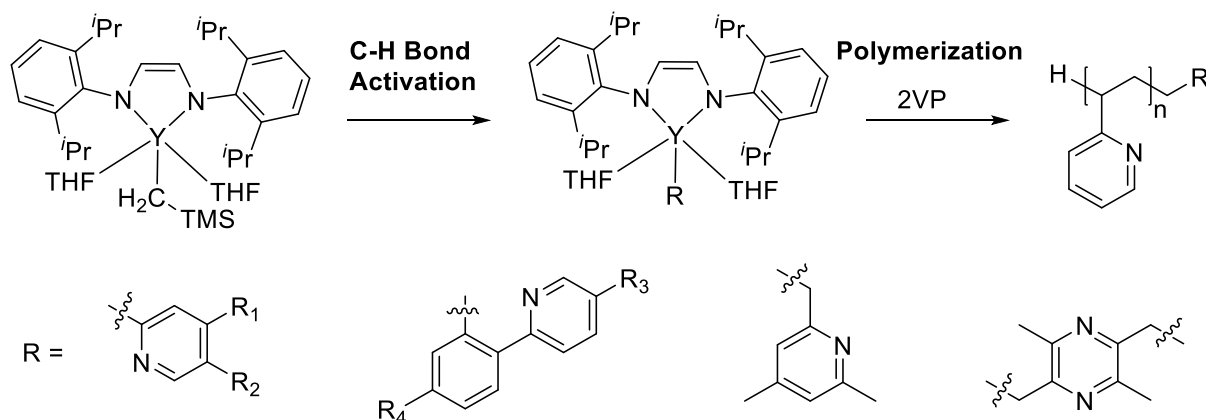


Figure 3. Characteristics of the MMA polymerization by group 4 CGC (modified and reprinted).^[2]

2.2.3 C-H Bond Activation

Besides the well-known salt metathesis route, the lanthanide catalysts can be synthesized by C-H bond activation. These $[2\sigma+2\sigma]$ cycloaddition reactions are one of the most effective tools in metalorganic chemistry for the cleavage of otherwise unreactive C-H bonds. After the first C-H activation for a lutetium complex presented in 1983, a wide range of catalysts were developed with this method.^[53]

The aforementioned yttrium-en-amido catalysts of *Mashima and coworkers* were prepared *in-situ* by σ -bond metathesis. After the successful C-H-bond activation of a variety of alkynes and heteroaromatic compounds such as 2,4,6-trimethylpyridine (*sym*-collidine), 1-trimethylsilyl-1-propyne, or 2,3,5,6-trimethylpyrazine, the easily accessible catalysts were tested in the polymerization of 2VP. Thereby, end-capping functional groups were introduced to P2VP combined with a well-controlled polymerization behavior (Scheme 4).^[38] Further nonmetallocene catalysts became more efficient in the polymerization of DEVP and DMAA after being activated with similar heteroaromatic initiators.^[48]



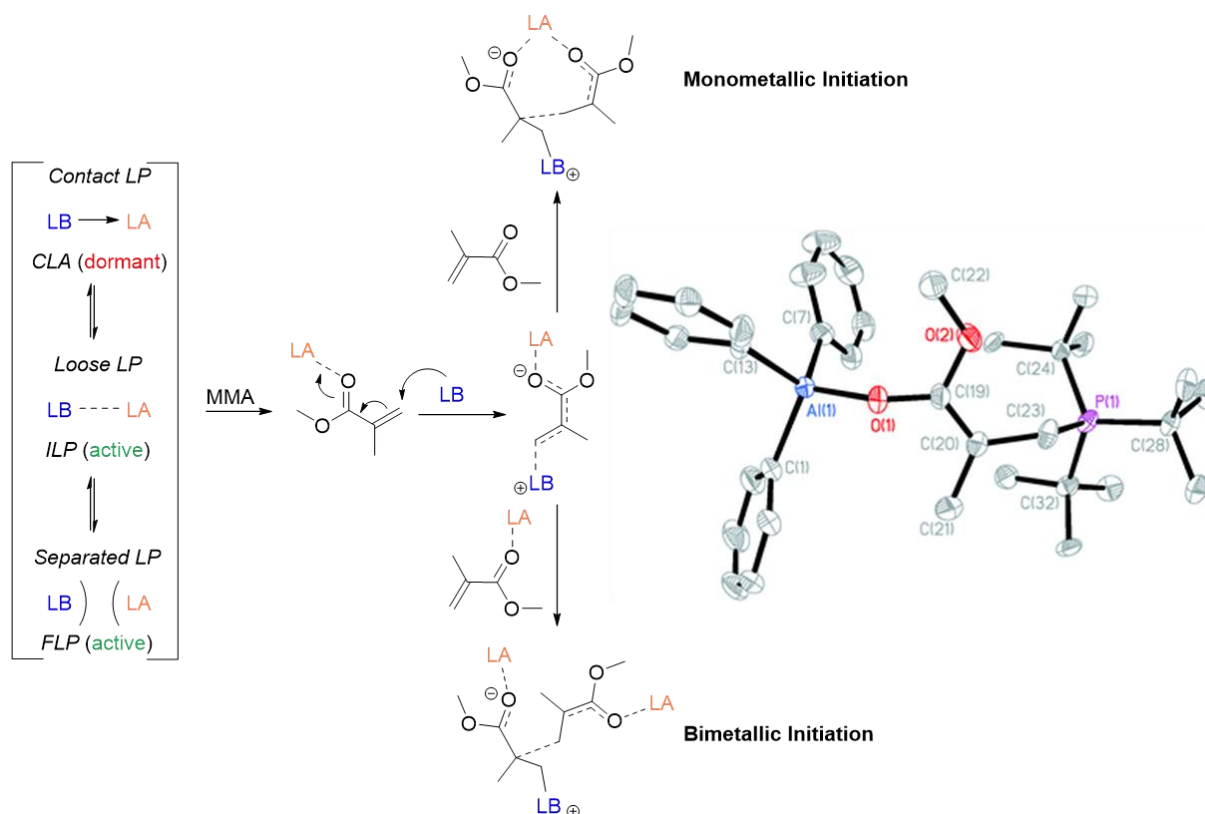
Scheme 4. Polymerization of 2VP with C-H-bond activated pyridyl-yttrium-en-diamido complexes.^[38]

Also for the polymerization of vinylphosphonates, *Rieger et al.* evidenced that C-H bond activated heteroaromatic initiators of lanthanide complexes outperform strongly basic alkyl initiators. Thus, side reactions like the deprotonation of the α -acidic DAVP could be avoided and the initiator efficiencies were increased.^[54] In addition, the same group applied three-fold C-H bond activation of 1,3,5-tris(3,5-dimethyl-4-pyridinyl)benzene with $\text{Cp}_2\text{YCH}_2\text{TMS}(\text{thf})$ to yield a trinuclear catalyst which enabled the fast synthesis of starshaped PDEVp and PIPOx structures.^[55] With a proficiently chosen design of the heteroaromatic initiator molecules, fluorescent as well as biocompatible PDAVP conjugates can be produced *via* initial σ -bond metathesis.^[19,20,56] Thereby, the fundamental precision polymerization of *Michael*-type monomers can be connected with tailor-made functions in biomedical applications.

2.3 Lewis Pair Polymerization

The beginnings of the *Lewis* pair polymerization (LPP) can be traced back to 1960, as a mixture of Et_3Al and PEt_3 (in a 2:1 ratio) was used for the polymerization of MMA with only marginal activity.^[57] In the following 50 years, a few additional approaches were presented in the literature without a resounding success.^[58,59] The common issues of these early examples can be summarized with the following points: 1. LPs were based on simple aluminum alkyls forming strong classical *Lewis* adducts (CLA), which result in a low activity; 2. The roles of *Lewis* acid (LA) and *Lewis* base (LB) were not understood in the polymerization system; 3. The polymerization mechanism was unclear.

In 2010, *Chen et al.* introduced the concept of frustrated *Lewis* pairs (FLP) and CLAs to the fields of polymerization catalysis.^[5] It was the uncovering of the first highly active and efficient polymerization of MMA with the strong and sterically encumbered LA $\text{Al}(\text{C}_6\text{F}_5)_3$ in combination with sterically demanding LBs like PtBu_3 or *N*-heterocyclic carbenes (NHCs). The LPP was proposed to proceed *via* a zwitterionic enoaluminate active species, formed in the initiation step through a nucleophilic attack of the LB onto MMA activated by the LA $\text{Al}(\text{C}_6\text{F}_5)_3$



Scheme 5. Illustrative example of the LPP of MMA by a CLA, an Interacting *Lewis* Pair (ILP), or FLP, showing a generic chain initiation step to generate the zwitterionic active species, evidenced by a SC-XRD analysis for $\text{Al}(\text{C}_6\text{F}_5)_3/\text{PtBu}_3$, and the two possible subsequent steps.^[60]

(Scheme 5).^[60] The next step can involve a nucleophilic attack of a non-activated (monometallic) or LA-activated (bimetallic) MMA by this zwitterion. Whereas *Chen et al.* only presented inconsistent theoretical and experimental data, the group of *Rieger* was able to corroborate the bimetallic mechanism in 2016.^[6]

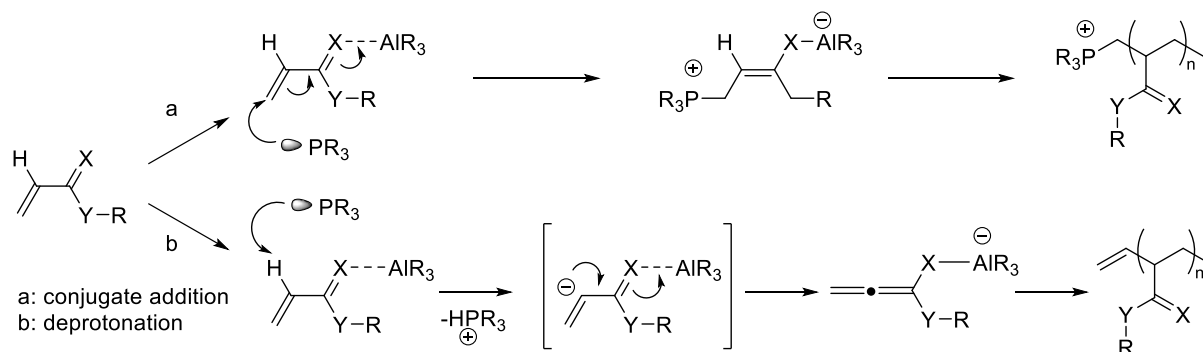
Again, *Chen and coworkers* extensively investigated the scopes of LA and LB and thereby, expanded the range of monomers to DMAA, 2VP, DEVP, IPOx and cyclic acrylic monomers.^[60] Additionally, they examined the chain termination mechanism for the LPP of methacrylates *via* a combined experimental and theoretical study, which revealed two chain termination pathways that compete with chain propagation cycles.^[61] However, the lack of a living polymerization behavior caused by these termination reactions was not the only drawback of the LPP method, since in most cases the initiator efficiencies were low (< 30%) and the dispersities broader (< 1.4) than expected for a precision polymerization. To overcome these issues and thus develop a controlled and living LPP, three different strategies have been explored.

The first strategy by *Hong et al.* replaced the strong *Lewis* acid $\text{Al}(\text{C}_6\text{F}_5)_3$ with the sterically encumbered, less acidic $\text{MeAl}(\text{BHT})_2$ (BHT = 2,6-di-*tert*-butyl-4-methylphenolate) which was proposed to suppress backbiting termination.^[62] Indeed, the MMA polymerization was found to be more controlled with this *Lewis* acid in combination with selected NHCs, which additionally exhibited higher initiator efficiencies. Nevertheless, the screening of the LA scope showed that $\text{MeAl}(\text{BHT})_2$ is unique for controlled LPP, while less sterically hindered or stronger LAs led to either less control or lower activity.

The second approach utilized the same LA, but in combination with N-heterocyclic olefins (NHO) to generate a non-interacting, true FLP catalytic system, enabling the suppression of both LA-induced chain termination and LB-induced reactivity quenching side reactions.^[63] The high to quantitative initiator efficiencies facilitated the synthesis of di- and triblock copolymers of diverse methacrylates with very narrow molecular weight distributions on a short time scale.

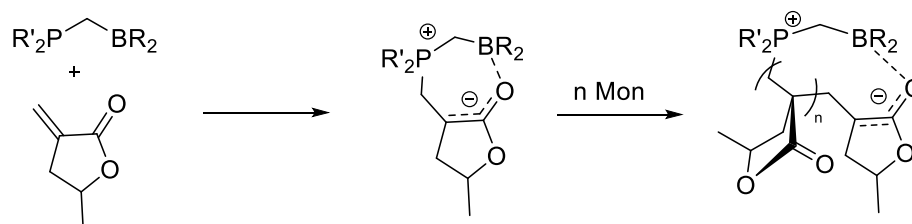
The last and more versatile strategy was presented by *Rieger et al.* when employing highly interacting LPs or CLAs comprising weaker LAs (simple aluminum alkyls and AlPh_3) and weaker LBs with less steric hindrance.^[6] The *Lewis* acidity and basicity as well as steric effects of the LB were quantified by the fluoride ion affinity index, protonation energy in the reaction with $\text{F}_3\text{CSO}_3\text{H}$ and *Tolman* angle, respectively. Based on this classification, a highly active and living method was established to produce well-defined polymers of methacrylates, DMAA, DEVP and even of the extended system 4VP. End group analysis of P4VP oligomers revealed

a phosphine chain end group, demonstrating the conjugate addition mechanism *via* the double-bond activation, which can be achieved even over several bonds. However, the end group analysis of PDEVp indicated two different series of masses, which were proposed to be caused by conjugate addition pathway **a** and deprotonation pathway **b**, leading to an active species with a cumulated double bond (Scheme 6). These common side reactions for α -acidic monomers, induced by a more basic phosphine, led to a slightly broadened dispersity, supporting the proposed competition of the two initiation mechanisms.



Scheme 6. Possible mechanisms of the initiation process for the LPP of α -acidic monomers.

The more user-friendly $B(C_6F_5)_3$ -based LPs were also tested for the polymerization of the cyclic and renewable γ -methyl- α -methylene- γ -butyrolactone (γ MMBL) by *Chen* and *Xu*.^[64] A surprising activity trend was observed when using a series of intermolecular and bridged P/B LPs (BLP). Counterintuitively, the CLA of $B(C_6F_5)_3$ with PPh_3 exhibited the highest activity with the drawback of multimodal molecular weight distributions, whereas intermolecular and bridged true FLPs were inactive. Hence, the most active system comprises a good compromise between B site acidity, P site basicity, steric crowding around P, and the strength of the P–B association in solution. Monomodal, but broader dispersities were achieved with methylene, ethylene and propylene bridged LPs. For the methylene linked BLP, a stoichiometric mixture with the monomer resulted in immediate formation of a cycloaddition intermediate, namely a zwitterionic phosphonium enolborate (Scheme 7). End group analysis of $P\gamma$ MMBL oligomers suggested that the propagation occurred *via* repeated conjugate addition.



Scheme 7. Postulated pathway for the polymerization of γ MMBL catalyzed by bridged LP.

2.4 Analysis of the Tacticity

The degree of stereoregularity of a polymer determines its thermal properties, such as melting-transition temperature (T_m) and glass-transition temperature (T_g). Stereoregular polymers are semi-crystalline materials, thus usually exhibiting both T_m and T_g , whereas their atactic (*at*), amorphous counterpart shows only T_g . In general, the physical and mechanical properties of the polymers having stereogenic centers in the repeating units depend largely on their stereochemistry.^[65] Crystallinity leads to superior material properties, such as enhanced solvent resistance, high modulus, as well as excellent impact strength and fatigue resistance.

Besides the thermal properties, there are several further techniques for determining the type of tacticity and degree of stereoregularity of a polymer sample. Commonly used methods include solubility, X-ray diffraction and IR spectroscopy. In the case of chiral polymers, optical rotation can be used to determine the absolute configuration as well as the degree of enantiomeric purity when the optically pure polymer is available. However, the most feasible method for classifying tacticity as well as quantifying a polymer's stereochemical purity is NMR. In many cases, the shifts for the various polymer nuclei are sensitive to adjacent stereogenic centers, resulting in fine structure that can provide quantitative information about the polymer microstructure once the shift identities are assigned.^[66,67] For example, ^{13}C NMR spectra showing the carbonyl region of PMMA significantly depend on the microstructure of the polymers: Highly *st*-PMMA produced by an *ansa*- C_s -ligated zirconocene shows a comparatively simple signal pattern,^[44] whereas 24 peaks can be found for the anionically synthesized (*at*-)PMMA (Figure 4).^[68]

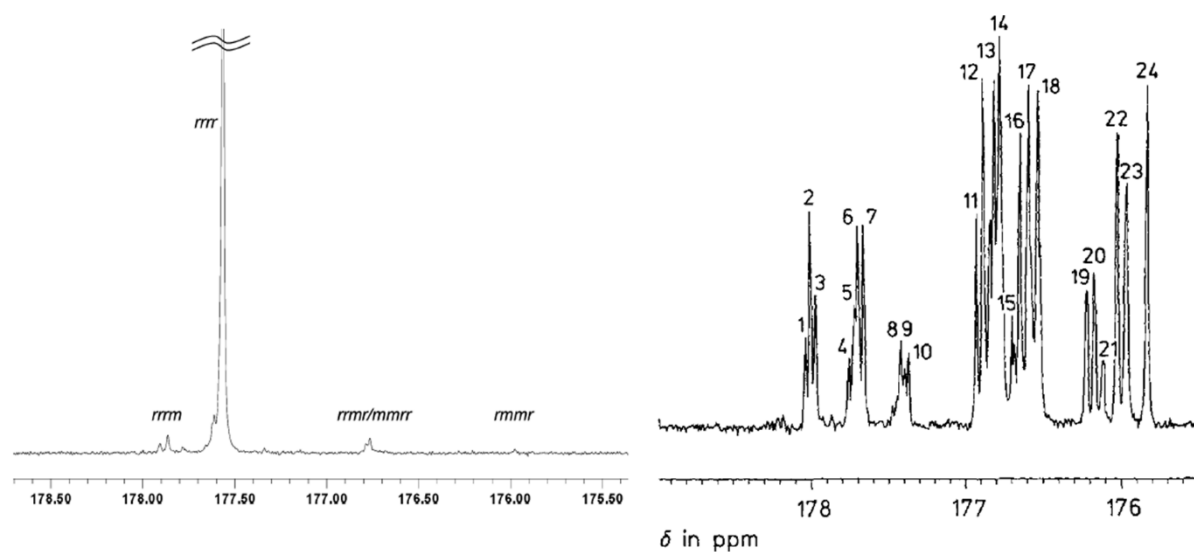


Figure 4. ^{13}C NMR spectra showing the carbonyl region of *st*- (left) and *at*- (right) PMMA.^[44,68]

Stereosequences based on the configuration of consecutive methine carbons and resulting in stereoregular or stereoirregular arrangements characterize the microstructure. Depending on the relative configuration of adjacent monomer pairs (diads), *meso* (*m*, same configuration) and *racemic* (*r*, opposite configuration) diads are distinguished as shortest stereosequences. Considering also the next nearest neighbor correlations complicates the stereochemical configuration assignments which is illustrated in Figure 5 on the left. The methylene protons in the middle of a *r* diad are expected to be magnetically equivalent due to their similar environment, while those in the middle of a *m* diad are nonequivalent. Hence, the ^{13}C methylene resonances of three tetrads, (*rrr*, *mrr* and *mrm*) are expected to have correlations to a single proton while the other three tetrad resonances, *mmm*, *mnr* and *rmr*, are expected to be correlated to two magnetically nonequivalent protons. As a result, the latter three ^{13}C resonances - *mmm*, *mnr* and *rmr* - show doublets in their single bond correlations to protons. It should be noted that the methylene proton resonances of *mrr* may show some nonequivalence since the protons are asymmetric with respect to the next nearest neighbor methine groups.^[69]

Using 2D NMR techniques is a powerful tool to observe and assign these correlations and after a first, scientifically reliable assignment (qualification) 1D NMR spectra are applied for the quantification. For example, the stereosequences of the aforementioned *at*-PMMA were investigated with a ^{13}C - ^1H COSY experiment by Kawamura *et al.* (Figure 5, right).^[68] The proton chemical shifts of the tetrads were determined from the ^1H - ^1H COSY spectrum, taking into consideration the more downfield shifted proton tetrad signals with increasing chemical shift differences from *mmm* to *rmr*.^[66] The expected doublets of the *m*-centered ^{13}C resonances are well identifiable. It is seen in the ^{13}C region that the *rrr*-centered tetrads overlap with the *rmr*-centered tetrads, and the *mrm*-centered tetrads shift higher up-field than the methoxy carbon absorption.

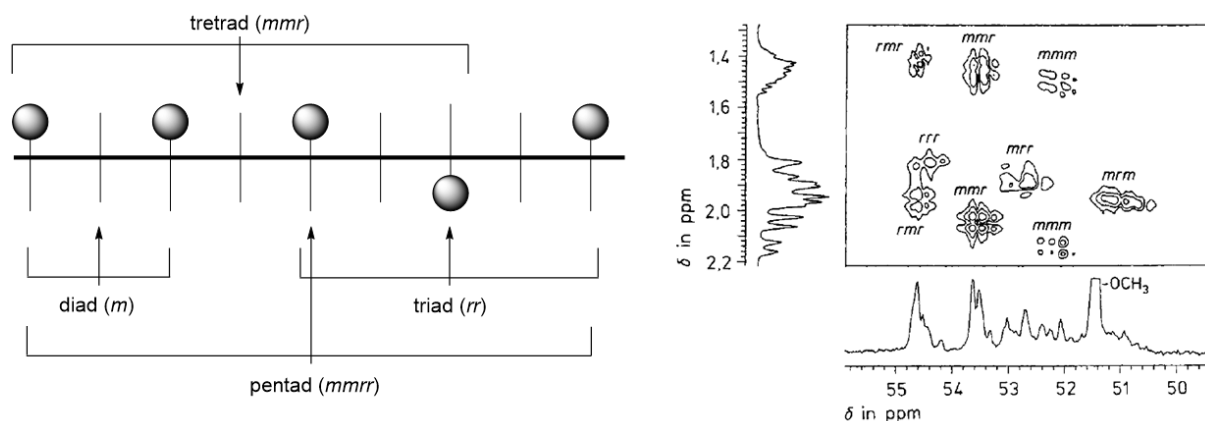


Figure 5. Left: A schematic representation of through-bond connectivities of stereosequences. Right: ^{13}C - ^1H COSY spectrum of the methylene region of *at*-PMMA.^[68]

In the case of PDMAA, the stereosequences of the specially synthesized dimer of DMAA were investigated for modeling the diad sequences in the homopolymer chains.^[70] After a detailed NMR study of this compound using 2D HETCOR spectroscopy (two-dimensional heteronuclear (^{13}C - ^1H) correlation) and the INEPTLR (long range insensitive nuclear enhanced by polarization transfer) experiment, the results facilitated the assignment of the diads for the carbonyl region of PDMAA. Whereas the polymers in this study were dissolved in CDCl_3 giving complicated, overlapped splitting patterns in the ^1H spectra, *Okamoto et al.* found that the methylene protons of PDMAA show a peak splitting pattern similar to those of polyacrylates by ^1H NMR measurement in DMSO-d_6 at a high temperature ($100\text{ }^\circ\text{C}$).^[71] The methylene proton peaks are split into three parts due to the main chain's stereochemistry. Thus, downfield *meso*, *racemic*, and upfield *meso* signals were clearly separated from the other peaks. The *group of Rieger* utilized both methods to quantify the isotacticity of PDMAA produced by their toolbox of bridged nonmetallocene lanthanides (Figure 2, 6).^[48]

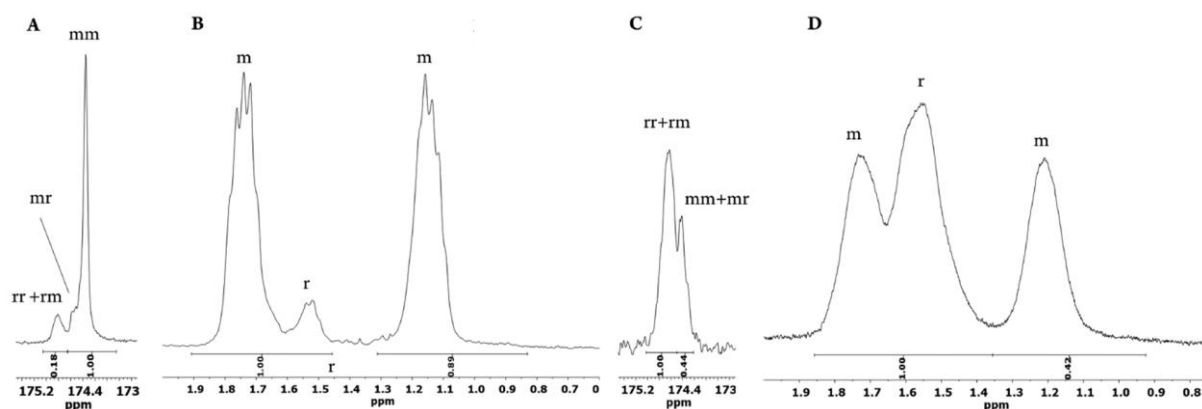


Figure 6. Carbonyl region of the ^{13}C NMR spectra (CDCl_3 , $25\text{ }^\circ\text{C}$) of *it*-(**A**) and *at*-(**C**) PDMAA. Backbone methylene signal in the ^1H NMR spectra (DMSO-d_6 , $140\text{ }^\circ\text{C}$) of *it*-(**B**) and *at*-(**D**) PDMAA.^[48]

A noteworthy method for the analysis of the tacticity was established for 2VP as a further *Michael*-type monomer. *Matsuzaki and coworkers* synthesized 2VP- $\beta,\beta\text{-d}_2$ and conducted the respective NMR measurements with deuterium decoupling in the 1970s.^[72] From the ^1H NMR spectra of nondeuterated polymer, only the fraction of isotactic triad could be obtained, while the ^1H NMR spectra of deuterated polymers showed no more overlapping signals and revealed triad tacticity. Later, they transferred this concept beneficially to ^{13}C signal assignments and to the regioisomer 4VP.^[73] Even after 50 years, these contributions are used to investigate the stereosequences of P2VP/P4VP, now tailor-made by coordinative-anionic approaches.^[74]

The tacticity analysis becomes more complicated for *Michael*-type monomers containing NMR active nuclei like phosphorus. The 100% natural abundance and high NMR sensitivity of ^{31}P causes scalar phosphorus proton ($^nJ_{\text{PH}}$) and phosphorus carbon ($^nJ_{\text{PC}}$) couplings, which vary

between ~ 135 Hz for one bond between phosphorus and carbon ($n = 1$) and 5-20 Hz for ${}^{2/3}J_{\text{PH}}$ and ${}^{2/3}J_{\text{PC}}$ also depending on stereochemistry, and made the study of poly(dimethyl vinylphosphonate) (PDMVP) more difficult.^[75] The separation of phosphonic ester groups on the polyvinyl backbone by only four bonds causes each proton or carbon to experience scalar couplings with two or three phosphorus atoms each, resulting in line broadening or splitting depending on the magnitude of the scalar couplings. Nevertheless, *Komber et al.* could distinguish three regions in the ${}^1\text{H}$ - ${}^{13}\text{C}$ HMQC spectrum (Figure 7, left). Region A covers the methylene group signals for which the resonances of the carbons can be defined with the before presented principle of equivalent and nonequivalent protons and with the characteristic trends in chemical shifts and their increasing differences. This assignment was confirmed by the TOCSY correlations with the methine protons (Figure 7, right). The analysis of the methine group signals (region B) showed a partial overlap of methine and methylene carbon signals. Besides, at least two methine proton as well as carbon signals could be distinguished, but the separations were superimposed by scalar phosphorus couplings. The direct couplings of the methine proton signals with the neighboring methylene groups facilitated the triad assignments in the TOCSY spectrum. The signals of the third region C originated from head to tail regioirregular structures which were caused by the applied radical polymerization. The catalytic precision polymerization of PDAVP is a very recent topic and no pronounced stereospecificity has been achieved up to now.

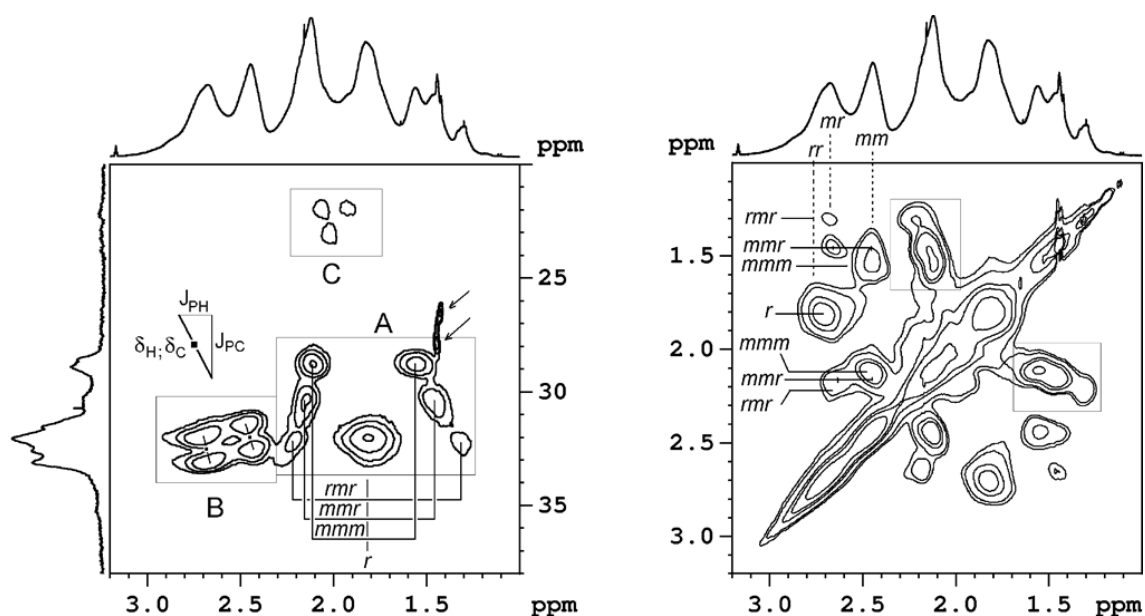


Figure 7. ${}^1\text{H}$ - ${}^{13}\text{C}$ HMQC and TOCSY (mixing time 20 ms) spectra of *at*-PDMVP in MeOD_4 .^[75]

The advent of 2D NMR greatly facilitated the characterization of stereosequences in polymers by providing better resolution and atomic connectivity information. However, due to severe

signal overlap in the case of some polymers, even 2D NMR cannot ensure sufficient resolution for unambiguous resonance assignment. 3D NMR structure characterization could provide additional information about distinct structure–property relationships which is already widely used in biological applications. Unfortunately, the same structural uniformity does not exist for non-biological applications of 3D NMR. The diversity of structures in these fields requires the use of unique instrument settings, and in some cases unique pulse sequences, to produce useful NMR data in each class of compounds to be studied. In formulating a suite of 3D NMR experiments to study structures in these diverse areas, the nature of the isotopes present and the magnitude of one-bond and multiple-bond couplings must be considered. Thus, triple resonance NMR investigations are scarcely applied in polymer chemistry.^[76]

One scholarly presented example was the characterization of the stereosequences in poly(vinyl fluoride) (PVF) using $^1\text{H}/^{13}\text{C}/^{19}\text{F}$ Triple Resonance NMR.^[77] The 3D NMR pulse sequence used by *Rinaldi and coworkers* was based on single quantum coherence transfer, which eliminated the complicated splitting patterns resulting from evolution of multiple-quantum coherence. In addition, selective excitation of the ^{19}F significantly reduced the folding of peaks from other spectral regions. This greatly simplified the spectra and made the assignment of resonances much easier. By performing a closer investigation of the H-C slices of the 3D spectrum, the resonances of both carbons are correlated with two nonequivalent protons for $\delta_{^{19}\text{F}} = -179.1$ ppm (Figure 8). Therefore, the ^{19}F between these methylene groups must exist in *mm* triads. According to this example, the carbon resonances could be assigned to the corresponding triads. Due to better dispersion in the ^{19}F dimension, it was possible to assign the signals of CFH-centered sequences to the pentad level. These data were obtained in relatively short experiment times (ca. 11 h) and provided unequivocal atomic connectivity information for studying the microstructures of PVF.

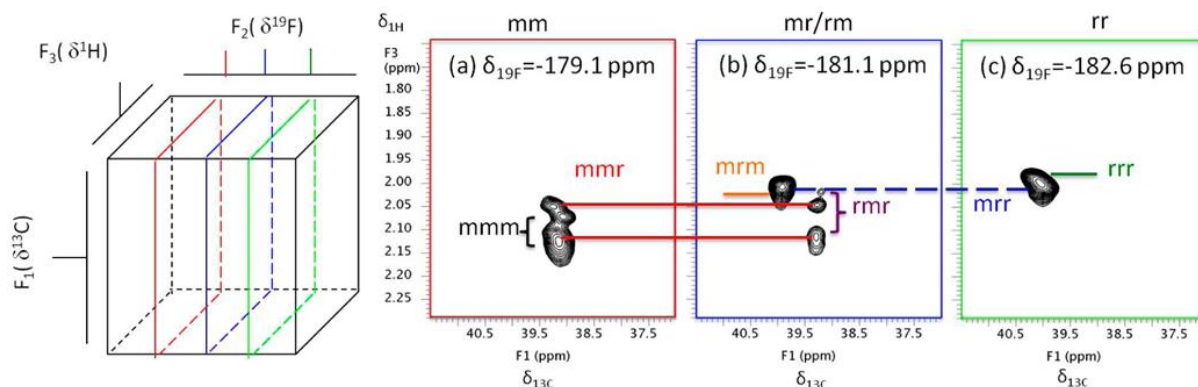
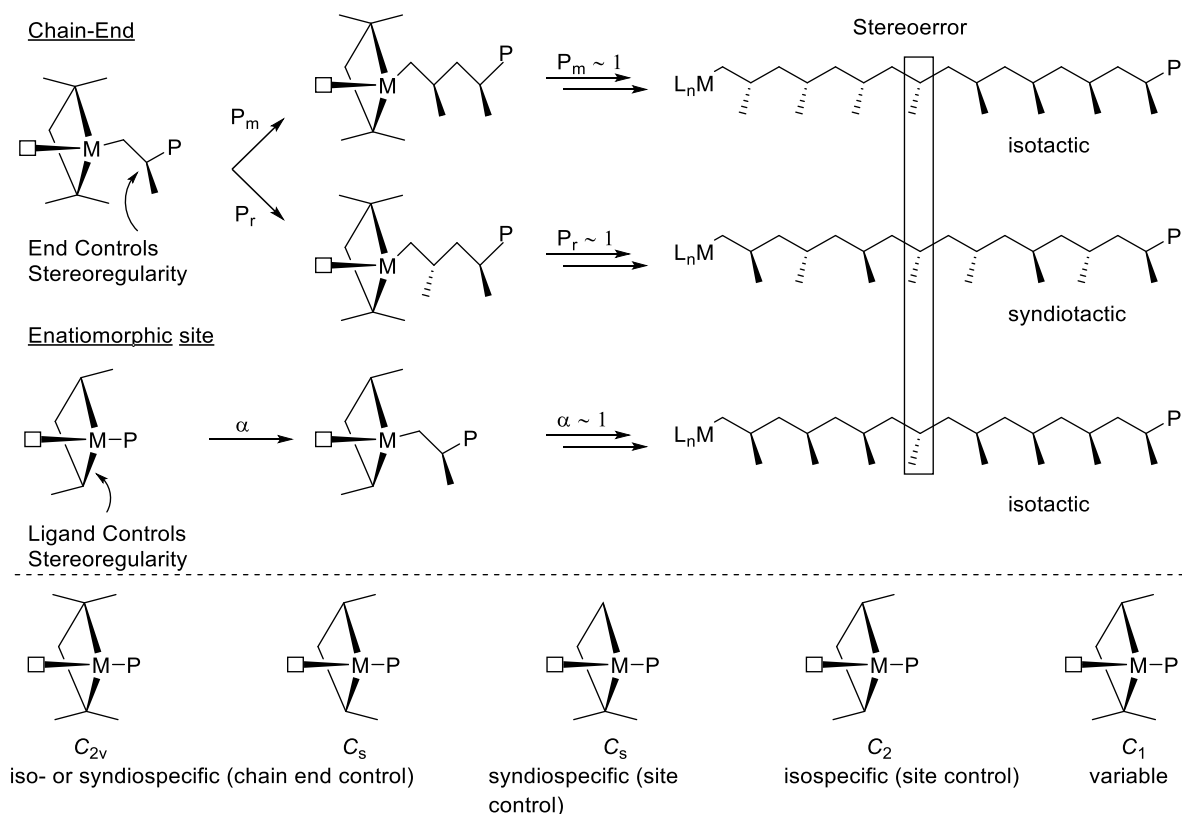


Figure 8. Low resolution H–C planes from the $^1\text{H}/^{13}\text{C}/^{19}\text{F}$ 3D NMR spectrum of PVF in DMSO at 110 °C.^[77]

2.5 Stereocontrol Mechanisms

Both the ligand sphere of a single-site catalyst and the growing polymer chain influence the stereochemistry of polymerization reactions.^[78] It is noteworthy that, unlike the catalytic synthesis of small molecules, during a chain-growth polymerization reaction a polymer chain remains bound to the active metal center during monomer enchainment. Thus, the stereogenic center from the last enchainment monomer unit will influence the stereochemistry of the following monomer addition. If this influence is significant, the mode of stereochemical regulation is referred to as “polymer chain-end control” (Scheme 8). It should be noted that in rare instances more than one stereogenic center of the chain can play a significant role. The parameters P_m and P_r refer to the probability of m and r placements, respectively. A P_m equal to unity indicates isotacticity, while a P_r equal to unity signifies syndiotacticity. Chain-end control can be statistically described by the *Bernoulli* and *Markov* model, respectively.^[79] The *Bernoulli* model assumes only an influence of the last monomer unit and therefore, enables the determination of probabilities for triad as well as pentads ($\frac{4(mm)(rr)}{(mr)^2} = 1$ for the isotactic case). The *Markov* model additionally takes the influence of the penultimate unit into consideration ($\frac{4(mmmm)(rmmr)}{(mmr)^2} = 1$ and $\frac{4(mrrm)(rrrr)}{(mrr)^2} = 1$ for the isotactic case).



Scheme 8. Chain-end and enantiomeric site mechanisms of stereocontrol and the stereoselectivities of different catalyst symmetries.^[80]

If the ligand set is chiral and overrides the influence of the polymer chain end, the mechanism of stereochemical direction is termed “enantiomorphic site control” (Scheme 8). The parameter α represents the degree of enantiotopic selectivity of the enchainment. When α is either 1 or 0 an isotactic polymer forms, while an α parameter of 0.5 produces an atactic polymer. The criteria for the isotactic case of this mechanism are $\frac{2(rr)}{(mr)} = 1$ and $1 - \frac{4}{(mr)+2(rr)} - \frac{1}{(rr)} = 1$. In the chain-end mechanism, a stereochemical error is propagated, while in the enantiomorphic site control a correction occurs since the ligands direct the stereochemical events.^[79]

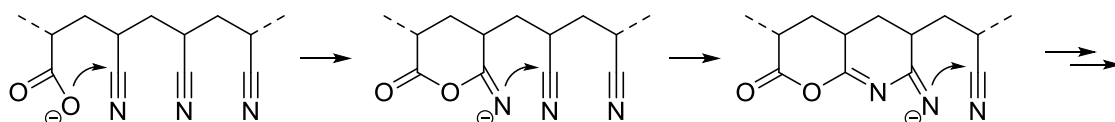
Single-site polymerization catalysts can be divided into five main symmetry categories which are supposed to be responsible for the respective stereocontrol (Scheme 8). Catalysts exhibiting C_{2v} symmetry typically produce atactic polymers or moderately stereoregular polymers by chain-end control mechanisms. C_s -symmetric catalysts that have mirror planes containing the two diastereotopic coordination sites behave similarly. However, C_s -symmetric catalysts that have a mirror plane reflecting two enantiotopic coordination sites frequently produce syndiotactic polymers. C_2 -symmetric complexes, both racemic mixtures and enantiomerically pure ones, typically produce isotactic polymers *via* a site-control mechanism. Stereoselectivities of asymmetric (C_1) complexes are unpredictable.^[80]

As an example, *Chen et al.* investigated in greater detail the stereocontrol mechanism for the syndiospecific polymerization of MMA catalyzed by the C_s -symmetric (CGC)Ti complexes illustrated in Figure 3 (chapter 2.2.2). Predominately isolated *m* meso diad stereoerrors (...rrrrmrrrr...) pointed to the apparent chain-end control nature of CGCs. Analysis of the stereomicrostructures at the pentad level revealed the *rrrm to rrmr* ratio to be approximately 1, thus also consistent with a catalyst site epimerization scheme in a chain-end control mechanism.^[50] The zero-order kinetics in MMA concentration implied that, in a unimetallic propagation cycle, displacement of the coordinated ester group by the incoming monomer is fast relative to intramolecular conjugate MMA addition within the catalyst-monomer complex, suggesting pathways leading to catalyst site epimerization at Ti before MMA additions. In contrast, monomer and catalyst concentrations as well as ion-pairing strength exhibited negligible effects on the syndiotacticity. Calculations supported the hypothesis of the catalyst site epimerization mechanism accounting for the formation of the predominately isolated *m* stereoerrors and indicated the driving force for an almost regular site epimerization reaction after a stereomistake being the higher energy of the eight-membered cycle formed after a mistake. This MMA- or anion-assisted catalyst site epimerization reaction converted the kinetic product after a stereoerror into a thermodynamically more stable resting state.^[81]

2.6 The Special Case Acrylonitrile

Whereas the fast, precise and even stereoregular coordinative-anionic polymerization of methacrylates and most of the further *Michael*-type monomers is well studied and understood, the controlled and catalytic conversion of AN still poses a big challenge to the polymer community. The highly reactive nitrile moiety and the resulting electron deficient structure makes it difficult to accomplish the control over the polymerization process and causes various side reactions like deprotonation of the highly acidic α -proton or cross-linking reactions. Nevertheless, academic as well as industrial research groups solely devote such great efforts to this topic because poly(acrylonitrile) (PAN) exhibits extremely interesting properties and the possibility of post-polymerization modifications, thus enabling a wide range of applications. The semi-crystalline PAN is characterized by excellent resistance against chemicals and solvents and by an enhanced strength and stiffness resulting from strong intermolecular interactions of the nitrile groups. Additionally, the hydrogen bonds between the nitriles and the adjacent methylene moieties effects the insolubility in most organic solvents, except the highly polar *N,N*-DMF and DMSO.^[82] Due to the bad processability caused by the poor solubility of PAN homopolymers, most of the commercial products, ranging from textile fibers to household and high technology items, are based on PAN copolymers. The most prominent examples are the four thermoplastics AN-styrene, AN-styrene-acrylate, AN-butadiene-styrene, and AN-butadiene rubber.^[83]

The low density and the fact that the melting point is above the decomposition temperature, makes PAN suitable as precursor for carbon fibers (CF), as the decomposition does not lead to depolymerization, but to a structure similar to that of graphite under appropriate conditions.^[84] Therefore, PAN fibers are assumed to be first stabilized and stretched at temperatures of 200 °C to 400 °C under oxidative conditions. In this process, the copolymerization of AN with acrylates has beneficial effects on the processability. While copolymers with acrylic acid facilitate the cyclization of the nitrile moieties, copolymers with esters of the acrylic acid ensure an enhanced meltability (Scheme 9).^[85] In the following carbonization process the previously stabilized fibers are heated temperatures of 800 °C to 1600 °C under an inert atmosphere to remove all noncarbon impurities. Depending on the quality of the resulting CF, a subsequent heat treatment to temperatures up to 3000 °C under stretching can be added.^[86]



Scheme 9. Assumed ionic stabilization of PAN with acrylic acid as comonomer.

For industrial and CF applications, the synthesis of PAN is still accomplished through radical polymerization of AN. To achieve precise control over the macromolecular parameters and tailor-made properties, living and controlled radical polymerization techniques are the methods of choice on a laboratory scale.^[87] Such controlled radical methods entail the major drawback of low reaction rates. Catalytic polymerization procedures are supposed to be the answer to this problem as these maintain the precision of the polymer architecture while ensuring higher velocities. Surprisingly, the literature provides catalytic polymerization techniques for AN to a lesser extent, although first approaches were established several decades ago.^[88] More recent concepts for a controlled, catalytic polymerization of AN share the issues of low reaction velocities, broadened molecular weight distributions (> 1.5) and requiring rare earth or transition metal-based catalysts (Figure 9).^[2,89] In addition, FLPs were already used for the polymerization of AN in the 1970s with moderate success.^[58,90] Almost none of the catalytic techniques showed a living behavior which impedes the fast and precise synthesis of the aforementioned, desired copolymer architectures.

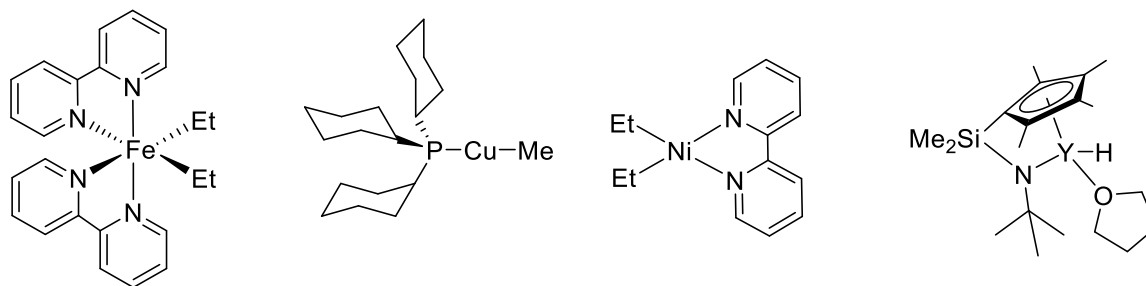
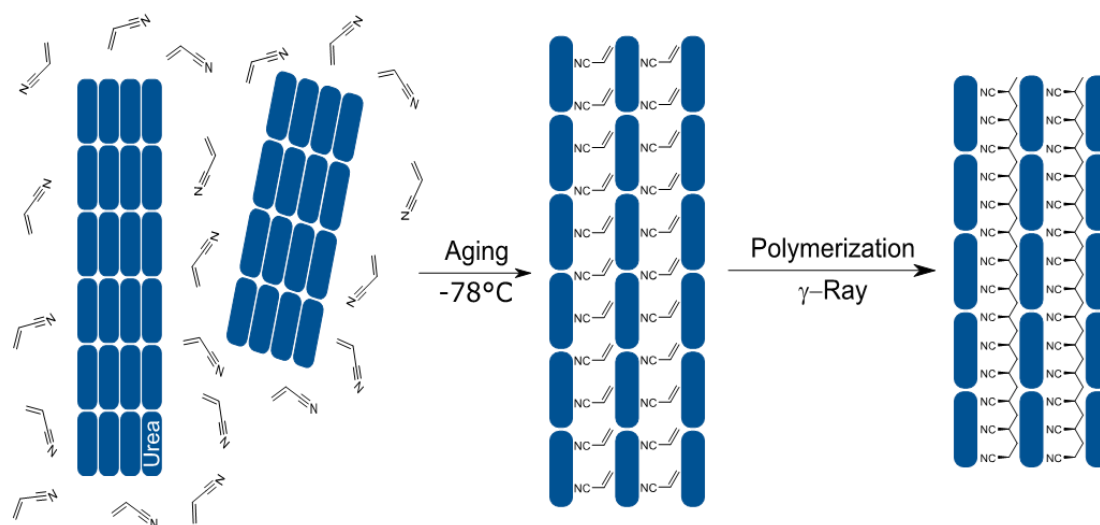


Figure 9. Examples for rare earth or transition metal-based catalysts for the catalytic polymerization of AN.

The lack of an adequate catalytic polymerization method for AN is furthermore responsible for the difficulties in controlling the tacticity. It is expected that *it*-PAN facilitates the cyclization process for CFs and that the number of connected segments after cyclization is higher compared to *at*-PAN which only enables up to five repetition units. Thereby, better mechanical properties of the resulting fiber could be the result of stereoregular PAN. Until now, the only and intricate way for the synthesis of *it*-PAN is the sophisticated preparation by template-assisted polymerization.^[91] Saturated solutions of urea crystallize to hexagonal structures upon cooling, comprising linear and parallel tunnels. The dimensions of the tunnels are suitable to include guest molecules like butadiene or AN. The monomers are confined in the cavity and restrained from rotation which enables stereoregular polymerization. A typical inclusion polymerization procedure consists of four crucial steps: 1. formation of the AN / urea inclusion compound, 2. polymerization initiated by γ -ray irradiation, 3. chain propagation, and 4. purification of the

polymer (Scheme 10). However, these time-consuming procedures with sensitive reaction conditions showed low monomer conversions.^[92]



Scheme 10. Schematic representation of the isospecific inclusion polymerization of AN in urea canals.

Due to the difficult preparation, only few studies for the CF synthesis based on stereoregular PAN can be found in the literature. Whereas *it*-rich PAN met the expectations and provided an increased concentration of cyclized rings in the stabilized fiber, *it*-PAN showed lower cyclization temperatures and a reduced activation energy.^[93] Though, the lower solubility and storage stability of *it*-PAN are believed to cause problems in CF production. The decreased solubility could cause the problem of a too fast solidification in coagulation baths for fiber spinning which results in poor fiber morphology control.

3. Aim of this Thesis

Over the last decades, a plethora of different catalysts has been synthesized and evaluated for the polymerization of polar olefins. Especially, the seminal work of *Yasuda et al.* for establishing the REM-GTP and the introduction of LPs as highly active polymerization catalysts by *Chen and coworkers* have attracted much attention.^[5,11] Without doubt, numerous advances have been made since the first reports, but the combination of the beneficial features of both methods is still a pending and desired goal. A comprehensive solution would comprise single-component and well accessible main group catalysts which are able to initiate a precision (co)polymerization of *Michael*-type monomers producing identical macromolecular chains while exhibiting high activities and initiator efficiencies at ambient conditions. Additionally, a tunable stereospecificity and an applicability for a broad scope of monomers is desirable.

Prior to the outset of this project, a decisive finding was made by the former group members *Maximilian Knaus* and *Marco Giuman*.^[94] While searching for the ideal LP combination for the polymerization of AN, they observed that the strong LA $\text{Al}(\text{C}_6\text{F}_5)_3$ initiates this reaction already before the addition of a LB. A closer investigation revealed an impressively high activity of $\text{Al}(\text{C}_6\text{F}_5)_3$ resulting in very high molecular weight PAN. Nonetheless, the following drawbacks of this method soon became obvious: 1. Broadened dispersities (> 1.5) 2. Low initiator efficiencies ($< 15\%$) 3. A solvent-dependent and non-living polymerization behavior.

In this thesis, we first set out to expand the scope of single-component aluminum and LP catalysts to screen the potential lying in this newly discovered approach. After gaining a deeper understanding of the underlying polymerization mechanisms and the origin of superior catalysts performances, we aim to transfer this knowledge to a longstanding problematic field in polymer catalysis. We would like to achieve a controlled polymerization of AN catalyzed by main group element complexes, focusing on the so far elusive narrow dispersities and a living polymerization behavior. In the last part, the received catalyst-monomer relationships should help us for tailoring complexes suitable for a stereoregular polymerization of selected monomers with the goal of achieving novel polymer properties. The outlined points are illustrated in Figure 10 and elaborated in the following.

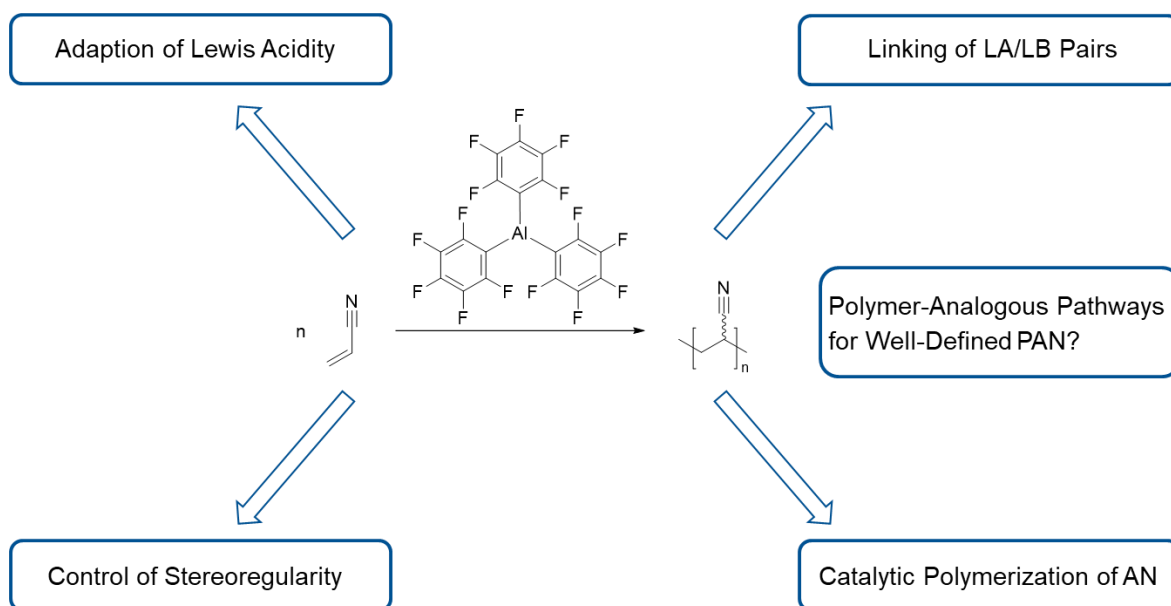


Figure 10. General outline of the different approaches within this thesis to establish single-component, main group catalysts for the precision polymerization of *Michael*-type monomers.

As a first step, additional alanes and potential catalyst candidates based on boron or magnesium will be synthesized to set up a library of catalysts with different *Lewis* acidities. Another option is to connect the LA and LB moiety with a methylene linker (Figure 11). Even though this idea is not completely new in the field of polymerization catalysis, the previously presented BLPs leave room for improvement.^[64] A systematic variation of the substituents and the synthesis of boron/phosphorus BLPs for the purpose of comparison is planned. Thereby, relationships between steric and electronic demand can be evaluated and the optimization of the polymerization process is facilitated. Both kinds of catalysts will be tested in the polymerization of *Michael*-type monomers. The monomer scope is not only restricted to AN but should also be expanded to different electronically and sterically challenging monomers. After a first screening, the active complexes are to be structurally investigated with single-crystal X-ray diffraction experiments to gain a first insight into the possible initiation mechanisms. Furthermore, end group analysis and kinetic studies will be performed and based on experimental evidence, it is expected to elucidate the respective polymerization mechanisms which will be corroborated by theoretical investigations. After solving this key issue, the catalyst structures and reaction conditions are adapted and the polymerization procedures are optimized to enable the synthesis of novel block copolymer architectures and analyze their properties. Finally, the polymerization results and mechanisms received are compared to previously presented methods to assess the benefits and limitations.

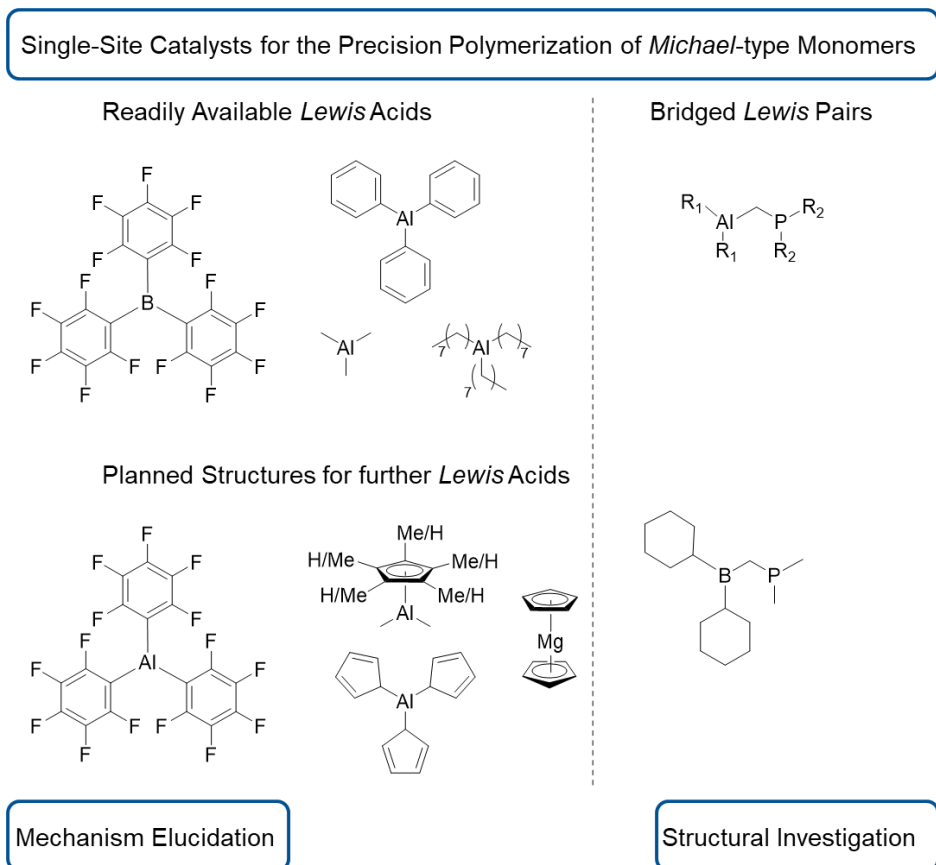


Figure 11. Two different approaches for the design of main group catalysts designated for the precise (co)polymerization of *Michael*-type monomers: Adapting the *Lewis* acidity of the complexes (left) and linking the LA and LB moieties covalently (right).

A special emphasis in this thesis is put on the catalytic polymerization of AN that is still a pending, but very important issue in polymer science. Naturally, the catalysts illustrated in Figure 11 will be extensively tested for the conversion of AN. Also, the reaction conditions will need to be modified, as a sufficient solubility of PAN is solely ensured in highly polar solvents. Suppressing known side reactions like deprotonation of the acidic proton in α -position or the nucleophilic attack of the nitrile group is necessary to establish a controlled and living polymerization. Due to the unpredictable outcome of the direct polymerization route, alternative pathways must be developed for the synthesis of well-defined PAN (Scheme 11). Polymer-analogous reactions are a promising option because the dehydration of amides into nitriles is an extensively investigated reaction on a molecular level. Since the necessary starting material poly(acrylamide) (PAA) cannot be synthesized using catalytic methods due to the acidic amide protons, a further polymer-analogous step is required. On the one hand, this could be enabled by cleaving suitable amide substituents in P(DAAA), on the other hand by amidating poly(acrylic acid) or its esters which is again a known reaction for the molecular case. After

broadening or splitting.^[75] Thus, the development of a triple resonance NMR methodology is indispensable to ensure scientifically sound signal assignments and quantification of the tacticity. After establishing a well-studied stereocontrolled approach for DEVP, this concept should be transferred to the synthesis of stereoregular PAN, which is supposed to be an enhanced precursor for the CF synthesis.

4. Single-site, Organometallic Aluminum Catalysts for the Precise Group Transfer Polymerization of Michael-type Monomers

Title: “Single-site, Organometallic Aluminum Catalysts for the Precise Group Transfer Polymerization of *Michael*-type Monomers”

Status: Full Paper, published online September 06, 2018

Journal: Chemistry – A European Journal, 2018, 24, 14950 - 14957

Publisher: Wiley-VCH

DOI: 10.1002/chem.201802075

Authors: Michael Weger,[‡] Marco M. Giuman,[‡] Maximilian G. Knaus,[‡] Maximilian Ackermann, Markus Drees, Julius Hornung, Philipp J. Altmann, Roland A. Fischer, Bernhard Rieger^a

Content: In 2016, our research group reported on the precise polymerization of diverse *Michael*-type monomers with highly interacting *Lewis* pairs. Some polymerizations showed broadened dispersities indicating side reactions like deprotonation or a transfer of a ligand originally bound to the aluminum compounds.^[6] The latter side reaction seemed to be a promising novel initiation pathway and led us to the synthesis of alanes with adapted *Lewis* acidity presented in this study. These single-component catalysts showed surprisingly high activity for the polymerization of diverse *Michael*-type monomers, even of the extended system 4-VP, without any *Lewis* base. Especially, the aluminum half-metallocenes exhibited almost quantitative initiator efficiency, affording high-molecular weight products with continuously narrow dispersities. Combined with a living behavior, they enabled the facile preparation of block architectures. Mechanistic investigations (DFT, XRD, end group and kinetic analyses) clearly suggested a main group element GTP proving a ligand transfer from the Al(III) center to the coordinated monomer as exclusive initiation step. Thereby, this work provides a new family of environmentally benign and highly active main group element catalysts acting analogously to the REM-GTP process.

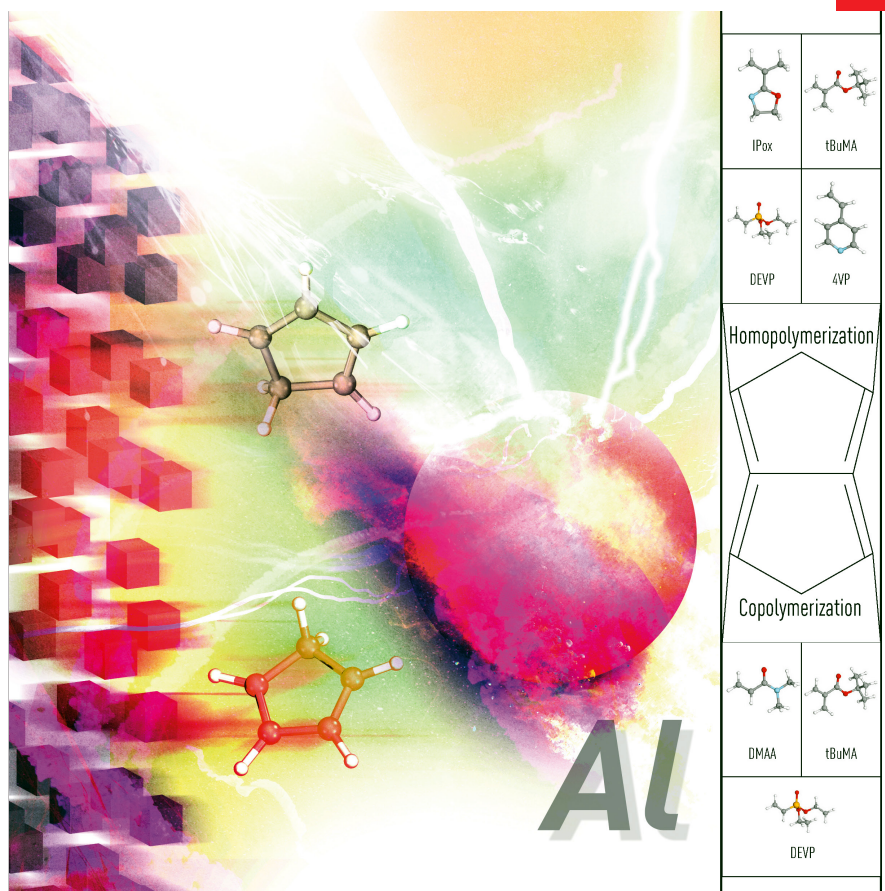
[‡] These authors contributed equally; ^aM. Weger planned and executed most of the experiments and wrote the manuscript. M. M. Giuman and M. G. Knaus had the initial idea and executed some of the experiments. M. Ackermann contributed with valuable intellectual input. M. Drees and J. Hornung performed all theoretical investigations under the supervision of R. A. Fischer. P. J. Altmann conducted all SC XRD-measurements and managed the processing of the respective data. All work was carried out under the supervision of B. Rieger.

Front Cover of Chemistry – A European Journal 2018, Volume 24, Issue 56

CHEMISTRY

A European Journal

www.chemeurj.org



A Journal of



2018-24/56

Front Cover:

B. Rieger et al.

Single-Site, Organometallic Aluminum Catalysts

for the Precise Group Transfer Polymerization of Michael-Type Monomers

Supported by



WILEY-VCH

Cover art designed and created by Jens Gronauer (Jens.Gronauer@adidas.com)

Copyright belongs to Wiley-VCH

Single-Site, Organometallic Aluminum Catalysts for the Precise Group Transfer Polymerization of Michael-Type Monomers



Michael Weger



Bernhard Rieger



Invited for the cover of this issue is the group of Bernhard Rieger and colleagues at the Technical University of Munich. The image depicts a polymerization process with an aluminum-based catalyst and its cyclopentadienyl-ligands. Read the full text of the article at [10.1002/chem.201802075](https://doi.org/10.1002/chem.201802075).

What was the biggest surprise on the way to the results presented in this paper?

Two years ago, we could present that the frustration of aluminum/phosphorus-based Lewis pairs is not mandatory to make them suitable as polymerization catalysts for Michael-type monomers. This fact made us quite curious if there is another underlying polymerization mechanism. To our surprise, we found some alanes with adapted Lewis acidity that can start the polymerization process without the help of any phosphine. We did not expect that organometallic aluminum compounds can initiate a group transfer polymerization (GTP) analogous to the rare earth metal-mediated variant. Therefore, we could establish the first single-component, main group element-based GTP catalysts.

How did the collaboration on this project start?

The starting point was the single-crystal X-ray analysis performed by P. Altmann. At that time, he was working in the subgroup of Dr. A. Pöthig at the chair of Inorganic and Metal-Organic Chemistry of Prof. R. Fischer. Mr. Altmann gave us the hint that DFT calculations would be useful for our topic, which were performed by Dr. M. Drees from Prof. Fischer's chair. In the course of the requested revisions, another member of Prof. Fischer's group, J. Hornung, supported us with different theoretical investigations.

What was the inspiration for this cover design?

The cover page was designed by Jens Gronauer, a professional graphic designer. Our aim for the cover design was the illustration of the most important features of our polymerization method at an abstract level. On the left side, we wanted to express the chaotic state of the monomeric building blocks before the polymerization. The center of the image shows our aluminum-based catalyst and its cyclopentadienyl-ligands, which are transferred onto a monomer to start the polymerization reaction. On the right side,

we used a completely different design element to present the order after the polymerization and the precise manner of the polymerization process.



Group Transfer Polymerization | Hot Paper |

Single-Site, Organometallic Aluminum Catalysts for the Precise
Group Transfer Polymerization of Michael-Type Monomers



Michael Weger^{+, [a]}, Marco M. Giومان^{+, [a]}, Maximilian G. Knaus^{+, [a]}, Maximilian Ackermann,^[a]
Markus Drees,^[b] Julius Hornung,^[b] Philipp J. Altmann,^[b] Roland A. Fischer,^[b] and
Bernhard Rieger^{*[a]}

Abstract: Unlike different types of Lewis pairs as polymerization catalysts for acrylic monomers, organometallic aluminum(III) compounds are reported that show a surprisingly high polymerization activity even without an additional Lewis base.^[1] DFT calculations, end group analysis and kinetic investigations clearly suggest a main group element (MGE) group transfer polymerization (GTP) mechanism analogous to the known metal-mediated GTP mechanism. The novel catalysts perform a precision polymerization of a

broad variety of monomers, ranging from 2-isopropenyl-2-oxazoline to *tert*-butylmethacrylate and *N,N*-dimethylacrylamide. Additionally, extended Michael-type structures like 4-vinyl pyridine are accessible. Especially the Al(III) half-metalocenes show an almost quantitative initiator efficiency, and, combined with the living character of the polymerization reactions, they enable the synthesis of block copolymers, even with unconventional monomers like vinyl phosphonates.

Introduction

Modern polymeric materials are developed with respect to targeting specific functions, like self-assembly or stimuli-responsivity. Precise control of the macromolecular architecture is a major requirement for producing identical polymer chains.^[2] One successful synthetic strategy is based on living and controlled radical polymerization methods.^[3] In contrast to those, catalytic polymerization routes combine extremely high reaction velocities with the necessary precision of the macromolecular structure.^[4]

Silyl ketene acetal (SKA)^[5] and rare-earth metal (REM)-based GTP reactions^[6–8,9,10] meet the mentioned requirements in perfection. Thereby, the initiation step of the single-component, metal-mediated approaches occurs through the nucleophilic transfer of a ligand to the coordinated monomer.^[6,10]

Beside these concepts, Chen et al. focused on frustrated Lewis pairs (FLPs). They pioneered the question of applying

FLPs for a controlled polymerization of a broad variety of acrylic monomers.^[11–13] The group of Chen discussed the importance of a zwitterionic intermediate for the initiation process of the polymerization reaction.^[13] Zwitterionic phosphonium and imidazolium enolaluminum species are formed by the reaction of the monomer-Al(C₆F₅)₃ adduct with the respective base.

Recently, we were able to demonstrate that even simple coordination compounds (e.g., Ph₃Al–PEt₃) with a strong Lewis interaction can act as remarkably active polymerization catalysts.^[14] The scope of the used Michael-type monomers includes conventional acrylic structures, as well as extended Michael-monomers, like 4-vinyl pyridine and even phosphorus-containing monomers, like vinyl phosphonates.^[14] This finding indicates that a precise and rapid polymerization is not dependent on the strength of the Lewis pair interaction, thus questioning the underlying polymerization mechanism.

Results and Discussion

Our ongoing research revealed that well-defined organoaluminum complexes act as impressively efficient polymerization catalysts even without a Lewis base.^[11] To elucidate the polymerization mechanism, we initially studied 2-isopropenyl-2-oxazoline (IPox) as an exemplary monomer, since P(oxazolines) have already proven their beneficial properties in various applications in the biomedical field.^[15] To our surprise triphenylaluminum (AlPh₃) turned out to be highly active for the polymerization of IPox as a single-component catalyst and produced high-molecular weight P(IPox) on a short timescale (Table 1, entry 1).^[16,17] Significantly enhanced initiator efficiencies and reaction rates were observed at elevated temperatures, ultimate-

[a] M. Weger,⁺ Dr. M. M. Giومان,⁺ Dr. M. G. Knaus,⁺ M. Ackermann,
Prof. Dr. B. Rieger
Catalysis Research Center & WACKER-Chair of Macromolecular Chemistry
Technical University of Munich
Lichtenbergstrasse 4, 85748 Garching bei München (Germany)
E-mail: rieger@tum.de

[b] Dr. M. Drees, J. Hornung, Dr. P. J. Altmann, Prof. Dr. R. A. Fischer
Catalysis Research Center &
Chair of Inorganic and Metal-Organic Chemistry
Technical University of Munich
Lichtenbergstrasse 4, 85748 Garching bei München (Germany)

[*] These authors contributed equally to this work.

Supporting information and the ORCID identification number(s) for the author(s) of this article can be found under:
<https://doi.org/10.1002/chem.201802075>.

Entry	Lewis acid	[Mon]/[LA]	T [°C]	t [min]	Yield [%] ^[b]	M _n [10 ³ g mol ⁻¹] ^[c]	D (M _w /M _n)	I [%] ^[d]
1	AlPh ₃	100	rt	60	61	61	1.05	11
2	AlPh ₃	100	60	10	74	19	1.09	45
3	AlMe ₂ Cp*	100	rt	30	67	15	1.28	48
4	AlMe ₂ Cp*	200	rt	30	49	18	1.12	61
5	Al(C ₆ F ₅) ₃	100	rt	60	0 ^[e]	–	–	–

[a] V_{Mon} = 0.25 mL, V_{solvent} = 2 mL (solvent toluene); Mon = monomer; LA = Lewis acid. [b] Measured gravimetrically and by ¹H NMR spectroscopy. [c] Determined by multi-angle laser light scattering (MALS) in H₂O/THF (9 g L⁻¹ tetrabutylammonium bromide) at 40 °C. [d] Initiator efficiency (M_n(theo)/M_n(determ.)). [e] ACF induces a ring-opening polymerization.^[20]

ly leading to defined polymers with narrow dispersities (Table 1, entry 2).

To vary the Lewis acidity of the aluminum center, the compounds pentamethylcyclopentadienyldimethylaluminum (AlMe₂Cp*) and tris(pentafluorophenyl)aluminum (Al(C₆F₅)₃) were employed.^[18,19] At ambient temperature, AlMe₂Cp* produces P(IPox) with an even higher initiator efficiency than AlPh₃ at elevated temperature (Table 1, entry 3). By further lowering the catalyst loading, both the initiator efficiency and the molecular dispersity of the resulting polymeric material could be enhanced (Table 1, entry 4). Thus, the half-metallocene AlMe₂Cp* constitutes an evident improvement to AlPh₃. In contrast to AlMe₂Cp*, the more acidic Al(C₆F₅)₃ induced a ring-opening polymerization of IPox (Table 1, entry 5), which is already known.^[20]

To gain a better understanding of the underlying polymerization mechanism, end group analysis by ESI-MS was performed on oligomers of IPox synthesized with AlPh₃ as catalyst. These experiments clearly revealed phenyl end groups bound to the oligomer chains, also after several precipitation steps (Figure S1 in the Supporting Information). Such a nucleophilic transfer of ligands,^[21] in combination with a narrow molecular weight distribution, is typically found in REM-GTP reactions.^[6,10] Therefore, the detection of C₆H₅-chain ends indicates that an analogous GTP-type reaction mechanism might also apply to aluminum(III) compounds.

To rationalize the experimental observations, quantum chemical calculations were performed at the B3LYP/6–31 + G** theory level. The density functional theory (DFT) calculations were carried out starting from AlPh₃ and Al(C₆F₅)₃ with toluene as solvent, according to the experimental setup.

The coordination of one IPox molecule was determined to be exergonic for both catalysts by either –5.7 kcal mol⁻¹ (AlPh₃, **1a**, ΔH = –19.0 kcal mol⁻¹) or –15.2 kcal mol⁻¹ (Al(C₆F₅)₃, **1b**, ΔH = –31.0 kcal mol⁻¹), whereas the respective calculations for a second coordinating monomer failed. The catalyst–IPox adducts are expected to be the active species and were thus defined as zero points to improve their comparability (Figure 1). It was possible to find feasible reaction pathways for the presumed initiation step, which is a nucleophilic aryl transfer to the olefin end of the coordinated monomer for both complexes. In the case of AlPh₃, the energy barrier for the nucleophilic aryl transfer could be optimized to 20.6 kcal mol⁻¹ in terms of ΔG[‡] (ΔH[‡] = 18.3 kcal mol⁻¹), while the reaction free

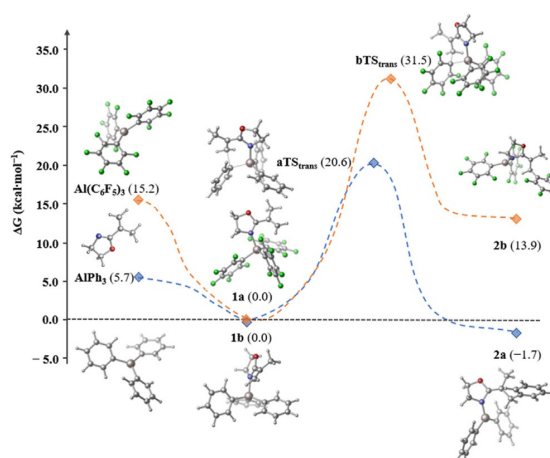


Figure 1. Energy profile of the initiation step induced by AlPh₃ (blue) and Al(C₆F₅)₃ (orange), respectively.

energy of the resulting intermediate **2a** was optimized to –1.7 kcal mol⁻¹ (ΔH = –1.9 kcal mol⁻¹). This barrier originates from the transition state, in which the exocyclic double bond of the coordinating monomer is required to bend over to the catalyst molecule in order to be functionalized by an aryl ligand (Figure 1, aTS_{trans}, and Figure 2).

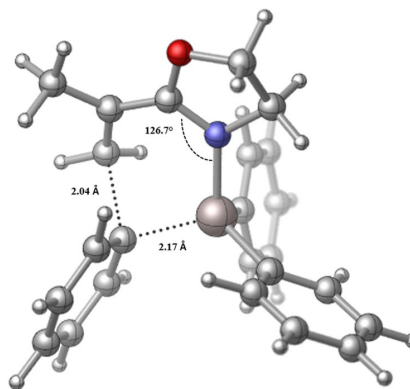


Figure 2. Transition state structure for the nucleophilic transfer in case of AlPh₃.

For the nucleophilic transfer of a pentafluorophenyl group, the energy barrier turned out to be significantly higher ($\Delta G^\ddagger = 31.5 \text{ kcal mol}^{-1}$, $\Delta H^\ddagger = 28.3 \text{ kcal mol}^{-1}$, Figure 1, **bTS_{trans}**) and endergonic in nature ($\Delta G = 13.9 \text{ kcal mol}^{-1}$, $\Delta H = 16.0 \text{ kcal mol}^{-1}$, **2b**). These results provide an explanation for the experimental observations in which AlPh_3 initiates a polymerization of IPox at ambient temperature, whereas $\text{Al}(\text{C}_6\text{F}_5)_3$ fails to polymerize IPox via the vinyl moiety.

Before continuing with DFT calculations it was necessary to obtain further information about the structural deviations of AlMe_2Cp^* . We investigated the solid-state structure of AlMe_2Cp^* by means of single-crystal X-ray analysis. Whereas cyclopentadienyldimethyl-aluminum AlMe_2Cp forms a polymeric structure in the solid state,^[22] we could prove a piano-stool structure for AlMe_2Cp^* (Figure 3).

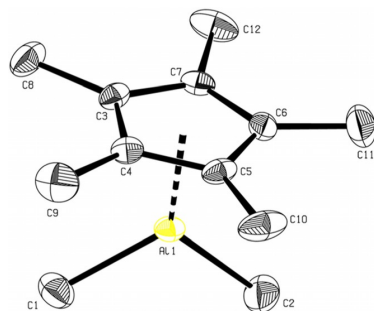


Figure 3. Solid-state structure of AlMe_2Cp^* from single-crystal X-ray analysis (CCDC 1815622 contains the supplementary crystallographic data. These data can be obtained free of charge by The Cambridge Crystallographic Data Centre).

Both compounds are easily accessible by a salt metathesis reaction of Me_2AlCl and the corresponding potassium salt of cyclopentadiene or its permethylated derivative. The ^1H NMR spectra of the compound AlMe_2Cp^* in $[\text{D}_6]$ toluene exhibit only one resonance for the ring methyl groups, which remains invariant upon a temperature decrease to -60°C . Thus, an η^5 -coordination of the Cp^* -ligand is evidenced, refuting the assumption of other groups that a trihapto geometry of the Cp^* ligand to aluminum (based on ^{27}Al -NMR spectroscopy) exists.^[19] In accordance with the work of Scherer and Kruck, AlMe_2Cp^* crystallizes at temperatures below 15°C . By comparing the methyl resonances of both compounds, a marginal upfield shift of the Al-Me groups can be observed for AlMe_2Cp^* . This shift might be attributed to a greater inductive effect of Cp^* relative to Cp .^[23]

Based on these findings, analogous calculations were performed for AlMe_2Cp^* in toluene. Upon the coordination of one IPox molecule the resulting adduct **3** could be optimized to a ΔG value of $6.0 \text{ kcal mol}^{-1}$, while the optimization procedure for the coordination of two monomer units failed. The reaction enthalpy was unexpectedly low for this reaction step ($\Delta H = -10.6 \text{ kcal mol}^{-1}$, Figure 4). The nucleophilic transfer of the Cp^* ligand showed a lower barrier ($\Delta G^\ddagger = 17.1 \text{ kcal mol}^{-1}$, $\Delta H^\ddagger =$

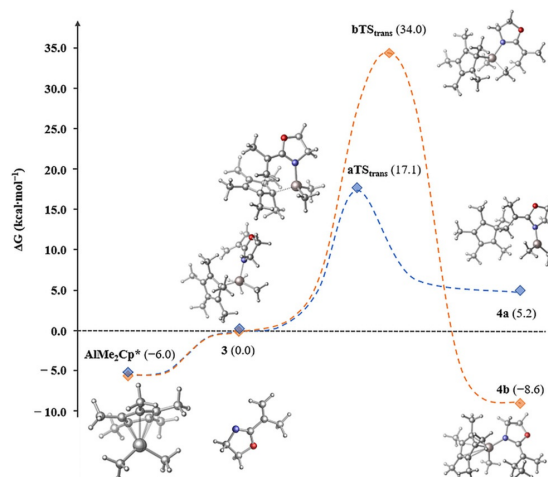


Figure 4. Energy profile of the initiation step induced by a methyl transfer (orange) and a Cp^* transfer (blue) starting from AlMe_2Cp^* .

$14.4 \text{ kcal mol}^{-1}$) compared to the transfer of a phenyl group of AlPh_3 , resulting in the endergonic reaction intermediate **4a** ($\Delta G = 5.2 \text{ kcal mol}^{-1}$, $\Delta H = 5.3 \text{ kcal mol}^{-1}$, Figure 4, **aTS_{trans}**). Thus, the theoretical values show that the Cp^* transfer is preferred over the phenyl transfer and can explain the higher initiator efficiencies of AlMe_2Cp^* (Figure S12 in the Supporting Information). To exclude the attack of an Al-Me group, the transition state energy was determined and the high barrier confirmed our assumptions ($\Delta G^\ddagger = 34.0 \text{ kcal mol}^{-1}$, $\Delta H^\ddagger = 32.3 \text{ kcal mol}^{-1}$, Figure 4, **bTS_{trans}**). For both AlMe_2Cp^* and AlPh_3 , a feasible pathway could only be found for an associative mechanism.

Most interestingly, during the transition state, the hapticity of the Cp^* ligand decreases from five to one. At that time, a carbon–aluminum bond length of 2.13 \AA can be calculated. The neighboring carbon atom of the Cp^* ligand is oriented towards the vinyl moiety of IPox with a distance of 2.01 \AA (Figure 5).

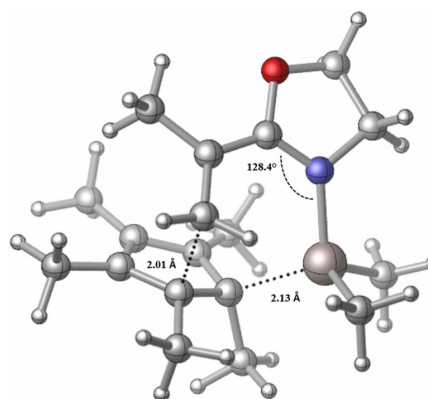


Figure 5. Transition state structure for the nucleophilic transfer in case of AlMe_2Cp^* .

For an alternative transfer of one Al–Me group to the coordinated monomer, the carbon–aluminum bond length shows an elongation of the relevant methyl group from 2.03 Å to 2.19 Å in the transition state. The distance to the vinyl group from the methyl carbon atom is 2.09 Å (Figure S11 in the Supporting Information). Compared to the Cp* transfer this transition state is located marginally earlier on the potential energy surface.

Comparing the distances of the forming carbon–carbon and breaking aluminum–carbon bonds at the transition state of the initiation reactions, it is evident that there are distinct differences in the transition states (see Supporting Information for structural comparison). For AlMe₂Cp* (in case of Cp* transfer) and AlPh₃, the structure of the transition state is more similar to the starting materials indicated by a long carbon–carbon bond of 2.00 and 2.04 Å, respectively. In contrast, the carbon–carbon distance for the transition state of the C₆F₅ transfer is significantly shorter (1.73 Å). Therefore, in the case of AlMe₂Cp* and AlPh₃ an early transition state is obtained, whereas for Al(C₆F₅)₃ a late transition state was found. To gain a deeper understanding of the factors determining the barrier of the initiation step, an energy decomposition analysis of the transition state was performed (see Supporting Information for further results) to obtain the interaction energy of the reactants at the transition state ($\Delta E_{\text{int}}^{\ddagger}$).^[24] Therefore, the transition state structure was fragmented into the IPox moiety and AlR₃. Within the activation strain model,^[25] the activation energy ΔE^{\ddagger} is the sum of the energy needed for structural distortion of the reactants $\Delta E_{\text{strain}}^{\ddagger}$ and $\Delta E_{\text{int}}^{\ddagger}$. Using the energy decomposition, $\Delta E_{\text{int}}^{\ddagger}$ can be further divided into Pauli repulsion and the attractive electrostatic and orbital interactions and dispersion forces (Table 2, see Supporting Information for full details).

Table 2. ΔE^{\ddagger} , $\Delta E_{\text{strain}}^{\ddagger}$ and $\Delta E_{\text{int}}^{\ddagger}$ as obtained from the energy decomposition analysis for the transition state of the initiation step.			
	AlMe ₂ Cp* ^[a]	AlPh ₃	Al(C ₆ F ₅) ₃
ΔE^{\ddagger} [kcal mol ⁻¹]	11.10	12.37	31.62
$\Delta E_{\text{int}}^{\ddagger}$ [kcal mol ⁻¹]	-75.04	-67.30	-94.57
$\Delta E_{\text{strain}}^{\ddagger}$ [kcal mol ⁻¹]	86.14	79.67	126.19

[a] In case of AlMe₂Cp*, only the Cp* transfer was considered.

The high $\Delta E_{\text{strain}}^{\ddagger}$ and $\Delta E_{\text{int}}^{\ddagger}$ values of Al(C₆F₅)₃ (126 and -95 kcal mol⁻¹) are in accordance to the assignment of a late transition state, which implies vast structural rearrangement (high $\Delta E_{\text{strain}}^{\ddagger}$) and strong interactions of the forming carbon–carbon bond ($\Delta E_{\text{int}}^{\ddagger}$) in contrast to the earlier transition state of AlMe₂Cp* ($\Delta E_{\text{int}}^{\ddagger} = -75$ kcal mol⁻¹, $\Delta E_{\text{strain}}^{\ddagger} = 86$ kcal mol⁻¹) and AlPh₃ ($\Delta E_{\text{int}}^{\ddagger} = -67$ kcal mol⁻¹, $\Delta E_{\text{strain}}^{\ddagger} = 80$ kcal mol⁻¹). Therefore, the reason for the high ΔE^{\ddagger} in the case of Al(C₆F₅)₃ can be found in the high $\Delta E_{\text{strain}}^{\ddagger}$ and a comparably low $\Delta E_{\text{int}}^{\ddagger}$ value, which is a result of the high steric repulsion (ΔE_{Pauli}) in the transition state.

The propagation step for the polymerizations after initiation through phenyl and Cp* transfer was again investigated with DFT calculations. The energy levels of the intermediates after

the initiation reaction **2a** (AlPh₃, see Figure 1) and **4a** (AlMe₂Cp*, see Figure 4) were chosen as starting points. The coordination of a second IPox moiety to the aluminum center showed exergonic character for both pathways (**5** and **7**, Figure 6). Also in both cases, the barriers of the transition

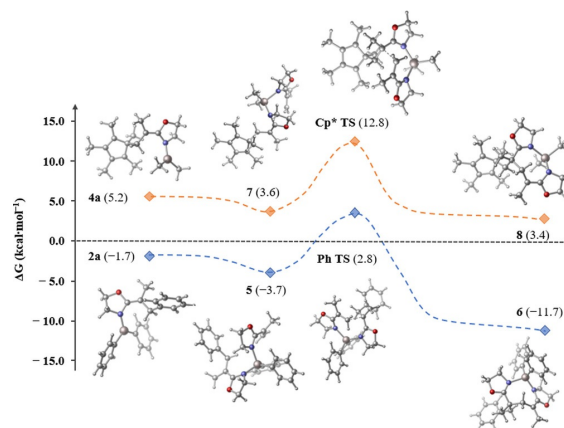


Figure 6. Energy profile of the propagation step after initiation through a phenyl (blue) and a Cp* transfer (orange).

states for the insertion of the second IPox unit were determined to be lower than the barriers of the initiation step ($\Delta G^{\ddagger} = 6.5$ kcal mol⁻¹, Ph TS, $\Delta G^{\ddagger} = 9.2$ kcal mol⁻¹, Cp* TS, Figure 6). After the first propagation step, the AlPh₃-catalyzed reaction ended up in the exergonic intermediate **6**. The AlMe₂Cp*-catalyzed polymerization was still optimized to an endergonic intermediate (**8**), but the tendency towards an exergonic process is clearly observable.

To learn more about the scope of the Al(III)-GTP, we screened different electronically and sterically challenging monomers, namely *tert*-butylmethacrylate (*t*BuMA), diethyl vinylphosphonate (DEVP), and the extended Michael-type monomer 4-vinylpyridine (4VP) (for an overview see Figure 7). Polymerization reactions were performed with commercially available Al(*n*Oct)₃ and AlMe₃ as well as freshly synthesized Al(C₆F₅)₃, B(C₆F₅)₃,^[26] AlMe₂Cp*, and AlMe₂Cp Lewis acids.

The polymerization activities of the above-mentioned catalysts were analyzed using the sterically demanding methacrylate *t*BuMA. Its polymers have not yet been satisfactorily acces-

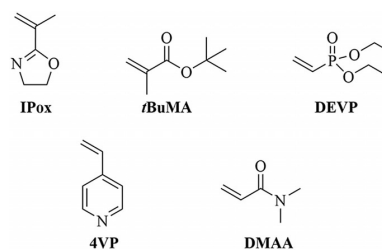


Figure 7. An overview of the investigated Michael-type monomers.

Table 3. Catalytic conversion of Michael-type monomers with main group element Lewis acids.^[a]

Entry	Monomer	Lewis acid	Solvent	T [°C]	t [min]	Yield [%] ^[b]	M_n [10 ³ g mol ⁻¹] ^[c]	\bar{D} (M_w/M_n)	I [%] ^[d]
1	tBuMA	Al(C ₆ F ₅) ₃	toluene	rt	60	0	–	–	–
2	tBuMA	AlMe ₃	toluene	rt	60	0	–	–	–
3	tBuMA	AlMe ₂ Cp	toluene	0	60	74	11	1.06	96
4	tBuMA	AlMe ₂ Cp	THF	0	15	100	18	1.28	79
5	tBuMA	AlMe ₂ Cp*	THF	0	15	100	15	1.14	98
6	tBuMA	Al(<i>n</i> Oct) ₃	toluene	rt	60	42	175	1.19	3
7	tBuMA	B(C ₆ F ₅) ₃	toluene	rt	60	0	–	–	–
8	DEVP	AlMe ₂ Cp	THF	0	15	100	19	1.21	87
9	4VP	AlMe ₂ Cp	THF	0	60	97	15	1.15	70

[a] $V_{\text{Mon}} = 0.5$ mL monomer, $V_{\text{solvent}} = 2$ mL, $[\text{Mon}]/[\text{LA}] = 100/1$; Mon = monomer; LA = Lewis acid. [b] Measured gravimetrically and by NMR spectroscopy (¹H, ³¹P NMR spectroscopy for entry 8). [c] Determined by GPC-MALS in H₂O/THF (9 g L⁻¹ tetrabutylammonium bromide) or dual-angle laser light scattering in THF at 40 °C. [d] Initiator efficiency ($M_{n(\text{theo.})}/M_{n(\text{determ.})}$).

sible with established lanthanoid-based catalysts.^[7] Similar to our research, it appears that the acidity of the applied Lewis acid has a crucial impact on the ability to catalyze a polymerization reaction. The strong Lewis acid Al(C₆F₅)₃ as well as the weak acid AlMe₃ failed to polymerize tBuMA (Table 3, entries 1 and 2). Interestingly, our aluminum half-metallocenes seem to meet the required conditions and provide Cp ligands that have been proven suitable as initiating groups in GTP. AlMe₂Cp can be applied to polymerize tBuMA with a remarkably high initiator efficiency (96%) and a narrow dispersity (1.06) at low temperatures (Table 3, entry 3). Mechanistic experiments that were analogous to the ones performed for P(IPox) confirmed our assumptions concerning group transfer initiation. ESI-MS analysis of purified oligomers produced by AlMe₂Cp again revealed the expected nucleophilic transfer of the Cp ligand (Figure S2 in the Supporting Information). Because both AlMe₂Cp and the growing P(tBuMA) chain are better soluble in THF (relative to toluene, Table 3, entry 3) the reaction was significantly accelerated by changing the solvent, although with a slightly lower initiator efficiency and broader dispersity (entry 4). When applying AlMe₂Cp* in THF, an almost quantitative initiator efficiency was observed, affording well-defined P(tBuMA) chains (Table 3, entry 5). Using Al(*n*Oct)₃ enabled the transfer of long alkyl substituents onto the polymer chain end (Figure S3 in the Supporting Information). In contrast to the easy transfer of cyclic ligands, the reaction rate and the initiator efficiency were reduced considerably, leading to a comparatively high molecular weight P(tBuMA) (Table 3, entry 6).

Furthermore, the catalysts were applied to produce the thermoresponsive P(DEVP). The relationship between Lewis acidity and activity also became evident in the polymerization of this highly polar monomer.^[8,27] While strong Lewis acids are only active at elevated temperatures,^[16] aluminum compounds with weak Lewis acidity fail as polymerization catalysts in the absence of a Lewis base.^[1] By far, the best results were once again produced by the two aluminum half-metallocenes. With AlMe₂Cp as catalyst in THF as solvent, DEVP could be quantitatively converted to the polymer in a rapid and controlled fashion at low temperatures and again, with a remarkably high initiator efficiency (Table 3, entry 8).

Additionally, the presented organoaluminum compounds provided access to the polymer of the non-classic Michael-monomer 4VP, which exhibits an extended unsaturated system.

P(4VP) has, to our knowledge, not been accessible by means of GTP thus far,^[14,28] even though the resulting polymer shows various promising application areas, for example, as interface layer for organic solar cells.^[29] AlMe₂Cp can produce P(4VP) in nearly quantitative yields with high molecular masses and narrow dispersities (Table 3, entry 9). Chain-end analysis by ESI-MS performed on purified short chained 4VP oligomers again confirmed the nucleophilic transfer of a Cp (or Cp*) ligand to the monomer. Furthermore, no signals were detected for an alternative reaction pathway such as a deprotonation reaction, which is in accordance with the narrow molecular weight distribution of the polymer products and the high initiator efficiency of the process (Figure 8). The fact that aluminum organyls can initiate the polymerization of polar monomers by itself could be a reason for broadened dispersities observed for Lewis pair polymerizations using certain Lewis pair combinations.^[12,14]

The linear dependence of the molecular weight of the polymer products upon monomer conversion underlines the living character of these polymerization reactions and leads to dispersities, which remain narrow over time. (Figure 9 and Figure S4 in the Supporting Information). This behavior was studied in detail using DEVP polymerized by AlMe₂Cp* as an example. Since it is possible to determine the conversion of DEVP by ³¹P NMR spectroscopy, the monitoring of the reaction progress is facilitated. Further evidence for the living nature of the polymerizations was the linear increase of the molecular weights from 20 to 49 and 88 kg mol⁻¹ when lowering the catalyst loadings from 100:1 to 250:1 and 450:1, respectively, and ensuring quantitative conversions.

Thus, we determined the order of the reaction with regard to the catalyst at different AlMe₂Cp* concentrations (constant toluene and monomer amounts at room temperature). The apparent rate constants (k_{app}) were obtained from the slopes of the best-fit lines for the plots of $[\text{DEVP}]_t/[\text{DEVP}]_0$ versus time. A double logarithmic diagram of k_{app} as a function of $\ln[\text{Mon}]/[\text{LA}]$ revealed a reaction order of 1 for AlMe₂Cp* (Figure S6 in

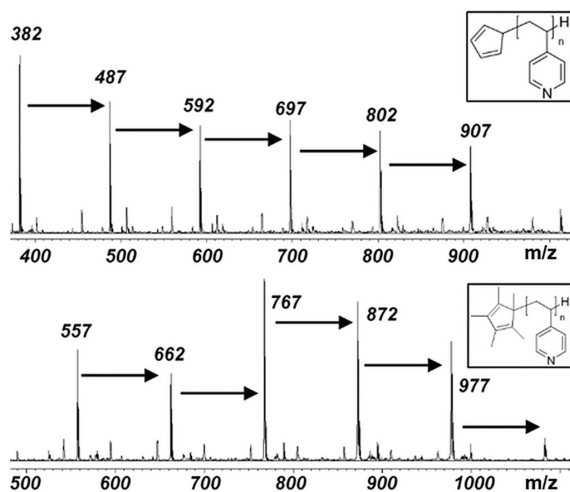


Figure 8. ESI-MS spectra of 4VP-oligomers produced with AlMe_2Cp and AlMe_2Cp^* , respectively; signals correspond to $M_{4VP} + M_H + M_{Cp}$ and M_{Cp^*} , respectively.

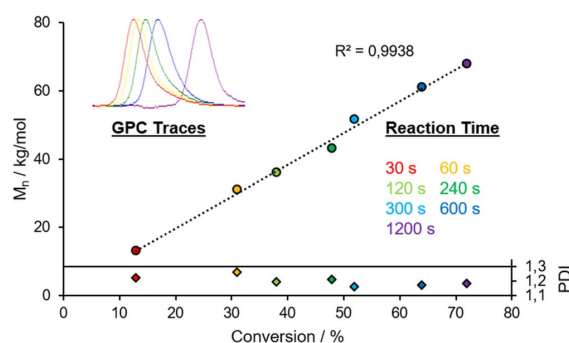


Figure 9. Linear growth of the molecular weight with increasing conversion and corresponding dispersities using the example of P(DEVP).

the Supporting Information). A similar set of experiments using different monomer concentrations also gave a reaction order of 1 for the DEVP monomer (Figure S5 in the Supporting Information).

From the discussion above, we postulate the following mechanism for our MGE-GTP reaction. After coordination of a monomer like DEVP via its phosphonate moiety to for example, AlMe_2Cp^* , the nucleophilic transfer of the Cp^* ligand initiates the polymerization reaction (Scheme 1). The oxophilicity of the aluminum center supports the coordination procedure. The activated species **9** gives rise to the coordination of the next monomer unit. Propagation occurs via an eight-electron process and affords the eight-membered ring intermediate **10**, already bearing the next DEVP fragment.^[6] This fivefold coordinated intermediate explains the inactivity of boron compounds, like $\text{B}(\text{C}_6\text{F}_5)_3$ (Table 3, entry 7), which can only adopt a fourfold coordinated ligand environment. As a result, the mechanism is analogous to the REM-GTP catalysis and has so far not been known for aluminum organyls.^[6,10,30]

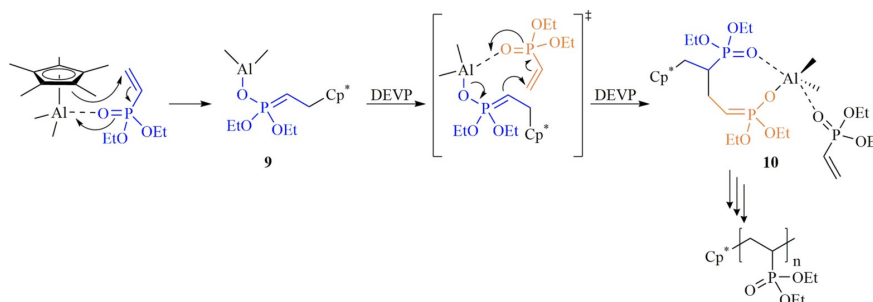
The living nature of this method and especially the exceptionally high initiator efficiencies of the aluminum half-metallocenes open up the possibility to design precise block-type macromolecular architectures. We demonstrated this feature by quantitatively converting *t*BuMA into its polymer by using AlMe_2Cp (Table 4, entry 1a). Subsequently, DEVP was added to form the second block. This sequential addition led to a polymer with narrow dispersity. The retention time shift of the GPC trace indicated an increasing molecular weight during block structure formation (Figure 10, Table 4, entry 1b).

To demonstrate the scope of the reaction, block copolymers comprising *N,N*-dimethylacrylamide (DMAA) and DEVP were prepared in addition (Figure S7 in the Supporting Information). The molecular weights increased here again from the homo- to the block polymer in the expected manner, depending on

Table 4. Block copolymerizations with AlMe_2Cp as catalyst.^[a]

Entry	Monomer	T [$^{\circ}\text{C}$]	M_n [10^3 g mol^{-1}]	D (M_w/M_n)
1a	<i>t</i> BuMA	0	23 ^[b]	1.05
1b	<i>t</i> BuMA-co-DEVP	0	51 ^[b]	1.15
2a	DMAA	-15	27 ^[c]	1.49
2b ^[c]	DMAA-co-DEVP	-15	66 ^[c]	1.78

[a] $V_{\text{Mon1}} = 0.5 \text{ mL}$, toluene as solvent (3.5 mL), $M_{\text{Mon1}}/M_{\text{Mon2}} = 1:1$, $[M_1]/[LA] = 200/1$, quantitative conversion ensured by NMR spectroscopy (^1H , ^{31}P NMR). [b] Determined by dual angle laser light scattering in *N,N*-DMF (2.2 g L^{-1} lithium bromide) at 30°C relative to PMMA. [c] Determined by GPC-MALS in $\text{H}_2\text{O}/\text{THF}$ (9 g L^{-1} tetrabutylammonium bromide) at 40°C .



Scheme 1. Postulated mechanism for the MGE-GTP exemplified by DEVP as monomer and AlMe_2Cp^* as catalyst.

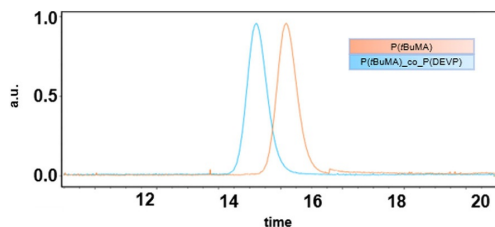


Figure 10. Retention time shift for P(tBuMA) and P(tBuMA)-co-P(DEVP) produced with AlMe_2Cp .

the monomer ratio and their molar masses (Table 4, entries 2a/b). To confirm the successful synthesis of block copolymers, we conducted experiments with different monomer ratios as well as time-dependent copolymerization experiments, (Figure S8–S10 in the Supporting Information). All of the obtained polymers are in accordance with block copolymer architectures, and the congruent light scattering data make an accidental overlap of separately formed homopolymers unlikely. The successful syntheses of both types of block copolymers were further proven by NMR spectroscopy and differential scanning calorimetry (DSC) analysis (Figures S11–S13 in the Supporting Information). The block copolymerization reactions did not work when using the monomers in reverse order. Consequently, the coordination strength of the monomers to the aluminum center has a decisive influence on the copolymerization experiments.

Conclusion

Herein we reported a group transfer polymerization mediated by Al(III)-based Lewis acids without any additional Lewis bases. Due to the variable ligand structure of these single-site aluminum organyls, this work provides a new family of environmentally benign and highly active main group element catalysts. The Al(III) compounds enable the controlled and precise GTP of important Michael-type monomers, affording high-molecular weight products with surprisingly narrow dispersities. Mechanistic investigations supported by DFT calculations provided proof that an aryl or alkyl group is transferred from the Al(III) center to the coordinated monomer, inducing a group transfer polymerization process and delivering an explanation for the varying initiator efficiencies. The broad applicability of this MGE-GTP is evidenced by the exemplary use of sterically and electronically diverse monomers as well as the extended Michael-system 4VP. The two half-aluminocenes in particular are the first single-component main group element catalysts to give surprisingly high initiator efficiencies. Therefore, they enable the facile preparation of polymer block architectures, even of unconventional monomer combinations.

Experimental Section

See Supporting Information for experimental details.

Acknowledgements

M.W. is grateful for a generous scholarship from the Studienstiftung des deutschen Volkes. M.K. is grateful for a generous scholarship from the Fonds der Chemischen Industrie. Financial support by the TUM Graduate School. M.D. thanks the LRZ computing center of the Bavarian Academy of Science for providing computing time. A. Pöthig is acknowledged for crystallographic advice and M. Weindl for the support with the low-temperature NMR experiments.

Conflict of interest

The authors declare no conflict of interest.

Keywords: block copolymers · density functional theory calculations · main group elements · polar monomers · group transfer polymerization

- [1] In this context, “without an additional Lewis base” means that no Lewis base like phosphine, amine, or NHC has to be added to start the polymerization, in contrast to Lewis pair polymerizations. In the initiation step, the ligands which are transferred to the monomer are acting as a base.
- [2] S. Salzinger, B. Rieger, *Macromol. Rapid Commun.* **2012**, *33*, 1327–1345.
- [3] a) C. J. Hawker, A. W. Bosman, E. Harth, *Chem. Rev.* **2001**, *101*, 3661–3688; b) M. Fantin, A. A. Isse, A. Venzo, A. Gennaro, K. Matyjaszewski, *J. Am. Chem. Soc.* **2016**, *138*, 7216–7219; c) W. A. Braunecker, K. Matyjaszewski, *Prog. Polym. Sci.* **2007**, *32*, 93–146; d) M. Kamigaito, T. Ando, M. Sawamoto, *Chem. Rev.* **2001**, *101*, 3689–3746.
- [4] B. S. Soller, S. Salzinger, B. Rieger, *Chem. Rev.* **2016**, *116*, 1993–2022.
- [5] a) W. J. Brittain, *J. Am. Chem. Soc.* **1988**, *110*, 7440–7444; b) J. Chen, R. R. Gowda, J. He, Y. Zhang, E. Y.-X. Chen, *Macromolecules* **2016**, *49*, 8075–8087; c) O. W. Webster, W. R. Hertler, D. Y. Sogah, W. B. Farnham, T. V. RajanBabu, *J. Am. Chem. Soc.* **1983**, *105*, 5706–5708; d) O. W. Webster, *J. Polym. Sci. Part A* **2000**, *38*, 2855–2860; e) K. Fuchise, Y. Chen, T. Satoh, T. Kakuchi, *Polym. Chem.* **2013**, *4*, 4278.
- [6] H. Yasuda, H. Yamamoto, K. Yokota, S. Miyake, A. Nakamura, *J. Am. Chem. Soc.* **1992**, *114*, 4908–4910.
- [7] H. Yasuda, E. Ihara, *Macromol. Chem. Phys.* **1995**, *196*, 2417–2441.
- [8] U. B. Seemann, J. E. Dengler, B. Rieger, *Angew. Chem. Int. Ed.* **2010**, *49*, 3489–3491; *Angew. Chem.* **2010**, *122*, 3567–3569.
- [9] a) B. S. Soller, N. Zhang, B. Rieger, *Macromol. Chem. Phys.* **2014**, *215*, 1946–1962; b) P. T. Altenbuchner, B. S. Soller, S. Kissling, T. Bachmann, A. Kronast, S. I. Vagin, B. Rieger, *Macromolecules* **2014**, *47*, 7742–7749; c) A. D. Bolig, E. Y.-X. Chen, *J. Am. Chem. Soc.* **2004**, *126*, 4897–4906; d) S. Collins, D. G. Ward, *J. Am. Chem. Soc.* **1992**, *114*, 5460–5462; e) F. Adams, P. Pahl, B. Rieger, *Chem. Eur. J.* **2018**, *24*, 509–518.
- [10] S. Salzinger, B. S. Soller, A. Plikhta, U. B. Seemann, E. Herdtweck, B. Rieger, *J. Am. Chem. Soc.* **2013**, *135*, 13030–13040.
- [11] J. He, Y. Zhang, L. Falivene, L. Caporaso, L. Cavallo, E. Y.-X. Chen, *Macromolecules* **2014**, *47*, 7765–7774.
- [12] Y. Zhang, G. M. Miyake, E. Y.-X. Chen, *Angew. Chem. Int. Ed.* **2010**, *49*, 10158–10162; *Angew. Chem.* **2010**, *122*, 10356–10360.
- [13] Y. Zhang, G. M. Miyake, M. G. John, L. Falivene, L. Caporaso, L. Cavallo, E. Y.-X. Chen, *Dalton Trans.* **2012**, *41*, 9119–9134.
- [14] M. G. M. Knaus, M. M. Giuman, A. Pöthig, B. Rieger, *J. Am. Chem. Soc.* **2016**, *138*, 7776–7781.
- [15] a) N. Adams, U. S. Schubert, *Adv. Drug Delivery Rev.* **2007**, *59*, 1504–1520; b) C. J. Waschinski, S. Barnert, A. Theobald, R. Schubert, F. Kleinschmidt, A. Hoffmann, K. Saalwächter, J. C. Tiller, *Biomacromolecules* **2008**, *9*, 1764–1771; c) C. Weber, T. Neuwirth, K. Kempe, B. Ozkahraman, E. Tamahkar, H. Mert, C. R. Becer, U. S. Schubert, *Macromolecules* **2012**, *45*, 20–27; d) N. Zhang, S. Salzinger, B. S. Soller, B. Rieger, *J. Am. Chem. Soc.* **2013**, *135*, 8810–8813.

- [16] M. Ackermann, Master's Thesis **2014**, Technische Universität München.
[17] M. G. M. Knaus, Dissertation **2016**, Technische Universität München.
[18] J. Klosin, G. R. Roof, E. Y.-X. Chen, K. A. Abboud, *Organometallics* **2000**, *19*, 4684–4686.
[19] M. Scherer, T. Kruck, *J. Organomet. Chem.* **1996**, *513*, 135–138.
[20] N. Zhang, Dissertation **2010**, Technische Universität München.
[21] J. D. Rainier, J. M. Cox, *Org. Lett.* **2000**, *2*, 2707–2709.
[22] J. Stadelhofer, J. Weidlein, *J. Organomet. Chem.* **1975**, *84*, C1–C4.
[23] C. T. Burns, P. J. Shapiro, P. H. M. Budzelaar, R. Willett, A. Vij, *Organometallics* **2000**, *19*, 3361–3367.
[24] a) A. Michalak, M. Mitoraj, T. Ziegler, *J. Phys. Chem. A* **2008**, *112*, 1933–1939; b) M. P. Mitoraj, A. Michalak, T. Ziegler, *J. Chem. Theory Comput.* **2009**, *5*, 962–975.
[25] F. M. Bickelhaupt, K. N. Houk, *Angew. Chem. Int. Ed.* **2017**, *56*, 10070–10086; *Angew. Chem.* **2017**, *129*, 10204–10221.
[26] A. G. Massey, A. J. Park, *J. Organomet. Chem.* **1964**, *2*, 461–465.
[27] S. Salzinger, U. B. Seemann, A. Plikhta, B. Rieger, *Macromolecules* **2011**, *44*, 5920–5927.
[28] a) A. J. Convertine, B. S. Sumerlin, D. B. Thomas, A. B. Lowe, C. L. McCormick, *Macromolecules* **2003**, *36*, 4679–4681; b) J. Xia, X. Zhang, K. Matyjaszewski, *Macromolecules* **1999**, *32*, 3531–3533.
[29] a) M. L. Hallensleben, H. Wurm, *Angew. Chem.* **1976**, *88*, 192; b) H. Nishide, E. Tsuchida, *Makromol. Chem.* **1976**, *177*, 2295–2310; c) A. Sharma, R. Kroon, D. A. Lewis, G. G. Andersson, M. R. Andersson, *ACS Appl. Mater. Interfaces* **2017**, *9*, 10929–10936.
[30] E. Y.-X. Chen, *Chem. Rev.* **2009**, *109*, 5157–5214.

Manuscript received: April 25, 2018

Revised manuscript received: July 26, 2018

Accepted manuscript online: July 26, 2018

Version of record online: September 6, 2018

5. Non-Innocent Methylene-Linker in Bridged Lewis Pair Initiators

Title: “Non-Innocent Methylene-Linker in Bridged *Lewis* Pair Initiators”

Status: Communication, published online June 12, 2019

Journal: *Angew. Chem. Int. Ed.*, 2019, 58, 9797 - 9801

Publisher: Wiley-VCH

DOI: 10.1002/anie.201902833

Authors: Michael Weger,[‡] Raphael K. Grötsch,[‡] Maximilian G. Knaus, Marco M. Giuman David C. Mayer, Philipp J. Altmann, Estelle Mossou, Birger Dittrich, Alexander Pöthig,* Bernhard Rieger*.^a

Content: As mentioned in chapter 4, we were searching for single-component catalysts which are less prone to side reactions in the polymerization of *Michael* monomers. Beside the aluminum half-metallocenes, a second approach was the covalent linkage of the *Lewis* acid and base moieties with a methylene bridge. These Al-P based BLPs were expected to initiate the polymerization of *Michael*-type monomers by the known conjugate addition mechanism.^[64] After the successful synthesis of variously substituted BLPs, SC XRD investigations revealed an unusually distributed electron density for the axial groups at the aluminum atom. Even though further diffraction experiments (XRD & neutron) and theoretical calculations could explain this phenomenon with hydrolysis, the selective reactivity of the axial groups pointed towards a possible tendency to initiate the polymerization *via* a nucleophilic transfer. The highly active BLPs polymerized the α -acidic DAVP and DMAA, but no methacrylates. Using NMR spectroscopy and ESI MS, this inactivity was attributed to a deprotonation of the α -acidic monomers instead of a group transfer or conjugate addition as initiation step. Additional DFT calculations and NBO analysis corroborated that the partly negatively charged methylene linker is not innocent, but likely responsible for the deprotonation. Consequently, the formerly unwanted deprotonation provides a living polymerization method with narrow molecular mass distributions and the possibility of copolymerization.

[‡] These authors contributed equally; * Corresponding authors; ^aM. Weger and R. K. Grötsch planned and executed all the experiments, M. Weger and A. Pöthig wrote the manuscript. M. M. Giuman and M. G. Knaus had the initial idea and contributed with valuable intellectual input. D. C. Mayer and B. Dittrich performed all theoretical investigations. P. J. Altmann and A. Pöthig conducted all SC-XRD measurements and managed the processing of the respective data. E. Mossou and A. Pöthig conducted all neutron diffraction measurements and managed the processing of the respective data. All work was carried out under the supervision of B. Rieger.

Polymerization

International Edition: DOI: 10.1002/anie.201902833
German Edition: DOI: 10.1002/ange.201902833

Non-Innocent Methylene Linker in Bridged Lewis Pair Initiators

Michael Weger[†], Raphael K. Grötsch[†], Maximilian G. Knaus, Marco M. Giuman,
David C. Mayer, Philipp J. Altmann, Estelle Mossou, Birger Dittrich, Alexander Pöthig,^{*} and
Bernhard Rieger^{*}

Abstract: Deprotonation usually occurs as an unwanted side reaction in the Lewis pair polymerization of Michael acceptors, for which the conjugated addition of the Lewis base to the acid-activated monomer is the commonly accepted initiation mechanism. This has also been reported for B–P-based bridged Lewis pairs (BLPs) that form macrocyclic addition products. We now show that the formerly unwanted deprotonation is the likely initiation pathway in the case of Al–P-based BLPs. In a detailed study of a series of Al–P-based BLPs, using a combination of single-crystal diffraction experiments (X-ray and neutron) and mechanistic investigations (experimental and computational), an active role of the methylene bridge was revealed, acting as a base towards the α -acidic monomers. Additionally, the polymerization studies proved a living behavior combined with significantly high activities, narrow molecular mass distributions, and the possibility of copolymerization.

The seminal work of the groups of Stephan and Erker in the field of frustrated Lewis pairs (FLPs) led to a renaissance in catalysis with main group elements.^[1,2] The cooperative interaction of Lewis acids and bases enables the heterolytic cleavage of hydrogen, which had been elusive for main group element compounds until then.^[3–5] The steric demand prevents the quenching of the Lewis pairs (LPs) and is a unique

property that additionally renders the activation of other small molecules possible.^[6]

Shortly after the revival of main group catalysis, Chen and co-workers introduced intermolecular frustrated and even classical LPs for the polymerization of diverse acrylic monomers.^[7] They proposed a novel conjugate-addition polymerization mechanism (Figure 1, pathway 1) based on a zwitterionic intermediate occurring in the initiation step.^[7,8] Further studies showed the broad applicability of this method and a more detailed elucidation of the mechanism, which identified deprotonation as a side reaction for α -acidic monomers (Figure 1, pathway 2).^[9] Furthermore, our group showed that organoaluminum compounds with adapted Lewis acidity initiate an impressively efficient nucleophilic group transfer polymerization (GTP) process (Figure 1, pathway 3).^[10]

As a subgroup of the intramolecular LPs,^[1,3–5,11] methylene-bridged Lewis pairs (BLPs) were already known for the activation of small molecules or for diverse catalytic purposes before the term “FLP” was introduced.^[12,13–15] Besides these applications, Xu and Chen demonstrated that boron-phos-


[*] M. Weger,^[†] R. K. Grötsch,^[†] Dr. M. G. Knaus, Dr. M. M. Giuman, Prof. Dr. B. Rieger
Catalysis Research Center & WACKER-Chair of Macromolecular Chemistry, Technical University of Munich
Lichtenbergstrasse 4, 85748 Garching (Germany)
E-mail: rieger@tum.de

D. C. Mayer, Dr. P. J. Altmann, Dr. A. Pöthig
Catalysis Research Center & Chair of Inorganic and Metal-Organic Chemistry, Technical University of Munich
Lichtenbergstrasse 4, 85748 Garching (Germany)
E-mail: alexander.poethig@tum.de

Dr. E. Mossou
Institute Laue-Langevin
71 avenue des Martyrs CS 20156, 38042 Grenoble (France)
and
Faculty of Natural Sciences, Keele University
Staffordshire, ST5 5BG (UK)

Dr. B. Dittrich
Inorganic Chemistry und Structural Chemistry 2
Heinrich Heine Universität
Universitätsstrasse 1, 40225 Düsseldorf (Germany)

[†] These authors contributed equally to this work.

Supporting information and the ORCID identification numbers for some of the authors of this article can be found under:
 <https://doi.org/10.1002/anie.201902833>.

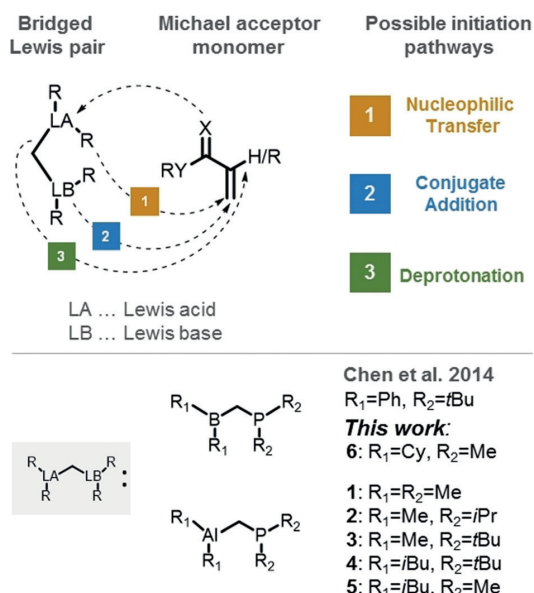


Figure 1. Top: Possible initiation pathways for the BLP-mediated polymerization of Michael-type monomers. Bottom: Known B–P-based BLP initiators^[16] and Al–P-based BLP initiators investigated in the present study.

phorus-based BLPs can serve as highly active catalysts for the polymerization of γ -methyl- α -methylene- γ -butyrolactone, however, with the drawback of broadened dispersities.^[16] The cycloaddition of the BLP to the monomer leads to a seven-membered, zwitterionic ring intermediate as the proposed active species, which is cleaved during quenching.

Herein, we introduce aluminum/phosphorus BLPs that act as polymerization initiators for polar monomers, present a detailed mechanistical elucidation of the initiation step, as well as significant differences to known boron/phosphorus BLPs.

We started our study with a thorough structural investigation of all employed Al–P-based initiator compounds by single-crystal X-ray diffraction (XRD). First, we redetermined the molecular structure of $\text{Me}_2\text{AlCH}_2\text{PMe}_2$ (**1**) at low temperature (100 K) and with higher resolution (0.65 Å) than reported for the original elucidation in 1985.^[13] In the independent atom model (IAM) derived from this initial experiment we observed a pronounced elongation of the axial Al1–C5 distance (2.0091(13) Å) compared to the equatorial Al1–C4 distance (1.9719(16) Å), together with an increased residual electron density on the axial carbon atom. As originally reported for the room-temperature measurements, all determined bond lengths were identical within statistical uncertainty. This finding sparked our interest as to whether the elongation at low temperature was possibly caused by a polarization of the bond towards the more electronegative carbon atom, and thus indicating a possible proneness to initiating polymerizations through a nucleophilic transfer of a methyl group (Figure 1, pathway 3).

To validate the plausibility of this unusually distributed electron density, we applied a more sophisticated model using aspherical atomic form factors. Thus, an invariom-like crystallographic least-squares refinement with Hansen–Coppens aspherical scattering factors predicted by DFT computations was carried out using the X-ray diffraction intensities (for details of the refinement see the Supporting Information).^[17] The charge accumulation in the dative bond observed in the residual electron density based on the IAM refinement hides the fact that the neutral Al and P atoms both carry too much charge when using neutral scattering factors, which is probably absorbed in the atomic displacement parameters. After the invariom refinement, the residual electron density included is small and the model thus fully consistent with the experimental X-ray data. However, this was only achieved when applying an artificially increased occupancy factor for the axially bound methyl carbon atom at the aluminum atom,

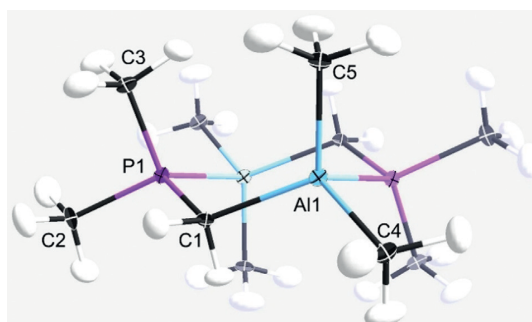


Figure 2. Molecular structure of $\text{Me}_2\text{AlCH}_2\text{PMe}_2$ (**1**), including hydrogen atom positions and displacements, determined by single-crystal neutron diffraction at 100 K.^[22] Displacement ellipsoids are shown at the 30% probability level.

which strongly indicates the possibility of a partial disorder of a heavier element.

To rule out a partial hydrolysis of the axial methyl group as the reason for the high residual electron density, we conducted a single-crystal neutron diffraction measurement on the ILL four-circle diffractometer D19 (Grenoble, France) at 100 K (Figure 2, for experimental and refinement details see the Supporting Information). The positions and occupancy of the hydrogen atoms were unequivocally determined, thereby confirming the absence of a partially occupying heteroatom at the C5-position. The actual geometry of the methyl groups significantly deviates from that derived from XRD, for which calculated hydrogen atom positions were used.

Interestingly, although the IAM model derived from the neutron data confirms the relative elongation of the axial Al–C bond, the determined bond length of 1.9877(14) Å is significantly shorter than that derived from the X-ray data. Therefore, to check for a possible decomposition of the smaller single crystal used in the XRD experiment, we reevaluated our results and were able to obtain a suitable data set from a quickly mounted single crystal using a short exposure time (see the Supporting Information). At 1.9858(12) Å, the now determined value of the axial Al–C bond length is significantly shorter and, furthermore, no suspicious residual electron density was observed. For the latter we were additionally able to document its formation over the course of a 12 h in situ diffraction experiment using one single crystal (Figure 3) and we can in fact attribute it to a selective

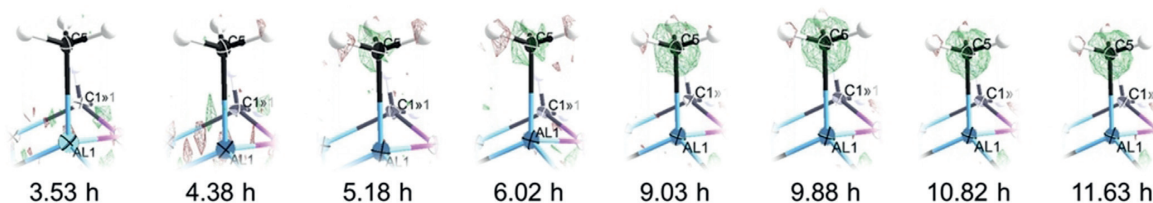


Figure 3. Formation of excessive residual electron density at the axial Al substituent of **1** upon hydrolysis, monitored over time by in situ single-crystal XRD.

hydrolysis of the axial methyl group, even in the solid state under a stream of protective nitrogen gas at 100 K.

Although a pronounced polarization of the Al–C bond was disproved by the findings of the diffraction experiments, the selective reactivity of the axial methyl group of **1** still suggests a possible tendency to initiate the polymerization by a nucleophilic transfer. We therefore tested the activity of compound **1** for initiating polymerization reactions of Michael-type monomers. We observed that the vinylphosphonates diethyl vinylphosphonate (DEVP) and diisopropyl vinylphosphonate (DIVP), as well as *N,N*-dimethylacrylamide (DMAA) can be polymerized with remarkably high turnover frequencies (TOF; Table 1, Exp. 1–3). The P(vinylphosphonates), a class of polymers of highest interest in the biomedical field,^[18] were obtained as high-molecular-weight products with narrow to extremely narrow dispersities.

The possible influence of steric effects at the LPs on the polymerization performance was investigated by employing four more BLPs with different substituents on the Al and P atoms (**2–5**).^[14,15] Single-crystal X-ray analyses of all the compounds confirmed their dimeric structure in the solid state. The elongation of the axial Al–C bond is not unique for **1**, but most pronounced, and the increased residual electron density at the axial C atom, indicative of hydrolysis, was also not observed for samples **2–5** (see the Supporting Information, also for the B–P-based BLP **6**).

When applied in polymerization experiments, the different BLPs also showed significant differences in their performance, depending on their substitution patterns. When the steric demand on the phosphorus atom is increased from a methyl to an isopropyl group, the resulting BLP **2** can polymerize DEVP and DMAA with slightly lower initiator efficiencies but with similar dispersities compared to Me₂AlCH₂PMe₂ (**1**; Table 1, Exp. 4 and 5). The TOF, however, is considerably lower in these polymerization reactions. Changing the ligand sphere at the aluminum center to isobutyl (*i*Bu₂AlCH₂PMe₂ (**5**)) impairs the activity for the polymerization of DEVP (Table S27, Exp. 9 and 10). A further increase in the steric demand on the phosphorus atom causes an inactivity towards DEVP under the chosen conditions. Me₂AlCH₂P*t*Bu₂ (**3**) only initiates the polymerization of DMAA with an again lower TOF, and polymeric material with a broad dispersity is received (Table S27, Exp. 13 and 14). Compound **4**, which is additionally equipped with isobutyl groups on the aluminum center, is only active in

neat DMAA with a lower TOF and shows a very low initiator efficiency (Table S27, Exp. 16). Consequently, the steric hindrance of the phosphorus atom has a tremendous impact on the activity, whereas bulkier ligands on the aluminum center seem to decelerate the propagation step, in particular for the more sterically challenging vinylphosphonates. For comparison, we also tested the activity of synthesized B–P BLP **6** towards different Michael-type monomers (Table S27). The inactivity of **6** supports the hypothesis of a GTP mechanism with a fivefold coordinated transition state in the propagation step, which boranes are incapable of.

To our surprise, none of the tested BLPs were able to polymerize methyl methacrylate (MMA) to PMMA, which is highly accessible by established GTP approaches.^[10,19] To understand the underlying mechanism we conducted end-group analysis and ³¹P NMR analysis of the reaction solutions of the oligomerization experiments. For oligomers of DEVP produced by Me₂AlCH₂P*i*Pr₂ (**2**), no methyl or any other end group was detectable using ESI-MS (Figure S17). In the corresponding NMR spectrum, the signals for P(DEVP), for residual monomer, and for the free phosphine MeP*i*Pr₂ were observed. The ³¹P NMR signal of the original compound **2** was no longer apparent (Figure 4). Therefore, the methylene moiety between the heteroatoms seems to be cleaved and afterwards, the free phosphine is released. These results indicate that the polymerization reactions are not initiated according to a GTP or a conjugate addition mechanism but through deprotonation (Figure 1).

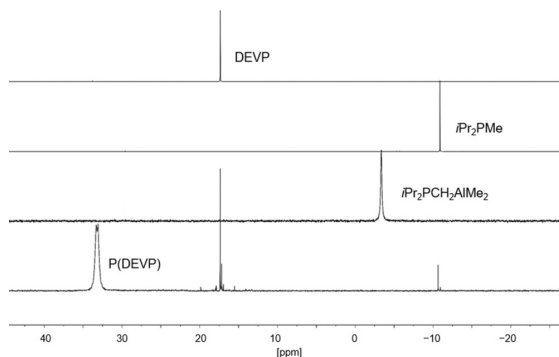


Figure 4. ³¹P NMR spectra of the reaction solution for the oligomerization of DEVP with Me₂AlCH₂P*i*Pr₂ (**2**; bottom) and reference spectra.

Table 1: Catalytic conversion of Michael-type monomers with BLPs.^[a]

Exp.	Mon	Cat.	[Mon]/[Cat.]	<i>t</i> [min]	Y [%] ^[b]	<i>M_n</i> /10 ³ g mol ⁻¹ ^[c]	<i>D</i> (<i>M_w</i> / <i>M_n</i>)	<i>I</i> [%] ^[d]	TOF [h ⁻¹]
1	DEVP	1	500	8	100	250	1.19	33	3700
2	DMAA	1	500	3	100	125	1.52	40	10 000
3	DIVP	1	500	65	100	250	1.05	38	450
4	DEVP	2	500	35	100	290	1.12	28	900
5	DMAA	2	500	4	100	140	1.59	36	3800
6 ^[e]	DMAA- <i>b</i> -DEVP	1	500	10	100	330	1.68	–	–
7 ^[e]	DEVP- <i>b</i> -DIVP	1	500	60	100	575	1.26	–	–
8 ^[f]	MMA	1	100	5	100	230	1.04	4	1200

[a] *V*_{Mon} = 0.5 mL, 4 mL toluene, r.t. [b] Measured gravimetrically and by NMR spectroscopy (¹H, ³¹P). [c] Determined by GPC-MALS in H₂O/THF (9 g L tetrabutylammonium bromide⁻¹) or by GPC-50 in tetrahydrofuran (6 g L tetrabutylammonium bromide⁻¹). [d] Initiator efficiency (*M_n*(theor.)/*M_n*(exp.)). [e] *M*_{Mon1}/*M*_{Mon2} = 1:1. [f] Preactivation of **1** with an equimolar amount of DEVP, after 30 s addition of MMA.

Further evidence for a deprotonation mechanism was established by theoretical calculations. Gas-phase geometry optimization for **1–5** did not show any pronounced elongation of the bond between the axial groups and the aluminum atom. Furthermore, natural bonding orbital (NBO)^[20] analysis on the optimized structures also showed no preferred bond polarization for Me₂AlCH₂PMe₂ relative to the other BLPs. However, NBO charges for the bridging methylene group between the phosphorus and aluminum atoms showed negative values (ca. $-1e$ for the CH₂ group) for **1–5** (see Section 5 in the Supporting Information). Hence, initiation could likely occur by deprotonation of the acidic α -position of the monomer by the partially negatively charged methylene bridge (Scheme 1), followed by its cleavage and release of free phosphine while the dialkylaluminum moiety activates the phosphonate unit. The propagation presumably occurs by a metal-mediated GTP mechanism. This most likely requires a fivefold ligand sphere in the transition state, which is possible for alanes in contrast to boranes.^[10,19,21]

We calculated the Gibbs free reaction enthalpies for the initial endergonic deprotonation step mediated by BLPs **1–5**. Geometry optimization of the intermediates showed the existence of two possible forms, namely a zwitterionic η^1 -ylide and a neutral, thermodynamically favorable η^2 -ylene form (Scheme 1, see also Section 5.1.2.3 in the Supporting Information). All the initiators bearing the sterically least demanding methyl substituents on the aluminum atom (**1–3**) consistently show the lowest Gibbs free reaction enthalpies (yielding the η^2 -ylene form), thereby explaining the experimentally observed higher TOFs for the methyl-substituted initiators.

After a detailed discussion of the mechanism, kinetic investigations with Me₂AlCH₂PPr₂ (**2**) and DEVP showed a living character of the polymerization method. The growth of the molecular weights of the polymer products showed linear dependence upon monomer conversion. The dispersities of the P(DEVP) chains remain narrow over time (Figures 5 and S19). The linear increase in the molecular weights when lowering the catalyst loadings stepwise and ensuring quantitative conversions was further evidence for the living nature enabling block copolymerizations (Figure S18).

The block-type architectures P(DMAA-*b*-DEVP) and P(DEVP-*b*-DIVP) are accessible with BLP **1**, whereas the combinations with reverse monomer order are not possible (Table 1, Exp. 6 and 7, Figures S12–S16). Consequently, the coordination strength of the monomers to the aluminum center has a decisive influence. Whereas **1** is neither active for

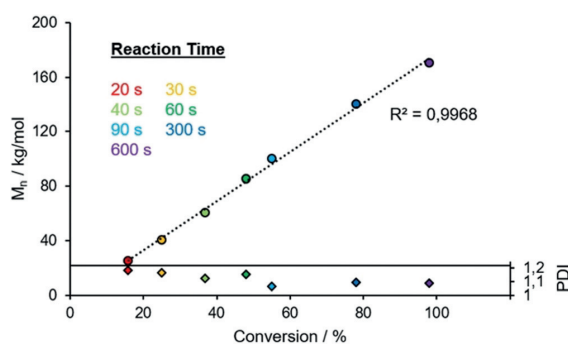


Figure 5. Linear growth of the molecular weight with increasing conversion using the polymerization of DEVP with **2** as an example.

homopolymerization of MMA nor for the block copolymerization of DEVP and MMA, the aforementioned allene-like intermediate is most likely present after a preactivation of the BLP with an equimolar amount of DEVP and can initiate the polymerization of MMA. Since the preactivation as well as the initiator efficiency of **1** is not quantitative, the high molecular weight of P(MMA) can be explained (Table 1, Exp. 6).

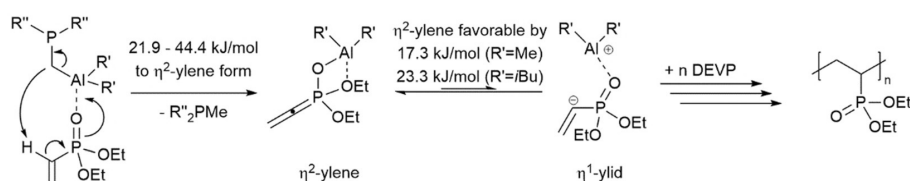
In summary, we were able to show that Al–P-based BLPs act as polymerization initiators of Michael-type monomers, most likely through a deprotonation mechanism. Less steric demand of the substituents at both Al and P is beneficial and the Al–P BLPs combine the benefits of only one initiation pathway with higher activities compared to intermolecular LPs.

Acknowledgements

M.W. is grateful for a scholarship from the Studienstiftung d. dt. Volkes. M.K. is grateful for a FCI scholarship. We acknowledge financial support by the TUM GS and provision of computing time by the LRZ of the Bavarian Academy of Science.

Conflict of interest

The authors declare no conflict of interest.



Scheme 1. Postulated initiation step by a deprotonation mechanism for the polymerization of Michael-type monomers, for example, DEVP, with two possible intermediates (η^2 -ylene and η^1 -ylide).

Keywords: Lewis pairs · Michael-type monomers · neutron diffraction · polymerization · X-ray diffraction

How to cite: *Angew. Chem. Int. Ed.* **2019**, *58*, 9797–9801
Angew. Chem. **2019**, *131*, 9902–9906

- [1] G. C. Welch, R. R. San Juan, J. D. Masuda, D. W. Stephan, *Science* **2006**, *314*, 1124–1126.
- [2] P. Spies, G. Erker, G. Kehr, K. Bergander, R. Fröhlich, S. Grimme, D. W. Stephan, *Chem. Commun.* **2007**, 5072–5074.
- [3] P. A. Chase, G. C. Welch, T. Jurca, D. W. Stephan, *Angew. Chem. Int. Ed.* **2007**, *46*, 8050–8053; *Angew. Chem.* **2007**, *119*, 8196–8199.
- [4] V. Sumerin, F. Schulz, M. Atsumi, C. Wang, M. Nieger, M. Leskelä, T. Repo, P. Pyykkö, B. Rieger, *J. Am. Chem. Soc.* **2008**, *130*, 14117–14119.
- [5] D. Chen, Y. Wang, J. Klankermayer, *Angew. Chem. Int. Ed.* **2010**, *49*, 9475–9478; *Angew. Chem.* **2010**, *122*, 9665–9668.
- [6] a) G. C. Welch, D. W. Stephan, *J. Am. Chem. Soc.* **2007**, *129*, 1880–1881; b) P. Spies, S. Schwendemann, S. Lange, G. Kehr, R. Fröhlich, G. Erker, *Angew. Chem. Int. Ed.* **2008**, *47*, 7543–7546; *Angew. Chem.* **2008**, *120*, 7654–7657; c) P. Spies, R. Fröhlich, G. Kehr, G. Erker, S. Grimme, *Chem. Eur. J.* **2008**, *14*, 333–343; d) T. A. Rokob, A. Hamza, A. Stirling, T. Soós, I. Pápai, *Angew. Chem. Int. Ed.* **2008**, *47*, 2435–2438; *Angew. Chem.* **2008**, *120*, 2469–2472; e) T. A. Rokob, A. Hamza, A. Stirling, I. Pápai, *J. Am. Chem. Soc.* **2009**, *131*, 2029–2036; f) C. M. Mömmling, E. Otten, G. Kehr, R. Fröhlich, S. Grimme, D. W. Stephan, G. Erker, *Angew. Chem. Int. Ed.* **2009**, *48*, 6643–6646; *Angew. Chem.* **2009**, *121*, 6770–6773; g) S. Grimme, H. Kruse, L. Goerigk, G. Erker, *Angew. Chem. Int. Ed.* **2010**, *49*, 1402–1405; *Angew. Chem.* **2010**, *122*, 1444–1447; h) M. Sajid et al., *Chem. Sci.* **2013**, *4*, 213–219.
- [7] Y. Zhang, G. M. Miyake, E. Y.-X. Chen, *Angew. Chem. Int. Ed.* **2010**, *49*, 10158–10162; *Angew. Chem.* **2010**, *122*, 10356–10360.
- [8] a) Y. Zhang, G. M. Miyake, M. G. John, L. Falivene, L. Caporaso, L. Cavallo, E. Y.-X. Chen, *Dalton trans.* **2012**, *41*, 9119–9134; b) J. He, Y. Zhang, L. Falivene, L. Caporaso, L. Cavallo, E. Y.-X. Chen, *Macromolecules* **2014**, *47*, 7765–7774.
- [9] a) M. G. M. Knaus, M. M. Giuman, A. Pöthig, B. Rieger, *J. Am. Chem. Soc.* **2016**, *138*, 7776–7781; b) M. McGraw, E. Y.-X. Chen, *ACS Catal.* **2018**, *8*, 9877–9887; c) Y.-B. Jia, W.-M. Ren, S.-J. Liu, T. Xu, Y.-B. Wang, X.-B. Lu, *ACS Macro Lett.* **2014**, *3*, 896–899; d) Y.-B. Jia, Y.-B. Wang, W.-M. Ren, T. Xu, J. Wang, X.-B. Lu, *Macromolecules* **2014**, *47*, 1966–1972; e) M. Hong, J. Chen, E. Y.-X. Chen, *Chem. Rev.* **2018**, *118*, 10551–10616; f) Y. Bai, J. He, Y. Zhang, *Angew. Chem. Int. Ed.* **2018**, *57*, 17230–17234; *Angew. Chem.* **2018**, *130*, 17476–17480.
- [10] M. Weger, M. M. Giuman, M. G. Knaus, M. Ackermann, M. Drees, J. Hornung, P. J. Altmann, R. A. Fischer, B. Rieger, *Chem. Eur. J.* **2018**, *24*, 14950–14957.
- [11] a) J. C. M. Pereira, M. Sajid, G. Kehr, A. M. Wright, B. Schirmer, Z.-W. Qu, S. Grimme, G. Erker, P. C. Ford, *J. Am. Chem. Soc.* **2014**, *136*, 513–519; b) X. Wang, G. Kehr, C. G. Daniliuc, G. Erker, *J. Am. Chem. Soc.* **2014**, *136*, 3293–3303; c) M. Harhausen, R. Fröhlich, G. Kehr, G. Erker, *Organometallics* **2012**, *31*, 2801–2809; d) Z. Jian, G. Kehr, C. G. Daniliuc, B. Wibbeling, G. Erker, *Dalton trans.* **2017**, *46*, 11715–11721.
- [12] a) J. Rathke, R. Schaeffer, *Inorg. Chem.* **1972**, *11*, 1150–1151; b) H. H. Karsch, A. Appelt, G. Mueller, *Organometallics* **1985**, *4*, 1624–1632; c) F.-G. Fontaine, D. Zargarian, *J. Am. Chem. Soc.* **2004**, *126*, 8786–8794; d) J. Boudreau, M.-A. Courtemanche, F.-G. Fontaine, *Chem. Commun.* **2011**, *47*, 11131–11133; e) J. Boudreau, M.-A. Courtemanche, V. M. Marx, D. Jean Burnell, F.-G. Fontaine, *Chem. Commun.* **2012**, *48*, 11250–11252.
- [13] H. H. Karsch, A. Appelt, F. H. Koehler, G. Mueller, *Organometallics* **1985**, *4*, 231–238.
- [14] F. Bertini, F. Hoffmann, C. Appelt, W. Uhl, A. W. Ehlers, J. C. Slootweg, K. Lammertsma, *Organometallics* **2013**, *32*, 6764–6769.
- [15] F. Bertini, V. Lyaskovskyy, B. J. J. Timmer, F. J. J. de Kanter, M. Lutz, A. W. Ehlers, J. C. Slootweg, K. Lammertsma, *J. Am. Chem. Soc.* **2012**, *134*, 201–204.
- [16] T. Xu, E. Y.-X. Chen, *J. Am. Chem. Soc.* **2014**, *136*, 1774–1777.
- [17] a) N. K. Hansen, P. Coppens, *Acta Crystallogr. Sect. A* **1978**, *34*, 909–921; b) B. Dittrich, C. B. Hübschle, K. Pröpper, F. Dietrich, T. Stolper, J. J. Holstein, *Acta Crystallogr. Sect. B* **2013**, *69*, 91–104.
- [18] a) C. Schwarzenböck, A. Schaffer, E. Nöbner, P. J. Nelson, R. Huss, B. Rieger, *Chem. Eur. J.* **2018**, *24*, 2584–2587; b) N. Mozner, T. Bock, Y. Catel, D. Pospiech, S. Starke, B. Voit, *EP* **3120827**, **2017**.
- [19] H. Yasuda, H. Yamamoto, K. Yokota, S. Miyake, A. Nakamura, *J. Am. Chem. Soc.* **1992**, *114*, 4908–4910.
- [20] A. E. Reed, R. B. Weinstock, F. Weinhold, *J. Chem. Phys.* **1985**, *83*, 735–746.
- [21] S. Salzinger, B. S. Soller, A. Plikhta, U. B. Seemann, E. Herdtweck, B. Rieger, *J. Am. Chem. Soc.* **2013**, *135*, 13030–13040.
- [22] CCDC contain the supplementary crystallographic data for this paper. These data can be obtained free of charge from The Cambridge Crystallographic Data Centre.

Manuscript received: March 6, 2019

Revised manuscript received: April 19, 2019

Accepted manuscript online: May 2, 2019

Version of record online: June 12, 2019

6. Taking Control over the Polymerization of Acrylonitrile with Highly Active Main Group Element Catalysts

Title: “Taking Control over the Polymerization of Acrylonitrile with Highly Active Main Group Element Catalysts”

Status: submitted

Journal: Angew. Chem. Int. Ed.

Publisher: Wiley-VCH

DOI: -

Authors: Michael Weger, Marco M. Giuman, Maximilian G. Knaus, Markus Drees, Alexander Pöthig, Bernhard Rieger^a

Content: The previously presented aluminum organyls and BLPs constitute excellent main group element catalysts for the polymerization of a broad variety of *Michael*-type monomers. Nonetheless, one important of compound is missing in the monomer scope: acrylonitrile, whose polymer is an interesting material in many respects. The highly interacting *Lewis* pairs (LPs) presented already in 2016 were able to polymerize AN with a high initiator efficiency, but the polymerization stopped long before a quantitative conversion. In addition to the obvious deprotonation side reaction, a second competing pathway became evident during the screening for the most fitting LP. The highly acidic *Lewis* acid $\text{Al}(\text{C}_6\text{F}_5)_3$ produced very high molecular weight PAN on extremely short time scales with the drawbacks of low initiator efficiency and broadened dispersities. Diverse mechanistic investigations could not substantiate our initial hypothesis of an aryl transfer to the olefin end of AN, but we tested further catalysts. The well-known Cp-donor MgCp_2 turned out to be the best and highly active option. Its remarkable performance included quantitative conversions of AN over a broad temperature range due to a living behavior, yielding polymers with very narrow molecular weight distributions. End group analysis and DFT calculations again evidenced a main group element GTP mechanism. To the best of our knowledge, MgCp_2 outperforms every previously reported catalyst for the polymerization of AN.

^aM. Weger planned and executed most of the experiments and wrote the manuscript. M. M. Giuman and M. G. Knaus had the initial idea and executed some of the experiments. M. Drees performed all theoretical investigations. A. Pöthig conducted all SC-XRD measurements and managed the processing of the respective data. All work was carried out under the supervision of B. Rieger.

COMMUNICATION

Taming the Polymerization of Acrylonitrile with Highly Active Main Group Element Catalysts

Michael Weger,^[a] Maximilian G. Knaus,^[a] Marco M. Giuman,^[a] Markus Drees,^[b] Alexander Pöthig,^[b] and Bernhard Rieger*^[a]

Abstract: The fast and controlled conversion of acrylonitrile (AN) is still a pending issue in polymerization catalysis. We now demonstrate that simple main group element catalysts enable the synthesis of high molecular weight PAN with very narrow molecular weight distributions on short time scales. Aluminum/phosphorus-based Lewis pairs facilitate the access to defined PAN with shorter chains due to their excellent initiator efficiency, whereas $\text{Al}(\text{C}_6\text{F}_5)_3$ converts AN to very high molecular weight products with extremely high TOFs (up to $110,000 \text{ h}^{-1}$). The easily accessible MgCp_2 performs even better as polymerization catalyst, achieving remarkable dispersities as narrow as 1.13 combined with high TOFs. As evidenced by kinetic studies, the living behavior allows the quantitative consumption of AN. End group analysis supported by DFT calculations clearly suggests the transfer of a Cp ligand to the olefin end of AN as the decisive initiation step.

Carbon fibers comprise a versatile, viable and widely used starting material for composite formation. Due to their high strength and stiffness, carbon fibers have become an integral part of a broad portfolio of high-performance materials. The lightweight properties especially constitute an important benefit over steel or aluminum. Currently, the majority of carbon fibers are produced by the carbonization of poly(acrylonitrile) (PAN).^[1] For industrial applications, the synthesis of PAN is still accomplished via radical polymerization of acrylonitrile (AN). To precisely control the macromolecular parameters and achieve tailor-made properties, living and controlled radical polymerization techniques are the methods of choice on a laboratory scale.^[2] Such controlled radical methods entail the major drawback of low reaction rates. Therefore, catalytic polymerization procedures are believed to be the answer to this problem since these maintain the precision of the polymer architecture while ensuring higher velocities. Surprisingly, the literature provides catalytic polymerization techniques for AN to a lesser extent, although first approaches were established several decades ago.^[3] More recent

concepts for a controlled, catalytic polymerization of AN share the issues of low reaction velocities, broadened molecular weight distributions and requiring rare earth or transition metal-based catalysts.^[4] In addition, main group element-based Lewis pairs (LPs) were already used for the polymerization of AN in the 1970s with moderate success.^[5]

Recently, the LP polymerization method was revived and we demonstrated the controlled polymerization of an expanded scope of *Michael*-type monomers (e.g. methacrylates, acrylamides) catalyzed by highly interacting LPs following a conjugate-addition mechanism.^[6,7] Furthermore, our group found evidence that organoaluminum compounds with adapted Lewis acidity initiate an impressively efficient group transfer polymerization (GTP) process for the same class of monomers.^[8] Within this work, we beneficially transfer the concepts of main group element-mediated LP and GTP to AN which is a member of the *Michael*-type monomers (Figure 1).

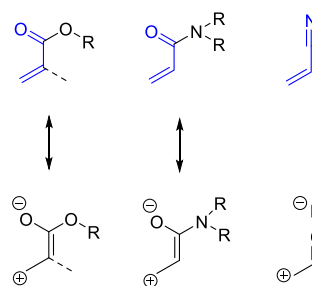


Figure 1. Proposed structural analogy of (meth)acrylates, acrylamides and acrylonitrile.

The investigation started with a detailed screening for the most suitable Lewis acid/base combination. The LP triphenylaluminum (AlPh_3)/trimethyl phosphine (PMe_3) constituted the best system as it has a very high initiator efficiency resulting in a PAN with a molecular weight distribution of 1.49 (Table 1, Exp. 1). However, no complete monomer conversions were able to be achieved for the LP polymerizations of AN (Table S1). This lack of a living polymerization behavior can most likely be substantiated with the existence of a known second initiation pathway, namely the deprotonation of AN by Lewis bases like PMe_3 (Table S1, run 4).^[6] During the initial screening we made an astonishing observation when using tris(pentafluorophenyl)alane ($\text{Al}(\text{C}_6\text{F}_5)_3$) as Lewis acid. The highly acidic compound already initiated the polymerization of AN before the addition of a Lewis base. Even though this pathway seemed to be an undesired side reaction at first, it was

[a] M. Weger, Dr. M. G. Knaus, Dr. M. M. Giuman, Prof. Dr. B. Rieger
Catalysis Research Center & WACKER-Chair of Macromolecular Chemistry
Technical University of Munich
Lichtenbergstraße 4, D-85748 Garching
E-mail: rieger@tum.de

[b] Dr. M. Drees, Dr. A. Pöthig
Catalysis Research Center & Chair of Inorganic and Metal-Organic Chemistry
Technical University of Munich
Lichtenbergstraße 4, D-85748 Garching

Supporting information for this article is given via a link at the end of the document.

COMMUNICATION

Table 1. Synthesis of PAN using different main group element-based catalysts.^[a]

Exp.	Catalyst	[Mon]/[LA]	t / min	Y / % ^[b]	$M_n / 10^3 \text{ g/mol}^{[c]}$	$\bar{D} (M_w/M_n)$	I / % ^[d]	TOF / h ⁻¹
1	AlPh ₃ /PMe ₃ ^[e]	500	10	26	7	1.49	88	800
2	Al(C ₆ F ₅) ₃	4000	0.25	10	140	1.62	15	96,000
3	Al(C ₆ F ₅) ₃	4000	0.5	23	n.d. ^[f]	n.d.	-	110,000
4	MgCp ₂	2000	12	100	185	1.29	57	10,000
5	MgCp ₂	1000	5	100	91	1.13	59	12,000
6	MgCp ₂	1000	27	100	82	1.32	64	2200

[a] $V_{\text{Mon}} = 0.5 \text{ mL}$, $V_{\text{solvent}} = 7.5 \text{ mL}$ *N,N*-DMF, $T = 0 \text{ }^\circ\text{C}$ (except for run 6: $-30 \text{ }^\circ\text{C}$). [b] measured gravimetrically and by ¹H NMR spectroscopy. [c] determined by dual-angle laser light scattering in *N,N*-DMF (2.2 g/L lithium bromide) at 30 $^\circ\text{C}$. [d] initiator efficiency ($M_n(\text{theo.})/M_n(\text{determ.})$). [e] [LA]/[LB] = 2:1, [f] $M_w = 700 \text{ kg/mol}$ determined by multi-angle laser light scattering.

then examined in greater detail revealing an enormous activity of Al(C₆F₅)₃ (turnover frequencies (TOF) > 100,000 h⁻¹, Table 1, Exp. 2). The molecular weight distribution of the obtained polymer was in the same range as for the LP polymerizations. This finding was even more surprising since our previously presented aluminum half-metallocenes produced solely oligomers in the polymerization of the *Michael*-type monomer AN (Table S1, run 7). From 30 seconds onwards, the molecular weights for the Al(C₆F₅)₃ induced polymerization started to exceed the exclusion volume of our GPC column. However, with the use of multi-angle laser light scattering, the weight-averaged molecular weight (M_w) of these ultra-high molecular weight samples was able to be determined. With a higher monomer to catalyst ratio of 8000:1, the molecular weight was actually able to be raised over a level of 1,000,000 g/mol until the reaction ran into viscosity limitations (Table S1, run 6). These exceptionally high molecular weights were caused by the low initiator efficiency of Al(C₆F₅)₃. To gain more insights into the initiation mechanism, we isolated the product of the coordination of AN to Al(C₆F₅)₃ at $-30 \text{ }^\circ\text{C}$ in toluene. Since this structure is believed to be the first intermediate of an initiation process, a single crystal X-ray diffraction study was performed (Figure 2). The aluminum center bears two monomer molecules in the axial positions of a trigonal bipyramidal coordination sphere which is one of the rare examples of a fivefold coordinated Al(III) aryl-based organometallic compound without chelating ligands.^[9] However, the structure does not correspond to the eight-membered ring intermediate which is characteristically found as the propagating species in GTP reactions.^[10]

To corroborate our experimental findings, we performed quantum chemical calculations at the B3LYP/6-31+G** theory level based on the assumption of the single crystal X-ray diffraction study. It was possible to find an energetically feasible reaction pathway for the aryl transfer from Al(III) to the olefin end of the coordinated AN monomer. We determined this crucial, energy demanding barrier to be 54.8 kcal mol⁻¹ in terms of ΔG^\ddagger ($\Delta H^\ddagger = 50.0 \text{ kcal mol}^{-1}$), while the reaction free energy of the resulting intermediate is $-11.3 \text{ kcal mol}^{-1}$ ($\Delta H = -11.0 \text{ kcal mol}^{-1}$, see ESI, section 4). Consequently, the high molecular masses of the PAN products are in line with the significantly high activation barrier, which causes a low initiator efficiency.

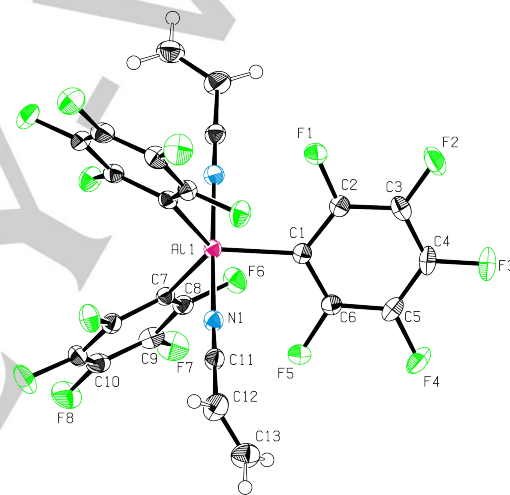


Figure 2. Molecular structure of the Al(C₆F₅)₃-acrylonitrile adduct in the solid state, determined by single crystal X-ray analysis (CCDC 1056884 contains the supplementary crystallographic data. These data can be obtained free of charge by The Cambridge Crystallographic Data Centre).

Furthermore, the polymerizations induced by Al(C₆F₅)₃ proceeded solely with *N,N*-dimethylformamide (*N,N*-DMF) as the solvent. The expected precipitation polymerization in solvents like toluene or tetrahydrofuran did not take place, which also suggested an alternative initiation mechanism. To recapitulate, Lewis pairs initiate a highly efficient polymerization of AN prone to side reactions, whereas Al(C₆F₅)₃ enables the synthesis of high molecular PAN products on very short time scales with an unclear initiation mechanism.

To combine a controlled polymerization process and high reaction velocities, we addressed magnesocene (MgCp₂) in addition to aluminum compounds. The donor of cyclopentadienyl (Cp) ligands known in literature is an interesting candidate for the coordinative polymerization of AN.^[11] Initial polymerization experiments conducted under comparable conditions resulted in

COMMUNICATION

PAN with a dispersity of 1.30 which is a quite good value with respect to the highly reactive monomer (Table 1, Exp. 4). In addition to the improved initiator efficiency compared to the values of $\text{Al}(\text{C}_6\text{F}_5)_3$, MgCp_2 enabled a quantitative consumption of AN for the first time. The TOF is somewhat diminished, but still remarkably high with $10,000 \text{ h}^{-1}$. When lowering the monomer to catalyst ratio, a very narrow molecular mass distribution of 1.13 was achieved (Table 1, Exp. 4). MgCp_2 maintained the high activity over a broad temperature range and ensured a quantitative conversion of AN (Table 1, Exp. 4, Table S1, runs 8–10). Additionally, the experiments catalyzed by MgCp_2 demonstrated a solvent independent process as the expected precipitation polymerization occurs in toluene or tetrahydrofuran. Subsequently, the end groups of purified short chained PAN produced by MgCp_2 were analyzed by matrix-assisted laser desorption/ionization time-of-flight (MALDI-TOF) mass spectrometry. Both spectra of the PAN polymerized at 0°C and -30°C exhibit only series of signals with a Cp moiety as the end group (Figures S1, S2). During kinetic experiments, the growth of the molecular weights of the polymer products showed linear dependence upon monomer conversion. The dispersities of the PAN chains remained narrow over time. Further evidence for the living nature of the polymerizations was the linear increase of the molecular weights when lowering the MgCp_2 loadings stepwise and ensuring quantitative conversions (Figures S3 – S5). End group analysis as well as kinetic studies strongly advocate a GTP initiation mechanism.

To rationalize the experimental observations, a different set of quantum chemical calculations was performed. The density functional theory (DFT) calculations were conducted starting from MgCp_2 and from $\text{MgCp}_2\text{-}N,N\text{-DMF}$ adduct, respectively. It was possible in both cases to find a feasible reaction pathway for the presumed initiation step which is a nucleophilic Cp transfer to the olefin end of the coordinated monomer (Figure 3). In the case of MgCp_2 , the coordination of AN was determined to be endergonic ($\Delta H = 8.1 \text{ kcal mol}^{-1}$, Figure 3, **2a**). The energy barrier for the nucleophilic aryl transfer was optimized to $36.3 \text{ kcal mol}^{-1}$ in terms of ΔG^\ddagger ($\Delta H^\ddagger = 23.4 \text{ kcal mol}^{-1}$) and the reaction free energy of the resulting intermediate **3a** to $18.1 \text{ kcal mol}^{-1}$ ($\Delta H = 8.16 \text{ kcal mol}^{-1}$).

For the $\text{MgCp}_2\text{-}N,N\text{-DMF}$ adduct, both the coordination of the solvent and the monomer resulted in an endergonic process ($\Delta H = 3.7$ and $9.5 \text{ kcal mol}^{-1}$ Figure 3, **1** and **2b**). The energy barrier for the nucleophilic aryl transfer was even lower with $28.7 \text{ kcal mol}^{-1}$ in terms of ΔG^\ddagger ($\Delta H^\ddagger = 5.5 \text{ kcal mol}^{-1}$), while the reaction free energy of the resulting intermediate **3b** was optimized to $7.0 \text{ kcal mol}^{-1}$ ($\Delta H = -13.3 \text{ kcal mol}^{-1}$). The barriers in both cases are significantly lower than for the hypothetical mechanism stated for $\text{Al}(\text{C}_6\text{F}_5)_3$ and provide an explanation for the improved initiator efficiencies. Calculations for the deprotonation of the α -acidic AN showed a considerably higher barrier, thus excluding this possibly concurring pathway (see ESI, section 4). More importantly, these theoretical investigations highlight the postulation of a main group element GTP mechanism analogous to the rare earth metal catalyzed GTP.^[8,10]

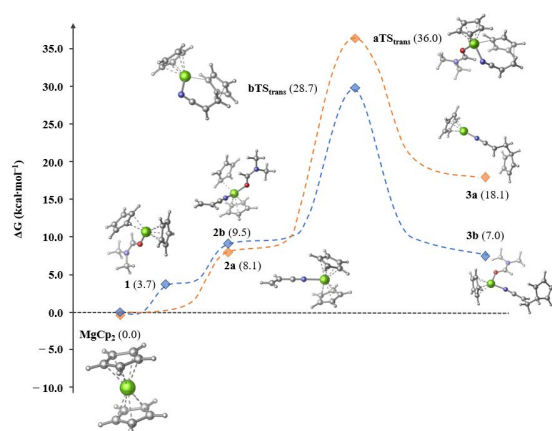


Figure 3. Energy profile of the initiation step starting from MgCp_2 (orange) and from $\text{MgCp}_2\text{-}N,N\text{-DMF}$ adduct (blue).

We reported herein on different main group element catalysts for the controlled polymerization of the scientifically as well as industrially important acrylonitrile. Since the aluminum-/phosphorus-based Lewis pairs were persuasive with high initiator efficiencies, the highly active Lewis acid $\text{Al}(\text{C}_6\text{F}_5)_3$ converted AN to very high molecular weight polymers. Furthermore, we utilized the easily accessible MgCp_2 as catalyst. This proved to be the best and most balanced approach because MgCp_2 quantitatively polymerizes AN with surprisingly narrow molecular weight distributions on a short time scale. End group and kinetic analysis pointed to a living group transfer process as the crucial initiation mechanism. This is strongly supported by theoretical calculations which delivered explanations for the good initiator efficiencies. To our knowledge, MgCp_2 represents the best catalyst thus far for the controlled polymerization of AN.

Acknowledgements

M.W. is grateful for a scholarship from the Studienstiftung des deutschen Volkes. M.K. is grateful for a FCI scholarship. We gratefully acknowledge financial support by the TUM GS and provision of computing time by the LRZ of the Bavarian Academy of Science.

Keywords: Poly(acrylonitrile) • Polymerization • Homogeneous Catalysis • Main Group elements • Density Functional Calculations

- [1] a) E. Frank, L. M. Steudle, D. Ingildeev, J. M. Spörl, M. R. Buchmeiser, *Angew. Chem. Int. Ed.* **2014**, *53*, 5262; b) E. A. Morris, M. C. Weisenberger in *ACS Symposium Series* (Eds.: A. K. Naskar, W. P. Hoffman), American Chemical Society, Washington, DC, **2014**, pp. 189–213.
- [2] a) M. Kamigaito, T. Ando, M. Sawamoto, *Chem. Rev.* **2001**, *101*, 3689; b) K. Matyjaszewski, *Macromolecules* **2012**, *45*, 4015; c) K.

COMMUNICATION

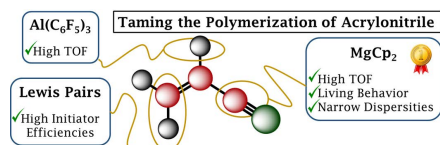
- Matyjaszewski, N. V. Tsarevsky, *Nature Chem.* **2009**, *1*, 276; d) K. Matyjaszewski, N. V. Tsarevsky, *J. Am. Chem. Soc.* **2014**, *136*, 6513.
- [3] a) A. Yamamoto, S. Ikeda, *J. Am. Chem. Soc.* **1967**, *89*, 5989; b) M. Ikeda, T. Hirano, A. Uchida, T. Tsuruta, *Makromol. Chem.* **1974**, *175*, 2039.
- [4] a) K. C. Hultsch, T. P. Spaniol, J. Okuda, *Angew. Chem. Int. Ed.* **1999**, *38*, 227; b) K. Nozaki, S. Kusumoto, S. Noda, T. Kochi, L. W. Chung, K. Morokuma, *J. Am. Chem. Soc.* **2010**, *132*, 16030; c) F. Schaper, S. R. Foley, R. F. Jordan, *J. Am. Chem. Soc.* **2004**, *126*, 2114; d) F. Wu, S. R. Foley, C. T. Burns, R. F. Jordan, *J. Am. Chem. Soc.* **2005**, *127*, 1841; e) E. Y.-X. Chen, *Chem. Rev.* **2009**, *109*, 5157; f) N. C. Billingham, P. D. Lees, *Makromol. Chem.* **1993**, *194*, 1445; g) U. Siemeling, L. Kölling, A. Stammer, H.-G. Stammer, E. Kaminski, G. Fink, *Chem. Commun.* **2000**, 1177; h) K. Tsuchihara, Y. Suzuki, M. Asai, K. Soga, *Chem. Lett.* **1999**, 28, 891.
- [5] a) M. Ikeda, T. Hirano, S. Nakayama, T. Tsuruta, *Makromol. Chem.* **1974**, *175*, 2775; b) M. Ikeda, T. Hirano, T. Tsuruta, *Makromol. Chem.* **1971**, *150*, 127.
- [6] M. G. M. Knaus, M. M. Giuman, A. Pöthig, B. Rieger, *J. Am. Chem. Soc.* **2016**, *138*, 7776.
- [7] Y. Zhang, G. M. Miyake, E. Y.-X. Chen, *Angew. Chem. Int. Ed.* **2010**, *49*, 10158.
- [8] M. Weger, M. M. Giuman, M. G. Knaus, M. Ackermann, M. Drees, J. Hornung, P. J. Altmann, R. A. Fischer, B. Rieger, *Chem. Eur. J.* **2018**, *24*, 14950.
- [9] a) G. Ménard, D. W. Stephan, *Dalton Trans.* **2013**, *42*, 5447; b) M.-C. Chen, J. A. S. Roberts, T. J. Marks, *Organometallics* **2004**, *23*, 932.
- [10] H. Yasuda, H. Yamamoto, K. Yokota, S. Miyake, A. Nakamura, *J. Am. Chem. Soc.* **1992**, *114*, 4908.
- [11] J. D. Fisher, M.-Y. Wei, R. Willett, P. J. Shapiro, *Organometallics* **1994**, *13*, 3324.

COMMUNICATION

Entry for the Table of Contents

Layout 2:

COMMUNICATION



Michael Weger, Maximilian G. Knaus,
Marco M. Giuman, Markus Drees,
Alexander Pöthig, and Bernhard Rieger*

Page No. – Page No.

**Taming the Polymerization of
Acrylonitrile with Highly Active Main
Group Element Catalysts**

Calm down, acrylonitrile! The desired precision polymerization of acrylonitrile can be achieved using different main group element-systems. MgCp₂ proved to be the superior catalyst, enabling narrow dispersities and a living behavior combined with high TOFs. Experimental as well as theoretical investigations revealed the transfer of a Cp ligand as the crucial initiation step.

7. Isospecific Group-Transfer Polymerization of Diethyl Vinylphosphonate and Multidimensional NMR Analysis of the Polymer Microstructure

Title: “Isospecific Group-Transfer Polymerization of Diethyl Vinylphosphonate and Multidimensional NMR Analysis of the Polymer Microstructure”

Status: Article, published online September 11, 2019

Journal: *Macromolecules*, 2019, 52, 7073 – 7080

Publisher: American Chemical Society

DOI: 10.1021/acs.macromol.9b01326

Authors: Michael Weger,[‡] Philipp Pahl,[‡] Fabian Schmidt,[‡] Benedikt S. Soller, Philipp J. Altmann, Alexander Pöthig, Gerd Gemmecker, Wolfgang Eisenreich,* Bernhard Rieger^{*,a}

Content: After establishing various catalysts for the precision polymerization of *Michael*-type monomers, it seemed natural to develop a methodology for controlling the stereoregularity of the polymers. We decided to focus on the thermoresponsive PDEVp, as the synthesis and the analysis of stereoregular PDEVp is poorly studied in the literature. We applied the well-known CGC ligands to synthesize the aluminum complexes and their yttrium pendants. The SC-XRD measurements of these compounds demonstrated differences in the molecular structures which later played a decisive role for the stereocontrol mechanism. Detailed polymerization studies revealed the superiority of the yttrium CGCs and the NMR spectra of the resulting polymers showed disparities dependent on the central atom of the catalyst used. Despite obstructive scalar ${}^nJ_{\text{PH}}$ and ${}^nJ_{\text{PC}}$ couplings, we were able to conduct a reliable signal assignment for the backbone signals with 2D- and 3D-NMR methods. The yttrium catalysts synthesized highly isotactic PDEVp, likely following an enantiomorphic site-control mechanism, whereas the aluminum complexes produced less defined polymers.

[‡] These authors contributed equally; * Corresponding authors; ^aM. Weger and F. Schmidt planned and executed all the experiments for the aluminum catalysts, M. Weger wrote the manuscript. P. Pahl planned and executed all the experiments for the yttrium catalysts. B. S. Soller had the initial idea and contributed with valuable intellectual input. P. J. Altmann and A. Pöthig conducted all SC-XRD measurements and managed the processing of the respective data. W. Eisenreich and M. Weger developed the NMR methods with the help of G. Gemmecker and managed the processing of the respective data. All work was carried out under the supervision of W. Eisenreich and B. Rieger.

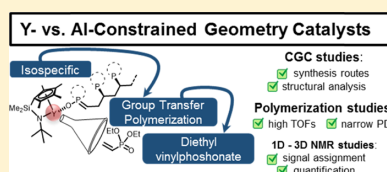
Isospecific Group-Transfer Polymerization of Diethyl Vinylphosphonate and Multidimensional NMR Analysis of the Polymer Microstructure

Michael Weger,^{†,‡} Philipp Pahl,^{†,‡} Fabian Schmidt,^{†,‡} Benedikt S. Soller,[†] Philipp J. Altmann,[‡] Alexander Pöthig,[‡] Gerd Gemmecker,[§] Wolfgang Eisenreich,^{*,||} and Bernhard Rieger^{*,†,‡}

[†]Catalysis Research Center & WACKER-Chair of Macromolecular Chemistry, [‡]Catalysis Research Center & Chair of Inorganic and Metal-Organic Chemistry, [§]Bavarian NMR Center, and ^{||}Chair of Biochemistry, Technical University of Munich, Lichtenbergstraße 4, D-85747 Garching, Germany

Supporting Information

ABSTRACT: Control of stereoregularity is an integral part of a precision polymerization method and for the development of functional materials. Yttrium- and aluminum-based catalysts are known for converting diethyl vinylphosphonate (DEVPh) into its stimuli-responsive polymer in a precise but stereoirregular way. Herein, we present Y- and Al-based constrained geometry complexes (CGCs) to induce isotacticity without losing control over other macromolecular parameters. After having established convenient synthesis routes and detailed structural analyses, these CGCs showed exceedingly high turn-over frequencies (up to 45 000 h⁻¹) in the group-transfer polymerization of DEVPh. The initiator efficiencies ($\leq 99\%$) and dispersities (≤ 1.02) strongly depended on the substitution pattern of the applied ligands. An analysis of the microstructure using multidimensional NMR (¹H–¹H and ¹H–¹³C(–³¹P)) correlation experiments demonstrated significant disparities for the stereospecificity of the CGCs and enabled a reliable signal assignment. The yttrium catalysts produced highly isotactic poly(diethyl vinylphosphonate), likely following a chain-end control mechanism, whereas the aluminum complexes produced less defined polymers.



INTRODUCTION

Precision polymerization is the major requirement for developing smart polymeric materials whose properties are reversibly switchable by physical or chemical stimuli. Group-transfer polymerization (GTP) represents a common method for the controlled conversion of acrylic monomers.^{1,2} It was already established several decades ago using silyl ketene acetals as initiators combined with an additional catalyst.³ In 1992, Yasuda et al. presented a further important GTP approach based on single-component, rare earth metal-mediated catalysis (REM-GTP).⁴

REM-GTP constitutes the most effective polymerization method for poly(dialkyl vinylphosphonates), which are known for various application areas.^{5–12} Especially, poly(diethyl vinylphosphonate) (PDEVPh) was extensively investigated, resulting in a wide variety of suitable REM-GTP catalysts.^{13–17} Detailed mechanistic investigations for the different initiation pathways and the propagation step of the polymerization of DEVPh revealed an exceptionally fast, precise, and living behavior to easily adjust the polymer properties.^{18,19} In particular, the widely tunable lower critical solution temperature of PDEVPh and its copolymers attracted serious attention.²⁰ Block copolymers with 2-vinylpyridine self-assembled into multiresponsive micelles, leading to the synthesis of a biocompatible and water-soluble material that can be further functionalized for biomedical applications.^{21–23}

In addition to the REM-GTP approaches, organoaluminum compounds enabled main group-catalyzed GTP of DEVPh following a Yasuda-like polymerization mechanism.²⁴

Even though the tacticity of polymers can significantly influence their properties,²⁵ the synthesis and analysis of stereoregular PDEVPh were scarcely investigated till now.^{26–28} For example, the so-called constrained geometry catalysts (CGCs) were already successfully applied in the polymerization of methyl methacrylate (MMA) and α -olefins, enabling high iso- and syndiotacticity.^{29–34} CGCs comprise linked cyclopentadienyl (Cp)-amido ligands and differ from bridged metallocene complexes in their sterically more accessible amido ligand and electronic configuration. Therefore, these well-known types of ligands seem to be promising candidates for the stereospecific polymerization of DEVPh.

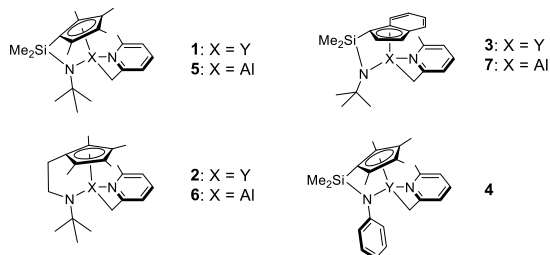
Since MMA and DEVPh belong to the class of Michael-type monomers, we synthesized the yttrium and aluminum CGCs depicted in Chart 1. These novel compounds were tested in the polymerization of DEVPh, and the tacticity of the resulting polymers was investigated by multidimensional NMR spectroscopy.

Received: June 26, 2019

Revised: August 23, 2019

Published: September 11, 2019

Chart 1. Overview of the Yttrium- and Aluminum-Based CGCs Used (Hapticities Assumed)



RESULTS AND DISCUSSION

We started our study with the synthesis and structural characterization of the CGCs. Since the synthesis of bridged RE complexes via salt metathesis can be affected by purification issues,^{35,36} we decided to take the route via simple alkane elimination of tetramethylsilane from the one-step reaction of $Y(CH_2TMS)_3(thf)_2$ and the corresponding ligand.³⁷ We used four different ligands to investigate the influence of the substitution pattern on the activity and stereospecificity in the polymerization reactions (Chart 1). The remaining $-CH_2TMS$ moiety was exchanged with 2,6-lutidine due to its higher efficiency as an initiating group (Table S9). REM catalysts equipped with the highly basic $-CH_2TMS$ moiety were shown to deprotonate DEVP as a side reaction during the initiation, whereas pyridine derivatives as initiating ligands exhibited unprecedented initiation rates because of an exclusive group-transfer pathway and mechanistic match between initiation and propagation.^{16,18} Additionally, the convenient C–H bond activation of these pyridine derivatives proceeds quantitatively via σ -bond metathesis.³⁸ After these straightforward synthesis steps, we confirmed the molecular structures of the yttrium CGCs **1** and **3** via single-crystal X-ray diffraction (XRD) (Scheme 1a and Figure S3). Compound **3** showed the expected dimeric structure, whereas **1** was obtained as a tetrahydrofuran (THF) adduct, arising from

residual THF in the crystallization solution. An η^5 -geometry was observed for the Cp as well as for the indenyl ring.

For the synthesis of the corresponding aluminum CGCs, a salt metathesis is the method of choice because aluminum alkyls cannot undergo C–H bond activation with cyclopentadienes.³⁹ Therefore, we synthesized (2,6-lutidynyl)aluminum dichloride and deprotonated the linked Cp-amido ligands with di-*n*-butylmagnesium (Scheme 1b). After the following successful salt metathesis reaction, we were able to obtain the solid-state structures of **5** and **7** via single-crystal XRD (Scheme 1 and Figure S5). Both compounds crystallized as dimers, with the respective nitrogen atom of the lutidynyl moiety coordinating to the adjacent aluminum center. The addition of THF to a solution of **5** in C_6D_6 led to the formation of a THF adduct by break up of the dimeric species monitored using diffusion-ordered NMR spectroscopy (DOSY) (Figure S1). This process suggests that the more strongly coordinating DEVP can break up the dimers during the initiation reaction. In contrast to yttrium CGCs and in accordance with the aluminum CGC known in the literature,³⁹ the Cp derivatives exhibit a hapticity of one. This feature of aluminum Cp compounds refers to a major difference in the steric and electronic situations.

When applied as catalysts for the polymerization reaction, the CGCs showed significant differences in their performance, depending on their substitution pattern and the central atom. PDEVPP produced with CGC **1** showed a very narrow molecular weight distribution independent of the reaction temperature (Table 1, runs 1–4). Enormous turn-over frequencies (TOFs) combined with high initiator efficiencies were observed for this catalyst down to -30 °C. By conducting the polymerization reaction at -78 °C, the activity and the initiator efficiency were significantly decreased while maintaining a narrow molecular dispersity. Catalyst **1** was the only one that exhibited such a high activity over a broad temperature range and could quantitatively convert DEVP at low temperatures on such a short timescale. The aluminum-based counterpart **5** polymerizes DEVP with a noticeably lower TOF and a broadened dispersity (Table 1, run 8). When changing the linker unit of the ligand to an ethylene moiety (**2**), the

Scheme 1. Two Different Routes to Yttrium (a) and Aluminum (b) CGCs Shown by the Illustrative Synthesis of **1 and **5** and Their Corresponding Molecular Structures in the Solid State as Determined by Single-Crystal XRD**

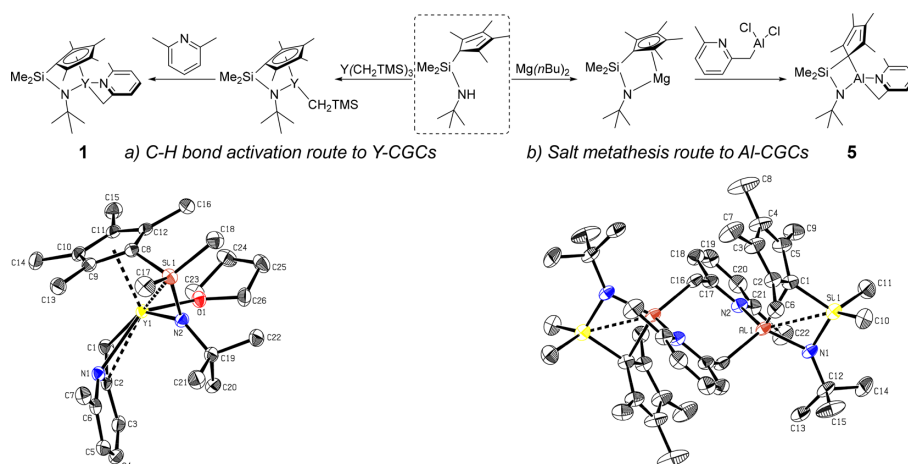


Table 1. Catalytic Conversion of DEVP with the Synthesized CGCs^a

run	catalyst	T/°C	t/min	yield/% ^b	M _n /kg/mol ^c	D (M _w /M _n)	I/% ^d	mmm/% ^e	TOF/h ⁻¹
1	1	30	0.4	100	49	1.02	99	68	45 000
2	1	0	0.9	100	50	1.03	98	85	20 000
3	1	-30	2	100	54	1.02	91	90	9000
4	1	-78	20	100	67	1.10	73	>98	900
5	2	30	0.8	100	250	1.48	38	73	23 000
6	3	30	45	66	22	1.85	^f		
7	4	30	3	100	130	1.26	47	88	6000
8	5	30	45	56	165	1.44	17	^g	200
9	6	30	45	traces					
10	7	30	45	79	200	1.73	19	^g	300

^aV_{DEVP} = 1.0 mL, V_{toluene} = 20 mL, [M]/[CGC] = 300/1. ^bMeasured gravimetrically and by NMR spectroscopy (³¹P NMR spectroscopy). ^cDetermined by GPC-MALS in H₂O/THF (9 g/L tetrabutylammonium bromide). ^dInitiator efficiency (M_{n(theo.)}/M_{n(determ.)}). ^eDetermined by deconvolution of ¹H{³¹P} NMR spectra (see the Supporting Information). ^fFalsified by oligomeric side products. ^gQuantification impossible due to strong signal overlapping, indicating low *mmm* content.

molecular weight distribution and activity were negatively influenced (Table 1, run 5). Due to the considerably lower initiator efficiency and the resulting higher molecular weights, no detailed temperature screening was performed.

The aluminum equivalent 6 was not even able to produce high-molecular PDEVP under the chosen conditions and was only active with a lower amount of solvent (Table 1, run 9; Table S1, run 4). In the literature, dimethylsilane bridges are discussed as being preferable over the two-membered ethylene connection because they provide higher rigidity, ideal bite angle, and favorable electronic characteristics for the metallocene-catalyzed migratory insertion polymerization reactions (Figure 1).^{30,40,41} Also, for the GTP of DEVP, we observed a

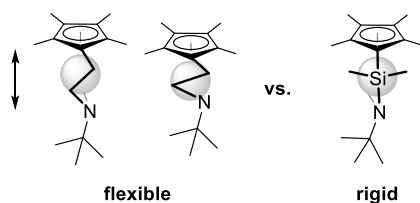


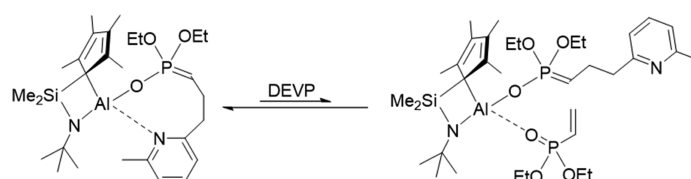
Figure 1. Higher flexibility for ethylene bridges in comparison to the corresponding silyl bridge.

strong positive impact of the silyl bridge, resulting in higher initiator efficiencies and narrower dispersities. Therefore, no further ligands with an ethylene linking unit were synthesized. The variation of the Cp derivative led us to the synthesis of complexes 3 and 7 substituted with indenyl ligands. This emerged as the sole case in which the aluminum catalyst outperformed the yttrium pendant. Whereas CGC 7 catalyzes the polymerization in a similar way to 5, the yttrium CGC 3 oligomerized DEVP (Table 1, runs 6 and 10). This weak performance is in accordance with the low yields in the

complex synthesis and the known lability of the precursor, which likely impairs the polymerization activity.⁴² The influence of the ligand sphere at the amido moiety was solely checked for the yttrium catalysts due to their superiority over the Al-CGCs. Compound 4 was again highly active for the polymerization of DEVP but could not reach the level of CGC 1, whose ligand system proved ideal when considering the requirements of a controlled polymerization process.

The mechanism of the REM-GTP of DEVP with methyl pyridines as initiating ligands has already been thoroughly investigated and revealed a six-electron as well as an eight-electron process as possible initiation pathways (Scheme S1).¹⁶ The living polymerization behavior was evidenced for Table 1, run 3 by the linear dependence of the molecular weights upon monomer conversion as well as upon stepwise variation of the catalyst loadings (Figures S11–S13). Since the initiation reaction for the aluminum-mediated GTP was previously studied only for half-metallocenes,²⁴ we conducted end-group and kinetic analyses (see the Supporting Information, Section 3). The electrospray ionization mass spectrometry (ESI-MS) performed on purified short-chained oligomers produced by CGC 5 confirmed the expected nucleophilic transfer of the lutidynil ligand to the monomer. Furthermore, no signals were detected for an alternative reaction pathway such as the deprotonation reaction. The reaction order with respect to the catalyst as well as to the monomer was determined to be one in both cases. Although the aluminum-catalyzed polymerization reactions proceed at much slower pace, the linear dependence of the molecular weight of the polymer products upon monomer conversion underlines the living character. Based on these experiments and the previous work, the aluminum-based CGCs most likely follow a polymerization mechanism, analogous to their yttrium pendants. The low initiator efficiencies of the aluminum CGCs and the broadened dispersities presumably arise from a comparatively stable

Scheme 2. Proposed Active Species for the Initiation Reaction Mediated by the Aluminum CGCs



species after the initial transfer of the lutidynyl moiety (Scheme 2). The nitrogen atom of the heteroaromatic ring coordinates stronger to the aluminum center than to the yttrium equivalent and occupies the crucial coordination site. This likely results in dormant species and time-delayed propagation.

Since the aluminum half-metallocenes already produced PDEVP with somewhat broader dispersities and lower TOFs,²⁴ the activity was further diminished when applying the bulkier ligands presented herein. These seem not to be particularly suitable for the small aluminum cation (effective ionic radius 53.5 pm). In contrast, the yttrium center (effective ionic radius 90 pm) is well accessible despite the high steric demand, resulting in exceptional activities and a confined propagation reaction.⁴³

Analyzing the PDEVP microstructure by NMR spectroscopy led us to additional disparities between the yttrium- and the aluminum-mediated GTP. We started with the comparison of the ¹H NMR spectra of the polymers produced by CGCs 1 and 5, which solely differ in their central atom, at 30 °C (Table 1, runs 1 and 8). While the PDEVP synthesized by the aluminum-based catalyst showed signals very similar to those of previously produced polymers, the spectrum of the PDEVP catalyzed by 1 demonstrated a significant change of the different signal sets in the backbone region (Figures 2I,a and

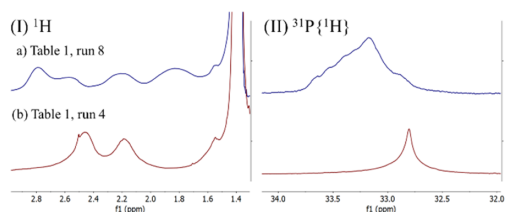


Figure 2. ¹H and ³¹P{¹H} NMR spectra of the PDEVP backbone of selected samples in MeOD₄.

S21). The polymer received at -78 °C delivered an even more simplified spectrum (Figure 2I,b). Its ³¹P{¹H} spectrum showed only one signal that was relatively sharp and slightly upfield shifted (Figure 2II). The ¹³C{¹H} NMR traces (Figure 3) confirmed the tendency, thus calling for a careful analysis of the stereoregularity.

To analyze the tacticity of PDEVP, we started a two-dimensional (2D) NMR study using the polymer produced by CGC 1 at -78 °C due to its simple splitting pattern. To

simplify the explanations, the polymer produced by CGC 5 at 30 °C (Table 1, run 8) is referred as polymer A and the one produced by CGC 1 at -78 °C as polymer B. The phosphonate moiety directly bound to the polymer backbone made the analysis more challenging. Depending on the magnitude, the scalar ⁿJ_{PH} and ⁿJ_{PC} couplings caused additional line broadening or splitting. Moreover, the couplings mentioned are passive in ¹H-¹H and ¹H-¹³C correlation experiments provoking signal splitting. In contrast to PDMVP, the signals of the PDEVP backbone overlapped with the methyl moiety of the ester side chains, further complicating the analysis.⁴⁴ We obtained initial indications for the signal assignments by phase-sensitive ¹H-¹³C-correlated DEPT-edited HSQC spectra.

In the case of polymer B, the signal at δ(¹H) = 2.46 ppm and δ(¹³C) = 30.9 ppm can be attributed to the methine group (Figure 3). This is supported by the coupling constant of ~139 Hz determined from the carbon NMR spectrum, which corresponds to the literature value of the ¹J_{PC} coupling.⁴⁵ The proton signal is additionally broadened due to the passive ²J_{PH} coupling. To ensure this assignment, we applied a ¹H-¹³C-³¹P triple-resonance HCP 2D experiment edited by J_{PC} = 20 Hz that suppressed the strong ¹J_{PC} coupling and only the correlations in the range of J_{PC} = 20 Hz remained detectable (acquisition parameters and further details can be found in Table S10). The result was an even simpler spectrum with two major proton backbone signals and no more methine group signal left (Figure S15). Therefore, the signals with δ(¹H) > 2.35 ppm belong to the methine group of the PDEVP backbone. In contrast, the methine region of polymer A shows a considerably more complicated splitting in the ¹³C{¹H} NMR spectra. Also, the at least two methine proton signals in the HSQC spectrum are caused by a less defined polymer microstructure (Figure 3).

In the HSQC spectrum of B, there remains only one carbon resonance with two magnetically nonequivalent protons, which is characteristic for a methylene moiety in a *meso* (*m*) diad. On the contrary, three carbon signals of this type can be distinguished in the spectrum of polymer A. The values Δδ, δ(¹H), and δ(¹³C) help us to assign the signals to the three possible tetrads *mmm*, *mmr*, *rmr*, as clear trends can be found for the methylene region of structurally similar acrylic polymers.^{44,46–50} Therefore, the increasing chemical shift difference enables the assignment of δ(¹³C) = 27.5 ppm (δ(¹H) = 1.55 and 2.14 ppm) to *mmm*, δ(¹³C) = 29.7 ppm (δ(¹H) = 1.49 and 2.19 ppm) to *mmr*, and δ(¹³C) = 31.8 ppm

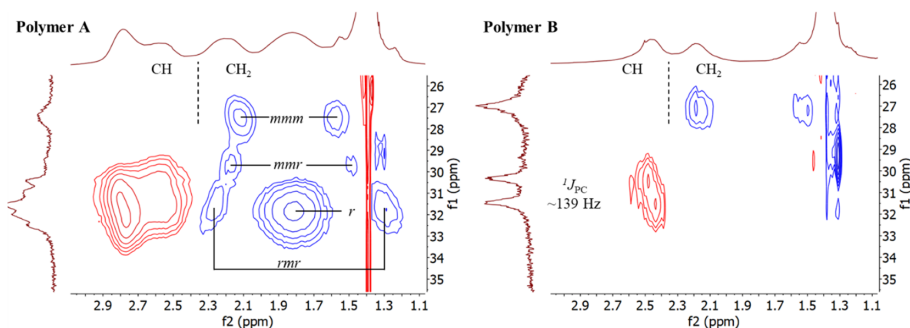


Figure 3. Phase-sensitive ¹H-¹³C DEPT-edited HSQC spectra of polymers A and B in MeOD₄. An assignment to tetrads and diads, respectively, was performed for the methylene signals.

($\delta(^1\text{H}) = 1.25$ and 2.27 ppm) to *mr*. The broad signal at $\delta(^{13}\text{C}) = 31.8$ ppm and $\delta(^1\text{H}) = 1.82$ ppm represents the magnetically equivalent methylene protons of the racemic (*r*) diad (Figure 3). A comparison of the two HSQC spectra indicates the high isotacticity of polymer B.

For the identification of the methine triads, we recorded TOCSY $\{^{31}\text{P}\}$ NMR spectra with a short mixing time to minimize long distance magnetization transfer. Since the methine protons directly couple with the neighboring methylene groups ($^3J_{\text{HH}}$) in *m* and *r* configurations, the cross peak at 2.57 ppm derives from the *mr* triad and the one at 2.78 ppm from the *rr* triad in the spectrum of polymer A (Figure 4).

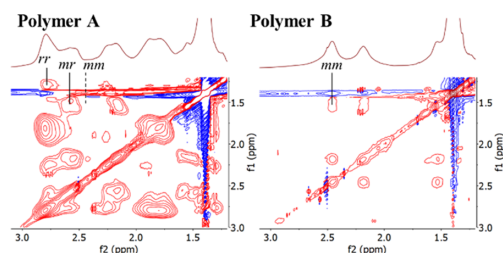


Figure 4. TOCSY $\{^{31}\text{P}\}$ NMR spectra of polymers A and B in MeOD₄. An assignment to triads was performed for the methine signals.

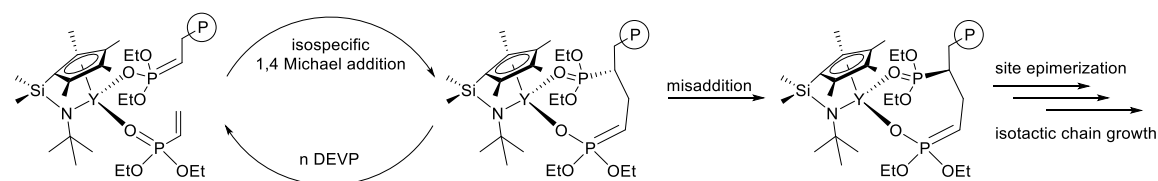
According to the literature regarding PDMVP, the *mm* triad should be more high-field shifted, but it can be hardly identified at 2.46 ppm in this case. To provide a more detailed assignment, we applied a ^1H - ^{13}C - ^{31}P triple-resonance HCP three-dimensional (3D) experiment, this time edited by $J_{\text{PC}} = 110$ Hz to observe the methine region. By performing a closer investigation of the H-C slices in the 3D spectrum of A, the *rr* triad ($\delta(^1\text{H}) = 2.78$ ppm) could be assigned to $\delta(^{13}\text{C}) = 31.2$ ppm for $\delta(^{31}\text{P}) = 33.5$ ppm and the *mr* triad ($\delta(^1\text{H}) = 2.57$ ppm) to $\delta(^{13}\text{C}) = 30.7$ ppm for $\delta(^{31}\text{P}) = 32.7$ ppm (Figure S31). The *mm* triad ($\delta(^1\text{H}) = 2.46$ ppm), which is hardly identifiable in the spectra of A, correlated in the 3D spectrum of B with $\delta(^{13}\text{C}) = 30.9$ ppm for the slice $\delta(^{31}\text{P}) = 32.8$ ppm (Figure S16, acquisition parameters and pulse program can be found in Tables S11 and S12). Since the TOCSY $\{^{31}\text{P}\}$ spectrum of B only shows the cross peaks of the *mm* triad and the *mmm* tetrads, a high degree of isotacticity for this PDEVP is evidenced, which is strongly supported by the ^1H - ^{13}C - ^{31}P correlation experiments. In general, the results of this NMR study are in accordance with a previous work, which used isotactic-enriched PDEVP with broad dispersities.²⁷ Additionally, differential scanning calorimetry (DSC) analysis showed a melting point for the highly isotactic polymer B unlike for A and the previously presented isotactic-enriched

ones (Figures S18 and S32). As expected, thermogravimetric analysis revealed no influence of the main chain tacticity on the temperatures of the two-step decomposition process (Figures S19 and S33).

Since the signal of PDEVP in $^{31}\text{P}\{^1\text{H}\}$ spectra shows an undefined splitting pattern and the methylene and methine regions in the $^{13}\text{C}\{^1\text{H}\}$ NMR spectra overlap for polymers with less defined microstructures, we applied a deconvolution method for the $^1\text{H}\{^{31}\text{P}\}$ spectra of the respective samples to quantify the degree of isotacticity. To minimize the overlapping of the signals, we recorded the $^1\text{H}\{^{31}\text{P}\}$ spectra on a 600 MHz spectrometer instead of the 400 MHz instrument, which was used for the signal assignment described above (see the Supporting Information, Section 4). As expected, the CGC 1 produces highly isotactic PDEVP at low temperatures (Table 1, runs 3 and 4) combined with very narrow molecular mass distributions and impressive initiator efficiencies. The proportion of *mmm* tetrads decreases with the increase in polymerization temperature, suggesting that the stereocontrol mechanism is less prone to errors at low temperatures (Table 1, runs 1 and 2). Surprisingly, the ligand sphere of CGC 4 constitutes a further improvement in the stereospecificity, resulting in a highly isotactic polymer even at room temperature (Table 1, run 7). However, this catalyst exhibits a lower activity, control, and initiator efficiency compared to those of 1. During the analysis of tacticity, it became once clearer that the silyl-bridge-containing complexes outperform the catalysts with ethylene-bridged ligands and are the method of choice for the desired highly active yttrium CGCs. In contrast, the aluminum pendants could not generate isotactic-enriched PDEVP microstructures. Due to the complexity of the spectra, we refrained from a precise quantification. The most likely explanation lies in the completely different electronic situations at the aluminum center and the concomitant hapticity of one for the Cp derivatives, which cannot enable a distinct stereocontrol mechanism.

For the elucidation of the stereocontrol mechanism mediated by the yttrium CGCs, we investigated the stereoerrors in the triad distributions. The CGCs 1 and 4 produce isotactic PDEVP with predominantly isolated *r* diad stereoerrors (...*mmmmrmmmm*...), as the abundance of the *rr* triad is extremely low. A possible pathway leading to such a *r*-type stereoerror could be a misaddition that is followed by catalyst-site epimerization, most likely leading to stereoblock PDEVP (Scheme 3). This points to an apparent isospecific chain-end control of these C_s -ligated catalysts. The polymerization with CGC 1 at low temperature (-78 °C) complied best with the necessary conditions for this probable mechanism. It is literature known that the chain-end control nature of coordination polymerization is more sensitive to the polymerization temperature, as compared to the site control one, which

Scheme 3. Proposed Stereocontrol Mechanism and Formation of Stereoerrors for the Isospecific Polymerization of DEVP Depicted with CGC 1



explains the strong temperature-depending stereospecificity of CGC **1**.⁵¹ Contrary to results of CGC **1** and **4**, the polymer produced by CGC **2** exhibits a more difficult triad distribution, which is attributed to a mixture of stereocontrol mechanisms caused by the more flexible ethylene linker in the ligand. A more detailed study of the stereocontrol mechanism including theoretical calculations is part of an ongoing research by our group.

The highly isotactic polymer **B** was additionally hydrolyzed to poly(vinyl phosphonic acid) (PVPA) according to a procedure from the literature.¹⁴ Even though the saponification was not quantitative, a comparison of the NMR spectra with radically produced PVPA revealed that the tacticity is apparently not affected by the hydrolysis (Figure S36). Therefore, stereoregular copolymers P(DEVP-co-VPA) can be synthesized, and as the GTP presented herein shows a living behavior, novel and precise co- and terpolymers are accessible. This enables the development of a wide range of smart polymeric materials using the stimuli-responsive and biocompatible PDEVP as a starting point.

CONCLUSIONS

We reported herein on highly active constrained geometry catalysts for the precise and stereoregular polymerization of DEVP. Suitable routes were established for the synthesis of yttrium as well as aluminum CGCs, and the purity of the novel compounds was confirmed by NMR, elemental, and single-crystal XRD analyses. A detailed study of the polymerization activities revealed the superiority of the yttrium catalysts and the importance of the ligand design. A thorough investigation of the polymer microstructure using ¹H–¹H and ¹H–¹³C (–³¹P) correlation experiments confirmed and expanded the literature-known signal assignment for PDEVP and evidenced a high degree of isotacticity for the samples produced by the yttrium CGCs. The proposed chain-end control mechanism explains the isospecific yttrium-mediated catalysis and contributes the last missing link in the understanding of the precise GTP of DEVP. The yttrium CGCs enable a fast, controlled, and, for the first time, stereoregular conversion of DEVP. Furthermore, the living polymerization behavior combined with the biocompatibility and stimuli responsivity opens up a high-precision pathway, enabling various smart materials.

ASSOCIATED CONTENT

Supporting Information

The Supporting Information is available free of charge on the ACS Publications website at DOI: 10.1021/acs.macromol.9b01326.

Experimental procedures; crystallographic data; polymerization studies and mechanism elucidation; further analytical and characterization data for polymers; ¹H DOSY NMR spectra; Ortep drawing with 50% ellipsoids for compounds **1**, **3**, **5**, and **7**; ESI-MS spectra of DEVP oligomers; DSC and thermogravimetric analysis; ¹H–³¹P NMR spectra; ¹H NMR spectra (PDF)

Compound **1** (CIF)

Compound **1** (PDF)

Compound **3** (CIF)

Compound **3** (PDF)

Compound **5** (CIF)

Compound **5** (PDF)

Compound **7** (CIF)

Compound **7** (PDF)

AUTHOR INFORMATION

Corresponding Authors

*E-mail: wolfgang.eisenreich@mytum.de (W.E.).

*E-mail: rieger@tum.de (B.R.).

ORCID

Alexander Pöthig: 0000-0003-4663-3949

Bernhard Rieger: 0000-0002-0023-884X

Author Contributions

¹M.W., P.P., and F.S. contributed equally.

Notes

The authors declare no competing financial interest.

ACKNOWLEDGMENTS

M.W. is grateful for a generous scholarship from the Studienstiftung des deutschen Volkes. We thank Deutsche Forschungsgemeinschaft (DFG) for financial support (project number 387680803). The authors thank Sergei I. Vagin, Thomas Pehl, Peter T. Altenbuchner, Stephan Salzinger, and Alexander Kronast for valuable discussions; Felix Getner, Florian Tschernuth, and Dmitri Starkov for their support on the preparative work; and Stefan Burger for his help with the thermal analysis.

ABBREVIATIONS

CGC, constrained geometry catalyst/complex; Cp, cyclopentadiene; DEPT, distortionless enhancement by polarization transfer; DEVP, diethyl vinylphosphonate; DMVP, dimethyl vinylphosphonate; ESI-MS, electrospray ionization mass spectrometry; GTP, group-transfer polymerization; HSQC, heteronuclear single quantum coherence spectroscopy; MMA, methyl methacrylate; TOCSY, total correlation spectroscopy; TOF, turn-over frequency; VPA, vinyl phosphonic acid

REFERENCES

- (1) Adams, F.; Pahl, P.; Rieger, B. Metal-Catalyzed Group-Transfer Polymerization: A Versatile Tool for Tailor-Made Functional (Co)Polymers. *Chem. - Eur. J.* **2018**, *24*, 509–518.
- (2) Chen, E. Y.-X. Coordination polymerization of polar vinyl monomers by single-site metal catalysts. *Chem. Rev.* **2009**, *109*, 5157–5214.
- (3) Webster, O. W.; Hertler, W. R.; Sogah, D. Y.; Farnham, W. B.; RajanBabu, T. V. Group-transfer polymerization. 1. A new concept for addition polymerization with organosilicon initiators. *J. Am. Chem. Soc.* **1983**, *105*, 5706–5708.
- (4) Yasuda, H.; Yamamoto, H.; Yokota, K.; Miyake, S.; Nakamura, A. Synthesis of monodispersed high molecular weight polymers and isolation of an organolanthanide(III) intermediate coordinated by a penultimate poly(MMA) unit. *J. Am. Chem. Soc.* **1992**, *114*, 4908–4910.
- (5) Banks, M.; Ebdon, J. R.; Johnson, M. The flame-retardant effect of diethyl vinyl phosphonate in copolymers with styrene, methyl methacrylate, acrylonitrile and acrylamide. *Polymer* **1994**, *35*, 3470–3473.
- (6) Berber, M. R.; Fujigaya, T.; Nakashima, N. High-Temperature Polymer Electrolyte Fuel Cell Using Poly(vinylphosphonic acid) as an Electrolyte Shows a Remarkable Durability. *ChemCatChem* **2014**, *6*, 567–571.
- (7) Berber, M. R.; Fujigaya, T.; Sasaki, K.; Nakashima, N. Remarkably Durable High Temperature Polymer Electrolyte Fuel Cell Based on Poly(vinylphosphonic acid)-doped Polybenzimidazole. *Sci. Rep.* **2013**, *3*, No. 1764.

- (8) Deng, N.; Ni, X.; Shen, Z. Syntheses and properties of amphiphilic poly (diethyl vinylphosphonate-co-2-chloroethyl methacrylate) copolymers. *Des. Monomers Polym.* **2015**, *18*, 470–478.
- (9) Ellis, J.; Wilson, A. D. The formation and properties of metal oxide poly(vinylphosphonic acid) cements. *Dent. Mater.* **1992**, *8*, 79–84.
- (10) Ellis, J.; Anstice, M.; Wilson, A. D. The glass polyphosphonate cement: A novel glass-ionomer cement based on poly(vinyl phosphonic acid). *Clin. Mater.* **1991**, *7*, 341–346.
- (11) Magnusson, C. D.; Liu, D.; Chen, E. Y.-X.; Kelland, M. A. Non-Amide Kinetic Hydrate Inhibitors: Investigation of the Performance of a Series of Poly(vinylphosphonate) Diesters. *Energy Fuels* **2015**, *29*, 2336–2341.
- (12) Tan, J.; Gemeinhart, R. A.; Ma, M.; Saltzman, W. M. Improved cell adhesion and proliferation on synthetic phosphonic acid-containing hydrogels. *Biomaterials* **2005**, *26*, 3663–3671.
- (13) Altenbuchner, P. T.; Soller, B. S.; Kissling, S.; Bachmann, T.; Kronast, A.; Vagin, S. I.; Rieger, B. Versatile 2-Methoxyethylaminobis(phenolate)yttrium Catalysts: Catalytic Precision Polymerization of Polar Monomers via Rare Earth Metal-Mediated Group Transfer Polymerization. *Macromolecules* **2014**, *47*, 7742–7749.
- (14) Salzinger, S.; Seemann, U. B.; Plikhta, A.; Rieger, B. Poly(vinylphosphonate)s Synthesized by Trivalent Cyclopentadienyl Lanthanide-Induced Group Transfer Polymerization. *Macromolecules* **2011**, *44*, 5920–5927.
- (15) Seemann, U. B.; Dengler, J. E.; Rieger, B. High-molecular-weight poly(vinylphosphonate)s by single-component living polymerization initiated by rare-earth-metal complexes. *Angew. Chem., Int. Ed.* **2010**, *49*, 3489–3491.
- (16) Soller, B. S.; Salzinger, S.; Jandl, C.; Pöthig, A.; Rieger, B. C–H Bond Activation by σ -Bond Metathesis as a Versatile Route toward Highly Efficient Initiators for the Catalytic Precision Polymerization of Polar Monomers. *Organometallics* **2015**, *34*, 2703–2706.
- (17) Zhang, N.; Salzinger, S.; Deubel, F.; Jordan, R.; Rieger, B. Surface-initiated group transfer polymerization mediated by rare earth metal catalysts. *J. Am. Chem. Soc.* **2012**, *134*, 7333–7336.
- (18) Salzinger, S.; Soller, B. S.; Plikhta, A.; Seemann, U. B.; Herdtweck, E.; Rieger, B. Mechanistic studies on initiation and propagation of rare earth metal-mediated group transfer polymerization of vinylphosphonates. *J. Am. Chem. Soc.* **2013**, *135*, 13030–13040.
- (19) Soller, B. S.; Sun, Q.; Salzinger, S.; Jandl, C.; Pöthig, A.; Rieger, B. Ligand Induced Steric Crowding in Rare Earth Metal-Mediated Group Transfer Polymerization of Vinylphosphonates: Does Enthalpy Matter? *Macromolecules* **2016**, *49*, 1582–1589.
- (20) Zhang, N.; Salzinger, S.; Rieger, B. Poly(vinylphosphonate)s with Widely Tunable LCST: A Promising Alternative to Conventional Thermoresponsive Polymers. *Macromolecules* **2012**, *45*, 9751–9758.
- (21) Adams, F.; Altenbuchner, P. T.; Werz, P. D. L.; Rieger, B. Multiresponsive micellar block copolymers from 2-vinylpyridine and dialkylvinylphosphonates with a tunable lower critical solution temperature. *RSC Adv.* **2016**, *6*, 78750–78754.
- (22) Schwarzenböck, C.; Schaffer, A.; Nöbner, E.; Nelson, P. J.; Huss, R.; Rieger, B. Fluorescent Polyvinylphosphonate Bioconjugates for Selective Cellular Delivery. *Chem. - Eur. J.* **2018**, *24*, 2584–2587.
- (23) Schwarzenböck, C.; Schaffer, A.; Pahl, P.; Nelson, P. J.; Huss, R.; Rieger, B. Precise synthesis of thermoresponsive polyvinylphosphonate-biomolecule conjugates via thiol–ene click chemistry. *Polym. Chem.* **2018**, *9*, 284–290.
- (24) Weger, M.; Giuman, M. M.; Knaus, M. G.; Ackermann, M.; Drees, M.; Hornung, J.; Altmann, P. J.; Fischer, R. A.; Rieger, B. Single-Site, Organometallic Aluminum Catalysts for the Precise Group Transfer Polymerization of Michael-Type Monomers. *Chem. - Eur. J.* **2018**, *24*, 14950–14957.
- (25) Chang, L.; Woo, E. M. Tacticity effects on glass transition and phase behavior in binary blends of poly(methyl methacrylate)s of three different configurations. *Polym. Chem.* **2010**, *1*, 198–202.
- (26) Soller, B. S.; Salzinger, S.; Rieger, B. Rare Earth Metal-Mediated Precision Polymerization of Vinylphosphonates and Conjugated Nitrogen-Containing Vinyl Monomers. *Chem. Rev.* **2016**, *116*, 1993–2022.
- (27) Rabe, G. W.; Komber, H.; Häussler, L.; Kreger, K.; Lattermann, G. Polymerization of Diethyl Vinylphosphonate Mediated by Rare-Earth Tris(amide) Compounds. *Macromolecules* **2010**, *43*, 1178–1181.
- (28) Pahl, P. Synthese funktionaler Polymere mittels Seltenerdmetall-mediierter Gruppentransferpolymerization. Dissertation, TU München, 2018 (As P. Pahl could not reproduce the isotactic-enriched microstructures of PDEVP stated in ref. 27 in his PhD Thesis, we started the present project to establish a reliable stereoregular synthesis of PDEVP and to verify the NMR signal assignments.).
- (29) Braunschweig, H.; Breitling, F. M. Constrained geometry complexes—Synthesis and applications. *Coord. Chem. Rev.* **2006**, *250*, 2691–2720.
- (30) McKnight, A. L.; Waymouth, R. M. Group 4 ansa-Cyclopentadienyl-Amido Catalysts for Olefin Polymerization. *Chem. Rev.* **1998**, *98*, 2587–2598.
- (31) Shapiro, P. J.; Bunel, E.; Schaefer, W. P.; Bercaw, J. E. Scandium complex $[\{(\eta^5\text{-C}_5\text{Me}_4)\text{Me}_2\text{Si}(\eta^1\text{-NCMe}_3)\}(\text{PMe}_3)\text{ScH}]_2$: a unique example of a single-component α -olefin polymerization catalyst. *Organometallics* **1990**, *9*, 867–869.
- (32) Shapiro, P. J.; Schaefer, W. P.; Labinger, J. A.; Bercaw, J. E.; Cotter, W. D. Model Ziegler-Natta α -Olefin Polymerization Catalysts Derived from $[\{(\eta^5\text{-C}_5\text{Me}_4)\text{SiMe}_2(\eta^1\text{-NCMe}_3)\}(\text{PMe}_3)\text{Sc}(\mu\text{-H})]_2$ and $[\{(\eta^5\text{-C}_5\text{Me}_4)\text{SiMe}_2(\eta^1\text{-NCMe}_3)\}(\mu\text{-CH}_2\text{CH}_2\text{CH}_3)]_2$. Synthesis, Structures, and Kinetic and Equilibrium Investigations of the Catalytically Active Species in Solution. *J. Am. Chem. Soc.* **1994**, *116*, 4623–4640.
- (33) Nguyen, H.; Jarvis, A. P.; Lesley, M. J. G.; Kelly, W. M.; Reddy, S. S.; Taylor, N. J.; Collins, S. Isotactic Polymerization of Methyl Methacrylate Using a Prochiral, Zirconium Enolate Initiator. *Macromolecules* **2000**, *33*, 1508–1510.
- (34) Rodriguez-Delgado, A.; Mariott, W. R.; Chen, E. Y.-X. Living and Syndioselective Polymerization of Methacrylates by Constrained Geometry Titanium Alkyl and Enolate Complexes. *Macromolecules* **2004**, *37*, 3092–3100.
- (35) Evans, W. J.; Seibel, C. A.; Ziller, J. W. Unsolvated Lanthanide Metallocene Cations $[(\text{C}_5\text{Me}_5)_2\text{Ln}][\text{BPh}_4]$: Multiple Syntheses, Structural Characterization, and Reactivity Including the Formation of $(\text{C}_5\text{Me}_5)_3\text{Nd}^+$. *J. Am. Chem. Soc.* **1998**, *120*, 6745–6752.
- (36) Tilley, T. D.; Andersen, R. A. Pentamethylcyclopentadienyl derivatives of the trivalent lanthanide elements neodymium, samarium, and ytterbium. *Inorg. Chem.* **1981**, *20*, 3267–3270.
- (37) Hultsch, K. C.; Spaniol, T. P.; Okuda, J. Half-Sandwich Alkyl and Hydrido Complexes of Yttrium: Convenient Synthesis and Polymerization Catalysis of Polar Monomers. *Angew. Chem., Int. Ed.* **1999**, *38*, 227–230.
- (38) Kaneko, H.; Nagae, H.; Tsurugi, H.; Mashima, K. End-functionalized polymerization of 2-vinylpyridine through initial C–H bond activation of N-heteroaromatics and internal alkenes by yttrium ene-diamido complexes. *J. Am. Chem. Soc.* **2011**, *133*, 19626–19629.
- (39) Pietryga, J. M.; Gorden, J. D.; Macdonald, C. L. B.; Voigt, A.; Wiacek, R. J.; Cowley, A. H. Main Group “Constrained Geometry” Complexes. *J. Am. Chem. Soc.* **2001**, *123*, 7713–7714.
- (40) Herrmann, W. A.; Rohrmann, J.; Herdtweck, E.; Spaleck, W.; Winter, A. The First Example of an Ethylene-Selective Soluble Ziegler Catalyst of the Zirconocene Class. *Angew. Chem., Int. Ed.* **1989**, *28*, 1511–1512.
- (41) Spaleck, W.; Kueber, F.; Winter, A.; Rohrmann, J.; Bachmann, B.; Antberg, M.; Dolle, V.; Paulus, E. F. The Influence of Aromatic Substituents on the Polymerization Behavior of Bridged Zirconocene Catalysts. *Organometallics* **1994**, *13*, 954–963.
- (42) Hultsch, K. C.; Voth, P.; Beckerle, K.; Spaniol, T. P.; Okuda, J. Single-Component Polymerization Catalysts for Ethylene and Styrene: Synthesis, Characterization, and Reactivity of Alkyl and Hydrido Yttrium Complexes Containing a Linked Amido–Cyclopentadienyl Ligand. *Organometallics* **2000**, *19*, 228–243.

(43) Shannon, R. D. Revised effective ionic radii and systematic studies of interatomic distances in halides and chalcogenides. *Acta Crystallogr., Sect. A: Found. Adv.* **1976**, *32*, 751–767.

(44) Komber, H.; Steinert, V.; Voit, B. ¹H, ¹³C, and ³¹P NMR Study on Poly(vinylphosphonic acid) and Its Dimethyl Ester. *Macromolecules* **2008**, *41*, 2119–2125.

(45) Berger, S.; Braun, S.; Kalinowski, H.-O. *NMR Spectroscopy of the Non-Metallic Elements*; John Wiley & Sons: New York, 1996.

(46) Beshah, K. Sequential assignments of polymers by 2D NMR techniques: application to stereochemical configuration assignment of poly(acrylic acid). *Makromol. Chem.* **1993**, *194*, 3311–3321.

(47) Chang, C.; Muccio, D. D.; St. Pierre, T. Determination of the tacticity and analysis of the pH titration of poly(acrylic acid) by proton and carbon-13 NMR. *Macromolecules* **1985**, *18*, 2154–2157.

(48) Kawamura, T.; Toshima, N.; Matsuzaki, K. Assignment of finely resolved ¹³C NMR spectra of poly(methyl methacrylate). *Makromol. Chem., Rapid Commun.* **1993**, *14*, 719–724.

(49) Kawamura, T.; Toshima, N.; Matsuzaki, K. Assignment of finely resolved ¹³C NMR spectra of polyacrylates. *Macromol. Chem. Phys.* **1995**, *196*, 3415–3424.

(50) Spěváček, J.; Suchopárek, M.; Al-Alawi, S. Characterization of the stereochemical structure of poly(acrylic acid) by one- and two-dimensional ¹³C-¹H nuclear magnetic resonance spectra. *Polymer* **1995**, *36*, 4125–4130.

(51) Chen, E. Y.-X. Transformation of polymerization of polar vinyl monomers by discrete and hybrid metal catalysts. *Dalton Trans.* **2009**, *41*, 8784–8793.

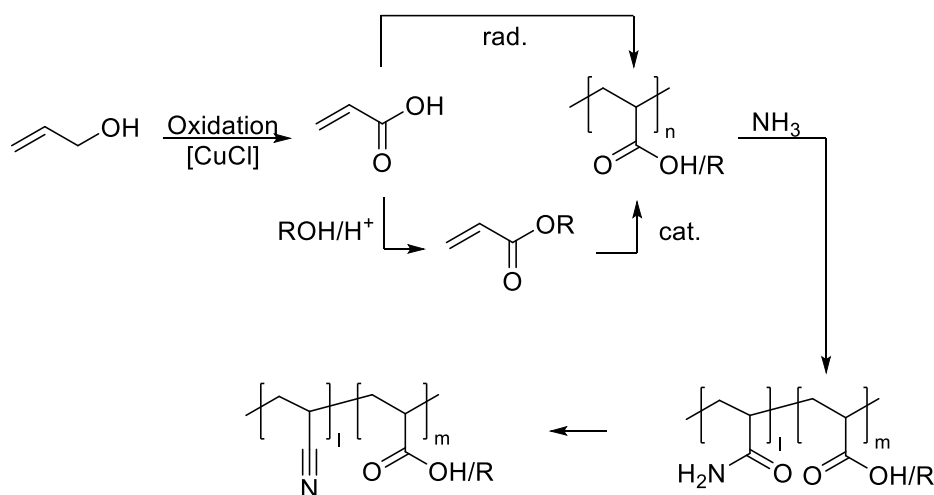
8. Excursus: Polymer-Analogous Reactions as Novel and Controlled Pathway to Polyacrylonitrile and its Well Adjustable Copolymers

Most of the produced carbon fibers are based on the carbonization of PAN. The required monomer AN is almost exclusively obtained from fossil resources, namely *via* the SOHIO process.^[97] In search of an alternative carbon source, glycerol synthesized by algae, seems to be a suitable feedstock worth pursuing. With respect to the three carbon backbone of AN, glycerol was already reported as a potential starting material. One pathway is its dehydration to acrolein, also a compound of industrial interest.^[98] A second pathway proceeds *via* the deoxydehydration of glycerol with formic acid to form allyl alcohol with high yields.^[99] In fact, acrolein as well as allyl alcohol are considered as potentially interesting intermediates for the production of AN. Both can be converted to the desired monomer *via* ammoxidation over heterogeneous redox catalysts.^[100]

Nowadays, AN is exclusively polymerized radically for industrial applications. To achieve precision of the macromolecular parameters and tailor-made properties, living and controlled radical polymerization techniques are the methods of choice. Using catalytic polymerization techniques would allow overcoming the low reaction rates, the major drawback of controlled radical methods, while maintaining the precision of the polymer architecture. Additionally, the control of the stereoregularity should be facilitated which is still an unsolved issue for the synthesis of high molecular weight PAN. Here, we propose a completely new polymer-analogous approach to PAN homo- and copolymer architectures starting from glycerol.

In the production of AN from glycerol, allyl alcohol is a straight forward intermediate. Similar to a broad range of primary alcohols, also allyl alcohol can be easily and selectively oxidized to acrylic acid under ambient conditions (Scheme 12).^[101] Acrylic acid or rather its polymers could be an approach to the synthesis of PAN, skipping the isolation and purification procedures of the toxic monomer AN. The radical polymerization of acrylic acid is a possible pathway as well as the simple esterification of acrylic acid under acidic conditions. The corresponding acrylate monomers can be applied in catalytic polymerization reactions by considering the aforementioned advantages. The resulting poly(acrylates) are modified by amidation with ammonia gas. Subsequently, the amide moieties of the copolymer should undergo a thermally or chemically induced dehydration reaction to PAN (Scheme 12). Additionally, the emerging copolymers of AN with acrylates will have some beneficial effects. As copolymers with acrylic acid facilitate the cyclization of the nitrile moieties, copolymers with esters of the acrylic acid

ensure an enhanced meltability.^[102] Therefore, different classes of copolymers will be synthesized and optimized for their use as precursor for carbon fibers. In conclusion, this route provides a sustainable and novel route to PAN and to a family of AN/acrylate copolymers, that could impact the polymer processability and the properties of the resulting fiber materials.



Scheme 12. Polymer analogous strategy to PAN and its acrylate copolymers.

The results for this excursus were obtained in collaboration with the two master's thesis students *Jonas Breitsameter* and *Waldemar Schmidt*. A compilation of the successfully performed experiments is presented on the following pages in form of a paper draft which is not yet ready to publish. In particular, the precision polymerization of the acrylates as well as the synthesis of acrylic acid starting from glycerol is still missing and are part of ongoing research in our group.



Journal Name

ARTICLE

Polymer-analogous reactions as novel and controlled pathway to polyacrylonitrile and its well adjustable copolymers

J. M. Breitsameter,^a M. Weger,^a W. Schmidt^a and B. Rieger^{a*}

Received 00th January 20xx,
Accepted 00th January 20xx

DOI: 10.1039/x0xx00000x

www.rsc.org/

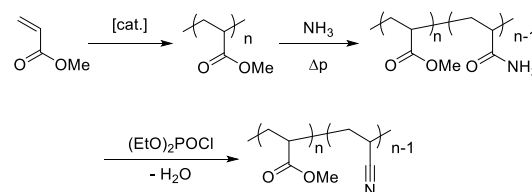
Herein we present a polymer-analogous pathway to poly(acrylonitrile) starting from poly(methyl acrylate). The synthesis begins with a pressurized reaction with ammonia which makes poly(methyl acrylate-co-acrylamide) copolymers with defined compositions accessible. The copolymers thus obtained can then be dehydrated with diethyl chlorophosphate yielding in poly(methyl acrylate-co-acrylonitrile) copolymers. NMR analysis shows that the dehydration is mild enough to prevent the hydrolysis of the methyl acrylate units which makes the method very convenient. The investigation of the thermal properties of different poly(MA-co-AN) copolymers reveals that the methyl acrylate moieties in the copolymer initiate the cyclization of the nitrile groups while heating.

Introduction

Post-polymerization modifications, also known as polymer-analogous reactions (PARs), arguably always were present since the beginnings of polymer science. Nowadays widely used materials like Rayon and rubber tires emerged from early-discovered PARs. With the discovery of the nitration of cellulose by Braconnot in 1833 as starting point, modified fibers from cellulose were finally recognized for the application as textile fiber in 1884.^{1,2} Recent studies are not only focused on the modification natural macromolecules, but on a wide variety of synthetic polymers. For the synthesis of functional polymers, PARs are today an interesting approach. Polymer functionalizations range from active esters over epoxides to pentafluorophenyl click or Thiol-yne acetal click linkers.^{3,4} Besides introducing functional groups, PARs allow to synthesize polymers which are not accessible directly from the monomer. Poly(vinyl alcohol) for example can only be obtained by the hydrolysis of poly(vinyl esters) such as poly(vinyl acetate).⁵ Polyacrylonitrile (pAN) and its copolymers are nowadays widely applied as starting material for fiber syntheses. Since pAN was thought to be insoluble comonomers were necessary in order to provide solubility. Even after finding suitable organic solvents for the homopolymer, pAN copolymers are often used to improve physical properties.⁶ The beneficial effect of copolymerizing pAN with different comonomers is also utilized for the carbon fiber precursor production. The addition of comonomers such as methyl acrylate or itaconic acid results in a higher quality carbon fiber since dipolar forces responsible for hindrances in molecular alignment during fiber spinning are reduced.⁷ Until now, such copolymers are almost exclusively produced by radical copolymerization.⁸ In order to achieve a

defined polymer in terms of molecular weight and weight distribution, controlled radical polymerization can be utilized.⁹ The major drawback here are the low reaction rates which can be overcome by using catalytic/coordinative polymerization procedures while maintaining the precision of the polymer architecture. In literature coordinative polymerization techniques for acrylonitrile can be found in a lesser extent, albeit first approaches were established a few decades ago.¹⁰ More recent concepts for a controlled, coordinative preparation of pAN share the issues of low reaction velocities and broadened molecular weight distributions.^{11–15} Combining the catalytic polymerization of a precursor compound with PARs gives the possibility to access defined pAN and additional to that allows easy incorporation of comonomers. This opens a new realm of acrylonitrile copolymers, which never has been investigated before.

Within this work, we present a new and convenient polymer-analogous pathway to polyacrylonitrile, which allows facile access to copolymers of defined compositions. As **Scheme 1** illustrates, synthesis begins with the catalytic polymerization of methyl acrylate. After an amidation reaction, the obtained



Scheme 1 Overview of the PARs starting from the catalytic polymerization of methyl acrylate to polyacrylonitrile.

poly(acrylamide) is converted into pAN in a dehydration reaction. The dehydration reaction can also be applied to

^a Catalysis Research Center & Wacker-Chair of Macromolecular Chemistry, Technical University of Munich, Lichtenbrgstraße 4, D-85748 Garching, E-mail: rieger@tum.de

Electronic Supplementary Information (ESI) available: Detailed experimental procedures, polymer characterisations. See DOI: 10.1039/x0xx00000x

copolymers of poly(methyl acrylate-co-acrylamide) to give well defined poly(methyl acrylate-co-acrylonitrile) copolymers.

Results and discussion

Polymerization of methyl acrylate with catalyst X.

Catalytic polymerization of methyl acrylate is not done yet.

Polymer-analogue amidation of poly(methyl acrylate).

Amidation reactions are performed by pressurizing pMA dissolved in a mixture of THF/MeOH (2:1, v/v) with ammonia (8 bar) at a temperature of 50 °C under variation of the reaction time. This solvent mixture is necessary to dissolve sufficient amounts of both the polymer and ammonia. As **Table 1** illustrates, the time dependency for the conversion of pMA to poly(acrylamide) (pAA) can be used to control the degree of amidation. This is an advantage not to be underestimated compared to conventional copolymerization methods because it allows an easy adjustment of the proportion of two different repeating units (methyl acrylate and acrylamide) by the reaction time. The acrylamide moieties evolving during the reaction causes an increasing insolubility. Therefore, quantitative amidation can be achieved by further reaction in water as solvent to overcome solubility problems. The reaction progress of the amidation can be monitored by proton NMR spectroscopy. As shown in **Figure 1**, the amide signals (1) evolve in the region of 6.57~ppm to 7.60~ppm (blue), while the integral of signal number 2 which is representing the pMA methoxy-protons (3.57~ppm, green) decreases. Additionally, a slight upfield shift of the backbone methine (5) and methylene (6-8) resonance is visible. The amide content can be calculated by integration of the amide- and methoxy signals and correcting them to the amount of protons representing the resonance by following equation:

$$\text{Degree of amidation (\%)} = \frac{I_{\text{NH}_2}}{I_{\text{OCH}_3}} \cdot \frac{3}{2} \cdot 100$$

Despite several cycles of freeze drying and appliance of high vacuum, THF is difficult to remove from the copolymer especially at higher amidation levels. Therefore, there is some overlap of the THF-signals (1.87~ppm and 3.71~ppm in DMSO-d₆) with the methoxy and methylene resonances (**Figure 1**, orange/green). This causes an error in the determination of the degree of amidation which is estimated to be up to 10~%.

Table 1 Time dependency of the amidation of poly(methyl acrylate) to poly(methyl acrylate-co-acrylamide) copolymers. Amide content determined by ¹H NMR spectroscopy

Time / d	Degree of amidation / %
1	17
2	33
3	50
4	65
5	77
7	92
10	98

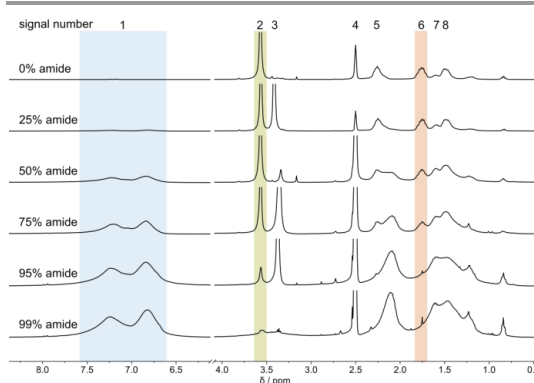


Figure 1 ¹H NMR spectra of different degrees of amidation in DMSO-d₆ (signal 4) as solvent. Explanation of the signals: NH₂ (1), OCH₃ (2), H₂O (3), methine (5), methylene (6, 7, 8). Signals 2 and 6 overlapped by THF resonances. Spectra intensities referred to the methine-signal of poly(methyl acrylate).

Polymer-analogue dehydration of poly(methyl acrylate-co-acrylamide) with diethyl chlorophosphate.

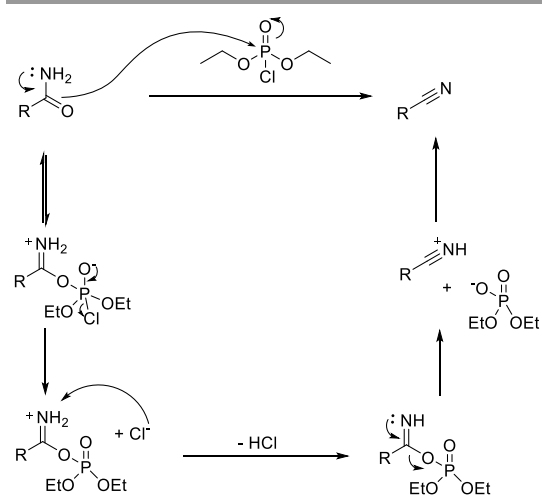
Diethyl chlorophosphate is reported to dehydrate common organic primary amides to nitriles.¹⁶ Varying the solvent to *N,N'*-dimethylformamide (DMF) enables the reaction to convert the amide-containing copolymers into poly(methyl acrylate-co-acrylonitrile). The mechanism is expected to take place analogue to the well investigated dehydration reaction with phosphorus pentoxide (**Scheme 2**).¹⁷ Since pAA is insoluble in DMF the copolymers with higher amide content used for the reaction give an inhomogeneous solution in the beginning. The copolymer becomes soluble with the formation of the nitrile groups, which gives an indication of the reaction being complete as soon as the solution is clear.

For analysis of the PAR products, attenuated total reflection infrared spectrophotometry (ATR-IR) is performed. **Figure 2** shows ATR-IR spectra of the two intermediate stages pMA and pAA, as well as the dehydration product pAN. The band at about 1600~cm⁻¹ to 1750~cm⁻¹ (blue) of pMA and pAA can be assigned to C=O. This band is significantly decreased for the spectrum of pAN. Compared to the spectrum of pAA, also the NH₂ band of pAA at 2930~cm⁻¹ to 3330~cm⁻¹ (orange) disappears completely. Instead, a sharp C≡N band at 2244~cm⁻¹ (green) is observable. The residual bands in the carbonyl region originate

Please do not adjust margins

Journal Name

ARTICLE



Scheme 2 Diethyl chlorophosphate-mediated dehydration of a primary amide to the nitrile with the reagent forming HCl and diethyl phosphate.

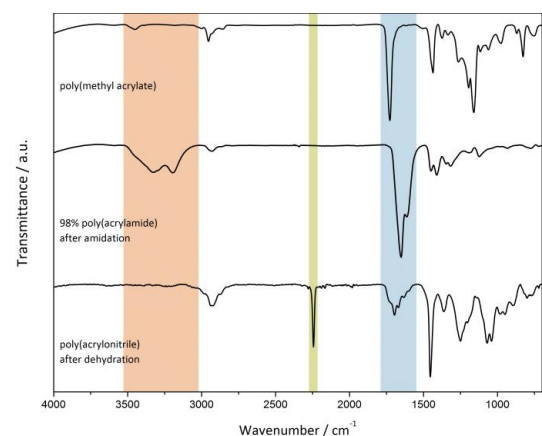


Figure 2 Comparison of IR-spectra of pMA, pAA and pAN with characteristic band regions: amide ($3000\text{--}3600\text{ cm}^{-1}$), nitrile (2244 cm^{-1} , green) and carbonyl ($1600\text{--}1750\text{ cm}^{-1}$, blue).

from non-amidated methyl acrylate units methyl acrylate units or residual DMF.

More detailed information about the PARs can be obtained from ^{13}C and ^1H NMR spectroscopy. As can be seen in **Figure 3** and **Figure 4** (spectrum 4), both show the expected signals for pAN. These are for proton NMR the methylene signal at 2.07 ppm and the methine-proton resonance at 3.14 ppm , respectively. Carbon NMR of pAN as homopolymer shows additional to methylene (27.2 ppm) and methine (32.7 ppm) signals a resonance of the nitrile group at a chemical shift of 120.0 ppm (**Figure 4**, spectrum 4). Other signals cannot be observed which indicates a complete conversion of the homopolymeric pAA as well as reaching a polymer of high

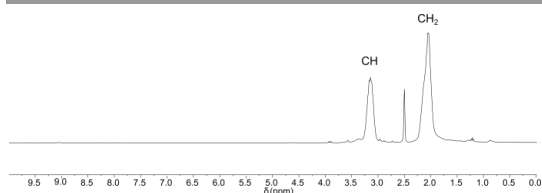


Figure 3 ^1H spectrum of pAN in $\text{DMSO-}d_6$ as solvent illustrating the methylene and methine proton resonances.

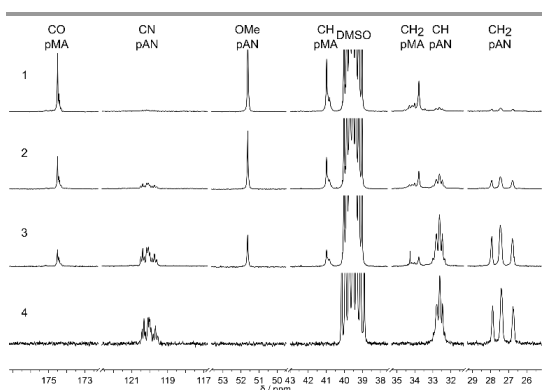


Figure 4 ^{13}C NMR spectra of poly(MA-co-AN) with nitrile contents of 25% (1), 50% (2), 75% (3) and pAN as homopolymer (4) in $\text{DMSO-}d_6$ as solvent.

purity. Since the amidation reaction provides access to MA-co-AA copolymers of defined proportions, the dehydration reaction can also be utilized to produce defined MA-co-AN polymers. For this, (MA-co-AA) copolymers with amide contents of 25%, 50% and 75% are used for the dehydration reaction. Again, carbon NMR can be used for verification of the resulting poly(MA-co-AN). The dehydration reaction with $(\text{EtO})_2\text{POCl}$ dehydrates selectively the amide-groups in the copolymers. Moreover, the reaction conditions are mild enough to leave the methyl ester groups of the pAM units unhydrolyzed since the spectra in **Figure 4** show no carboxylic acid resonances.

The homo- and copolymers received from the polymer-analogous pathway are further investigated to their thermal properties by thermogravimetric analysis (TGA) and differential scanning calorimetry (DSC). According to the measurement of pAN as homopolymer under an inert argon atmosphere, decomposition starts slowly at a temperature of about $280\text{ }^\circ\text{C}$. At this temperature, only 10% weight loss can be observed while beginning at a temperature of about $500\text{ }^\circ\text{C}$ the main decomposition step takes place which ends up in a complete decomposition (see **Figure 5**). This behaviour coincides with data from literature.^{18,19} Measuring the same polymer under the presence of oxygen reveals a different decomposition behaviour, the onset of the decomposition can be observed at a much lower temperature of $280\text{ }^\circ\text{C}$. In contrast to the measurement before, thermal decomposition under oxidative conditions terminates with a residue of 43% . This is due to the cyclization reaction of adjacent nitrile groups which is assumed

Please do not adjust margins

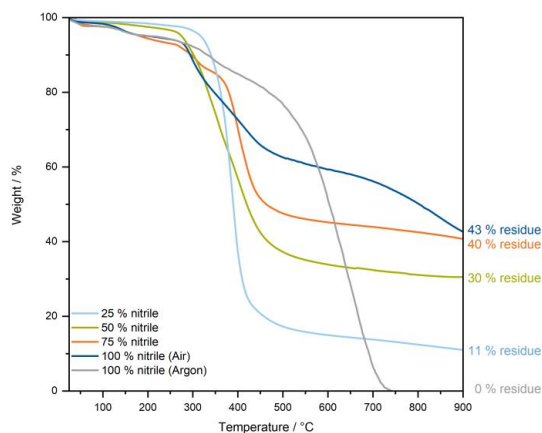


Figure 5 TGA measurements of poly(MA-co-AN) copolymers with different proportions.

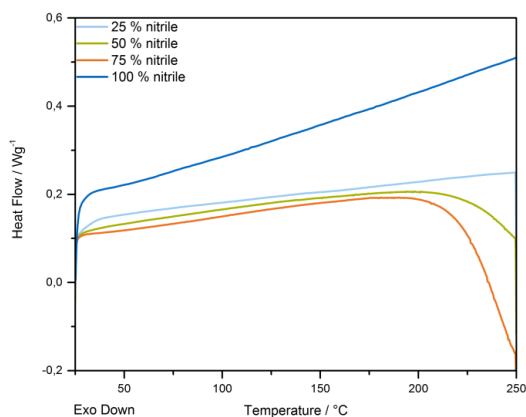


Figure 6 DSC measurements of poly(MA-co-AN) copolymers with different compositions.

to follow a radical mechanism initiated by oxidation and results in a stabilized polymer. Stabilization reactions can also be initiated ionically by comonomers, which can be observed in the residues of the methyl acrylate containing polymers after heating to 900°C (compare residues in Figure 5). Here, the stabilization occurs independently of the atmosphere during the heating process.^{20,21}

Keeping in mind that the cyclization is an exothermic reaction, the outcome of the DSC-measurement shown in Figure 6 can be explained. For the polymers containing 50% and 75% acrylonitrile, respectively, the heat flow decreases at a temperature around 200 °C. This indicates an exothermic reaction and coincides with the onset temperatures of the decomposition the TGA-curves show. The copolymers with 25% and 100% do not show an exothermic process. The homopolymeric pAN is most likely unable to undergo the stabilization reaction under these conditions. For the 25% nitrile containing polymer there might be too less neighbouring nitrile groups for the cyclization to affect the measurement.

Conclusions

Herein we reported a new and convenient pathway to poly(acrylonitrile) which is achieved by two polymer-analogous reactions starting from poly(methyl acrylate). The first synthetic step is the amidation of pMA by pressurizing it in solution with ammonia. Within this reaction it is possible to adjust the degree of amidation by the reaction time allowing to obtain poly(methyl acrylate-co-acrylamide) copolymers of defined proportions. The right choice of the solvent allows to gain poly(acrylamide) as homopolymer starting from previously amidated polymer. The content of amide groups in the copolymer can be determined by proton NMR spectroscopy. The final dehydration reaction from pAA to pAN can be performed with diethyl chlorophosphate in DMF. The reaction can be also applied to poly(MA-co-AA) copolymers with varying proportions. As carbon NMR spectroscopy shows, the method is mild enough to leave the methyl acrylate units unhydrolyzed resulting in poly(methyl acrylate-co-acrylonitrile) copolymers. Investigations on the thermal properties gives hints towards the cyclization of the adjacent nitrile groups which is most probably initiated ionically by the methyl acrylate units. This is observable in residues after the heating process in relation to the nitrile content in the copolymer, pointing towards the stabilized polymer. DSC measurements confirm this showing an exothermic process starting at the decomposition temperature originating from the cyclization.

Conflicts of interest

There are no conflicts to declare.

Acknowledgements

The acknowledgements come at the end of an article after the conclusions and before the notes and references.

Notes and references

- 1 C. Woodings, *Regenerated cellulose fibres*, 2010.
- 2 R. E. Oesper, *J. Chem. Educ.*, 1929, **6**, 677.
- 3 C. E. Hoyle, A. B. Lowe and C. N. Bowman, *Chem. Soc. Rev.*, 2010, **39**, 1355–1387.
- 4 W. Wang, Y. Shi, X. Wang, A. Qin, J. Z. Sun and B. Z. Tang, *Polym. Chem.*, 2017, **8**, 2630–2639.
- 5 M. L. Hallensleben, R. Fuss and F. Mumby, in *Ullmann's Encyclopedia of Industrial Chemistry*, Wiley-VCH Verlag GmbH & Co. KGaA, Weinheim, Germany, 2015, pp. 1–23.
- 6 R. B. Beevers, *J. Polym. Sci. Macromol. Rev.*, 1968, **3**, 113–254.
- 7 J.-B. Donnet, T. K. Wang and J. C. M. Peng, *Carbon Fibers*, CRC Press, Boca Raton, 3rd edn., 1998.
- 8 W. M. Thomas, *Fortschritte der Hochpolym.*, 1961, **2**, 401–441.
- 9 T. Fukuda, T. Terauchi, A. Goto, Y. Tsujii, T. Miyamoto and Y. Shimizu, *Macromolecules*, 1996, **29**, 3050–3052.
- 10 A. Yamamoto and S. Ikeda, *J. Am. Chem. Soc.*, 1967, **89**,

Excursus: Polymer-Analogous Reactions as Novel and Controlled Pathway to Polyacrylonitrile and its Well Adjustable Copolymers

Please do not adjust margins

Journal Name

ARTICLE

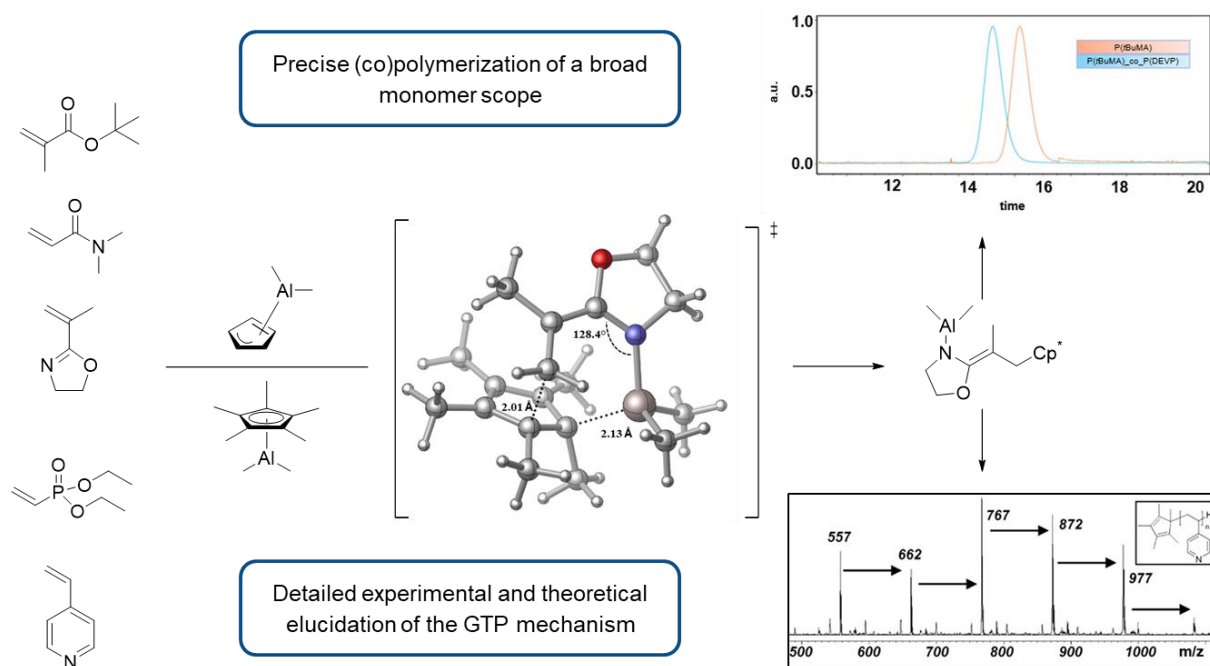
- 5989–5990.
- 11 E. Y.-X. Chen, *Chem. Rev.*, 2009, **109**, 5157–5214.
 - 12 K. C. Hultzsich, T. P. Spaniol and J. Okuda, *Angew. Chemie Int. Ed.*, 1999, **38**, 227–230.
 - 13 K. Nozaki, S. Kusumoto, S. Noda, T. Kochi, L. W. Chung and K. Morokuma, *J. Am. Chem. Soc.*, 2010, **132**, 16030–16042.
 - 14 F. Schaper, S. R. Foley and R. F. Jordan, *J. Am. Chem. Soc.*, 2004, **126**, 2114–2124.
 - 15 F. Wu, S. R. Foley, C. T. Burns and R. F. Jordan, *J. Am. Chem. Soc.*, 2005, **127**, 1841–1853.
 - 16 Z. Shahsavari-Fard and A. R. Sardarian, *J. Iran. Chem. Soc.*, 2011, **8**, 204–208.
 - 17 R. Brückner, in *Organic Mechanisms*, Springer Berlin Heidelberg, Berlin, Heidelberg, 2010, pp. 321–338.
 - 18 E. Ismar and A. S. Sarac, *Polym. Adv. Technol.*, 2016, **27**, 1383–1388.
 - 19 H. F. Moafi, A. F. Shojaie and M. A. Zanjanchi, *J. Chil. Chem. Soc.*, 2011, **56**, 610–615.
 - 20 J. Kim, Y. C. Kim, W. Ahn and C. Y. Kim, *Polym. Eng. Sci.*, 1993, **33**, 1452–1457.
 - 21 L. M. Manocha and O. P. Bahl, *Fibre Sci. Technol.*, 1980, **13**, 199–212.

Please do not adjust margins

9. Summary and Outlook

In the first part of this thesis, a novel precise GTP method using organometallic complexes of the main group element aluminum was established for a broad scope of monomers. This catalytic polymerization type combines the advantages of two well-known and important techniques which are widely used for the conversion of *Michael*-type monomers: The LPP reported by *Chen et al.* in 2010 and the REM-GTP based on the seminal works of *Yasuda et al.* in 1992.^[5, 11] The catalysts of our main group element-catalyzed GTP comprised exclusively aluminum as central atom and easily accessible or even commercially available ligands. Their tailor-made *Lewis* acidity allowed to initiate the polymerizations without any additional LB and no side reactions occurred like the deprotonation of α -acidic monomers in the LPP. A detailed end group analysis using ESI-MS clearly pointed towards a group transfer initiation process *via* nucleophilic transfer of the aromatic ligands to the olefin end of the respective monomer. The absence of detectable concurring initiation pathways represents a crucial requirement for establishing a precision polymerization method. Especially the use of the aluminum half-metallocenes provided access to a broad range of different sterically and electronically challenging monomers including *t*BuMA, DEVP, DMAA, IPOx and even the extended *Michael*-system 4VP and enabled the synthesis of high molecular weight polymer with narrow dispersities (Scheme 13). To evidence a GTP mechanism analogous to the REM-catalysis, a thorough elucidation combining experimental and theoretical investigations was performed. Kinetic studies uncovered the desired living polymerization behavior and revealed a reaction order of one for both monomer and catalyst concentration. DFT calculations confirmed the proposed group transfer process as initiation step and underlined the Yasuda-type propagation mechanism. The lower energy demanding barrier for the initiation reaction explained the improved initiator efficiencies of the aluminum half-metallocenes compared to other alanes. An additional energy decomposition analysis determined the steric repulsion and the interaction energy of the reactants as decisive for the barrier of the initiation step. The living nature of our method and especially the exceptionally high initiator efficiencies of the aluminum half-metallocenes opened the possibility to design precise block-type macromolecular architectures. This feature was demonstrated by the synthesis of the unconventional copolymers *Pt*BuMA-*co*-PDEVp and PDMAA-*co*-PDEVp. Thus, our novel main group element-catalyzed GTP method fulfills the decisive characteristics of a catalytic precision polymerization. The convenient synthesis facilitates a tailoring of the *Lewis* acidity to further expand the monomer scope and the introduction of more sophisticated initiating groups like pyridine derivatives which serve as functional end groups. The high precision (co)polymerization method catalyzed

by these single-site aluminum catalysts could replace the REM-GTP because of the cheaper and better available starting materials. An open challenge for the main group alternative is the increase of the catalyst activities to the level of REM pendants.



Scheme 13. Aluminum-catalyzed GTP for a wide variety of *Michael*-type monomers including a detailed mechanistic elucidation.

A second approach to overcome the side reactions occurring in the LPP was the covalent bridging of the LA and LB moiety. Neither the synthesis nor the application of such compounds as polymerization catalysts was completely new to the literature. But since the boron/phosphorus-based BLPs reported by *Chen et al.* produced polymers with broadened dispersities,^[64] we were curious how a replacement of boron with aluminum would influence the polymerization process. After the synthesis of BLPs bearing systematically varied substituents and first successful screenings, we intended to redetermine the molecular structure of the simplest Al/P-BLP $\text{Me}_2\text{AlCH}_2\text{PMe}_2$ by single-crystal XRD diffraction. Beside the expected dimeric structure, a pronounced elongation of the axial Al-Me bond was observed (Figure 11, left). This surprising finding sparked our interest and with the help of a single crystal neutron diffraction experiment and DFT computations, the partial hydrolysis of this bond was excluded. However, the neutron diffraction data pointed to a less pronounced elongation of the axial Al-Me bond. After a re-evaluation of the XRD data by conducting a 12h *in situ* experiment with one crystal, we were able to attribute this phenomenon to a rare example of a selective hydrolysis, even under a protective nitrogen stream at 100 K. The assumption that this highly reactive bond initiates a group transfer process was refuted by polymerization studies and

mechanistic analysis. Whereas the BLPs catalyzed a very fast and precise polymerization of α -acidic monomers like DAVP and DMAA, no activity towards methacrylates, a very common monomer class for GTP methods, was observable. For further insights, PDEVOP oligomers were examined with NMR spectroscopy and ESI-MS. Their combined and complementary results suggested a cleavage of the methylene linker caused by a deprotonation of the acidic α -proton of the monomer (Figure 11, right). Thereby, the free phosphine is cleaved and the dialkyl aluminum moiety stays coordinated to the phosphonate group. The likely following *Yasuda*-type propagation process was only possible with Al-based BLPs, since boranes are not capable of forming the required fivefold transition state. Theoretical investigations confirmed this hypothesis and natural bonding analysis explained the nucleophilic character of the methylene linker. This unexpected and formerly unwanted deprotonation as initiation step ensured a living polymerization behavior and enabled block copolymerizations. The Al/P-BLPs by far outperform their intermolecular pendants in the polymerization of *Michael*-type monomers without an α -methyl group, mainly because they use the side reaction as exclusive and highly efficient pathway.

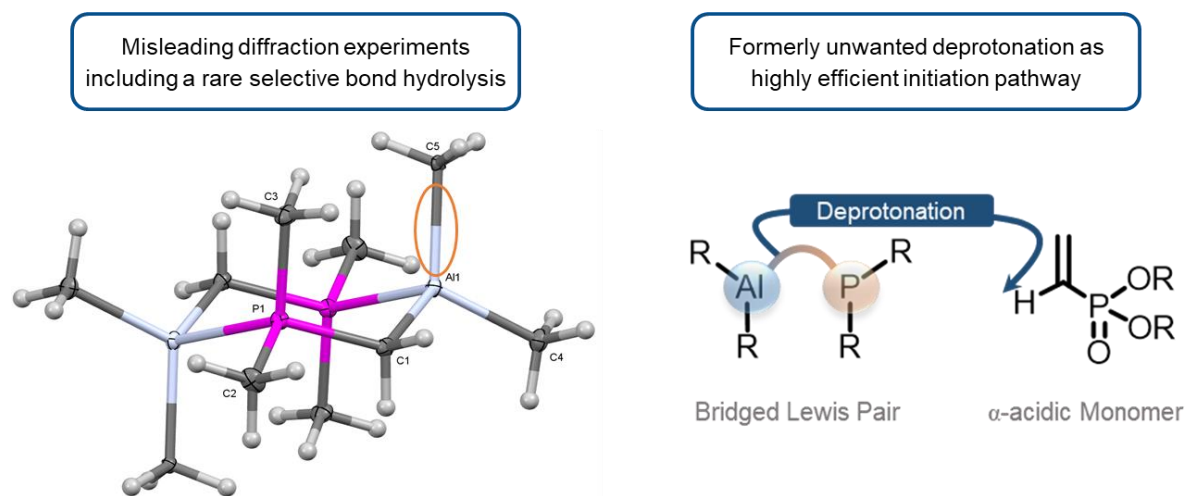
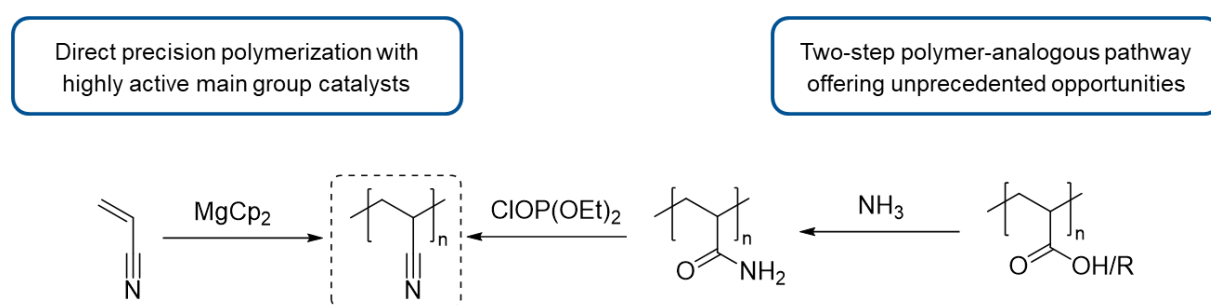


Figure 11. Combined study for the suitability analysis of BLPs regarding their polymerization activity: Unexpected bond characteristics during the single-crystal XRD and neutron diffraction experiments (left) and conclusive experimental and theoretical evidences for the initiation process (right).

Unfortunately, the aluminum half-metallocenes as well as the BLPs exhibited low activity for the polymerization of AN. The catalytic precision polymerization of AN is still a pending issue and a desired goal in material science. Therefore, the polymerization behavior of our diverse main group catalysts was investigated in more detail. While intermolecular LPs showed high initiator efficiencies but low activity, the strong LA $\text{Al}(\text{C}_6\text{F}_5)_3$ was the only alane which was able to initiate the polymerization of AN without LB, resulting in very high molecular weight products within seconds, due to a low initiator efficiency. The solvent-dependency of the

$\text{Al}(\text{C}_6\text{F}_5)_3$ -catalyzed reactions complicated the mechanism elucidation and an improvement of the polymerization process. LPP and using $\text{Al}(\text{C}_6\text{F}_5)_3$ as a single-component catalyst shared the drawback of a non-living polymerization behavior caused by side and termination reactions. Also, the molecular weight distributions were not satisfying, and we sought to solve these problems. Thus, we switched to a further main group metal, namely magnesium, utilizing the known Cp donor MgCp_2 as catalyst. This idea revealed an impressive catalyst improvement and provided access to well-defined PAN (Scheme 14). The unprecedented narrow dispersities were achieved on short time scales and the initiator efficiencies of MgCp_2 were determined to decent values. Kinetic studies evidenced the desired living nature of this polymerization, enabling quantitative consumption of AN. End group analysis confirmed the expected nucleophilic Cp transfer to the olefin end of AN, which was corroborated by DFT calculations. Applying the easily accessible MgCp_2 as catalyst constitutes to our knowledge the best catalytic approach for the polymerization of AN and provides a high-quality answer to this highly important issue.

In parallel to the direct catalytic polymerization method, we developed a novel route to well-defined PAN by focusing on polymer-analogous reactions. We started with the anionic polymerization of acrylic acid and its esters, that were converted in a first step into amide moieties in a pressurized reaction with ammonia gas. After a detailed analysis to ensure the purity and an optimization of the reaction conditions, a second polymer-analogous reaction was applied. The dehydration of the amide to nitrile groups was successfully achieved using diethyl chlorophosphate, resulting in high molecular weight PAN (Scheme 14).



Scheme 14. Unprecedented performance of main group catalysts (left) and a smart polymer-analogous route (right) as convenient pathways for the synthesis of well-defined PAN.

This straight-forward approach is a promising alternative to the direct polymerization of AN with important benefits and options: 1. Acrylates are catalytically polymerizable and a control of the microstructure is possible. 2. Co- or even terpolymer architectures are easily accessible with a defined composition. 3. The properties of PAN and its copolymers can be precisely tuned

for further applications, e.g. for CF synthesis. 4. Acrylic acid can be synthesized based on biogenic starting materials like glycerol.

The last topic of this thesis concentrated on GTP catalysts, which were supposed to control the stereoregularity of the *Michael*-type monomers. Representatively, we decided to focus on DEVP as monomer, because the synthesis and the analysis of stereoregular PDEVP is scarcely explored in the literature and the well-known CGCs served as examples for the ligand design of our catalyst. Again, we used aluminum as central metal and established a salt metathesis route to synthesize the Al-CGCs. For comparison, the synthesis of structurally identical Y-CGCs was realized *via* a convenient CH bond activation pathway. The polymerization experiments revealed a significant influence of the applied ligands on the catalyst performance and a superiority of the Y-CGCs which produced PDEVP with narrow molecular weight distributions exhibiting high TOFs and initiator efficiencies (Figure 12).

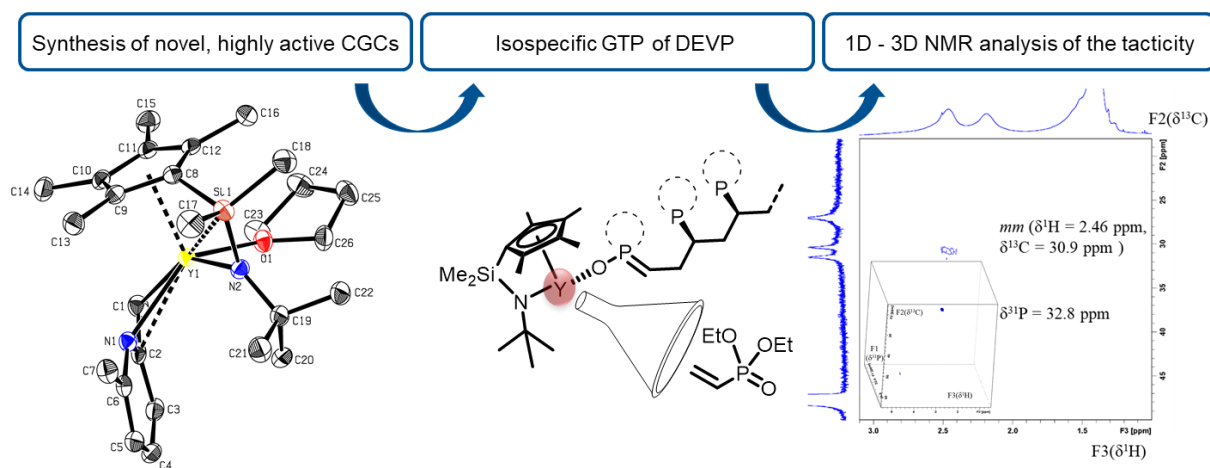


Figure 12. Tailor-made CGCs for the synthesis of *it*-PDEVP and an extensive NMR study for the qualification and quantification of the tacticity.

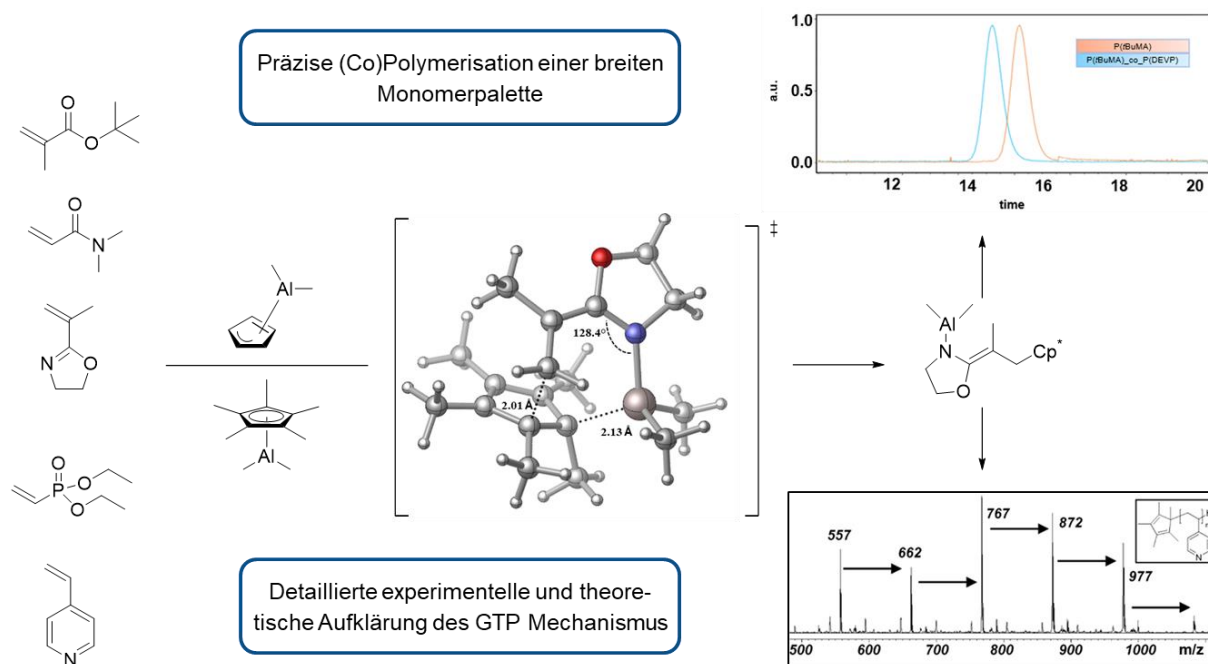
The disparities in the 1D NMR spectra of the resulting polymers depending on the ligands and on the central atom of the catalysts made us perform a more detailed analysis of the PDEVP microstructure. The use of 2D NMR methods (HSQC, TOCSY) allowed for a preliminary assignment of the signals for the polymer backbone and suggested that the Y-CGCs induce isotacticity whereas PDEVP produced by Al-CGCs is atactic. Due to the complexity of this analysis caused by the scalar J_{HP} and J_{CP} couplings, we established 2D and 3D triple resonance NMR methods. This latter sophisticated type of NMR spectroscopy confirmed the scientific reliability of the 2D results and expanded the assignments. The universal applicability of the presented triple resonance method constitutes an important simplification and enhancement for the microstructure analysis of polymers containing heteroatoms with NMR-active nuclei. Furthermore, this detailed NMR study helped us to identify chain-end control as the dominant

stereocontrol mechanism and to quantify the isotacticity of the PDEVp produced by Y-CGCs. The novel properties of the highly isotactic PDEVp and its possible copolymers should be investigated in further works. The absence of stereospecificity in the case of the Al catalysts was attributed to the difference in the hapticity of the Cp derivatives (five for Y-CGCs, one for Al pendants) and the resulting discrepancy in the electronic and steric situation. In general, the combination of *ansa*-metallocene ligands and aluminum as central atom did not seem to work and made us aware of the limitations in main group catalysis. Nevertheless, the versatile main group polymerization catalysts presented in this thesis proved to be a serious competition for established methods and offer enormous potential for further improvements and promising applications.

10. Zusammenfassung und Ausblick

Im ersten Teil dieser Arbeit wurde eine neuartige, präzise Gruppentransferpolymerisation (GTP)-Methode für eine breite Monomerpalette mit Hilfe von metallorganischen Komplexen des Hauptgruppenelements Aluminium etabliert. Diese katalytische Polymerisationsart kombiniert die Vorzüge von zwei äußerst bekannten und bedeutenden Techniken, die häufig für die Umsetzung von *Michael*-artigen Monomeren verwendet werden: Die *Lewis* Paar-Polymerisation (LPP) veröffentlicht in 2010 von *Chen et al.* und die Seltenerdmetall-(REM-) vermittelte GTP basierend auf den grundlegenden Arbeiten von *Yasuda et al.* aus dem Jahre 1992.^[5,11] Die Katalysatoren der Hauptgruppenelement-katalysierten GTP enthielten ausschließlich aus Aluminium als Zentralatom zusammen mit leicht zugänglichen oder kommerziell erhältlichen Liganden. Ihre maßgeschneiderte *Lewis*-Azidität verhalf dabei die Polymerisationen ohne zusätzliche *Lewis*-Base (LB) zu starten und es traten keine Nebenreaktionen wie die Deprotonierung α -azider Monomeren in der LPP auf. Eine detaillierte Endgruppenanalyse mit ESI-MS legte einen Gruppentransferinitiationsprozess durch nukleophilen Transfer der aromatischen Liganden auf die aktivierte Doppelbindung des jeweiligen Monomers nahe. Das Fehlen von anderen detektierbaren Initiationswegen stellt eine entscheidende Voraussetzung für das Etablieren einer präzisen Polymerisationsmethode dar. Insbesondere der Einsatz von Aluminium-Halbmetalloenen machte eine große Bandbreite von sterisch und elektronisch unterschiedlichen Monomeren einschließlich *t*BuMA, DEVP, DMAA, IPOx und sogar des erweiterten *Michael*-Systems 4VP zugänglich. Zusätzlich wurde die Synthese von hochmolekularen Polymeren mit engen Molmassenverteilungen ermöglicht (Schema 15). Um die mechanistische Analogie zur REM-GTP nachzuweisen, wurde eine sorgfältige Mechanismusaufklärung mit experimentellen und theoretischen Untersuchungen durchgeführt. Kinetische Studien bewiesen das gewünschte lebende Polymerisationsverhalten und eine Reaktionsordnung von eins sowohl für Monomer- als auch für Katalysator-konzentration. DFT-Berechnungen bestätigten den vorgeschlagenen Gruppentransferprozess als Initiationsschritt und den *Yasuda*-artigen Propagationsmechanismus. Die niedrigere Energiebarriere im Initiationsschritt erklärte die besseren Initiatoreffizienzen der Aluminium-Halbmetalloenen im Vergleich zu den restlichen Aluminiumorganylen. Eine zusätzliche Energiezersetzungsanalyse zeigte den entscheidenden Einfluss der sterischen Abstoßung und der Interaktion der Reaktanten auf die Aktivierungsbarriere des Initiationsschritts. Das lebende Verhalten der Methode und speziell die außergewöhnlich hohen Initiatoreffizienzen der Aluminium-Halbmetalloenen ermöglichte die Synthese von Blockcopolymerstrukturen. Dies wurde mit der Herstellung der unkonventionellen Copolymere *Pt*BuMA-*co*-PDEVp und

PDMAA-*co*-PDEVP nachgewiesen. Somit erfüllt unsere neuartige Hauptgruppenelement-katalysierte GTP-Methode die entscheidenden Anforderungen einer katalytischen Präzisionspolymerisation. Die variable Katalysatorsynthese ermöglicht weitere Anpassungen der *Lewis*-Azidität für die Polymerisation weiterer Monomere und den Einsatz von weniger bekannten Initiatoren wie Pyridin-Derivaten, die folglich als funktionelle Endgruppe dienen. Diese hochpräzise (Co)Polymerisationsmethode mit den vorgestellten single-site Aluminium-katalysatoren könnte die REM-GTP aufgrund der billigeren und besser verfügbaren Edukte ersetzen. Eine Herausforderung für die Zukunft der Hauptgruppenelement-Variante stellt die Steigerung der katalytischen Aktivität auf das Level der REM-Pendants dar.



Schema 15: Aluminium-katalysierte GTP einsetzbar für verschiedene *Michael*-artige Monomere samt ausführlicher Mechanismusaufklärung.

Ein zweiter Ansatz für die Vermeidung der Nebenreaktionen, die in der LPP auftreten, war die kovalente Verknüpfung der *Lewis*-Säure- (LS) und LB-Einheit. Sowohl die Synthese als auch die Anwendung solcher Verbindungen als Polymerisationskatalysatoren waren in einem gewissen Maße bereits literaturbekannt. Da allerdings Bor/Phosphor-basierte verbrückte *Lewis*-Paare (VLP) gemäß *Chen et al.* Polymere mit breiten Molmassenverteilungen produzieren,^[64] stellten wir uns die Frage, welchen Einfluss das Austauschen von Bor mit Aluminium auf den Polymerisationsverlauf haben könnte. Nach der Synthese von VLPs mit systematisch variierten Substituenten und ersten erfolgreichen Screeningversuchen waren wir an der Wiederbestimmung der molekularen Struktur vom einfachsten Al/P-VLP $\text{Me}_2\text{AlCH}_2\text{PMe}_2$ mittels Röntgenkristallstrukturanalyse interessiert. Neben der erwarteten dimeren Struktur wurde dabei eine deutliche Verlängerung der axialen Al-Me Bindung beobachtet

(Abbildung 13, links). Dieser überraschende Befund zog unsere Aufmerksamkeit auf sich und mit Hilfe eines Einkristall-Neutronenbeugungsexperimentes und theoretischen Berechnungen konnte die partielle Hydrolyse dieser Bindung ausgeschlossen werden. Allerdings wiesen die Daten der Neutronenbeugung auf eine weniger deutliche Verlängerung der axialen Al-Me-Bindung hin. Nach einer erneuten Evaluierung der XRD-Daten durch ein zwölfstündiges *in situ* Experiment mit einem Kristall konnten wir dieses Phänomen einem seltenen Beispiel einer selektiven Hydrolyse zurechnen, das sogar unter Schutzgasatmosphäre bei 100 K auftritt. Die Vermutung, dass diese hochreaktive Bindung einen Gruppentransferprozess initiiert, konnte durch Polymerisations- und Mechanismusstudien widerlegt werden. Auch wenn die VLPs eine sehr schnelle und präzise Polymerisation von α -aziden Monomeren wie DAVP und DMAA katalysierten, waren sie gegenüber Methacrylaten, eine sehr gängige Monomerklasse für GTP-Methoden, inaktiv. Weitere Einblicke wurden durch NMR-Spektroskopie und ESI-MS an PDEVPOligomeren erhalten. Deren kombinierte und komplementären Resultate legten eine Spaltung der Methylenbrücke nahe, verursacht durch eine Deprotonierung des sauren α -Protons des Monomers (Abbildung 13, rechts).

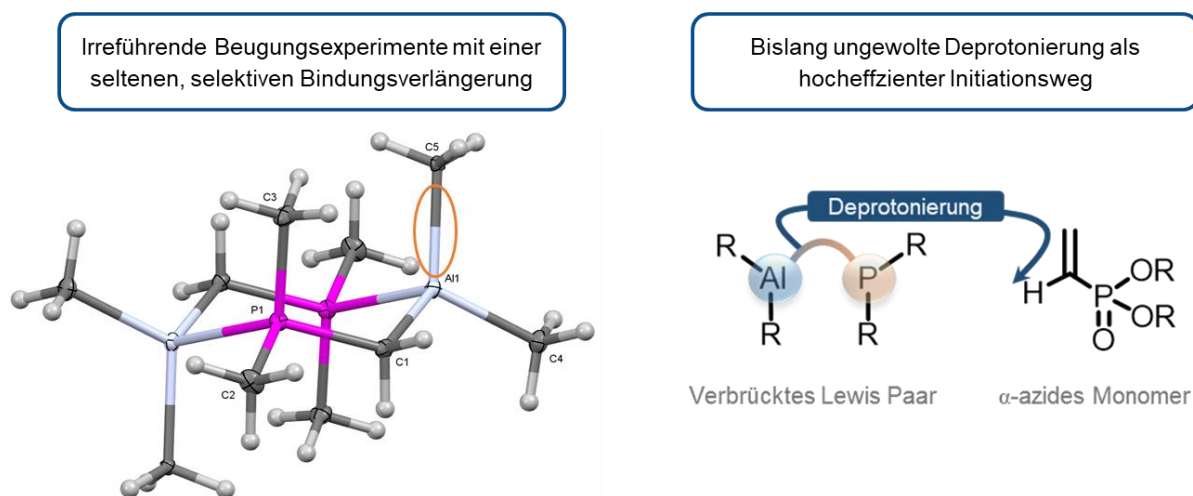


Abbildung 13: Untersuchung der Polymerisationsaktivität von VLPs : Unerwartete Bindungseigenschaften während der Einkristall-XRD- und Neutronenbeugungsexperimente (links) und aufschlussreiche experimentelle und theoretische Beweise für den Initiationsprozess (rechts).

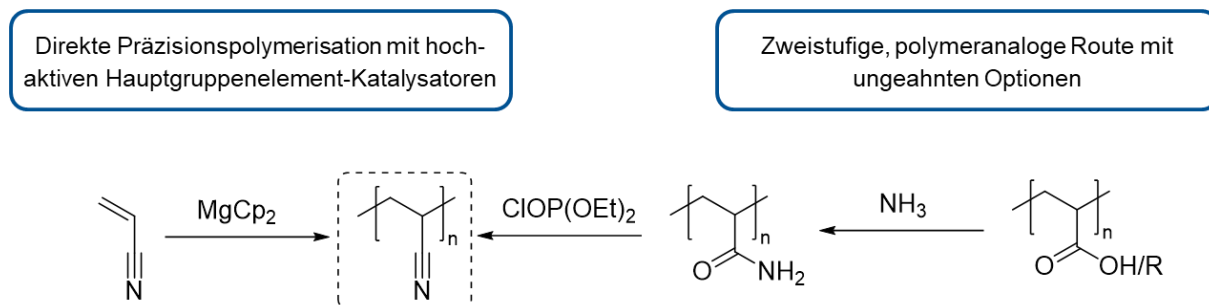
Dabei wird das freie Phosphan abgespalten und das Dialkylaluminium-Kation verbleibt an der Phosphonatgruppe. Der wohl *Yasuda*-artige Propagationsprozess war nur mit Al-basierten VLPs möglich, da Borane den benötigten fünffach koordinierten Übergangszustand nicht bilden können. Theoretische Untersuchungen bestätigten diese Hypothese und eine NBO-Analyse erklärte den nukleophilen Charakter der Methylenbrücke. Diese unerwartete und bisher ungewollte Deprotonierungsreaktion als Initiationsschritt stellte ein lebendes Polymerisationsverhalten sicher und ermöglichte wiederum Blockcopolymerisationen. Die

Al/P-VLPs sind ihren intermolekularen Pendants in der Polymerisation *Michael*-artiger Monomere ohne α -Methylgruppe weit überlegen, hauptsächlich da sie eine Nebenreaktion als exklusiven und hocheffizienten Initiationsweg nutzen.

Unglücklicherweise zeigten sowohl die Aluminium-Halbmetailocene als auch die VLPs geringe Aktivitäten für die Polymerisation von Acrylnitril (AN). Die katalytische Präzisionspolymerisation von AN ist immer noch ein ausstehendes Problem und ein erstrebenswertes Ziel in den Materialwissenschaften. Daher wurde das Polymerisationsverhalten unserer verschiedenen Hauptgruppenelement-Katalysatoren noch genauer untersucht. Während intermolekulare LP zwar hohe Initiatoreffizienzen, aber geringe Aktivitäten aufwies, war die starke LS $\text{Al}(\text{C}_6\text{F}_5)_3$ die einzige Aluminiumverbindung, die die Polymerisation von AN ohne LB starten konnte. Die in wenigen Sekunden erhaltenen Produkte zeigten aufgrund der niedrigen Initiatoreffizienzen allerdings eine sehr breite Molmassenverteilung. Die Lösemittelabhängigkeit der $\text{Al}(\text{C}_6\text{F}_5)_3$ -katalysierten Reaktionen erschwerte die Mechanismusaufklärung und eine Verbesserung des Polymerisationsprozesses zusätzlich. LPP und die Verwendung von $\text{Al}(\text{C}_6\text{F}_5)_3$ als Einkomponenten-Katalysator hatten den Nachteil eines nichtlebenden Polymerisationsverhaltens gemeinsam, bedingt durch Neben- und Abbruchreaktionen. Folglich waren auch die Molmassenverteilungen nicht zufriedenstellend. Auf der Suche nach einer Lösung wechselten wir das Hauptgruppenmetall und verwendeten den bekannten Cp-Donor MgCp_2 als Katalysator. Diese Idee stellte eine beeindruckende Verbesserung der katalytischen Performance und einen Weg zu wohldefinierten PAN dar (Schema 16). Sehr gute PDI-Werte wurden in sehr kurzen Reaktionszeiten erreicht und die Initiatoreffizienzen von MgCp_2 lagen in einem guten Bereich. Kinetische Studien bewiesen das angestrebte lebende Polymerisationsverhalten, das quantitative Umsätze von AN ermöglichte. Endgruppenanalyse bestätigte den erwarteten nukleophilen Cp-Transfer auf die aktivierte Doppelbindung von AN, was durch DFT Untersuchungen unterstrichen wurde. Der Einsatz des einfach synthetisierbaren MgCp_2 als Katalysator stellt nach unserem Wissensstand die beste katalytische Methode für die Polymerisation von Acrylnitril dar und liefert eine hochwertige Lösung für dieses langjährige Problem.

Parallel zur direkten Polymerisation entwickelten wir eine neuartige Route zu wohldefiniertem PAN unter Verwendung von polymeranalogen Reaktionen. Wir wählten die anionische Polymerisation von Methylacrylat und dessen Ester als Startpunkt. Die funktionellen Gruppen der Polymere wurden zuerst in einer Druckreaktion mit Ammoniakgas in Amide umgewandelt. Nach einer ausgiebigen Analyse der Reinheit und Optimierung der Reaktionsbedingungen folgte eine zweite polymeranaloge Reaktion. Die Dehydratisierung der Amid- zu Nitril-

Gruppen konnte erfolgreich mit Diethylchlorophosphat durchgeführt werden und resultierte in hochmolekularem PAN (Schema 16).



Schema 16: Beispiellose Eignung von Hauptgruppenelement-Katalysatoren (links) und eine elegante polymeranaloge Route (rechts) als geeignete Wege für die Synthese von wohldefiniertem PAN.

Dieses unkomplizierte Konzept ist eine vielversprechende Alternative zur direkten Polymerisation von AN mit wichtigen Vorteilen und Optionen: 1. Acrylate sind katalytisch polymerisierbar und die Kontrolle der Mikrostruktur ist möglich. 2. Co- oder sogar Terpolymere mit einer definierten Zusammensetzung sind problemlos zugänglich. 3. Die Eigenschaften von PAN und dessen Copolymeren können präzise für weitere Anwendungen, wie Carbonfasersynthese, justiert werden. 4. Acrylsäure kann aus biogenen Edukten gewonnen werden.

Der letzte Bereich dieser Arbeit setzte sich mit GTP-Katalysatoren auseinander, die für die Kontrolle der Stereoregularität von *Michael*-artigen Monomeren angedacht waren. Wir entschieden, uns auf DEVP als stellvertretendes Monomer zu fokussieren, da die Synthese und Analyse von stereoregularem PDEVP bisher kaum untersucht wurde. Die bereits bekannten CGC-Liganden dienten als Vorbild, für die wir eine Syntheseroute *via* Salzmetathese mit Aluminium als Zentralatom etablierten. Zu Vergleichszwecken wurden die strukturell identischen Y-CGCs mittels CH-Bindungsaktivierung synthetisiert. Die Polymerisationsexperimente zeigten den erheblichen Einfluss der verwendeten Liganden auf die Katalysatorleistung und die Überlegenheit der Y-CGCs, die PDEVP mit engen Molmassenverteilungen bei hohen Wechselzahlen und Initiatoreffizienzen herstellten (Abbildung 14). Die Unterschiede in den 1D-NMR Spektren der resultierenden Polymere abhängig von Liganden und Zentralatom der Katalysatoren ließ uns eine genauere Analyse der PDEVP-Mikrostruktur durchführen. Die Anwendung von 2D-NMR Methoden (HSQC, TOCSY) erlaubten eine vorläufige Signalzuordnung für das Polymerrückgrat und legten nahe, dass die Y-CGCs Isotaktizität induzieren, wohingegen das von Al-CGCs katalysierte PDEVP ataktisch ist. Wegen der Komplexität der Analyse, die durch die skalaren J_{HP} und J_{CP} Kopplungen hervorgerufen wird, konzipierten wir 2D und 3D Tripelresonanz-NMR-Methoden. Diese

anspruchsvolleren Arten der NMR-Spektroskopie bestätigten die Wissenschaftlichkeit der 2D Ergebnisse und präzisierten die Zuordnungen. Die universelle Anwendbarkeit der präsentierten Tripelresonanz-Methode stellt eine bedeutende Vereinfachung und Verbesserung der Mikrostrukturanalyse von Polymeren mit NMR-aktiven Heteroatomkernen dar. Des Weiteren half uns die detaillierte NMR-Studie, Kettenendkontrolle als dominierenden Stereokontrollmechanismus zu identifizieren und die Isotaktizität des mit Y-CGCs hergestellten PDEVp zu quantifizieren. Die neuartigen Eigenschaften des hochisotaktischen PDEVp und der möglichen Copolymere sollten in weiteren Arbeiten untersucht werden. Die fehlende Stereospezifität der Al-Katalysatoren war sehr wahrscheinlich der Unterschiede in der Haptizität der Cp-Liganden (fünf für Y-CGCs, eins für die Al-Pendants) und der resultierenden Diskrepanz bei der elektronischen und sterischen Umgebung geschuldet. Generell schien die Kombination von *ansa*-Metallocenliganden und Aluminium als Zentralatom nicht zu funktionieren und zeigte uns die Grenzen der Hauptgruppenelement-Katalyse auf. Dennoch erwiesen sich die vielseitigen Polymerisationskatalysatoren dieser Arbeit als ernsthafte Konkurrenten für etablierte Methoden und bieten enormes Potential für weitere Verbesserungen und vielversprechende Anwendungen.

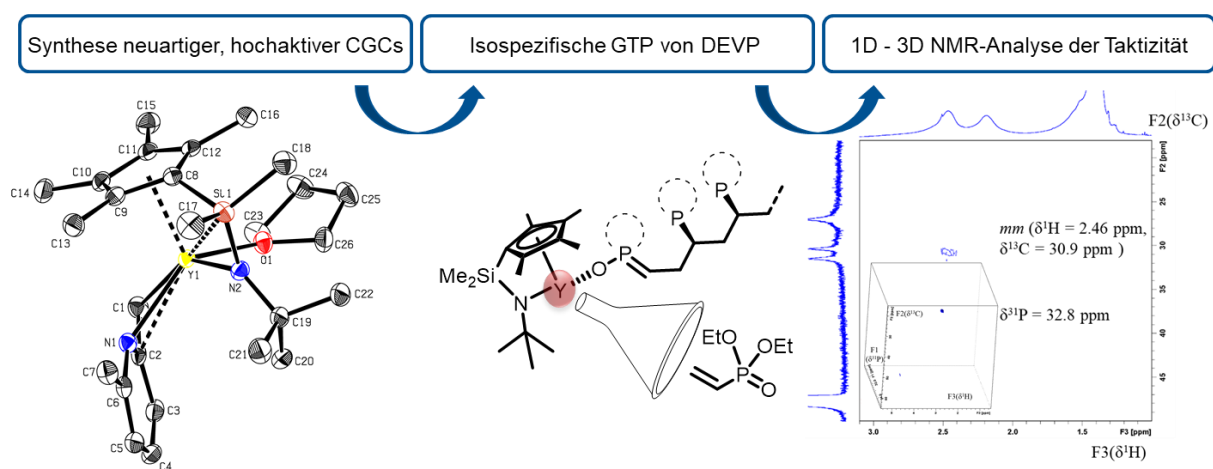


Abbildung 14: Maßgeschneiderte CGCs für die Synthese von *it*-PDEVp und eine ausführliche NMR-Studie zur Quali- und Quantifizierung der Taktizität.

11. Bibliography

- [1] S. Salzinger, B. Rieger, *Macromol. Rapid Commun.* **2012**, *33*, 1327.
- [2] E. Y.-X. Chen, *Chem. Rev.* **2009**, *109*, 5157.
- [3] R. Mülhaupt, *Macromol. Chem. Phys.* **2003**, *204*, 289.
- [4] P. Corradini, *Macromol. Symp.* **1995**, *89*, 1.
- [5] Y. Zhang, G. M. Miyake, E. Y.-X. Chen, *Angew. Chem. Int. Ed.* **2010**, *49*, 10158.
- [6] M. G. M. Knaus, M. M. Giuman, A. Pöthig, B. Rieger, *J. Am. Chem. Soc.* **2016**, *138*, 7776.
- [7] B. Rieger, L. S. Baugh, S. Kacker, S. Striegler, *Late Transition Metal Polymerization Catalysis*, Wiley, **2003**.
- [8] a) H. Abe, K. Imai, M. Matsumoto, *J. Polym. Sci., Part B* **1965**, *3*, 1053; b) H. Abe, K. Imai, M. Matsumoto, *J. Polym. Sci., Part C* **1968**, *23*, 469; c) C. Simionescu, N. Asandei, I. Benedek, C. Ungurenasu, *Eur. Polym. J.* **1969**, *5*, 449.
- [9] D. G. H. Ballard, P. W. van Lienden, *Makromol. Chem.* **1972**, *154*, 177.
- [10] S. Collins, D. G. Ward, *J. Am. Chem. Soc.* **1992**, *114*, 5460.
- [11] H. Yasuda, H. Yamamoto, K. Yokota, S. Miyake, A. Nakamura, *J. Am. Chem. Soc.* **1992**, *114*, 4908.
- [12] O. W. Webster in *Advances in Polymer Science*, Springer Berlin Heidelberg, Berlin, Heidelberg, **2004**, pp. 1–34.
- [13] a) A. D. Celiz, J. G. W. Smith, A. K. Patel, R. Langer, D. G. Anderson, D. A. Barrett, L. E. Young, M. C. Davies, C. Denning, M. R. Alexander, *Biomater. Sci.* **2014**, *2*, 1604; b) E. Goiti, M. B. Huglin, J. M. Rego, *Eur. Polym. J.* **2004**, *40*, 219; c) C. Tarducci, J. P. S. Badyal, S. A. Brewer, C. Willis, *Chem. Commun.* **2005**, 406.
- [14] A. A. Kavitha, N. K. Singha, *Macromol. Chem. Phys.* **2007**, *208*, 2569.
- [15] P. Q. Ashton Acton, *Acrylates-Advances in Research and Application*, ScholarlyMedia LLC, Atlanta, **2012**.
- [16] a) M. Banks, J. R. Ebdon, M. Johnson, *Polymer* **1994**, *35*, 3470; b) M. R. Berber, T. Fujigaya, N. Nakashima, *ChemCatChem* **2014**, *6*, 567; c) M. R. Berber, T. Fujigaya, K. Sasaki, N. Nakashima, *Sci Rep* **2013**, *3*, 2430; d) N. Deng, X. Ni, Z. Shen, *Designed Monomers and Polymers* **2015**, *18*, 470; e) J. Ellis, A. D. Wilson, *Dent. Mater.* **1992**, *8*,

- 79; f) J. Ellis, M. Anstice, A. D. Wilson, *Clinical Materials* **1991**, 7, 341; g) C. D. Magnusson, D. Liu, E. Y.-X. Chen, M. A. Kelland, *Energy Fuels* **2015**, 29, 2336; h) J. Tan, R. A. Gemeinhart, M. Ma, W. M. Saltzman, *Biomaterials* **2005**, 26, 3663.
- [17] B. S. Soller, S. Salzinger, B. Rieger, *Chem. Rev.* **2016**, 116, 1993.
- [18] F. Adams, P. T. Altenbuchner, P. D. L. Werz, B. Rieger, *RSC Adv.* **2016**, 6, 78750.
- [19] C. Schwarzenböck, A. Schaffer, E. Nößner, P. J. Nelson, R. Huss, B. Rieger, *Chem. Eur. J.* **2018**, 24, 2584.
- [20] C. Schwarzenböck, A. Schaffer, P. Pahl, P. J. Nelson, R. Huss, B. Rieger, *Polym. Chem.* **2018**, 9, 284.
- [21] J. M. J. Fréchet, M. V. de Meftahi, *Brit. Poly.J.* **1984**, 16, 193.
- [22] A. Sharma, R. Kroon, D. A. Lewis, G. G. Andersson, M. R. Andersson, *ACS Appl. Mater. Interfaces* **2017**, 9, 10929.
- [23] a) N. Adams, U. S. Schubert, *Adv. Drug Delivery Rev.* **2007**, 59, 1504; b) C. J. Waschinski, S. Barnert, A. Theobald, R. Schubert, F. Kleinschmidt, A. Hoffmann, K. Saalwächter, J. C. Tiller, *Biomacromolecules* **2008**, 9, 1764; c) C. Weber, T. Neuwirth, K. Kempe, B. Ozkahraman, E. Tamahkar, H. Mert, C. R. Becer, U. S. Schubert, *Macromolecules* **2012**, 45, 20.
- [24] N. Zhang, S. Salzinger, B. S. Soller, B. Rieger, *J. Am. Chem. Soc.* **2013**, 135, 8810.
- [25] K. Fuchise, *Design and Precise Synthesis of Thermoresponsive Polyacrylamides*, Springer Japan, Tokyo, **2014**.
- [26] T. Kodaira, H. Tanahashi, K. Hara, *Polym. J.* **1990**, 22, 649.
- [27] O. W. Webster, W. R. Hertler, D. Y. Sogah, W. B. Farnham, T. V. RajanBabu, *J. Am. Chem. Soc.* **1983**, 105, 5706.
- [28] a) A. H. E. Müller, G. Litvinenko, D. Yan, *Macromolecules* **1996**, 29, 2346; b) R. P. Quirk, J.-S. Kim, *J. Phys. Org. Chem.* **1995**, 8, 242; c) R. Quirk, G. Bidinger, *Polym. Bull.* **1989**, 22.
- [29] E. Ihara, M. Morimoto, H. Yasuda, *Proc. Jpn. Acad.* **1995**, 71 (B), 126.
- [30] H. Yasuda, H. Tamai, *Prog. Polym. Sci.* **1993**, 18, 1097.
- [31] H. Yasuda, H. Yamamoto, M. Yamashita, K. Yokota, A. Nakamura, S. Miyake, Y. Kai, N. Kanehisa, *Macromolecules* **1993**, 26, 7134.

- [32] G. Qi, Y. Nitto, A. Saiki, T. Tomohiro, Y. Nakayama, H. Yasuda, *Tetrahedron* **2003**, *59*, 10409.
- [33] a) H. Frauenrath, H. Keul, H. Höcker, *Macromolecules* **2001**, *34*, 14; b) T. Stuhldreier, H. Keul, H. Höcker, *Macromol. Rapid Commun.* **2000**, *21*, 1093.
- [34] G. G. Odian, *Principles of polymerization*, Wiley, Hoboken, N.J, **2010**.
- [35] E. Ihara, M. Morimoto, H. Yasuda, *Macromolecules* **1995**, *28*, 7886.
- [36] U. B. Seemann, J. E. Dengler, B. Rieger, *Angew. Chem. Int. Ed.* **2010**, *49*, 3489.
- [37] S. Salzinger, B. S. Soller, A. Plikhta, U. B. Seemann, E. Herdtweck, B. Rieger, *J. Am. Chem. Soc.* **2013**, *135*, 13030.
- [38] H. Kaneko, H. Nagae, H. Tsurugi, K. Mashima, *J. Am. Chem. Soc.* **2011**, *133*, 19626.
- [39] P. T. Altenbuchner, B. S. Soller, S. Kissling, T. Bachmann, A. Kronast, S. I. Vagin, B. Rieger, *Macromolecules* **2014**, *47*, 7742.
- [40] W. R. Mariott, E. Y.-X. Chen, *Macromolecules* **2004**, *37*, 4741.
- [41] W. R. Mariott, E. Y.-X. Chen, *Macromolecules* **2005**, *38*, 6822.
- [42] a) E. Kirillov, C. W. Lehmann, A. Razavi, J.-F. Carpentier, *Organometallics* **2004**, *23*, 2768; b) M. H. Lee, J.-W. Hwang, Y. Kim, J. Kim, Y. Han, Y. Do, *Organometallics* **1999**, *18*, 5124; c) C. Qian, W. Nie, J. Sun, *Organometallics* **2000**, *19*, 4134; d) M. A. Giardello, Y. Yamamoto, L. Brard, T. J. Marks, *J. Am. Chem. Soc.* **1995**, *117*, 3276.
- [43] A. D. Bolig, E. Y.-X. Chen, *J. Am. Chem. Soc.* **2004**, *126*, 4897.
- [44] Y. Ning, E. Y.-X. Chen, *J. Am. Chem. Soc.* **2008**, *130*, 2463.
- [45] J. W. Strauch, J.-L. Fauré, S. Bredeau, C. Wang, G. Kehr, R. Fröhlich, H. Luftmann, G. Erker, *J. Am. Chem. Soc.* **2004**, *126*, 2089.
- [46] C. Cui, A. Shafir, C. L. Reeder, J. Arnold, *Organometallics* **2003**, *22*, 3357.
- [47] S. A. Ahmed, M. S. Hill, P. B. Hitchcock, S. M. Mansell, St., *Organometallics* **2007**, *26*, 538.
- [48] F. Adams, M. R. Machat, P. T. Altenbuchner, J. Ehrmaier, A. Pöthig, T. N. V. Karsili, B. Rieger, *Inorg. Chem.* **2017**, *56*, 9754.
- [49] H. Nguyen, A. P. Jarvis, M. J. G. Lesley, W. M. Kelly, S. S. Reddy, N. J. Taylor, S. Collins, *Macromolecules* **2000**, *33*, 1508.

- [50] A. Rodriguez-Delgado, W. R. Mariott, E. Y.-X. Chen, *Macromolecules* **2004**, *37*, 3092.
- [51] B. Lian, C. M. Thomas, C. Navarro, J.-F. Carpentier, *Macromolecules* **2007**, *40*, 2293.
- [52] K. C. Hultsch, T. P. Spaniol, J. Okuda, *Angew. Chem. Int. Ed.* **1999**, *38*, 227.
- [53] a) P. L. Watson, *Chem. Commun.* **1983**, 276; b) P. L. Watson, *J. Am. Chem. Soc.* **1983**, *105*, 6491.
- [54] B. S. Soller, S. Salzinger, C. Jandl, A. Pöthig, B. Rieger, *Organometallics* **2015**, *34*, 2703.
- [55] P. Pahl, C. Schwarzenböck, F. A. D. Herz, B. S. Soller, C. Jandl, B. Rieger, *Macromolecules* **2017**, *50*, 6569.
- [56] C. Schwarzenböck, S. I. Vagin, W. R. Heinz, P. J. Nelson, B. Rieger, *Macromol. Rapid Commun.* **2018**, *39*, 1800259.
- [57] S. Murahashi, S. I. Nozakura, K. Hatada, S. Takeuchi, T. Aoki, *Sen-iken. Nenpo.* **1960**, 99.
- [58] M. Ikeda, T. Hirano, T. Tsuruta, *Makromol. Chem.* **1971**, *150*, 127.
- [59] a) T. Kitayama, T. Iijima, T. Nishiura, K. Hatada, *Polym. Bull.* **1992**, *28*, 327; b) T. Kitayama, E. Masuda, M. Yamaguchi, T. Nishiura, K. Hatada, *Polym. J.* **1992**, *24*, 817.
- [60] Y. Zhang, G. M. Miyake, M. G. John, L. Falivene, L. Caporaso, L. Cavallo, E. Y.-X. Chen, *Dalton Trans.* **2012**, *41*, 9119.
- [61] J. He, Y. Zhang, L. Falivene, L. Caporaso, L. Cavallo, E. Y.-X. Chen, *Macromolecules* **2014**, *47*, 7765.
- [62] X. Wang, Y. Zhang, M. Hong, *Molecules (Basel, Switzerland)* **2018**, *23*.
- [63] Q. Wang, W. Zhao, S. Zhang, J. He, Y. Zhang, E. Y.-X. Chen, *ACS Catal.* **2018**, *8*, 3571.
- [64] T. Xu, E. Y.-X. Chen, *J. Am. Chem. Soc.* **2014**, *136*, 1774.
- [65] K. Hatada, T. Kitayama, K. Ute, *Progress in Polymer Science* **1988**, *13*, 189.
- [66] F. A. Bovey, P. A. Mirau, *NMR of polymers*, Academic Press, San Diego, **1996**.
- [67] H. G. Barth, J. W. Mays, *Modern methods of polymer characterization*, Wiley, New York, **1991**.

- [68] T. Kawamura, N. Toshima, K. Matsuzaki, *Makromol. Chem., Rapid Commun.* **1993**, *14*, 719.
- [69] K. Beshah, *Makromol. Chem.* **1993**, *194*, 3311.
- [70] A. Bulai, M. L. Jimeno, A.-A. Alencar de Queiroz, A. Gallardo, J. San Román, *Macromolecules* **1996**, *29*, 3240.
- [71] W. Liu, T. Nakano, Y. Okamoto, *Polym. J.* **2000**, *32*, 771.
- [72] K. Matsuzaki, T. Kanai, T. Matsubara, S. Matsumoto, *J. Polym. Sci. Polym. Chem. Ed.* **1976**, *14*, 1475.
- [73] K. Matsuzaki, T. Matsubara, T. Kanai, *J. Polym. Sci. Polym. Chem. Ed.* **1977**, *15*, 1573.
- [74] P. T. Altenbuchner, F. Adams, A. Kronast, E. Herdtweck, A. Pöthig, B. Rieger, *Polym. Chem.* **2015**, *6*, 6796.
- [75] H. Komber, V. Steinert, B. Voit, *Macromolecules* **2008**, *41*, 2119.
- [76] P. L. Rinaldi, *Analyst* **2004**, *129*, 687.
- [77] L. Li, B. Zhang, F. Wyzgoski, X. Li, E. F. McCord, P. L. Rinaldi, *ACS Macro Lett.* **2013**, *2*, 141.
- [78] E. L. Eliel, S. H. Wilen *Topics in stereochemistry*, Wiley, New York, **1987**.
- [79] F. Adams, *Gruppentransferpolymerisation von Michael-Monomeren*, Springer Fachmedien Wiesbaden, **2016**.
- [80] G. W. Coates, *Chem. Rev.* **2000**, *100*, 1223.
- [81] Y. Ning, L. Caporaso, A. Correa, L. O. Gustafson, L. Cavallo, E. Y.-X. Chen, *Macromolecules* **2008**, *41*, 6910.
- [82] a) H. F. Mark, *Encyclopedia of polymer science and technology*, John Wiley & Sons Inc, Hoboken, New Jersey, **2014**; b) K. Ohlrogge *Membranen. Grundlagen, Verfahren und industrielle Anwendungen*, Wiley-VCH, Weinheim, **2006**; c) V. Pitto, B. I. Voit, T. J. A. Loontjens, R. A. T. M. van Benthem, *Makromol. Chem. Phys.* **2004**, *205*, 2346.
- [83] a) J. M. Margolis, *Engineering plastics handbook*, McGraw-Hill, New York, **2006**; b) J. Pietrasik, H. Dong, K. Matyjaszewski, *Macromolecules* **2006**, *39*, 6384; c) N. V. Tsarevsky, T. Sarbu, B. Göbelt, K. Matyjaszewski, *Macromolecules* **2002**, *35*, 6142.

- [84] A. Gupta, I. R. Harrison, *Carbon* **1997**, *35*, 809.
- [85] J. Kim, Y. C. Kim, W. Ahn, C. Y. Kim, *Polym. Eng. Sci.* **1993**, *33*, 1452.
- [86] J. L. Figueiredo, C. A. Bernardo, R. T. K. Baker, K. J. Hüttinger, *Carbon Fibers Filaments and Composites*, Springer Netherlands, Dordrecht, **1990**.
- [87] a) M. Kamigaito, T. Ando, M. Sawamoto, *Chem. Rev.* **2001**, *101*, 3689; b) K. Matyjaszewski, *Macromolecules* **2012**, *45*, 4015; c) K. Matyjaszewski, N. V. Tsarevsky, *Nature Chem.* **2009**, *1*, 276; d) K. Matyjaszewski, N. V. Tsarevsky, *J. Am. Chem. Soc.* **2014**, *136*, 6513.
- [88] a) A. Yamamoto, S. Ikeda, *J. Am. Chem. Soc.* **1967**, *89*, 5989; b) M. Ikeda, T. Hirano, A. Uchida, T. Tsuruta, *Makromol. Chem.* **1974**, *175*, 2039.
- [89] a) K. C. Hultsch, T. P. Spaniol, J. Okuda, *Angew. Chem. Int. Ed.* **1999**, *38*, 227; b) K. Nozaki, S. Kusumoto, S. Noda, T. Kochi, L. W. Chung, K. Morokuma, *J. Am. Chem. Soc.* **2010**, *132*, 16030; c) F. Schaper, S. R. Foley, R. F. Jordan, *J. Am. Chem. Soc.* **2004**, *126*, 2114; d) F. Wu, S. R. Foley, C. T. Burns, R. F. Jordan, *J. Am. Chem. Soc.* **2005**, *127*, 1841; e) U. Siemeling, L. Kölling, A. Stammler, H.-G. Stammler, E. Kaminski, G. Fink, *Chem. Commun.* **2000**, 1177; f) K. Tsuchihara, Y. Suzuki, M. Asai, K. Soga, *Chem. Lett.* **1999**, *28*, 891.
- [90] M. Ikeda, T. Hirano, S. Nakayama, T. Tsuruta, *Makromol. Chem.* **1974**, *175*, 2775.
- [91] D. M. White, *J. Am. Chem. Soc.* **1960**, *82*, 5678.
- [92] M. Minagawa, H. Yamada, K. Yamaguchi, F. Yoshii, *Macromolecules* **1992**, *25*, 503.
- [93] a) R. V. Ghorpade, D. W. Cho, S. C. Hong, *Carbon* **2017**, *121*, 502; b) J. Hao, W. Li, X. Suo, H. Wei, C. Lu, Y. Liu, *Polymer* **2018**, *157*, 139.
- [94] M. G. M. Knaus, M. M. Giuman, B. Rieger, WO 2017162784 A1, **2017**.
- [95] G. W. Rabe, H. Komber, L. Häussler, K. Kreger, G. Lattermann, *Macromolecules* **2010**, *43*, 1178.
- [96] a) H. Braunschweig, F. M. Breitling, *Coord. Chem. Rev.* **2006**, *250*, 2691; b) P. J. Shapiro, E. Bunel, W. P. Schaefer, J. E. Bercaw, *Organometallics* **1990**, *9*, 867; c) P. J. Shapiro, W. P. Schaefer, J. A. Labinger, J. E. Bercaw, W. D. Cotter, *J. Am. Chem. Soc.* **1994**, *116*, 4623; d) A. L. McKnight, R. M. Waymouth, *Chem. Rev.* **1998**, *98*, 2587.
- [97] R. K. Grasselli, F. Trifirò, *Top Catal* **2016**, *59*, 1651.

- [98] B. Katryniok, S. Paul, V. Bellière-Baca, P. Rey, F. Dumeignil, *Green Chem.* **2010**, *12*, 2079.
- [99] X. Li, Y. Zhang, *ACS Catal.* **2016**, *6*, 2785.
- [100] a) C. Guillon, C. Liebig, S. Paul, A.-S. Mamede, W. F. Hölderich, F. Dumeignil, B. Katryniok, *Green Chem.* **2013**, *15*, 3015; b) C. Liebig, S. Paul, B. Katryniok, C. Guillon, J.-L. Couturier, J.-L. Dubois, F. Dumeignil, W. F. Hoelderich, *Applied Catalysis B: Environmental* **2013**, *132-133*, 170.
- [101] S. Mannam, G. Sekar, *Tetrahedron Letters* **2008**, *49*, 2457.
- [102] V.A. Bhanu, P. Rangarajan, K. Wiles, M. Bortner, M. Sankarpandian, D. Godshall, T.E. Glass, A.K. Banthia, J. Yang, G. Wilkes, *Polymer* **2002**, *43*, 4841.

12. Appendix

12.1 Supporting Information for Chapter 4

The supporting information is available free of charge under:

<https://onlinelibrary.wiley.com/doi/abs/10.1002/chem.201802075>

Rightslink® by Copyright Clearance Center

<https://s100.copyright.com/AppDispatchServlet>

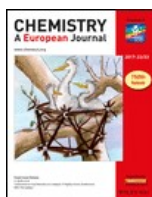


RightsLink®

Home

Account Info

Help



Title: Front Cover: Single-Site, Organometallic Aluminum Catalysts for the Precise Group Transfer Polymerization of Michael-Type Monomers (Chem. Eur. J. 56/2018)

Publication: Chemistry - A European Journal

Publisher: John Wiley and Sons

Date: Sep 7, 2018

Copyright © 2018, John Wiley and Sons

Logged in as:

Michael Weger

Account #:

3001467353

LOGOUT

Order Completed

Thank you for your order.

This Agreement between Mr. Michael Weger ("You") and John Wiley and Sons ("John Wiley and Sons") consists of your license details and the terms and conditions provided by John Wiley and Sons and Copyright Clearance Center.

Your confirmation email will contain your order number for future reference.

[printable details](#)

License Number	4680181048703
License date	Oct 01, 2019
Licensed Content Publisher	John Wiley and Sons
Licensed Content Publication	Chemistry - A European Journal
Licensed Content Title	Front Cover: Single-Site, Organometallic Aluminum Catalysts for the Precise Group Transfer Polymerization of Michael-Type Monomers (Chem. Eur. J. 56/2018)
Licensed Content Date	Sep 7, 2018
Licensed Content Pages	1
Type of use	Dissertation/Thesis
Requestor type	Author of this Wiley article
Format	Print and electronic
Portion	Full article
Will you be translating?	No
Title of your thesis / dissertation	Precision Polymerization of Michael-type Monomers: Benefits and Limitations of Main Group Element-Catalysts
Expected completion date	Nov 2019
Expected size (number of pages)	200
Requestor Location	Mr. Michael Weger Lichtenbergstr 4 Garching, 85747 Germany Attn: Mr. Michael Weger
Publisher Tax ID	EU826007151
Total	0.00 USD

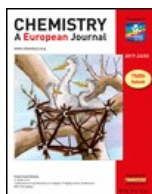


RightsLink®

Home

Account Info

Help



Publication: Chemistry - A European Journal
Publisher: John Wiley and Sons
Date: Dec 31, 1969
Copyright © 1969, John Wiley and Sons

Logged in as:
Michael Weger
Account #:
3001467353

LOGOUT

Order Completed

Thank you for your order.

This Agreement between Mr. Michael Weger ("You") and John Wiley and Sons ("John Wiley and Sons") consists of your license details and the terms and conditions provided by John Wiley and Sons and Copyright Clearance Center.

Your confirmation email will contain your order number for future reference.

[printable details](#)

License Number	4680181212645
License date	Oct 01, 2019
Licensed Content Publisher	John Wiley and Sons
Licensed Content Publication	Chemistry - A European Journal
Licensed Content Date	Dec 31, 1969
Licensed Content Pages	1
Type of use	Dissertation/Thesis
Requestor type	Author of this Wiley article
Format	Print and electronic
Portion	Full article
Will you be translating?	No
Title of your thesis / dissertation	Precision Polymerization of Michael-type Monomers: Benefits and Limitations of Main Group Element-Catalysts
Expected completion date	Nov 2019
Expected size (number of pages)	200
Requestor Location	Mr. Michael Weger Lichtenbergstr 4 Garching, 85747 Germany Attn: Mr. Michael Weger
Publisher Tax ID	EU826007151
Total	0.00 USD

Would you like to purchase the full text of this article? If so, please continue on to the content ordering system located here: [Purchase PDF](#)

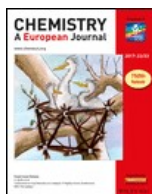
If you click on the buttons below or close this window, you will not be able to return to the



Home

Account Info

Help



Title: Single-Site, Organometallic Aluminum Catalysts for the Precise Group Transfer Polymerization of Michael-Type Monomers

Author: Michael Weger, Marco M. Giuman, Maximilian G. Knaus, et al

Publication: Chemistry - A European Journal

Publisher: John Wiley and Sons

Date: Sep 6, 2018

Copyright © 2018, John Wiley and Sons

Logged in as:

Michael Weger

Account #:

3001467353

LOGOUT

Order Completed

Thank you for your order.

This Agreement between Mr. Michael Weger ("You") and John Wiley and Sons ("John Wiley and Sons") consists of your license details and the terms and conditions provided by John Wiley and Sons and Copyright Clearance Center.

Your confirmation email will contain your order number for future reference.

[printable details](#)

License Number	4680181413814
License date	Oct 01, 2019
Licensed Content Publisher	John Wiley and Sons
Licensed Content Publication	Chemistry - A European Journal
Licensed Content Title	Single-Site, Organometallic Aluminum Catalysts for the Precise Group Transfer Polymerization of Michael-Type Monomers
Licensed Content Author	Michael Weger, Marco M. Giuman, Maximilian G. Knaus, et al
Licensed Content Date	Sep 6, 2018
Licensed Content Pages	1
Type of use	Dissertation/Thesis
Requestor type	Author of this Wiley article
Format	Print and electronic
Portion	Full article
Will you be translating?	No
Title of your thesis / dissertation	Precision Polymerization of Michael-type Monomers: Benefits and Limitations of Main Group Element-Catalysts
Expected completion date	Nov 2019
Expected size (number of pages)	200
Requestor Location	Mr. Michael Weger Lichtenbergstr 4 Garching, 85747 Germany Attn: Mr. Michael Weger
Publisher Tax ID	EU826007151

12.2 Supporting Information for Chapter 5

The supporting information is available free of charge under:

<https://onlinelibrary.wiley.com/doi/abs/10.1002/anie.201902833>

Rightslink® by Copyright Clearance Center

<https://s100.copyright.com/AppDispatchServlet>

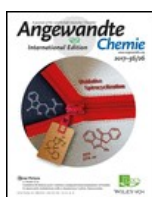


RightsLink®

Home

Account Info

Help



Publication: Angewandte Chemie International Edition

Publisher: John Wiley and Sons

Date: Dec 31, 1969

Copyright © 1969, John Wiley and Sons

Logged in as:

Michael Weger

Account #:

3001467353

LOGOUT

Order Completed

Thank you for your order.

This Agreement between Mr. Michael Weger ("You") and John Wiley and Sons ("John Wiley and Sons") consists of your license details and the terms and conditions provided by John Wiley and Sons and Copyright Clearance Center.

Your confirmation email will contain your order number for future reference.

[printable details](#)

License Number	4681530145197
License date	Oct 03, 2019
Licensed Content Publisher	John Wiley and Sons
Licensed Content Publication	Angewandte Chemie International Edition
Licensed Content Date	Dec 31, 1969
Licensed Content Pages	1
Type of use	Dissertation/Thesis
Requestor type	Author of this Wiley article
Format	Print and electronic
Portion	Full article
Will you be translating?	No
Title of your thesis / dissertation	Precision Polymerization of Michael-type Monomers: Benefits and Limitations of Main Group Element-Catalysts
Expected completion date	Nov 2019
Expected size (number of pages)	200
Requestor Location	Mr. Michael Weger Lichtenbergstr 4 Garching, 85747 Germany Attn: Mr. Michael Weger
Publisher Tax ID	EU826007151
Total	0.00 USD

Would you like to purchase the full text of this article? If so, please continue on to the content ordering system located here: [Purchase PDF](#)

If you click on the buttons below or close this window, you will not be able to return to the

12.3 Supporting Information for Chapter 6

WILEY-VCH

SUPPORTING INFORMATION

Supporting Information
©Wiley-VCH 2016
69451 Weinheim, Germany

Taming the Polymerization of Acrylonitrile with Highly Active Main Group Element Catalysts

Michael Weger, Maximilian G. Knaus, Marco M. Giuman, Markus Drees, Alexander Pöthig, and Bernhard Rieger*

Abstract: The fast and controlled conversion of acrylonitrile (AN) is still a pending issue in polymerization catalysis. We now demonstrate that simple main group element catalysts enable the synthesis of high molecular weight PAN with very narrow molecular weight distributions on short time scales. Aluminum/phosphorus-based Lewis pairs facilitate the access to defined PAN with shorter chains due to their excellent initiator efficiency, whereas $\text{Al}(\text{C}_6\text{F}_5)_3$ converts AN to very high molecular weight products with extremely high TOFs (up to $110,000 \text{ h}^{-1}$). The easily accessible MgCp_2 performs even better as polymerization catalyst, achieving remarkable dispersities as narrow as 1.13 combined with high TOFs. As evidenced by kinetic studies, the living behavior allows the quantitative consumption of AN. End group analysis supported by DFT calculations clearly suggests the transfer of a Cp ligand to the olefin end of AN as the decisive initiation step.

DOI: 10.1002/anie.2016XXXXX

SUPPORTING INFORMATION

0. Table of Contents

0. Table of Contents	2
1. Experimental Procedures	2
2. Single Crystal Diffraction Experiments	4
3. End Group Analysis and Kinetic Studies	7
4. Theoretical Calculations	9
5. References	22

1. Experimental Procedures

Materials and Methods: Unless otherwise stated, all chemicals were purchased from Sigma-Aldrich, VWR-International or ABCR and used as received. Toluene, pentane, diethyl ether and tetrahydrofuran were dried using an MBraun SPS-800 solvent purification system. Acrylonitrile and *N,N*-dimethylformamide were dried over CaH₂ and distilled prior to use. NMR spectra were recorded on a Bruker AV-NEO 400. ¹H NMR spectroscopic chemical shifts δ are reported in ppm relative to tetramethylsilane. δ (¹H) is calibrated to the residual proton signal of the solvent. Deuterated solvents were obtained from Eurisotop or Sigma Aldrich.

For the MALDI-TOF measurements a Bruker Daltonics ultraflex TOF/TOF was used and analyzed using FlexAnalysis software. The samples were prepared according to a literature procedure.^[1]

GPC was carried out on a Varian PL GPC-50 equipped with two PL Polargel columns. As eluent *N,N*-dimethylformamide (2.2 g/L lithium bromide) was used. Absolute molecular weights have been determined by two angle laser light scattering analysis using a concentration and viscosity detector, coupled with GPC.

Elemental analysis was performed at the microanalytic laboratory of the Department of Inorganic Chemistry at the Technical University of Munich.

General procedure for the polymerization of acrylonitrile: Polymerizations were performed in 15 mL oven-dried glass reactors interfaced to a dual-manifold Schlenk line at the stated temperatures under argon atmosphere. A predetermined amount of the respective catalyst was first dissolved in DMF. Then the polymerization was started by addition of acrylonitrile *via* a gastight syringe under vigorous stirring. After the measured time interval, a 0.2 mL aliquot was taken from the reaction mixture *via* a syringe and quickly quenched into a 4 mL vial containing 0.4 mL of undried "wet" DMSO-d₆. The quenched aliquots were later analyzed by ¹H NMR to obtain the percent polymer yield data. The polymerization was immediately quenched after the removal of the aliquot by addition of 0.5 mL 4N HCl in dioxane. The solvents were evaporated from the quenched mixtures under reduced pressure, the polymers were purified by precipitation in methanol and dried in a vacuum oven at 40 °C overnight to a constant weight.

Activity measurements: The stated amount of catalyst is dissolved in DMF and the reaction mixture is thermostated to the desired temperature. Then, the stated amount of monomer is added. During the course of the measurement, the temperature is monitored with a digital thermometer and aliquots (0.5 ml) are taken and quenched by addition to deuterated DMSO (0.2 ml). After the stated reaction time, the reaction is quenched by addition of 4N HCl in dioxane (0.5 ml). The procedure was performed at least twice for every polymerization to obtain accurate activity values. The TOFs are calculated corresponding to the following equation:^[2]

$$TOF = \frac{n(Mon)}{n(Cat) \times t} = \frac{n(Mon)_0 \times X}{n(Cat) \times t}$$

Characterization of synthesized organometallic compounds:

Synthesis of tris(pentafluorophenyl)aluminum: Al(C₆F₅)₃ was synthesized according to a literature known procedure.^[3]

¹⁹F NMR (376 MHz, C₆D₆, 298 K): δ = -160.5 (s, m-F), -152.5 (s, p-F), -126.7 (s, o-F).

Synthesis of magnesocene: MgCp₂ was synthesized according to a literature known procedure.^[4]

¹H NMR (400 MHz, C₆D₆, 298 K): δ = 6.01 (s, 10H).

¹³C NMR (100 MHz, C₆D₆, 298 K): δ = 107.8 (s, 10C).

Synthesis of tris(pentafluorophenyl)alane-acrylonitrile adduct: To a solution of tris(pentafluorophenyl)aluminum (100 mg, 161 μ mol) in dry toluene (5 mL) acrylonitrile (500 μ L) was added at -78 °C. The solvent and excess acrylonitrile were removed under high vacuum. Crystals suitable for single X-ray analysis could be obtained out of a toluene / pentane solution at -30 °C *via* a vapor diffusion technique.

¹H NMR (400 MHz, C₆D₆, 298 K): δ = 5.11 (d, ³J = 18.0 Hz, 1H), 4.72 (d, ³J = 12.3 Hz, 1H), 3.88 (dd, ³J = 18.0, 12.3 Hz).

¹⁹F NMR (376 MHz, C₆D₆, 298 K): δ = 160.6 (s, 2F), 151.0 (s, 1F), 123.2 (s, 2F).

EA: calculated: C 43.40, H 0.52, N 2.41; found: C 43.46, H 0.58, N 2.58.

SUPPORTING INFORMATION

Additional polymerization studies

Table S1. Synthesis of PAN using different main group element-based catalysts.^[a]

Exp.	Catalyst	[Mon]/[LA]	t / min	T / °C	Y / % ^[b]	M _n / 10 ³ g/mol ^[c]	Đ (M _w /M _n)	I / % ^[d]	TOF / h ⁻¹
1	AlPh ₃ /PCy ₃ ^[e]	1000	60	0	16	16	1.42	54	160
2	AlMe ₃ /PMe ₃ ^[e]	2000	60	0	31	44	2.01	76	620
3	AlPh ₃ /PCy ₃ ^[e]	2000	60	0	25	65	1.46	40	500
4	PMe ₃	1000	60	0	75	n.d.	bimodal	-	-
5	Al(C ₆ F ₅) ₃	4000	0.08	0	4	105	1.59	8	115,000
6	Al(C ₆ F ₅) ₃	8000	2.5	0	46	n.d. ^[f]	n.d.	-	88,000
7	AlMe ₂ Cp	200	60	30	<10	n.d.	n.d.	-	-
8	MgCp ₂	2000	49	-30	100	195	1.41	54	2500
9	MgCp ₂	1000	4	30	100	120	1.25 ^[g]	44	15,000
10	MgCp ₂	2000	8.5	30	100	270	1.38	39	7000

[a] V_{Mon} = 0.5 mL, V_{solvent} = 7.5 mL *N,N*-DMF. [b] measured gravimetrically and by ¹H NMR spectroscopy. [c] determined by dual-angle laser light scattering in *N,N*-DMF (2.2 g/L lithium bromide) at 30 °C. [d] initiator efficiency (M_{n(theo.)}/M_{n(determ.)}). [e] [LA]/[LB] = 2:1, [f] M_w = 1600 kg/mol determined by multi-angle laser light scattering, [g] slightly bimodal.

SUPPORTING INFORMATION

2. Single Crystal Diffraction Experiments

A clear light yellow fragment-like specimen of $C_{24}H_6AlF_{15}N_2$, approximate dimensions 0.034 mm x 0.044 mm x 0.390 mm, was used for the X-ray crystallographic analysis. The X-ray intensity data were measured on a Bruker Kappa APEX II CCD system equipped with a MONTEL mirror monochromator and a Mo FR591 rotating anode ($\lambda = 0.71073 \text{ \AA}$).

A total of 1456 frames were collected. The total exposure time was 4.04 hours. The frames were integrated with the Bruker SAINT software package using a narrow-frame algorithm. The integration of the data using a monoclinic unit cell yielded a total of 19947 reflections to a maximum θ angle of 27.10° (0.78 \AA resolution), of which 2638 were independent (average redundancy 7.561, completeness = 99.7%, $R_{int} = 4.35\%$) and 2210 (83.78%) were greater than $2\sigma(F^2)$. The final cell constants of $a = 15.9964(7) \text{ \AA}$, $b = 11.4071(5) \text{ \AA}$, $c = 13.8644(5) \text{ \AA}$, $\beta = 109.0790(10)^\circ$, volume = $2390.90(17) \text{ \AA}^3$, are based upon the refinement of the XYZ-centroids of 119 reflections above $20 \sigma(I)$ with $4.479^\circ < 2\theta < 62.02^\circ$. Data were corrected for absorption effects using the multi-scan method (SADABS). The ratio of minimum to maximum apparent transmission was 0.833. The calculated minimum and maximum transmission coefficients (based on crystal size) are 0.9190 and 0.9930.

The final anisotropic full-matrix least-squares refinement on F^2 with 204 variables converged at $R1 = 3.20\%$, for the observed data and $wR2 = 8.37\%$ for all data. The goodness-of-fit was 1.035. The largest peak in the final difference electron density synthesis was $0.403 \text{ e}/\text{\AA}^3$ and the largest hole was $-0.191 \text{ e}/\text{\AA}^3$ with an RMS deviation of $0.048 \text{ e}/\text{\AA}^3$. On the basis of the final model, the calculated density was $1.762 \text{ g}/\text{cm}^3$ and $F(000)$, 1248 e^- .

Table S2. Sample and crystal data for the tris(pentafluorophenyl)alane-acrylonitrile adduct.

Identification code	KnaMa2 AP6206-123	
Chemical formula	$C_{24}H_6AlF_{15}N_2$	
Formula weight	317.14	
Temperature	123(2) K	
Wavelength	0.71073 \AA	
Crystal size	0.034 x 0.044 x 0.390 mm	
Crystal habit	clear light yellow fragment	
Crystal system	monoclinic	
Space group	C 1 2/c 1	
Unit cell dimensions	$a = 15.9964(7) \text{ \AA}$	$\alpha = 90^\circ$
	$b = 11.4071(5) \text{ \AA}$	$\beta = 109.0790(10)^\circ$
	$c = 13.8644(5) \text{ \AA}$	$\gamma = 90^\circ$
Volume	$2390.90(17) \text{ \AA}^3$	
Z	8	
Density (calculated)	$1.762 \text{ g}/\text{cm}^3$	
Absorption coefficient	0.221 mm^{-1}	
$F(000)$	1248	

Table S3. Data collection and structure refinement for the tris(pentafluorophenyl)alane-acrylonitrile adduct.

Diffractometer	Bruker Kappa APEX II CCD	
Radiation source	FR591 rotating anode, Mo	
Theta range for data collection	2.24 to 27.10°	
Index ranges	$-20 \leq h \leq 20$, $-11 \leq k \leq 14$, $-16 \leq l \leq 17$	
Reflections collected	19947	
Independent reflections	2638 [$R_{int} = 0.0435$]	
Coverage of independent reflections	99.7%	
Absorption correction	multi-scan	
Max. and min. transmission	0.9930 and 0.9190	
Refinement method	Full-matrix least-squares on F^2	
Refinement program	SHELXL-2014 (Sheldrick, 2014)	
Function minimized	$\Sigma w(F_o^2 - F_c^2)^2$	
Data / restraints / parameters	2638 / 0 / 204	
Goodness-of-fit on F^2	1.035	
Final R indices	2210 data; $l > 2\sigma(l)$	$R1 = 0.0320$, $wR2 = 0.0785$
	all data	$R1 = 0.0414$, $wR2 = 0.0837$
Weighting scheme	$w = 1/[\sigma^2(F_o^2) + (0.0361P)^2 + 2.3918P]$ where $P = (F_o^2 + 2F_c^2)/3$	

SUPPORTING INFORMATION

Largest diff. peak and hole	0.403 and -0.191 eÅ ⁻³
R.M.S. deviation from mean	0.048 eÅ ⁻³

Table S4. Bond lengths (Å) for the tris(pentafluorophenyl)alane-acrylonitrile adduct.

F1-C2	1.3538(17)	Al1-C7	1.996(2)
Al1-C1	2.0086(14)	Al1-C1	2.0086(14)
Al1-N1	2.0963(12)	Al1-N1	2.0963(12)
C1-C2	1.383(2)	C1-C6	1.384(2)
N1-C11	1.1384(19)	C2-C3	1.380(2)
F2-C3	1.3410(17)	C3-C4	1.377(2)
F3-C4	1.3444(17)	C4-C5	1.377(2)
F4-C5	1.3469(18)	F5-C6	1.3581(16)
C5-C6	1.379(2)	F6-C8	1.3575(17)
F7-C9	1.3455(17)	C7-C8	1.3832(17)
C7-C8	1.3832(17)	F8-C10	1.338(2)
C8-C9	1.379(2)	C11-C12	1.435(2)
C10-C9	1.3743(19)	C10-C9	1.3744(19)
C12-C13	1.293(3)	C12-H12	0.96(3)
C13-H13B	0.95(3)	C13-H13A	0.96(2)

Table S5. Bond angles (°) for the tris(pentafluorophenyl)alane-acrylonitrile adduct.

C7-Al1-C1	117.96(4)	C7-Al1-C1	117.96(4)
C1-Al1-C1	124.07(8)	C7-Al1-N1	91.15(4)
C1-Al1-N1	89.31(5)	C1-Al1-N1	89.61(5)
C7-Al1-N1	91.15(4)	C1-Al1-N1	89.61(5)
C1-Al1-N1	89.31(5)	N1-Al1-N1	177.71(7)
C2-C1-C6	114.03(13)	C2-C1-Al1	123.82(11)
C6-C1-Al1	122.13(10)	C11-N1-Al1	178.64(12)
F1-C2-C3	116.49(13)	F1-C2-C1	119.13(13)
C3-C2-C1	124.39(14)	F2-C3-C4	119.77(14)
F2-C3-C2	121.46(14)	C4-C3-C2	118.77(14)
F3-C4-C3	120.32(14)	F3-C4-C5	120.05(15)
C3-C4-C5	119.63(14)	F4-C5-C4	119.65(14)
F4-C5-C6	121.20(14)	C4-C5-C6	119.15(14)
F5-C6-C5	116.48(13)	F5-C6-C1	119.49(13)
C5-C6-C1	124.03(14)	C8-C7-C8	113.71(18)
C8-C7-Al1	123.15(9)	C8-C7-Al1	123.15(9)
F6-C8-C9	116.53(13)	F6-C8-C7	119.16(13)
C9-C8-C7	124.32(14)	N1-C11-C12	179.38(19)
F8-C10-C9	120.32(9)	F8-C10-C9	120.32(9)
C9-C10-C9	119.36(19)	F7-C9-C10	120.08(14)
F7-C9-C8	120.77(14)	C10-C9-C8	119.14(14)
C13-C12-C11	122.06(17)	C13-C12-H12	120.6(15)
C11-C12-H12	117.3(15)	C12-C13-H13B	119.0(15)
C12-C13-H13A	120.9(13)	H13B-C13-H13A	120.(2)

Table S6. Torsion angles (°) for the tris(pentafluorophenyl)alane-acrylonitrile adduct.

C6-C1-C2-F1	-179.80(12)	Al1-C1-C2-F1	1.61(19)
C6-C1-C2-C3	-0.3(2)	Al1-C1-C2-C3	-178.91(11)
F1-C2-C3-F2	0.0(2)	C1-C2-C3-F2	-179.48(13)
F1-C2-C3-C4	-179.63(13)	C1-C2-C3-C4	0.9(2)
F2-C3-C4-F3	-0.5(2)	C2-C3-C4-F3	179.20(13)
F2-C3-C4-C5	179.68(14)	C2-C3-C4-C5	-0.7(2)
F3-C4-C5-F4	0.3(2)	C3-C4-C5-F4	-179.85(13)
F3-C4-C5-C6	-179.91(13)	C3-C4-C5-C6	0.0(2)
F4-C5-C6-F5	0.6(2)	C4-C5-C6-F5	-179.17(13)
F4-C5-C6-C1	-179.56(13)	C4-C5-C6-C1	0.6(2)
C2-C1-C6-F5	179.34(12)	Al1-C1-C6-F5	-2.04(18)
C2-C1-C6-C5	-0.4(2)	Al1-C1-C6-C5	178.17(11)

SUPPORTING INFORMATION

C8-C7-C8-F6	179.78(15)	Al1-C7-C8-F6	-0.22(15)
C8-C7-C8-C9	-0.67(11)	Al1-C7-C8-C9	179.33(11)
F8-C10-C9-F7	-1.58(16)	C9-C10-C9-F7	178.42(16)
F8-C10-C9-C8	179.38(10)	C9-C10-C9-C8	-0.62(10)
F6-C8-C9-F7	1.9(2)	C7-C8-C9-F7	-177.71(11)
F6-C8-C9-C10	-179.12(11)	C7-C8-C9-C10	1.3(2)

SUPPORTING INFORMATION

3. End Group Analysis and Kinetic Studies

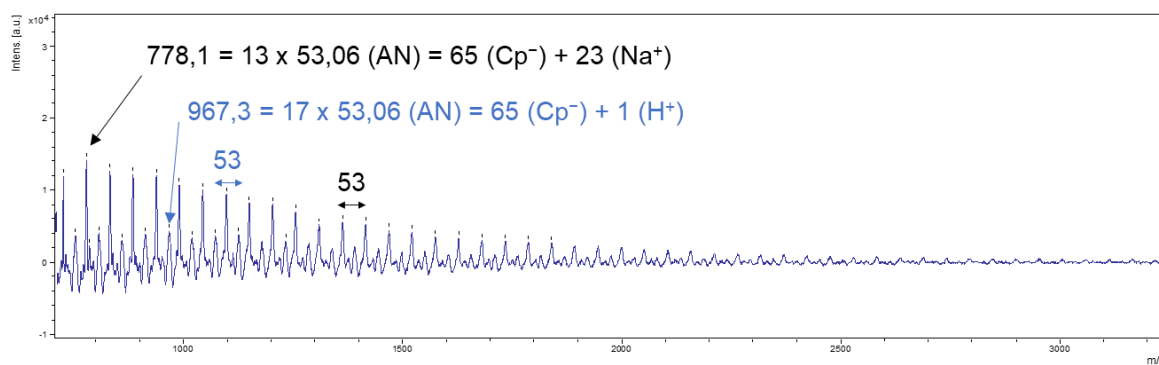


Figure S1. MALDI TOF analysis of AN oligomers produced with MgCp_2 (monomer to catalyst ratio of 30/1, 0 °C, 2.5 mL DMF, 0.1 mL AN).

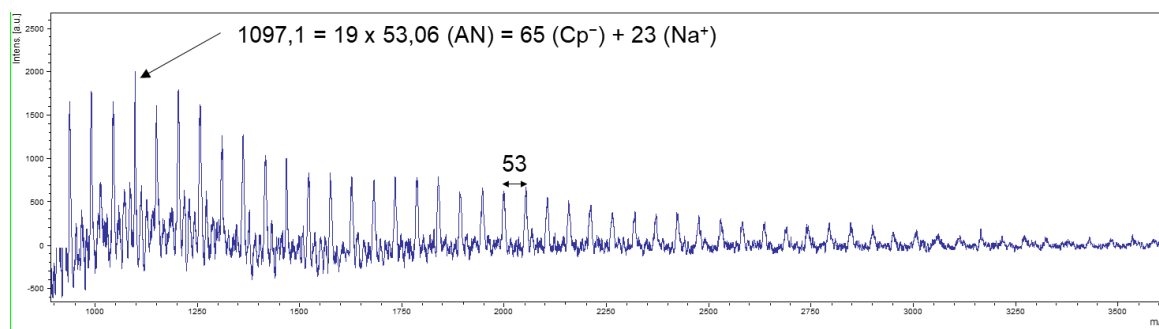


Figure S2. MALDI TOF analysis of AN oligomers produced with MgCp_2 (monomer to catalyst ratio of 30/1, -30 °C, 2.5 mL DMF, 0.1 mL AN).

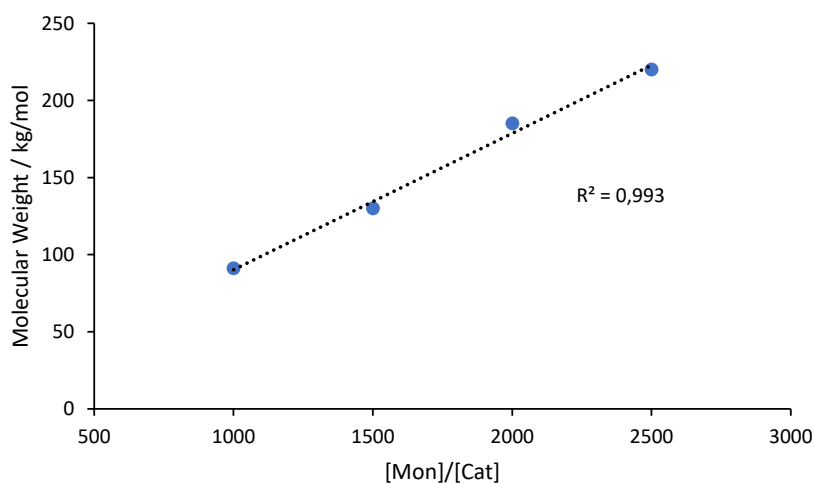


Figure S3. Molecular weight vs. $[\text{Mon}]/[\text{Cat}]$ plot for polymerization of acrylonitrile with MgCp_2 ensuring quantitative conversions (0 °C, 7.5 mL DMF, 0.5 mL AN).

SUPPORTING INFORMATION

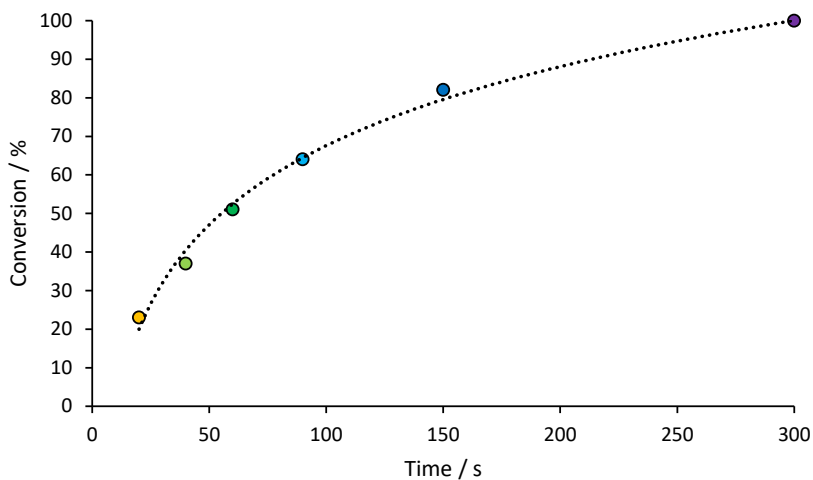


Figure S4. Time vs. conversion plot for polymerization of acrylonitrile with MgCp₂ (monomer to catalyst ratio of 1000/1, 0 °C, 7.5 mL DMF, 0.5 mL AN).

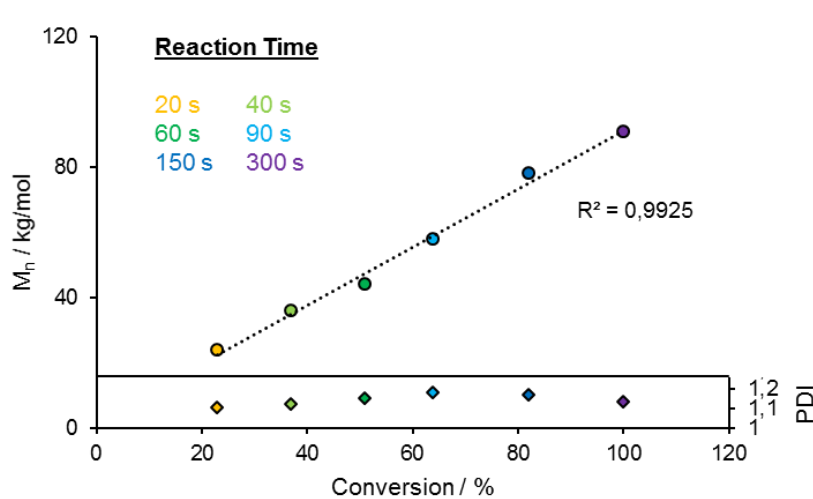


Figure S5. Linear growth of the molecular weight with increasing conversion for the polymerization of acrylonitrile with MgCp₂ (monomer to catalyst ratio of 1000/1, 0 °C, 7.5 mL DMF, 0.5 mL AN).

SUPPORTING INFORMATION

4. Theoretical Calculations

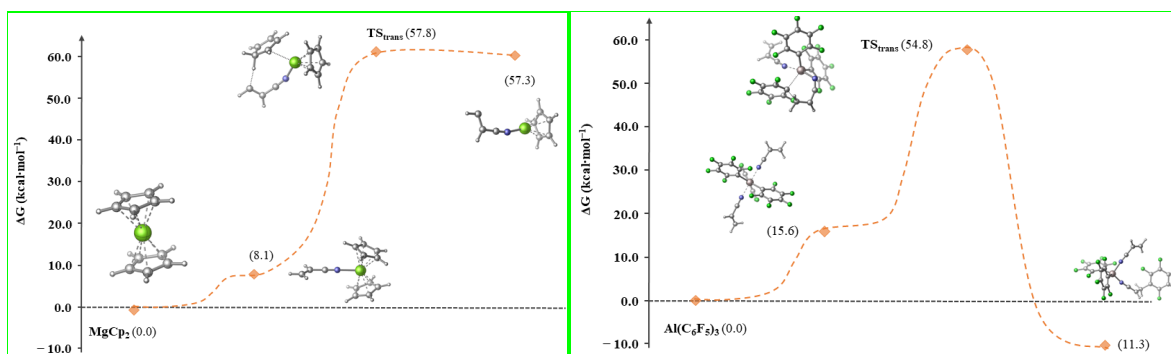


Figure S6. Energy profile for deprotonation initiation step starting from MgCp₂ (left) and energy profile for the hypothetical group transfer initiation step starting from Al(C₆F₅)₃-2 AN adduct (right).

Computational Details

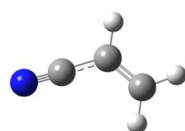
All calculations regarding geometry optimization and frequency calculations to determine the mechanistic behaviors of these Mg and Al compounds have been carried out using the software package Gaussian09.^[5]

As level of theory, the hybrid functional B3LYP^[6] has been chosen together with the basis set 6-31+G**^[7] for all atoms. All reported energies are ΔG values in kcal/mol relative to all starting materials with respect to T=298.15 K and p=1 atm. The number of imaginary frequencies ensures to have either a ground state (NImag=1) or a transition state (NImag=1).

DFT calculations: details of calculated molecules and transition states (geometries, energies)

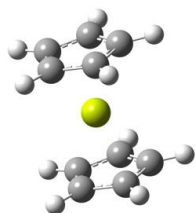
Magnesium based complexesI) Mechanism I: MgCp₂

Acrylonitrile

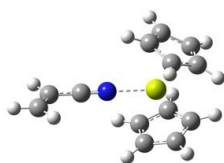


Center Number	Atomic Number	Atomic Type	Coordinates (Angstroms)		
			X	Y	Z
1	6	0	-0.783470	0.087939	0.000029
2	7	0	-1.905097	-0.223578	-0.000017
3	6	0	0.586550	0.505254	0.000000
4	6	0	1.612197	-0.357573	-0.000004
5	1	0	0.752520	1.579586	-0.000018
6	1	0	2.635263	0.003203	-0.000025
7	1	0	1.456243	-1.431463	0.000015
Sum of electronic and thermal Enthalpies=			-170.789176		
Sum of electronic and thermal Free Energies=			-170.820185		
HF=-170.8450003 / NImag=0					

SUPPORTING INFORMATION

MgCp₂

Center Number	Atomic Number	Atomic Type	Coordinates (Angstroms)		
			X	Y	Z
1	12	0	0.000006	0.000142	0.000063
2	6	0	-1.912849	1.369212	-0.241646
3	6	0	-2.347711	0.013154	-0.281266
4	6	0	-1.076487	1.596403	-1.372358
5	1	0	-2.185119	2.103453	0.506481
6	6	0	-1.780230	-0.597645	-1.436371
7	1	0	-3.008725	-0.464411	0.431479
8	6	0	-0.994532	0.380820	-2.110672
9	1	0	-0.601876	2.533793	-1.635117
10	1	0	-1.934448	-1.620885	-1.756081
11	1	0	-0.446970	0.232051	-3.033197
12	6	0	1.464326	-1.702431	0.740458
13	6	0	0.897123	-1.091678	1.895726
14	6	0	2.249339	-0.723726	0.065705
15	1	0	1.336144	-2.734544	0.438246
16	6	0	1.332487	0.264204	1.935666
17	1	0	0.261875	-1.578000	2.625769
18	6	0	2.168503	0.491506	0.804716
19	1	0	2.823196	-0.881465	-0.839175
20	1	0	1.086215	0.989595	2.701236
21	1	0	2.669825	1.419798	0.559864
Sum of electronic and thermal Enthalpies=			-587.033102		
Sum of electronic and thermal Free Energies=			-587.081015		
HF=-587.210259 / NImag=0					

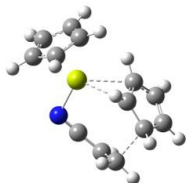
MgCp₂-ACN adduct (2a)

Center Number	Atomic Number	Atomic Type	Coordinates (Angstroms)		
			X	Y	Z
1	12	0	0.676210	0.001862	-0.021447
2	6	0	0.456561	-2.348171	-0.811185
3	6	0	0.234911	-2.377716	0.591137
4	6	0	1.790669	-1.910847	-1.036642
5	1	0	-0.260236	-2.620843	-1.576401
6	6	0	1.429072	-1.954275	1.235574
7	1	0	-0.682283	-2.674265	1.085260
8	6	0	2.395102	-1.678035	0.229142
9	1	0	2.272402	-1.802282	-2.000966
10	1	0	1.587885	-1.886926	2.305270

SUPPORTING INFORMATION

11	1	0	3.410272	-1.342094	0.397040
12	6	0	0.757474	2.192757	1.128008
13	6	0	0.106891	2.465393	-0.103709
14	6	0	2.081805	1.758645	0.836436
15	1	0	0.337662	2.331656	2.117402
16	6	0	1.010853	2.172235	-1.158094
17	1	0	-0.907989	2.823987	-0.219753
18	6	0	2.238519	1.746546	-0.575969
19	1	0	2.838783	1.490357	1.562825
20	1	0	0.817535	2.292170	-2.217611
21	1	0	3.135853	1.468028	-1.114245
22	7	0	-1.511263	-0.011618	-0.221465
23	6	0	-2.668868	-0.038735	-0.313242
24	6	0	-4.086952	-0.073209	-0.456270
25	6	0	-4.924618	0.044735	0.586002
26	1	0	-4.452149	-0.203057	-1.471671
27	1	0	-5.997607	0.011390	0.432220
28	1	0	-4.564322	0.174930	1.601115
Sum of electronic and thermal Enthalpies=					-757.823151
Sum of electronic and thermal Free Energies=					-757.888285
HF=-758.0578861 / NImag=0					

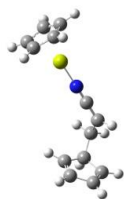
Transition state Cp transfer (aTStrans)



Center Number	Atomic Number	Atomic Type	Coordinates (Angstroms)		
			X	Y	Z
1	12	0	-0.953633	-0.300889	-0.140682
2	6	0	3.087866	1.302070	-0.242807
3	6	0	2.466652	0.859445	0.980140
4	6	0	2.103721	1.593323	-1.164719
5	1	0	4.155035	1.289761	-0.434217
6	6	0	1.039976	1.080310	0.816087
7	1	0	2.940825	0.915886	1.954835
8	6	0	0.827209	1.499045	-0.505054
9	1	0	2.250375	1.876978	-2.199934
10	1	0	0.323620	1.117213	1.632824
11	1	0	-0.104231	1.876907	-0.919498
12	6	0	-2.752044	0.208506	1.327072
13	6	0	-3.181286	-0.874841	0.508224
14	6	0	-2.546701	1.341446	0.486955
15	1	0	-2.647081	0.188924	2.405287
16	6	0	-3.225386	-0.421406	-0.835473
17	1	0	-3.412078	-1.876472	0.848005
18	6	0	-2.830324	0.950032	-0.852360
19	1	0	-2.246883	2.330039	0.812303
20	1	0	-3.515986	-1.010542	-1.696416
21	1	0	-2.802030	1.593130	-1.723954
22	7	0	-0.120605	-2.166992	-0.447844
23	6	0	1.059684	-2.038461	-0.477494
24	6	0	2.411958	-1.800127	-0.387069
25	6	0	2.878974	-1.227256	0.810188
26	1	0	3.000285	-1.794962	-1.296725
27	1	0	3.950549	-1.105848	0.926888
28	1	0	2.353642	-1.453922	1.731553
Sum of electronic and thermal Enthalpies=					-757.785059
Sum of electronic and thermal Free Energies=					-757.843428
HF= -758.0184528 / NImag=1 (-297.4246 cm ⁻¹)					

SUPPORTING INFORMATION

Intermediate 3a (CpMg-ACN-Cp)

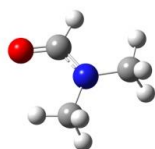


Center Number	Atomic Number	Atomic Type	Coordinates (Angstroms)		
			X	Y	Z
1	12	0	-2.481607	-0.162370	-0.123638
2	6	0	4.846668	-0.355558	-0.426427
3	6	0	3.903305	-0.401715	0.752258
4	6	0	4.975734	0.920071	-0.853520
5	1	0	5.340849	-1.230268	-0.835153
6	6	0	3.497890	1.043847	0.903800
7	1	0	4.488200	-0.691819	1.644442
8	6	0	4.134390	1.793749	-0.022283
9	1	0	5.598407	1.263628	-1.673082
10	1	0	2.799765	1.396095	1.655015
11	1	0	4.050121	2.868068	-0.148965
12	6	0	-4.115786	1.497159	-0.041176
13	6	0	-4.188244	0.751141	1.171818
14	6	0	-4.436458	0.619142	-1.118257
15	1	0	-3.881761	2.551027	-0.127223
16	6	0	-4.557136	-0.587770	0.844799
17	1	0	-4.023228	1.140289	2.168963
18	6	0	-4.710608	-0.669230	-0.570091
19	1	0	-4.493578	0.890575	-2.165172
20	1	0	-4.718527	-1.393743	1.549943
21	1	0	-5.008877	-1.547970	-1.128403
22	7	0	-0.645319	-0.641264	-0.286697
23	6	0	0.524527	-0.910416	-0.411086
24	6	0	1.815017	-1.220984	-0.542078
25	6	0	2.739900	-1.428256	0.635640
26	1	0	2.213884	-1.287310	-1.550057
27	1	0	3.193463	-2.429783	0.592163
28	1	0	2.162602	-1.398571	1.567674
Sum of electronic and thermal Enthalpies=					-757.809279
Sum of electronic and thermal Free Energies=					-757.872422
HF= -758.0450598 / NImag=0					

II) Mechanism II: MgCp₂-N,N-DMF

Acetonitrile (see Mechanism I)

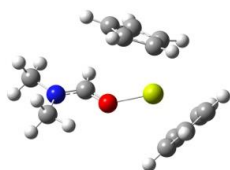
N,N-DMF



Center Number	Atomic Number	Atomic Type	Coordinates (Angstroms)		
			X	Y	Z
1	6	0	-0.863515	-0.649457	-0.000001
2	8	0	-1.956263	-0.096947	-0.000003
3	1	0	-0.762207	-1.750879	0.000057

SUPPORTING INFORMATION

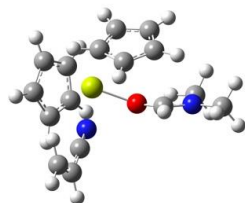
4	7	0	0.345919	-0.019495	-0.000007
5	6	0	0.421639	1.433695	0.000015
6	1	0	0.953899	1.790707	0.890362
7	1	0	0.952853	1.790807	-0.890941
8	1	0	-0.593507	1.831124	0.000567
9	6	0	1.593809	-0.761889	-0.000003
10	1	0	1.384379	-1.834634	-0.000084
11	1	0	2.190855	-0.524535	-0.889672
12	1	0	2.190809	-0.524634	0.889722
Sum of electronic and thermal Enthalpies=					-248.424036
Sum of electronic and thermal Free Energies=					-248.460332
HF= -248.5333895 / NImag=0					

MgCp₂-N,N-DMF (1)

Center Number	Atomic Number	Atomic Type	Coordinates (Angstroms)		
			X	Y	Z
1	12	0	1.101173	0.015166	-0.005098
2	6	0	-0.662898	2.204684	1.286800
3	6	0	-1.427774	2.406267	0.120370
4	6	0	0.702955	2.127585	0.917112
5	1	0	-1.046309	2.131833	2.298465
6	6	0	-0.554258	2.448737	-0.989668
7	1	0	-2.507407	2.512616	0.083041
8	6	0	0.771786	2.281114	-0.519231
9	1	0	1.550035	2.162501	1.595235
10	1	0	-0.836665	2.618629	-2.023419
11	1	0	1.677872	2.450608	-1.092151
12	6	0	2.428875	-1.703742	-1.036863
13	6	0	2.263751	-2.060191	0.329512
14	6	0	3.205614	-0.510386	-1.088332
15	1	0	2.052460	-2.256535	-1.889229
16	6	0	2.928465	-1.082900	1.122511
17	1	0	1.727664	-2.924880	0.700956
18	6	0	3.517623	-0.131050	0.243671
19	1	0	3.517704	0.006742	-1.987657
20	1	0	3.002605	-1.083118	2.203474
21	1	0	4.098422	0.733966	0.539644
22	8	0	-0.697888	-0.888922	-0.092249
23	6	0	-1.812226	-0.622659	-0.589386
24	1	0	-1.900377	0.003783	-1.481961
25	7	0	-2.969465	-1.089012	-0.109928
26	6	0	-4.239987	-0.730155	-0.728460
27	1	0	-4.787649	-1.632675	-1.019995
28	1	0	-4.854555	-0.154734	-0.027329
29	1	0	-4.060967	-0.122338	-1.617270
30	6	0	-3.018839	-1.894682	1.107040
31	1	0	-3.535572	-2.838684	0.905487
32	1	0	-2.001849	-2.097197	1.438810
33	1	0	-3.558655	-1.353792	1.892114
Sum of electronic and thermal Enthalpies=					-835.467005
Sum of electronic and thermal Free Energies=					-835.535396
HF=-835.755497 / NImag=0					

SUPPORTING INFORMATION

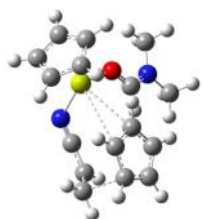
MgCp2-DMF-ACN adduct (2b)



Center Number	Atomic Number	Atomic Type	Coordinates (Angstroms)		
			X	Y	Z
1	6	0	0.535940	-3.271506	-0.175524
2	6	0	1.651813	-2.952810	0.644548
3	6	0	2.572901	-2.206924	-0.136701
4	6	0	2.030462	-2.074496	-1.447143
5	6	0	0.774509	-2.732908	-1.469973
6	12	0	0.528743	-0.828349	0.072701
7	8	0	-1.097175	-0.175534	-0.959532
8	6	0	-1.840667	0.819640	-0.848444
9	7	0	-3.132390	0.823418	-1.203694
10	6	0	-3.795757	-0.396848	-1.651074
11	6	0	-3.962560	2.002332	-1.000470
12	7	0	1.720327	0.974674	-0.568955
13	6	0	2.463796	1.840598	-0.782708
14	6	0	3.376208	2.903042	-1.060184
15	6	0	4.156107	3.446372	-0.113159
16	6	0	0.311004	-0.074926	2.246188
17	6	0	-0.139987	1.280477	2.192396
18	6	0	-1.543664	1.276292	2.250853
19	6	0	-1.985928	-0.069967	2.348608
20	6	0	-0.857581	-0.905509	2.360463
21	1	0	-2.181622	2.155326	2.240212
22	1	0	0.496320	2.158325	2.155718
23	1	0	-3.018025	-0.399712	2.406929
24	1	0	1.324266	-0.388208	2.488069
25	1	0	-0.858438	-1.980563	2.498185
26	1	0	3.531529	-1.828084	0.198015
27	1	0	2.499446	-1.570296	-2.283645
28	1	0	1.773586	-3.225075	1.686062
29	1	0	0.111350	-2.808951	-2.323061
30	1	0	-0.335834	-3.838314	0.128117
31	1	0	3.405661	3.244757	-2.091349
32	1	0	4.842178	4.248812	-0.361944
33	1	0	4.128878	3.106290	0.916879
34	1	0	-1.464072	1.773438	-0.466764
35	1	0	-4.446051	2.293608	-1.939446
36	1	0	-4.737237	1.798662	-0.252216
37	1	0	-3.346846	2.831110	-0.646245
38	1	0	-4.301165	-0.215956	-2.605598
39	1	0	-3.048751	-1.179803	-1.771944
40	1	0	-4.537823	-0.714697	-0.909637
Sum of electronic and thermal Enthalpies=					-1006.260429
Sum of electronic and thermal Free Energies=					-1006.346399
HF=-1006.6063463 / NImag=0					

SUPPORTING INFORMATION

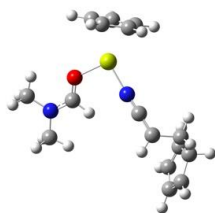
Transition state Cp transfer (bTStrans)



Center Number	Atomic Number	Atomic Type	Coordinates (Angstroms)		
			X	Y	Z
1	6	0	-1.345596	0.359044	-1.400364
2	6	0	-2.527686	-0.364004	-1.205493
3	6	0	-3.589968	0.573881	-1.017447
4	6	0	-3.049626	1.884029	-1.188289
5	6	0	-1.676106	1.762739	-1.384258
6	6	0	-3.546200	0.579054	1.471217
7	6	0	-2.329718	1.039358	1.915829
8	6	0	-1.234924	0.179771	1.985984
9	7	0	-0.322448	-0.563509	2.054359
10	12	0	0.602847	-1.264055	0.316288
11	8	0	1.814092	0.336728	0.062480
12	6	0	1.579489	1.566322	0.049197
13	7	0	2.532007	2.499454	0.003800
14	6	0	2.192272	3.919514	-0.026174
15	6	0	3.949350	2.143944	-0.031637
16	6	0	-0.129027	-3.489732	-0.041681
17	6	0	0.293608	-2.967799	-1.299733
18	6	0	1.694018	-2.726924	-1.225635
19	6	0	2.135663	-3.093340	0.077125
20	6	0	1.010552	-3.570014	0.805415
21	1	0	-3.609447	2.811569	-1.136544
22	1	0	-4.644872	0.323784	-0.990361
23	1	0	-0.992361	2.580951	-1.589889
24	1	0	-2.630518	-1.443296	-1.215109
25	1	0	-0.393505	-0.056194	-1.725459
26	1	0	1.017841	-3.925792	1.828310
27	1	0	3.153653	-3.037697	0.443631
28	1	0	-1.137189	-3.789515	0.216384
29	1	0	2.314916	-2.338276	-2.023529
30	1	0	-0.336305	-2.805767	-2.165624
31	1	0	-2.140217	2.096036	2.068623
32	1	0	-3.753594	-0.480157	1.405770
33	1	0	-4.395662	1.248708	1.444861
34	1	0	0.549131	1.942672	0.058265
35	1	0	2.626352	4.429719	0.840168
36	1	0	2.581492	4.381308	-0.939646
37	1	0	1.107939	4.040404	-0.003992
38	1	0	4.462835	2.578209	0.832511
39	1	0	4.042659	1.059479	-0.007195
40	1	0	4.406424	2.532003	-0.947928
Sum of electronic and thermal Enthalpies=			-1006.237525		
Sum of electronic and thermal Free Energies=			-1006.315771		
HF= -1006.5825804 / NImag=1 (-76.5198 cm ⁻¹)					

SUPPORTING INFORMATION

Intermediate 3b (CpDMFMg-ACN-Cp)



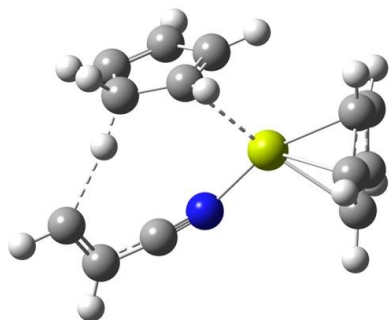
Center Number	Atomic Number	Atomic Type	Coordinates (Angstroms)		
			X	Y	Z
1	6	0	-3.755187	-2.159234	0.323651
2	6	0	-2.846060	-2.502314	1.378387
3	6	0	-1.767999	-3.251189	0.814797
4	6	0	-1.997698	-3.375154	-0.578385
5	6	0	-3.225102	-2.696551	-0.875616
6	12	0	-1.532001	-1.121231	-0.127796
7	8	0	-2.607066	0.645743	-0.044488
8	6	0	-2.507519	1.749241	0.530402
9	7	0	-3.206152	2.832529	0.189181
10	6	0	-4.223693	2.776062	-0.854380
11	7	0	0.231390	-0.297907	-0.485871
12	6	0	1.303082	0.294238	-0.737548
13	6	0	2.507433	0.854231	-0.944428
14	6	0	3.645250	0.126384	-1.616135
15	6	0	4.893196	-0.147496	-0.722847
16	6	0	5.576866	1.080064	-0.170437
17	6	0	5.724235	0.954240	1.167368
18	6	0	5.147795	-0.328617	1.596211
19	6	0	4.654227	-0.973575	0.516191
20	6	0	-2.996156	4.109375	0.850189
21	1	0	5.900782	1.914316	-0.783463
22	1	0	5.621125	-0.683164	-1.360219
23	1	0	6.193690	1.671615	1.832974
24	1	0	4.150980	-1.933953	0.508657
25	1	0	5.127626	-0.682371	2.621900
26	1	0	-0.938500	-3.677757	1.366431
27	1	0	-1.389940	-3.913475	-1.295164
28	1	0	-2.980456	-2.258416	2.425206
29	1	0	-3.690339	-2.620601	-1.851323
30	1	0	-4.651685	-1.561986	0.423697
31	1	0	2.673126	1.852260	-0.549726
32	1	0	4.003521	0.687223	-2.494353
33	1	0	3.288973	-0.836975	-2.001748
34	1	0	-1.781066	1.915394	1.334125
35	1	0	-2.330403	3.984545	1.705935
36	1	0	-2.549946	4.835423	0.159720
37	1	0	-3.955246	4.502548	1.201699
38	1	0	-4.227506	1.778294	-1.286945
39	1	0	-5.201896	3.003222	-0.422676
40	1	0	-3.994985	3.512097	-1.632960
Sum of electronic and thermal Enthalpies=			-1006.267538		
Sum of electronic and thermal Free Energies=			-1006.350413		
HF= -1006.6152245 / NImag=0					

SUPPORTING INFORMATION

III) Alternative to I – hydrogen transfer from Olefin to Cp

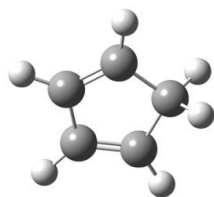
MgCp₂ and MgCp₂-ACN adduct see I)

TS hydrogen transfer



Center Number	Atomic Number	Atomic Type	Coordinates (Angstroms)		
			X	Y	Z
1	12	0	0.883990	-0.137444	-0.137212
2	6	0	-0.809042	1.470779	1.055920
3	6	0	-2.254889	1.271901	0.778117
4	6	0	-0.224168	2.084677	-0.037010
5	1	0	-0.336498	1.297743	2.018680
6	6	0	-2.437696	1.865209	-0.567952
7	1	0	-2.673123	0.170514	0.793477
8	6	0	-1.242175	2.303196	-1.055868
9	1	0	0.792852	2.463591	-0.084389
10	1	0	-3.384546	1.876704	-1.095265
11	1	0	-1.059023	2.741183	-2.030157
12	6	0	2.999721	-0.711940	-1.034932
13	6	0	2.776457	-1.560258	0.082112
14	6	0	3.083209	0.631349	-0.558846
15	1	0	3.112414	-1.030220	-2.064050
16	6	0	2.708476	-0.747011	1.248920
17	1	0	2.662337	-2.636383	0.050229
18	6	0	2.909180	0.607767	0.853330
19	1	0	3.288326	1.507276	-1.162532
20	1	0	2.572816	-1.100597	2.263824
21	1	0	2.947166	1.464438	1.515323
22	7	0	-0.588234	-1.405948	-0.691491
23	6	0	-1.625989	-1.914354	-0.501004
24	6	0	-2.911954	-2.396799	-0.165275
25	6	0	-3.594397	-1.517015	0.627216
26	1	0	-3.196195	-3.383258	-0.542861
27	1	0	-4.584398	-1.907674	0.913549
28	1	0	-2.892775	1.702646	1.562786
Sum of electronic and thermal Enthalpies=			-757.748163		
Sum of electronic and thermal Free Energies=			-757.809029		
HF=-757.977775 / NImag=1 (-96.6571 cm ⁻¹)					

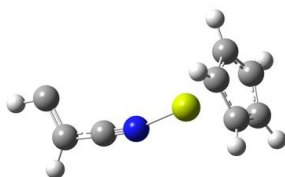
SUPPORTING INFORMATION

C₅H₆ (Cp)

Center Number	Atomic Number	Atomic Type	Coordinates (Angstroms)		
			X	Y	Z
1	6	0	-0.001099	-1.218191	0.000389
2	1	0	-0.001693	-1.881644	-0.877731
3	1	0	-0.001705	-1.880830	0.879149
4	6	0	1.181137	-0.284322	-0.000384
5	1	0	2.213973	-0.612175	-0.000594
6	6	0	0.735617	0.992439	0.000122
7	1	0	1.350934	1.885709	0.000238
8	6	0	-1.181647	-0.282192	-0.000408
9	1	0	-2.215073	-0.608179	-0.000635
10	6	0	-0.733825	0.993763	0.000161
11	1	0	-1.347530	1.888140	0.000297

Sum of electronic and thermal Enthalpies= -194.022285
 Sum of electronic and thermal Free Energies= -194.053998
 HF=-194.1198158 / NImag=0

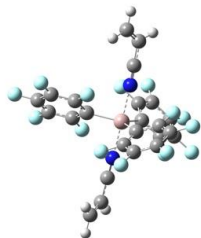
CpMg-ACN



Center Number	Atomic Number	Atomic Type	Coordinates (Angstroms)		
			X	Y	Z
1	12	0	0.416537	-0.156659	-0.000017
2	6	0	2.509560	-0.836761	-0.715950
3	6	0	2.510257	-0.840089	0.711211
4	6	0	2.305900	0.506299	-1.153776
5	1	0	2.669761	-1.696657	-1.354485
6	6	0	2.307011	0.500891	1.155507
7	1	0	2.671079	-1.702983	1.345533
8	6	0	2.180372	1.333063	0.002874
9	1	0	2.282841	0.844181	-2.182394
10	1	0	2.285077	0.833978	2.185711
11	1	0	2.043604	2.407296	0.005410
12	7	0	-1.491348	-0.517123	0.000145
13	6	0	-2.669583	-0.458899	0.000034
14	6	0	-4.058794	-0.338834	-0.000002
15	6	0	-4.468819	0.982339	-0.000003
16	1	0	-4.631046	-1.276077	-0.000011
17	1	0	-5.575754	1.001966	0.000050

Sum of electronic and thermal Enthalpies= -563.704514
 Sum of electronic and thermal Free Energies= -563.755849
 HF=-563.8373881 / NImag=0

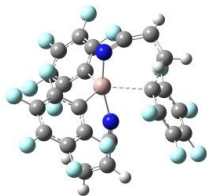
SUPPORTING INFORMATION

Aluminium based complexesAl(C₆F₅)₃ * 2 ACN adduct

Center Number	Atomic Number	Atomic Type	Coordinates (Angstroms)		
			X	Y	Z
1	13	0	-0.078018	-0.000043	0.000010
2	6	0	0.935497	-1.749608	-0.055529
3	6	0	2.135853	-1.952151	0.620622
4	6	0	0.481991	-2.855180	-0.771534
5	6	0	2.848966	-3.148399	0.603449
6	6	0	1.151729	-4.075580	-0.827239
7	6	0	2.348812	-4.220970	-0.130500
8	6	0	-2.096815	-0.000460	0.000117
9	6	0	-2.849178	-0.983240	0.638814
10	6	0	-2.849641	0.982009	-0.638520
11	6	0	-4.241829	-1.009612	0.656011
12	6	0	-4.242304	1.007780	-0.655628
13	6	0	-4.943474	-0.001068	0.000213
14	6	0	0.934658	1.750003	0.055422
15	6	0	0.480809	2.855294	0.771644
16	6	0	2.134763	1.953178	-0.620984
17	6	0	1.149997	4.075998	0.827322
18	6	0	2.847324	3.149757	-0.603858
19	6	0	2.346848	4.222021	0.130319
20	7	0	-0.060245	-0.075449	2.144305
21	6	0	0.012337	-0.134325	3.298270
22	6	0	0.088245	-0.204106	4.721634
23	6	0	1.243559	-0.454222	5.354976
24	1	0	-0.844500	-0.042490	5.254629
25	1	0	2.170899	-0.614728	4.814506
26	1	0	1.274077	-0.501920	6.438180
27	7	0	-0.060615	0.075229	-2.144300
28	6	0	0.011658	0.133972	-3.298291
29	6	0	0.087270	0.203583	-4.721680
30	6	0	1.242075	0.455541	-5.355220
31	1	0	-0.845263	0.040252	-5.254523
32	1	0	1.272374	0.503076	-6.438437
33	1	0	2.169209	0.617742	-4.814901
34	9	0	-0.680055	-2.773241	-1.471346
35	9	0	0.664533	-5.108383	-1.538351
36	9	0	3.014417	-5.385395	-0.165334
37	9	0	4.003839	-3.283374	1.282194
38	9	0	2.673625	-0.942722	1.359807
39	9	0	-0.681046	2.772760	1.471702
40	9	0	2.672848	0.944078	-1.360385
41	9	0	4.001978	3.285325	-1.282860
42	9	0	3.011917	5.386754	0.165119
43	9	0	0.662478	5.108499	1.538652
44	9	0	-2.219801	1.990897	-1.297564
45	9	0	-4.915847	1.983805	-1.291648
46	9	0	-2.218860	-1.991847	1.297830
47	9	0	-4.914911	-1.985922	1.292082
48	9	0	-6.285278	-0.001357	0.000256
Sum of electronic and thermal Enthalpies=					-2767.419399
Sum of electronic and thermal Free Energies=					-2767.544063

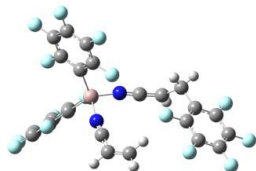
SUPPORTING INFORMATION

HF= -2767.7147723 / NImag=0

TS C₆F₅⁻-Transfer to ACN

Center Number	Atomic Number	Atomic Type	Coordinates (Angstroms)		
			X	Y	Z
1	13	0	-0.138671	0.143102	-0.697994
2	6	0	1.056442	1.741511	-0.434486
3	6	0	2.300475	1.773466	0.191853
4	6	0	0.618431	2.977694	-0.915122
5	6	0	3.076942	2.922650	0.322737
6	6	0	1.351672	4.157117	-0.811053
7	6	0	2.596796	4.125426	-0.187757
8	6	0	-2.089135	0.261107	-0.152538
9	6	0	-2.492641	1.079506	0.901901
10	6	0	-3.137159	-0.390619	-0.802079
11	6	0	-3.814977	1.259307	1.296376
12	6	0	-4.479314	-0.248529	-0.452922
13	6	0	-4.820547	0.586309	0.607322
14	7	0	-0.390660	0.316060	-2.656360
15	6	0	-0.457303	-0.656421	-3.332011
16	6	0	-0.220859	-1.943157	-3.721304
17	6	0	0.999937	-2.358358	-3.114366
18	1	0	-1.035770	-2.614605	-3.956951
19	6	0	0.995851	-2.069083	-1.168733
20	6	0	2.341750	-1.984648	-0.762511
21	6	0	0.260360	-3.068895	-0.505083
22	6	0	2.913144	-2.773369	0.225286
23	6	0	0.779910	-3.888998	0.486886
24	6	0	2.116225	-3.729361	0.860213
25	7	0	0.271362	-0.541515	1.271160
26	6	0	0.382688	-0.640631	2.420402
27	6	0	0.515393	-0.747744	3.836079
28	6	0	-0.119396	0.102410	4.657730
29	1	0	1.158712	-1.543421	4.200560
30	1	0	-0.003344	0.011447	5.732369
31	1	0	-0.755782	0.896511	4.280079
32	9	0	-5.442697	-0.908379	-1.117595
33	9	0	-6.102884	0.736406	0.966348
34	9	0	-4.131298	2.062798	2.328764
35	9	0	-1.557745	1.762677	1.624145
36	9	0	-2.881232	-1.230491	-1.835395
37	9	0	3.153723	-1.119314	-1.405569
38	9	0	4.199301	-2.642668	0.583192
39	9	0	2.636538	-4.500539	1.821086
40	9	0	0.028490	-4.817303	1.103434
41	9	0	-1.030886	-3.263535	-0.845715
42	9	0	-0.598613	3.073507	-1.500893
43	9	0	2.824903	0.640131	0.731631
44	9	0	0.875310	5.318351	-1.290293
45	9	0	4.273367	2.886753	0.936541
46	9	0	3.323455	5.245762	-0.071241
47	1	0	1.869797	-1.727774	-3.264027
48	1	0	1.228485	-3.421864	-3.158589
Sum of electronic and thermal Enthalpies=			-2767.336201		
Sum of electronic and thermal Free Energies=			-2767.453617		

SUPPORTING INFORMATION

HF=-2767.6300358 / NImag=1 (-362.5119 cm⁻¹)ACN-Al(C₆F₅)₂-ACN-C₆F₅ adduct

Center Number	Atomic Number	Atomic Type	Coordinates (Angstroms)		
			X	Y	Z
1	13	0	-1.351816	-0.076150	-0.135075
2	6	0	-2.181500	1.730389	-0.287135
3	6	0	-1.458956	2.883330	0.012592
4	6	0	-3.489560	1.950019	-0.715384
5	6	0	-1.973675	4.171812	-0.090439
6	6	0	-4.057101	3.216735	-0.838117
7	6	0	-3.289163	4.335180	-0.520943
8	6	0	-2.558313	-1.654190	-0.032445
9	6	0	-3.341176	-1.897806	1.093085
10	6	0	-2.710093	-2.575526	-1.067435
11	6	0	-4.212505	-2.975394	1.215898
12	6	0	-3.568610	-3.671011	-1.000349
13	6	0	-4.323602	-3.870492	0.153632
14	7	0	0.101859	-0.296712	-1.191639
15	6	0	1.188074	-0.476989	-1.671664
16	6	0	2.392351	-0.652287	-2.215816
17	6	0	3.461397	0.423841	-2.175276
18	1	0	2.612381	-1.607287	-2.681321
19	1	0	3.902559	0.558286	-3.167049
20	1	0	3.015407	1.381671	-1.892939
21	6	0	4.582397	0.107113	-1.195192
22	6	0	4.444819	0.325891	0.176460
23	6	0	5.795166	-0.453087	-1.602144
24	6	0	5.438415	0.011427	1.095999
25	6	0	6.814081	-0.780939	-0.708053
26	6	0	6.634549	-0.547723	0.652738
27	7	0	-0.507411	-0.014224	1.664220
28	6	0	0.083409	0.038375	2.658410
29	6	0	0.788754	0.097240	3.893372
30	6	0	2.063120	0.516293	3.952072
31	1	0	0.228731	-0.213337	4.771013
32	1	0	2.577505	0.555444	4.906393
33	1	0	2.613806	0.819057	3.067618
34	9	0	7.961569	-1.317646	-1.147543
35	9	0	7.600249	-0.857311	1.528608
36	9	0	5.249741	0.244682	2.410660
37	9	0	3.298904	0.868150	0.657157
38	9	0	6.012466	-0.698818	-2.910240
39	9	0	-3.270193	-1.040997	2.149912
40	9	0	-2.007712	-2.420255	-2.213418
41	9	0	-3.679121	-4.532231	-2.024559
42	9	0	-5.153803	-4.917858	0.241994
43	9	0	-4.939725	-3.164049	2.330371
44	9	0	-4.276246	0.896506	-1.042383
45	9	0	-5.323579	3.375548	-1.254551
46	9	0	-3.812370	5.563220	-0.629831
47	9	0	-1.230737	5.249297	0.215902
48	9	0	-0.170731	2.769481	0.436922
Sum of electronic and thermal Enthalpies=			-2767.437915		
Sum of electronic and thermal Free Energies=			-2767.562106		
HF=			-2767.7348225 / NImag=0		

SUPPORTING INFORMATION

5. References

- [1] K. Linnemayr, P. Vana, G. Allmaier, *Rapid Commun. Mass Spectrom.* **1998**, *12*, 1344.
- [2] A. Behr, *Angewandte homogene Katalyse*, Wiley-VCH Verlag GmbH & Co. KGaA, Weinheim, **2008**.
- [3] J. Klosin, G. R. Roof, E. Y.-X. Chen, K. A. Abboud, *Organometallics* **2000**, *19*, 4684.
- [4] A. W. Duff, P. B. Hitchcock, M. F. Lappert, R. G. Taylor, J. A. Segal, *J. Organomet. Chem.* **1985**, *293*, 271.
- [5] Gaussian 09, Revision E.02, M. J. Frisch, G. W. Trucks, H. B. Schlegel, G. E. Scuseria, M. A. Robb, J. R. Cheeseman, G. Scalmani, V. Barone, G. A. Petersson, H. Nakatsuji, X. Li, M. Caricato, A. Marenich, J. Bloino, B. G. Janesko, R. Gomperts, B. Mennucci, H. P. Hratchian, J. V. Ortiz, A. F. Izmaylov, J. L. Sonnenberg, D. Williams-Young, F. Ding, F. Lipparini, F. Egidi, J. Goings, B. Peng, A. Petrone, T. Henderson, D. Ranasinghe, V. G. Zakrzewski, J. Gao, N. Rega, G. Zheng, W. Liang, M. Hada, M. Ehara, K. Toyota, R. Fukuda, J. Hasegawa, M. Ishida, T. Nakajima, Y. Honda, O. Kitao, H. Nakai, T. Vreven, K. Throssell, J. A. Montgomery, Jr., J. E. Peralta, F. Ogliaro, M. Bearpark, J. J. Heyd, E. Brothers, K. N. Kudin, V. N. Staroverov, T. Keith, R. Kobayashi, J. Normand, K. Raghavachari, A. Rendell, J. C. Burant, S. S. Iyengar, J. Tomasi, M. Cossi, J. M. Millam, M. Klene, C. Adamo, R. Cammi, J. W. Ochterski, R. L. Martin, K. Morokuma, O. Farkas, J. B. Foresman, and D. J. Fox, *Gaussian, Inc., Wallingford CT* **2016**.
- [6] a) S. H. Vosko, L. Wilk, M. Nusair, *Can. J. Phys.* **1980**, *58*, 1200; b) P. J. Stephens, F. J. Devlin, C. F. Chabalowski, M. J. Frisch, *J. Phys. Chem.* **1994**, *98*, 11623; c) Lee, Yang, Parr, *Phys. Rev. B* **1988**, *37*, 785; d) A. D. Becke, *J. Chem. Phys.* **1993**, *98*, 5648.
- [7] a) R. Ditchfield, W. J. Hehre, J. A. Pople, *J. Chem. Phys.* **1971**, *54*, 724; b) W. J. Hehre, R. Ditchfield, J. A. Pople, *J. Chem. Phys.* **1972**, *56*, 2257; c) M. M. Francl, W. J. Pietro, W. J. Hehre, J. S. Binkley, M. S. Gordon, D. J. DeFrees, J. A. Pople, *J. Chem. Phys.* **1982**, *77*, 3654.

12.4 Supporting Information for Chapter 7

The supporting information is available free of charge under:

<https://pubs.acs.org/doi/10.1021/acs.macromol.9b01326>

Rightslink® by Copyright Clearance Center

<https://s100.copyright.com/AppDispatchServlet#formTop>



RightsLink®

Home

Create Account

Help



ACS Publications
Most Trusted. Most Cited. Most Read.

Title: Isospecific Group-Transfer Polymerization of Diethyl Vinylphosphonate and Multidimensional NMR Analysis of the Polymer Microstructure

Author: Michael Weger, Philipp Pahl, Fabian Schmidt, et al

Publication: Macromolecules

Publisher: American Chemical Society

Date: Sep 1, 2019

Copyright © 2019, American Chemical Society

LOGIN

If you're a [copyright.com user](#), you can login to RightsLink using your copyright.com credentials.

Already a [RightsLink user](#) or want to [learn more?](#)

Quick Price Estimate

Permission for this particular request is granted for print and electronic formats, and translations, at no charge. Figures and tables may be modified. Appropriate credit should be given. Please print this page for your records and provide a copy to your publisher. Requests for up to 4 figures require only this record. Five or more figures will generate a printout of additional terms and conditions. Appropriate credit should read: "Reprinted with permission from {COMPLETE REFERENCE CITATION}. Copyright {YEAR} American Chemical Society." Insert appropriate information in place of the capitalized words.

I would like to... ?

reuse in a Thesis/Dissertation

Requestor Type ?

Author (original work)

Portion ?

make a selection

Format ?

Print

Select your currency

USD - \$

Quick Price

Click Quick Price

This service provides permission for reuse only. If you do not have a copy of the article you are using, you may copy and paste the content and reuse according to the terms of your agreement. Please be advised that obtaining the content you license is a separate transaction not involving Rightslink.

QUICK PRICE

CONTINUE

To request permission for a type of use not listed, please contact [the publisher](#) directly.

Copyright © 2019 [Copyright Clearance Center, Inc.](#) All Rights Reserved. [Privacy statement](#). [Terms and Conditions](#). Comments? We would like to hear from you. E-mail us at customer@copyright.com